



**University of
Nottingham**

UK | CHINA | MALAYSIA

Health and Environmental Impact Assessment of Landfill Mining Activities

By

Mohammed Zari

Thesis submitted to the University of Nottingham

for the degree of Doctor of Philosophy

School of Engineering

Department of Chemical and Environmental Engineering

University of Nottingham

September 2023

Abstract

The adoption of landfill mining (LFM) has the potential to reduce the negative environmental effects of landfills while also recovering critical and secondary raw materials, energy, and land space by a series of on-site mechanical operations. However, there is a fundamental lack of understanding of how these activities could impact the environment and human health during LFM mining operations through atmospheric transport of contaminants. Therefore, this research aims to bridge this gap and optimize the benefits of LFM activities by shedding light on the potential health and environmental impacts associated with these practices.

A sampling programme was devised for an existing landfill site and recovered waste material characterised for physical, chemical, and biological properties. Almost 40 kg of municipal solid waste (MSW) was collected from 4 different wells (~10 kg each from wells 1901, 1904, 1906, and 1907) using a rotary drilling rig with depth ranging from surface of 7 - 8 metres. Samples were subjected to a wide array of laboratory analysis to meet the objectives for a risk assessment of LFM on human health and the environment. Characterisation results were used to derive pollution and health impact indices and other key indicators. Additionally, a method for computing the amount of dust, coupled with adoption of surface mining activities equations was proposed for each individual LFM activity. Subsequently, air dispersion modelling software (ADMS 5) was used to determine the potential air quality impact of LFM, with a focus on dust emissions as the main emission associated with landfill mining processes. Different scenarios were considered based on locally derived site meteorological data. Well-established statistical methods were used in the assessment to draw meaningful interpretation, identify parameter trends and support the research findings.

Results of potentially toxic elements were assessed against regulatory soil guideline values (SGVs). The concentrations of As, Cd, Cr, Pb, Cu, and Zn were above permissible limits set

for soil in the UK. The Zn and Pb concentrations were found to be the highest in wells 1901 and 1904, respectively, compared to the SGVs. The concentrations also varied significantly among the four wells and decreased in the following order: Zn>Mn>Pb>Cu>Ba>Cr>Ni>As>Co>Cd. The pollution load index was >1, indicating that unacceptable pollution could arise. The study predicts that the landfill could pose a significant risk to human health due to LFM, with potential non-carcinogenic risks of Zn and Pb being higher than the levels set by the USEPA. Carcinogenic assessment suggests that Cr was the most prominent metal followed by As, which could cause human health impacts. Emission estimation results showed that point source activities are the major sources of emission, with cover removal loading activity being the highest as an individual activity. Air dispersion modelling results suggest that dust concentrations are most intense in low wind and maximum emission rate scenarios. Results also suggest that some dust concentration values were above the Air Quality Strategy for England PM10s limit, especially with the inclusion of background concentrations. Therefore, the risk to the human health and environment is potentially significant.

Design and implementation of LFM processes must adequately consider environmental and health impacts to allow safe practices from an occupational health (protection of site workers), off-site human health and the surrounding environment.

Acknowledgments

First of all, I would like to express my genuine gratitude and appreciation to both my academic supervisors, Dr Rebecca Ferrari and Dr Richard Smith who greatly supported me with invaluable academic guidance and advice throughout the research. They provided me with useful information and participated actively during the research of this intensive and rewarding experience. A special thanks also goes to Dr Eleanor Binner for her continuous monitoring after the submission of the thesis. I would like also to thank all the technicians for their great help in laboratories during the PhD journey including Vikki Archibald, Joseph Meehan, Adrian Quinn, and Dr Elisabeth Steer.

It was a delight to work with these individuals because I gained a great deal from their keen scientific insight, their problem-solving skills, and their exceptional ability to communicate complex ideas in simple terms.

Additionally, I want to convey my profound gratitude to my family for their unwavering support and belief in all my endeavours.

Table of Contents

Abstract	i
Acknowledgment	iii
Table of Contents	iv
List of Figures	ix
List of Tables	xii
Chapter 1: Introduction	1
1.1 Background	1
1.2 Aim and Objectives	3
1.3 Thesis Overview	4
Chapter 2: Literature Review	7
2.1 Overview of Landfill Mining Concepts	7
2.2 International LFM Project	8
2.3 Europe Landfill Population	10
2.4 UK Landfill Population	11
2.5 Case Studies	13
2.6 Concepts for Aftercare and Completion	14
2.7 Potential Analytes in MSW Landfills	19
2.8 Conclusion	21
Chapter 3: Site Sampling and Material Characterisation	23

3.1 Site Location and History	23
3.2 Geology and Hydrogeology.....	27
3.3 Conceptual Site Model	28
3.4 Sampling Strategy and Location of Samples	32
3.5 Excavation and Storage.....	34
3.6 Sample Processing Methodology	36
3.7 MSW Characterisation and Laboratory Work	37
Chapter 4: Results and Discussion of MSW Characterisation	39
4.1 Moisture Content (MC).....	39
4.2 Leaching test	43
4.2.1 Procedure of Leaching Test	43
4.3 Chemical Oxygen Demand (COD).....	44
4.4 pH.....	46
4.5 Statistical Analysis of (MC, COD, and pH).....	48
4.6 Comparison and Relationship Between the Data of the Studied Site and Seven Other UK Landfill Sites	50
4.6.1 Moisture Content.....	50
4.6.2 Chemical Oxygen Demand (COD)	51
4.6.3 pH	53
4.7 Oven Drying.....	53
4.8 Particle Size Distribution (PSD).....	53
4.9 Heavy Metals.....	58
4.9.1 Heavy Metals Pollution Assessment	70
4.9.2 Health Risk Assessment	76

4.10 Total Organic Carbon (TOC).....	81
4.11 Waste Degradation Stages in Landfills.....	87
4.12 Mineral Composition.....	90
Chapter 5: ADMS Methods and Modelling.....	110
5.1 Introduction to Air Dispersion Modelling.....	110
5.2 Factors Affecting Dispersion of Pollutants in the Atmosphere	111
5.2.1 Meteorology	111
5.3 Air Dispersion Models.....	114
5.4 ADMS	116
5.5 ADMS Modelling Methodology.....	118
5.6 Emission Estimation	119
5.7 Meteorological and Terrain Data.....	125
5.8 LFM Assumed Process Plan	126
5.9 Selection of Scenarios	128
5.10 Formatting Input Data to ADMS Format.....	130
5.11 Inputs of Dry Deposition Modelling.....	130
Chapter 6: Results and Discussion of Air Dispersion Models	135
6.1 Emission Estimation	135
6.2 Meteorological and Terrain Data.....	138
6.3 LFM Process Plan.....	141
6.4 ADMS Modelling	144
Chapter 7: Conclusions and Further Work	167

7.1 Introduction.....	167
7.2 Review of the Thesis Objectives.....	167
7.3 Contribution to Knowledge.....	172
7.4 Limitations of the Research	173
7.5 Future Work and Recommendations.....	174
7.6 Conclusion	175
References.....	179
Appendices.....	224
Appendix 1. Mean values of (COD, pH, and MC) in different wells	224
Appendix 2. One-Way ANOVA test of (COD, pH, and MC) for all wells	225
Appendix 3. Multiple comparisons analysis between (COD, pH, and MC) of the four wells.....	226
Appendix 4. Correlation analysis between variables of (COD, pH, and MC) for all wells using Pearson’s correlation (2-tailed) analysis.....	227
Appendix 5. Multiple linear regression analysis between COD and (MC and pH) for all wells.....	228
Appendix 6. Correlation analysis between variables of the studied site (COD, MC, and pH) and the 7 previous landfill sites in the UK using Pearson’s correlation (2-tailed) analysis.....	229
Appendix 7. Descriptive statistics of heavy metals within the different wells.....	230
Appendix 8. One-Way ANOVA test of heavy metals for all wells	231

Appendix 9. Multiple comparisons analysis between heavy metal values of the four wells.....	232
Appendix 10. Correlation analysis between various heavy metals using Pearson’s correlation (2-tailed) analysis	233
Appendix 11. Correlation analysis between TOC and heavy metals using Pearson’s correlation (2-tailed) analysis	234
Appendix 12. Descriptive statistics of minerals within the four different wells	235
Appendix 13. One-Way ANOVA test of minerals for all wells	236

List of Figures

Figure 1. Basic overview of PhD thesis and objectives fulfilment.	6
Figure 2. Number of known landfill sites in UK and their regulatory status (Gregory, 2018).	12
Figure 3. Locations of historic landfill sites in England (Brand et al., 2018).	13
Figure 4. Different management stages throughout the life-cycle of a MSW landfills (Laner et al., 2012a).	15
Figure 5. (a) Image showing an aerial photograph of the study area marked in a red boundary. (b) Map of the site location illustrating the boundary of Norfolk and the study area marked with a red boundary, obtained using ArcMap 10.4.1.	25
Figure 6. Historic maps of 1880s and 1970s (Edina, 2022b).	26
Figure 7. (a) Geological Map of the study site location (Edina, 2019). (b) Map of the Norfolk site location illustrating the hydrogeological settings and the study area marked with a red boundary, obtained using ArcMap 10.4.1.	28
Figure 8. Generic block diagram of the conceptual site model. Produced by using Coreldraw Software.	31
Figure 9. Site-specific SPR conceptual model diagram of the studied area.	31
Figure 10. A land cover map showing the land uses within 2 km of the site (Edina, 2022a).	32
Figure 11. (a) Map showing the gas wells location plan and drill logs by Norfolk County Council. (b) Aerial photograph of the study area marked with a red boundary and sample locations illustrated in purple squares with corresponding well numbers.	34
Figure 12. Photographs of the recovered wastes from drilling (a) well 1901 (b) well 1904 (c) well 1906 (d) well 1907.	35
Figure 13. (a) Coning and quartering method was utilized to first split the sample into 4 segments, the diagonally opposite of which are rejected. Quartering was continued till a favourable sample volume is reached. (b) Riffle sample splitter was used to divide the samples into two equal parts. The process of dividing was repeated till a suitable sample size is achieved for analysis (Gerlach et al., 2002).	36
Figure 14. Chart illustrating the sample processing steps followed in the methodology.	37
Figure 15. Flowchart diagram of the laboratory sequence.	38
Figure 16. Mean of moisture content from the four wells.	41
Figure 17. Maps of climate variables in the UK for previous years (Met-Office, 2020).	42

Figure 18. (a) Mean of COD fixed to 150 mg/l as a maximum value with error bars: +/- 1 SE. (b) Mean of COD of both used range kits (0-150 & 0-1000 mg/l) in comparison with the generic acceptance criteria marked with a red line for the effluent discharge regulations.....	45
Figure 19. Mean of pH from the four wells.	48
Figure 20. Correlation graph between pH and COD using linear regression line.	49
Figure 21. Mean moisture content in the UK landfill sites, including the current site.	51
Figure 22. Mean COD in the UK landfill sites, including the current site.	52
Figure 23. Correlation graph between COD and landfill age using linear regression line.	52
Figure 24. Mean pH in the UK landfill sites, including the current site.	53
Figure 25. Particle size distribution cumulative passing curve for different sieve sizes of all wells.	55
Figure 26. Different size fractions of all wells. (a) well 1901 (b) well 1904 (c) well 1906 (d) well 1907.....	57
Figure 27. Heavy metals correlated using linear regression.	63
Figure 28. Heavy metals concentration with their different size fractions.	65
Figure 29. Comparison of heavy metal concentrations from landfill samples recovered from the four wells. The numbers above/below boxplots indicate which observation in the dataset (Table 11) is the outlier (numbers are arranged in descending order).	67
Figure 30. Boxplots of the contamination factor values of five heavy metals within the four wells.	74
Figure 31. Cancer risk (CR) values of heavy metals.	80
Figure 32. TOC values of different size fractions from wells 1901 and 1904.....	83
Figure 33. TOC and MC values of wells 1901 and 1904.	84
Figure 34. Correlation graph between TOC and various heavy metals using linear regression line.....	86
Figure 35. (a) Theoretical MSW landfill gas and leachate evolution (b) waste degradation stages (Brown et al., 2018).	88
Figure 36. Pie diagrams of minerals found in two different waste size fractions.....	95
Figure 37. Photos of selected mineral phases showing fiberglass particles in light blue colour adhered on the top of other particles using SEM-MLA analysis.....	104
Figure 38. Glass noodle and rod-like fibre particles of well 1907 in blue light colours.....	105
Figure 39. Photomicrographs displaying fine-grained and heterogeneously composed parts in intergrowth with ferroan clay in purple colour.	107

Figure 40. A simplified schematic representation of the input-output of the air dispersion model.....	118
Figure 41. Assumed plan of LFM phases.	127
Figure 42. Boxplots of the real-recorded wind speed data from 2016 to 2019.....	129
Figure 43. Boxplots of the real-recorded temperature data from 2016 to 2019.....	129
Figure 44. The ADMS interface.	130
Figure 45. The Source screen.....	131
Figure 46. Box and whisker plot showing the point source activities emission rates.....	137
Figure 47. Wind rose diagram of the study area.	140
Figure 48. Topography 3D view of the upper part of Norfolk showing the land height above sea level in m with a red circle showing the study area. Produced by using Mapper Software.	140
Figure 49. Flowsheet illustrating the LFM processes and defining volumetric throughput/number of loading frequencies/timeframe ranges for each unit operation with their respective emission rate.	143
Figure 50. Contour plots of each individual activity source of the 3 wind speed scenarios considering maximum and minimum emissions rate against the UK regulatory standard for PM10 24-hour mean stated in terms of percentile.	153
Figure 51. Contour plots of all five sources of activities of the 3 wind speed scenarios considering maximum and minimum emissions rate against the UK regulatory standards for PM10 24-hour mean stated in terms of percentile.	155
Figure 52. Correlation between the modelled percentiles concentration of three- and twelve-months meteorological data.	158

List of Tables

Table 1: Principal drivers for historic and current LFM activities globally (Ford et al., 2013).	9
Table 2: Receptor locations around the studied landfill.	29
Table 3: Conceptual site model of the studied area.	29
Table 4: Gas extraction well details for recovered waste samples.	33
Table 5: Mean samples of moisture content.	39
Table 6: Literature COD values compared to the present COD values.	46
Table 7: Characteristics of the previous UK studied landfill sites.	50
Table 8: Selected heavy metal concentrations of the four wells of various size fractions.	58
Table 9: Correlation analysis between waste size fractions and heavy metals.	63
Table 10: Descriptive statistics of heavy metals according to the generic Assessment Criteria of UK Soil Guideline Values (Defra and Agency, 2009).	69
Table 11: Permissible limit of heavy metal concentrations in soil (mg/kg) for different countries (Jani et al., 2016; Kamunda et al., 2016).	70
Table 12: Classification levels of geoaccumulation index (I_{geo}).	71
Table 13: Results of the geo-accumulation index of heavy metals.	72
Table 14: Classification levels of contamination factor (CF).	73
Table 15: Results of the contamination factor of the heavy metals.	74
Table 16: Potential human health non-carcinogenic risk assessment index (HQ) of heavy metals categorised by intended future land use.	77
Table 17: Overall potential for non-carcinogenic (HI) effects of heavy metals and the associated risk-level categories.	78
Table 18: TOC values of different waste size fractions.	82
Table 19: Literature TOC values from different landfills.	83
Table 20: Correlation analysis between waste size fractions and TOC values.	85
Table 21: Development of acetogenic to methanogenic leachate quality in a landfill (Brown et al., 2018).	89
Table 22: Modals mineralogy of samples 53-38 μm of well 1901.	96
Table 23: Modals mineralogy of samples 53-38 μm of well 1904.	97
Table 24: Modals mineralogy of samples 53-38 μm of well 1906.	98
Table 25: Modals mineralogy of samples 53-38 μm of well 1907.	99
Table 26: Modals mineralogy of samples < 38 μm of well 1901.	100

Table 27: Modals mineralogy of samples < 38 µm of well 1904.	101
Table 28: Modals mineralogy of samples < 38 µm of well 1906.	102
Table 29: Modals mineralogy of samples < 38 µm of well 1907.	103
Table 30: MLA particles size distribution.	108
Table 31: Stability categories in ADMS (CERC, 2016).	116
Table 32: Emission inventory and mathematical expressions for emission rate.	122
Table 33: Inputs of the dry deposition model.	131
Table 34: Descriptive statistics results of emission estimation of 9 different LFM activities.	136
Table 35: Results of the modelled 24-h/annual ground-level long-term average airborne highest concentrations in (ug/m ³) and their respective percentiles of 24-hour average using 3- and 12-months meteorological data.	159

Chapter 1: Introduction

1.1 Background

Landfill mining (LFM) involves the extraction of waste that has a potential economic value from a landfill site, usually following site closure (Frändegård et al., 2013; Krook et al., 2012; Somani et al., 2018; Zhou et al., 2015). It involves the excavation of waste from a landfill site following a prolonged period of closure, usually measured in decades, during which time the site has stopped receiving waste (Hogland et al., 2004; Hull et al., 2005; Krook et al., 2012; Rodriguez et al., 2018; Somani et al., 2018). LFM is not a new concept; many projects have been cited since the later 1940s and perhaps earlier, when unrecorded practices took place (Wagner and Raymond, 2015). It is a global practice that is carried out in many countries and in many parts of the world for various reasons (Krook et al., 2012; Somani et al., 2018). One primary opportunity associated with the increase in LFM from a global perspective is the recycling of resources and the rejuvenation of the development agenda (Somani et al., 2018; Van der Zee et al., 2004) to bring sites back into beneficial use. According to (Hogland et al., 2004), there are several fundamental reasons for LFM to be proposed at the feasibility stage. These include, but are not limited to, conserving available landfill void space for future use (prolonging landfill life), mitigating a pre-existing source of contamination or eliminating a potential source of contamination from a risk perspective, recovery of energy from excavated waste, reuse of recovered waste materials, and site redevelopment (Burlakovs et al., 2016; Jones et al., 2013; Maheshi, 2015). In the shorter-term, LFM may also be attractive dependent on local land value and opportunities for redevelopment. LFM serves multiple purposes aimed at protecting and preserving the environment, as well as producing energy (Wolfsberger et al., 2015). In turn, some landfills especially those created before the development of modern engineered containment systems, might have emitted hazardous substances to the environment,

which can be problematic if mined without proper management and treatment (Chandana et al., 2020; Qi et al., 2013).

LFM activities can create episodic fugitive dust/airborne particulate matter (PM) from physically extracting and processing waste through excavation, shredding, and screening/trommeling, with some of these particulates potentially adversely impacting on human health and the environment (Appleton et al., 2006; Ilse et al., 2018; Pastre et al., 2018; Smart-Ground, 2018). These emissions are of great importance because the presence of fine fractions within a landfill body is usually high, typically accounting for >50% of the total excavated MSW mass within the size range <10 mm to >4 mm (Datta et al., 2020; Kaartinen et al., 2013; Parrodi et al., 2018a; Quaghebeur et al., 2013; Wagland et al., 2019). Small fine fractions have close association with human health because particulates <3.5 µm penetrate the bronchioles, that can give rise to severe lung damage (Chu et al., 2008; Ghorbel et al., 2014; Pecorini and Iannelli, 2020; Wang et al., 2022a). Also, particularly potentially toxic elements usually accumulate in fine fractions of waste materials owing to its higher surface area (Hölzle, 2018; Wei et al., 2015) and can be transported over long distances in the atmosphere (Liu et al., 2023). Several studies have reported links between airborne PM and negative health outcomes, including morbidity and mortality due to cardiovascular and respiratory disorders (Burnett et al., 2014; Kloog et al., 2013; Tsiouri et al., 2015). In addition, methane, which may only be present in residual concentrations or localised hotspots, is a potent greenhouse gas produced by organic waste degradation and can pose a risk to local residents because of its flammability and explosivity (Chandana et al., 2020; Jacobs, 2008; Rong et al., 2017; Weng et al., 2015). Hence, these problems should be fully understood from a risk point of view for projects to be beneficial and cost-effective (Atkinson, 2010; Ziyang et al., 2015).

A critical review of studies on LFM revealed that research has primarily focused on material and energy recovery (Dino et al., 2018; Frändegård et al., 2013; Mehta et al., 2020; Ortner et

al., 2014; Pecorini and Iannelli, 2020). However, there is a fundamental lack of understanding of how these activities can affect the environment and human health (Frändegård et al., 2013; Krook et al., 2012; Nguyen et al., 2018; Ortner et al., 2014; Padoan et al., 2020). Therefore, this gap in research initiated this study to inform the potential impacts of LFM which is of value at the site-specific LFM feasibility stage. A sampling and analysis programme was applied to recovered waste samples from a typical ex-Local Authority operated and predominantly MSW UK closed landfill site. Physical, chemical, and biological properties of landfilled waste were characterised.

1.2 Aim and Objectives

The aim of this research is to determine the potential health and environmental impacts of landfill mining activities.

The overarching aim is underpinned by a series of specific objectives:

1. To identify the landfill pollutant linkages based on site specific conditions;
2. To characterize the landfill waste to determine the state of degradation and its relevant impact for determining the suitability for landfill mining;
3. To identify the components within the waste known for their established health impact based on chemical analysis;
4. To estimate the dust that can be airborne during landfill mining activities;
5. To model dust emissions impact of landfill mining activities on air quality; and
6. To quantify the risk compared to appropriate standards and legislation.

The following scientific hypotheses were formulated at the start of the PhD project:

“LFM activities can pose potential human health and environmental impact.”

“Experimental tests would enable the assessment of the potential health and environmental risk associated with LFM activities.”

Following the achievement of a developed method for health and environmental impact assessment of LFM based on the application of laboratory tests, additional work was carried out and thus the following hypothesis was formulated:

“The use of air dispersion modelling system would allow for air quality assessment of LFM activities.”

As mentioned earlier, the focus of previous research has been on aspects of energy and resource recovery with a knowledge gap being the potential health and environmental impacts associated with LFM activities. Consequently, this thesis shows a number of important scientific developments in the assessment approach used for determining potential risks to human health and the environment from LFM activities.

1.3 Thesis Overview

The format in which this thesis is presented follows that the experimental Chapter contains a method, result and discussion section of each parameter characterised. In contrast, the technical part of the thesis which involves the air dispersion modelling of dust is divided into two Chapters regarding methods, results, and discussion. Portions of this thesis have been published or accepted for publication in peer-reviewed journals and conference proceedings. In addition, a part of thesis is currently being prepared for submission and publication. These are the following:

Zari M, Smith R, Wright C, Ferrari R. Health and environmental impact assessment of landfill mining activities: A case study in Norfolk, UK. *Heliyon* 2022: e11594. (Published).

Zari M, Smith R, Ferrari R. Evaluation of dust emission rate of landfill mining activities. Proceedings Sardinia 2023, 19th international symposium on waste management, resource recovery and sustainable landfilling, S. Margherita di Pula, Cagliari, Italy, CISA. (Accepted).

Zari M, Smith R, Ferrari R. Evaluation of dust emission rate from landfill mining activities. *Detritus* 2023. Invited for publication. (Accepted).

Zari M, Smith R, Ferrari R. Air quality assessment of landfill mining activities. (In preparation).

The structure of this thesis is shown in Figure 1.

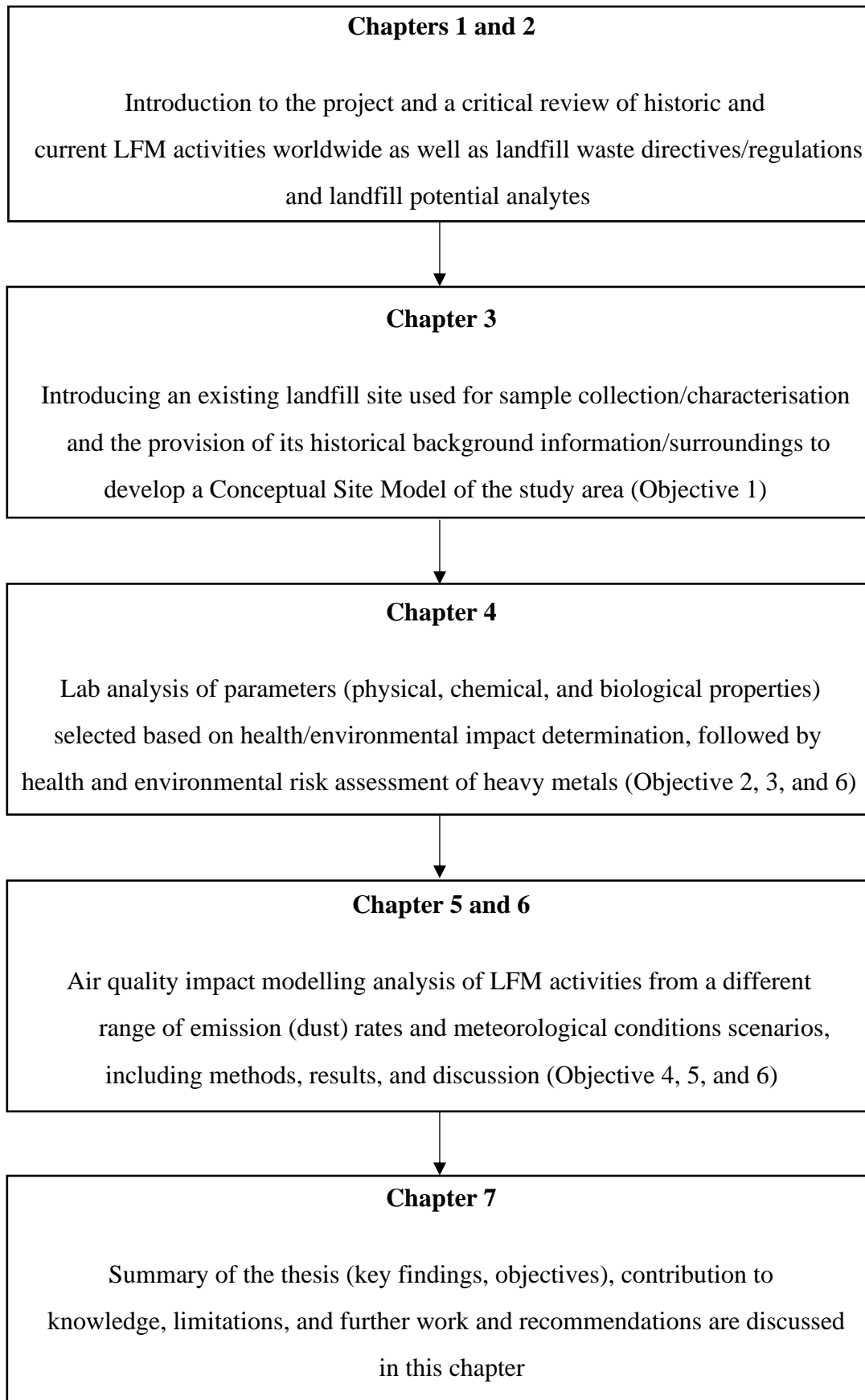


Figure 1. Basic overview of PhD thesis and objectives fulfilment.

Chapter 2: Literature Review

2.1 Overview of Landfill Mining Concepts

"Landfill mining" is defined by (Krook et al., 2012) as the process of recovering materials or other solid natural resources from landfill wastes that have previously been buried in the ground for disposal. However, traditional LFM activities were typically restricted to methane extraction, partial valuable metal recovery, and/or land reclamation (Jones et al., 2013; Prechthai et al., 2008). As corroborated by (Krook et al., 2012), *“so far, landfill mining has primarily been seen as a way to solve traditional management issues related to landfills such as lack of landfill space and local pollution concerns. Although most initiatives have involved some recovery of deposited resources, mainly cover soil and in some cases waste fuel, recycling efforts have often been largely secondary. Typically, simple soil excavation and screening equipment have therefore been applied, often demonstrating moderate performance in obtaining marketable recyclables”*. Scientists have developed a comprehensive concept known as Enhanced landfill mining (ELFM) in response to the need for a framework to solve LFM difficulties, technical advancement, and additional research on this topic (Parrodi et al., 2019a; Parrodi et al., 2019c). ELFM can be defined as the process of excavating waste materials from landfills that has previously been disposed of and integrating valorisation of historic and/or future waste streams as both materials (waste-to-material) and energy (waste-to-energy) (Jones et al., 2013). It aims to utilise cutting-edge transformational technology while adhering to the strictest social and ecological criteria (Danthurebandara et al., 2015; Jones et al., 2013; Lucas et al., 2019b). ELFM is distinct from traditional landfill mining in that it strives for integrated material and energy recovery optimization, reduces the end residue volume to almost zero, and employs a number of methods to reduce CO₂ emissions (Danthurebandara, 2015). ELFM is still a developing field with the utility of mined materials in many applications (Chandana et al., 2021; Parrodi et al., 2019b; Somani et al., 2018).

2.2 International LFM Project

LFM was first introduced in Israel in 1953 as a means of obtaining manure for farming (Savage et al., 1993; Somani et al., 2018). This project remained the only recorded investigation of LFM until the early 1980s (Singh and Chandel, 2020). By the 1990s, this practice had become more popular since it was becoming increasingly difficult with modern regulation to obtain regulatory approvals for new landfills, thus, the excavation of old landfills was adopted to create new void space by extending the life of existing landfills (Dickinson, 1995). However, by the mid-1990s, the popularity of LFM had dropped especially due to the introduction of superior modern engineering methods and standards for waste disposal in many localities (Dhar, 2015). The popularity of the practice also became diminished by the fact that the marketable recyclables from these landfills were not as valuable as first anticipated (Krogmann and Qu, 1997). In Europe and Asia, urban development was impeded due to the increasing need for removal of waste and treatment of old landfills, leading to an increase in LFM activities (Cossu et al., 1996). Owing to the expansion of big cities particularly in densely inhabited areas, opening new landfills has become a problem due to shortage of land space (Hogland et al., 2014; Ortner et al., 2014; Van Passel et al., 2013). Thus, LFM has become an innovative solution in some countries (Burlakovs et al., 2016; Burlakovs et al., 2017; Singh and Chandel, 2020).

A summary of reported LFM projects globally in the literature with their different principal drivers is shown in Table 1, which identifies 57 projects. Since the first project reported in 1953, the adoption of LFM activities has not been plentiful. Table 1 shows that the USA has undertaken most of the LFM projects of any individual country. The UK has six documented LFM projects to date. Improvement of landfill engineering was the main driver for three of the projects to meet regulatory requirements, whereas the other three were driven by site redevelopment.

Table 1: Principal drivers for historic and current LFM activities globally (Ford et al., 2013).

Principal project driver	UK no. projects	Europe excl. UK no. projects	North America (no. projects)	Asia no. projects	Total projects
Unknown		12	4	2	18
Recovery of landfill capacity		3	4		7
Site redevelopment	3	2		1	6
Pollution mitigation		2	5	1	8
Landfill engineering improvement	3	1	2	1	7
Resource recovery		3	2	6	11
Overall projects	6	23 Projects across 8 countries	17 projects. 1 in Canada and 16 in the USA	11 projects within 7 countries	57

Whilst there were various drivers that lead to these LFM projects, some barriers have been identified. The challenge of assessing the resource and technical potential is the most encountered barrier in LFM owing to the heterogeneity of waste deposited in landfill sites (Frändegård et al., 2013; Johansson, 2013; Somani et al., 2018). Additionally, there has often been local opposition (usually by residents) to LFM because of drilling activities (Smart-Ground, 2018) and poor public perception (Einhäupl et al., 2021), perhaps as a result of lack of knowledge. Furthermore, at present, the current policy in most countries considers landfilling as an eternal storage of waste, which is on the contrary to the current LFM vision of landfills as a resource reservoir for future valorisation (Jones et al., 2013; Ziyang et al., 2015) addressed as ELM (Van Passel et al., 2013). Therefore, the same waste can be taxed twice due to the back re-filling into landfills (Smart-Ground, 2018). Moreover, LFM activities can also give rise to short-term local pollution in spite of their broader environmental benefits (Einhäupl et al., 2018).

2.3 Europe Landfill Population

There are around 500,000 old landfill sites in Europe, some of which are closed with others still in operation (Damigos et al., 2016). Among EU member states, the UK, Finland, and Greece are some of the most reliant countries on direct landfilling (Laner et al., 2012a). Many of these sites are situated in semi-urban environments adjacent to water bodies or residential areas, rising concern to many experts in the landfill sector (Brand et al., 2018; Maheshi, 2015; Nguyen et al., 2018). As a consequence of EU's Landfill and Waste Directives, some of these sites still in action are sanitary and equipped with state-of-the-art environmental protection and methane-collection systems. Nevertheless, there is still a significant number of these sites lacking modern environmental technology "non-sanitary", which estimated to be 90% of these landfill sites that predate the EU's Landfill and Waste Directives in 1999 (Nguyen et al., 2018; Smart-Ground, 2018). These sites are of major concern to the whole ecosystem (water, health, air, soil, and land) (Chandana et al., 2020). These landfill sites posing environmental problems will most likely have to be mined (Jones et al., 2013) to manage waste legacy contained with as secondary raw materials (Chandana et al., 2020; Machiels et al., 2017) that can become part of the circular economy (Canopoli et al., 2020), as well as to reduce cost and time in aftercare long-term monitoring (Ortner et al., 2014). Other reasons coupled with recovering untapped valuable materials include mitigation of potential contaminant sources to avoid environmental and health problems and at the same time allowing for temporary storage place (Jones et al., 2013; Van Passel et al., 2013).

These sites constitute very high potential risk to the human health and the environment due to the uncertainty about landfill biodegradation completion (Nguyen et al., 2018; Savage et al., 1993). Harm may also be caused by dispersing odour, noise, dust, and contaminants during LFM operations, harming the ecosystem (Einhäupl et al., 2018). Local community members of Belgium stated that *"Poor execution could lead to bigger environmental problems than*

before: These are huge risks, also on the environmental level the risk of creating a bigger environmental problem than before is still there” (Einhäupl et al., 2018).

2.4 UK Landfill Population

There are over 21,000 known landfills in the UK of which 90% have been closed before 1996 (Gregory, 2018; Wagland et al., 2019). The timing is important as the EU Landfill Directive (Council, 1999) was implemented in 1999 which resulted in the reclassification of landfills and changes to technical requirements. Thus, many UK landfill sites, that were regulated under different legislation, were closed at this time.

Approximately 13,429 of known UK landfill sites are under unknown ownership/management and about 6,000 landfills are unpermitted sites under known ownership (Gregory, 2018). On the other hand, only 1,900 landfill sites are permitted under Environmental Permitting Regulations and 94% of them under private management. A summary of these landfill sites is illustrated in Figure 2. Some of the unknown ownership landfill sites may fall under the provisions of contaminated land legislation and as orphan sites become the responsibility of government if they are identified to be causing a risk to the environment or human health. As it is shown in Figure 2, most of the landfill sites in the UK are not known by the competent authorities, and most of these sites are historic landfills (Figure 3).

These sites might be heavily contaminated and contain valuable resources at the same time (Hogland et al., 2014; Hogland et al., 2004). For example, an investigation of two landfills in Essex, UK, focusing on climate impacts and potential sea level changes, has found that contamination levels in a range of solid waste materials were above sediment quality standards, indicating that the erosion of historic landfills and the incorporation of waste into coastal sediments could have a negative impact on the flora and fauna (Brand, 2017). In turn, a recent study from Cranfield University suggests that UK landfill sites could contain up to £90m of valuable metals (Allen, 2015) including rare and precious metals; the challenge is how to

recover and extract them. Another UK study has investigated four landfill sites and results have revealed that copper and aluminium present within these sites has a value approaching £400m (Gutiérrez-Gutiérrez et al., 2015). These landfills cannot be mined for remediation of contaminated land or resource recovery unless the ownership or management responsible for these landfill sites is known.

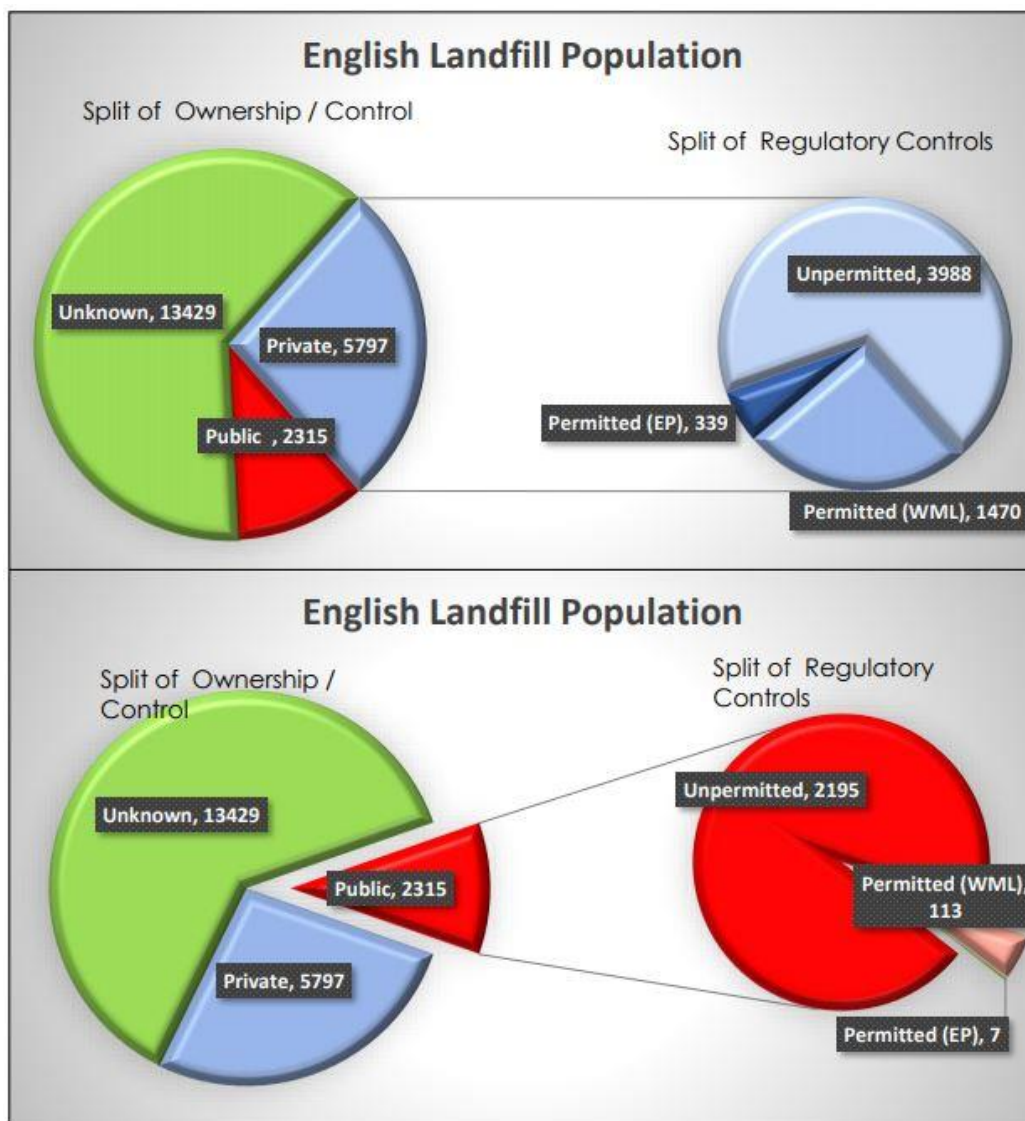


Figure 2. Number of known landfill sites in UK and their regulatory status (Gregory, 2018).

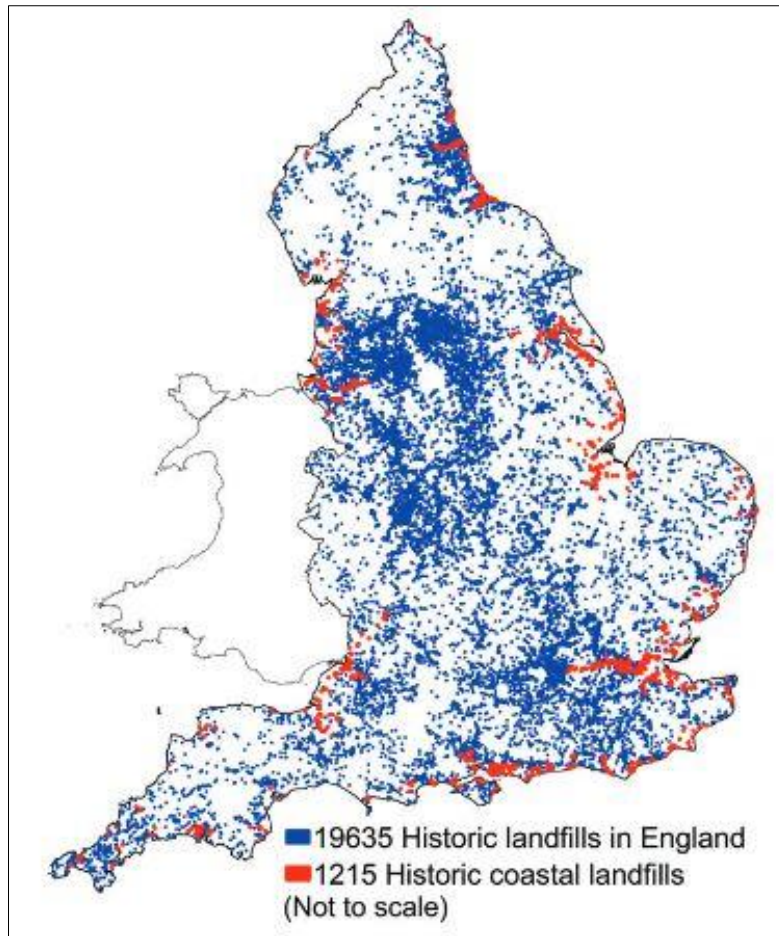


Figure 3. Locations of historic landfill sites in England (Brand et al., 2018).

2.5 Case Studies

Case studies were identified from several landfills that represent different eras of waste management practices and waste material composition. A case study in Halbenrain, Austria aimed at developing a new ELFM scenario for the combined recovery of resources and remediation strategies. The case study emphasized the unsuitability of LFM activities in areas that have hazardous materials and contaminated soils which severely lowers the potential of landfills as feasible resources (López et al., 2018). The implementation of the strategy can reduce the expected remediation costs and aid in the reclamation of valuable land while at the same time reveal vital resources. Likewise, the remediation strategies can be used to prevent any harm in the long-term.

A Swedish case study demonstrated the extraction of materials and energy resources derived from “high risk” landfills. The research revealed that the remediation of the landfills could lead to a reduction estimated at 30 million tonnes of greenhouse gas emissions (Frändegård et al., 2013). Similar research findings have stated that LFM activities for resource recovery present immense potential for mitigating the global climate impact (Jones et al., 2013). The case study also recommended that extensive research should be executed in the future to assess the various environmental impacts ranging from human toxicity to air pollution that can be eradicated from LFM initiatives (Frändegård et al., 2013).

Another notable case study was conducted at Kuopio Landfill, Finland from 2001 to 2011. The landfill was found to hold 38-54 % of fine fractions, which contained numerous organic matter amounts, nutrients, and soluble organic compounds (Kaartinen et al., 2013). The organic matter and biomethane were identified to be greater in the top stratum of the new landfill (fresher waste), whereas the bottom layer of the landfill was older and more decomposed material. The case study emphasized the importance of requiring an appropriate exploration phase in the LFM projects aimed at valid full-scale planning procedures for the recovery of materials. The exploratory phase includes the site-specific assessment of landfill waste composition for recoverable waste fractions (metals, waste fuel, and possibly soil) and for proper treatment processes using test excavations or drilling sampling techniques.

2.6 Concepts for Aftercare and Completion

“Landfills are considered as places where the life cycle of products ends and materials have been disposed of forever” (Burlakovs et al., 2013). This consideration had been in practice until the newer ELFM concept introduced by (Jones et al., 2013). Prior to the installation of a final cover also referred as containment system/capping/soil cover, it is usually mandatory under different legislation that various landfill management phases are fulfilled, such as enhanced emission reduction from landfill operating sites (Dijkstra et al., 2013). The illustrative Figure

4 below shows the chronological process of landfill management phases. The post-operational care period starts when a landfill reaches its end of accepting waste for disposal, while the aftercare period starts when the landfill has reached the ultimate layout of capping to effectively contain emissions and prevent further leachate generation as much as possible.

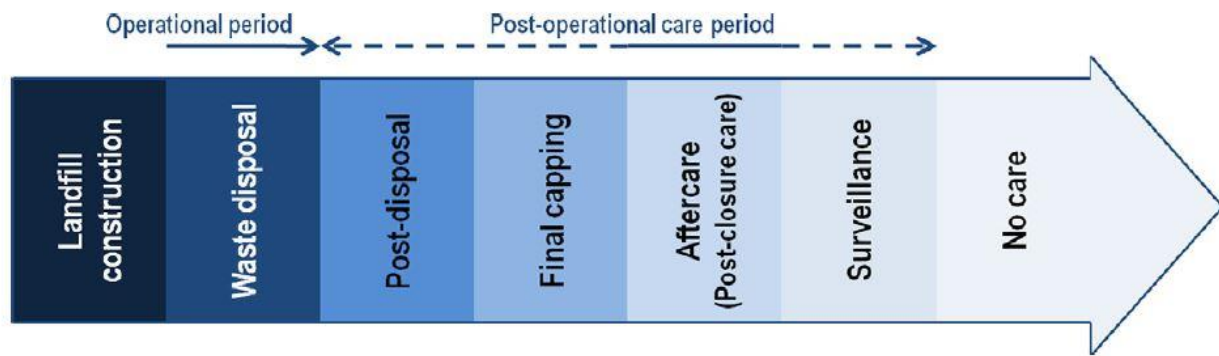


Figure 4. Different management stages throughout the life-cycle of a MSW landfills (Laner et al., 2012a).

The aftercare completion differs from site to site depending on the quality and quantity of materials being disposed (Bour et al., 2005). In addition, the climatic conditions in the surrounding area greatly affect the type of landfill management carried out (Mathlener et al., 2006). The management process of closed landfills (also referred to as post-closure period), involves three steps (Bour et al., 2005; Brand et al., 2016). These stages include the monitoring of the potential emissions and groundwater, the treatment of the potential emissions such as leachate treatment, maintenance of a landfill cover, and leachate/gas collections of landfill sites. Aftercare period ends when the landfill is not likely to pose a threat to human health and the environment (Laner et al., 2012b). In other words, aftercare completion can be defined as the point at which the competent authorities are satisfied with the end of regulated aftercare, since the landfill is not likely to constitute a threat to human health and the environment in the absence of aftercare (Ford et al., 2013).

LFM activities commence after the aftercare phase because, at this point, the landfill potential gaseous emissions are not as concentrated as the initial stages within a few decades (Bučinskas et al., 2018; Ziyang et al., 2015). Nevertheless, LFM practices might need to be carried out prior to this stage due to some improvements or maintenance of landfill engineering systems to meet the necessary regulatory requirements or to remediate the landfill site due to unacceptable risks (Ehrig and Krümpelbeck, 2001). Moreover, LFM activities as said “*are focused on older landfill as the recovery potential is highest due to the lack of recycling schemes in the past*” (Jacobs, 2008); in other words, there has increasingly been a tendency in modern times to segregate and recover wastes prior to disposal of residual materials (Singh and Chandel, 2020). Recent research has shown that landfill management plays an important role in significant issues of contemporary solid waste management, including mitigation of potential global warming, LFM, and land reclamation (Weng et al., 2015).

For closed landfills with building and construction waste (C&D), the aftercare completion management is much shorter and environmentally acceptable after a few years (Laner, 2011). According to the conclusion stated by (Laner et al., 2012b), there is a low environmental risk associated with building and construction waste because of the low emissions potential of the deposited waste. In the case of a large municipal solid waste, the post-closure care period is estimated to last a century or more (Mathlener et al., 2006). The aftercare period of a small municipal solid waste, with annual precipitation of around 2,000 millimetres per year, might be terminated within the first few decades (Mathlener et al., 2006), where moisture content is more optimum. However, the aftercare of municipal solid waste landfills may require several decades or possibly stretch over a number of centuries, which is not compatible with the aim of aftercare completion of one generation (Heyer et al., 2005) in terms of inter-generational equity. The aftercare (post-closure) minimum monitoring period identified for municipal solid waste landfills in Europe is 30 years and a financial provision should be assured for this period

unless the regulatory agency shortens or extends this period on a site-by-site basis (Laner et al., 2012a; Weng et al., 2015).

In England and Wales particularly, a combined target value and risk assessment approach have to be met in order to release a landfill owner from aftercare obligations termed ‘permit surrender’, which requires concentrations of CH₄ and CO₂, for example, to be similar to the established background levels in the surrounding environment (Environment Agency, 2010). However, to support such aftercare management measures, large financial aids are required. Thus, central governments may be responsible for the aftercare maintenance of closed landfills rather than local municipalities since the budgets for local municipalities may be inadequate (Weng et al., 2013).

Due to the increased rigid regulations set by the European Community Directive 1999 and the later European Waste Directive 2008 in the landfill sector (Council, 1999; Directive, 2008), many landfill sites have been closed based on the failure to comply with the enforceable regulations, and the overall cost of landfilling has increased considerably that owners of landfills are seeking alternative business opportunities (Laner, 2011; Ortner et al., 2014; Van der Zee et al., 2004). In this regard, what are predominantly MSW landfills have become the focus of many studies in regard to aftercare and long-term management schemes within the last few decades (Laner et al., 2012a).

Additionally, as a result of the increase in stringent environmental regulations and the cost, there was a reduction in the number of new landfills, including municipal solid waste landfills (Laner, 2011; Ortner et al., 2014; Van der Zee et al., 2004). For instance, there was a significant reduction of the municipal solid waste landfills from 6,300 in the 1990s to about 1,800 in the 2000s in the US, Washington, DC (Morris et al., 2012). A similar case is evidenced in Germany where the number of landfills decreased from 550 in the 1990s to around 320 in the 2000s

(Laner et al., 2012a). Moreover, there was a substantial decrease of the MSW landfills from 2000 in 2004 to about 465 landfills remained active in 2009 in the UK with a Landfill Directive 1999 compliant permit (Environment Agency, 2010; García et al., 2016; Laner et al., 2012a; Morris et al., 2012). Some industry insiders believe that LFM activities will be a part of the waste management strategy in the UK due to the rigid restrictions on opening new landfill sites (Roberts, 2013). In addition to circular economy principles, during the second ELFM Seminar in the European Parliament (Commission, 2018), the vision of dynamic landfill management was introduced. It included a multidisciplinary approach to landfill management, resources, and land recovery as well as pollution control as regards the European policy and legislation (Canopoli et al., 2020; Hölzle et al., 2022).

According to (Stegmann et al., 2003), the biodegradation processes are completed to a great extent at the end of the post-closure care period and may not be reactivated in the future due to the changing conditions within the landfill site (Bour et al., 2005; Stegmann et al., 2003). Because stabilisation of organic wastes is significant prior to LFM, in-situ aeration and leachate recirculation into landfill waste bodies have become the major strategies for the achievement of low potential emissions and odours (Hupe et al., 2003; Stegmann et al., 2003). In-situ aeration has emerged as a promising strategy to accelerate the biodegradation processes within the landfill waste, improve leachate quality, and complete or accelerate the main landfill settlements (Heyer et al., 2005; Raga and Cossu, 2010). Furthermore, in situ aeration strategy was suggested to be a landfill pre-treatment prior to LFM activities (Raga and Cossu, 2010; Ziyang et al., 2015).

There are various studies carried out on the municipal solid waste landfills to investigate the potential emissions and the results highlighted their perceived long-term effects on the environment (Brand et al., 2016). Therefore, it is mandatory to develop a long-term

management concept for closed landfill sites for the prevention of negative effects on human health and the environment (Laner et al., 2012a; Morris and Barlaz, 2011; Ziyang et al., 2015).

2.7 Potential Analytes in MSW Landfills

Landfills are considered an environmental hazard due to landfill gas and leachate generation (Burlakovs et al., 2017; Omar and Rohani, 2015; Singh and Chandel, 2020; Ziyang et al., 2015). A landfill site consists of many components, but the main emission from the site is landfill gas (Macklin et al., 2011). When the waste products are deposited in a landfill, the biodegradable fractions start to decompose through the aerobic and anaerobic processes, which undergo complex physical, chemical, and biological changes and as a result, release landfill gas and leachate (Danthurebandara, 2015; Zhao et al., 2007; Ziyang et al., 2015). Landfill gas consists of various gases based on the type of waste. Bulk gases include methane, carbon dioxide and trace components of organic and vapour found in the proportion of 65%, 35%, and 1% respectively (Parker et al., 2002). Accumulation of methane at landfills is the primary reason for explosions due to its flammability (Hogland, 2002; Weng et al., 2015). Hence, methane emission collection and reduction are important in terms of public health as prevention of fires (caused by waste streams or often over extraction of landfill gas and pulling in oxygen) and for global warming mitigation (Frändegård et al., 2013; Weng et al., 2015), as methane is converted to carbon dioxide when oxidized in the presence of landfill cover materials (Laner et al., 2016). Varying landfill gas composition is also attributed to evaporation of some volatile substances and exchange of gaseous compounds between the atmosphere and landfill (Fisher et al., 1999). Volatile organic compounds (VOC's) and hydrogen sulphide (H₂S) are also potential gases that can be emitted into the air during the operation of LFM and should not be neglected (Ziyang et al., 2015). These landfill gases can have significant environmental and health impact, such as the explosive potential of methane and the poisonous effects of VOC's and H₂S (Smart-Ground, 2018).

In addition, according to (Jia et al., 2013), the greatest problem linked to landfill sites is the generation of fine dust since fine fractions of soil-like materials within the size range of <10 mm to >4 mm can account for up to 40–80 wt.% of the total waste excavated (Chandana et al., 2020; Datta et al., 2020; Hölzle, 2019; Jani et al., 2016; Kaartinen et al., 2013; Masi et al., 2014; Parrodi et al., 2018a; Quaghebeur et al., 2013; Somani et al., 2018; Somani et al., 2019). This was evidenced by a recent investigation of nine landfill sites in the UK that showed that fine soil-like material accounted for 30–74% (w/w) of the total waste excavated (Parrodi et al., 2018a; Wagland et al., 2019). PM in the form of dust released from landfill sites may also consist of heavy metals like lead, cobalt, arsenic, manganese, cadmium, chromium, and copper (Hogland et al., 2014; Rodriguez et al., 2018; Zilenina et al., 2017). Some researchers believe that heavy metals contamination can represent up to 51% in landfills. This high weighting factor underlies the potential risk that heavy metals contamination can cause to the environment (Abu-Daabes et al., 2013). Additionally, the dust from landfill wastes can be composed of fungi, bacteria and microbial toxins in the form of bioaerosols (Kim et al., 2018; Macklin et al., 2011; Ziyang et al., 2015).

Dust particles from landfills are likely to be airborne from activities, such as vehicle movements on site, handling, storage and waste processing activities during LFM (Ilse et al., 2018), and the rate of travelling particles is influenced by wind speed, particle size fractions, and the topography (Jia et al., 2013; Leelőssy et al., 2014; Wu et al., 2018). Smaller particles are blown the farthest (Mariraj Mohan, 2016), whereas intermediate size ranging from 10 to 30 µm are likely to travel up to 200–500 m (Sairanen and Pursio, 2020).

Because landfilled waste is heterogeneous comprising materials such as decomposed organics, mineral waste, asbestos and heavy metals, the dust may cause significant environmental and health problems (Bastian et al., 2018; Mathew, 2017). These emissions in large amounts have considerable health effects on the workers and people living nearby (Douglas et al., 2017;

Hogland et al., 2014; Kim et al., 2015). These compounds are most likely to be released during landfill excavation, and there is a potential risk that these chemicals will drift into natural waters in the landfill's vicinity or into the air (Smart-Ground, 2018; Ziyang et al., 2015).

Historic landfills that lack modern environmental standards are the primary sources of long-term methane and carbon dioxide emissions which contribute to global warming and acidification (Danthurebandara et al., 2015), and requiring extensive aftercare periods (Laner et al., 2016). They are also the main source of groundwater pollution owing to the leaching of toxic substances (Hogland et al., 2014; Van Passel et al., 2013). Countries with good environmental performance show that local authorities favour closure of these landfills to minimize risks and build new sanitary landfills with modern engineering systems (Burlakovs et al., 2017).

According to (Ford et al., 2013), a waste management plan to develop appropriate human health and environmental risk assessments is needed prior to LFM operations primarily to consider the potential of uncovering hazardous wastes during LFM (Dhar, 2015). Furthermore, according to (Krook et al., 2012), the reviewed literature lacks information on pollutant emissions that occur after the landfill has been excavated. Hence, understanding the key elements affecting the performance of LFM from health and environmental perspective is a significant aspect to move ELM from the conceptual to the practical stage.

2.8 Conclusion

The literature review has revealed significant gaps in understanding the health and environmental impacts of landfill mining (LFM) activities. Previous studies have recommended the need for comprehensive risk assessments, considering appropriate human health risk assessments (Ford et al., 2013), emissions implications of LFM activities (Einhäupl et al., 2018; Krook et al., 2012; Krook et al., 2019), and uncertainties surrounding landfill

biodegradation completion (Nguyen et al., 2018). Additionally, it has been highlighted that understanding potential risks from an occupational health standpoint is crucial (Márquez et al., 2019). Environmental impacts related to LFM activities are poorly quantified, potentially leading to significant underestimation of adverse effects on health and the environment (Nguyen et al., 2018; Sauve and Van Acker, 2018). Consequently, there is a pressing need to establish a methodology for assessing health and environmental impacts associated with LFM activities. This research intends to address these gaps by investigating the potential health and environmental risks of LFM activities, considering physical, chemical, and biological properties of the landfill waste in the study area. By identifying pollutant linkages based on site-specific conditions, this study aims to gain insights into how different landfill characteristics and conditions can influence pollutant migration and dispersion, ultimately impacting human health and the environment. Characterizing the landfill waste and assessing its state of degradation will inform decisions on the suitability of landfill mining at various sites. The research will also identify specific hazardous components within the waste, contributing to the understanding of potential health risks associated with exposure during landfill mining operations. Through modelling dust emissions impact on air quality, the study will provide valuable information about how LFM activities may affect the surrounding environment. By quantifying risks and comparing them to relevant standards and legislation, this research aims to inform decision-making and policy formulation related to landfill mining practices. In conclusion, this research aims to fill the existing knowledge gaps surrounding LFM activities and their potential impacts on health and the environment. By investigating the specific aims and objectives outlined in 1.2, the research will contribute to comprehensive risk assessments, aid in the formulation of appropriate regulations, and promote sustainable waste management practices that prioritize human health and environmental protection.

Chapter 3: Site Sampling and Material Characterisation

3.1 Site Location and History

The study site is located in Norfolk, eastern England. The area where the site is situated called Docking Common, and named by Norfolk County Council as Landfill Docking number 1 and 2. Both landfill phases were operated and are now managed by Norfolk County Council. Specifically, Landfill Docking 1 is the area considered in this study (Figure 5 a and b). The site grid reference for the centre of the site is TF790356, easting 579041, northing 335638 and the nearest postcode is PE31 8NN. The site was operational from 1978 to 1986, is approximately 10 m deep, and has surface area of 3.12 hectares (approximately 7.71 acres). The site selection for this study was made based on it being representative of the many ex-Local Authority sites that were operated on a dilute and disperse or natural attenuation basis in contrast to modern engineered landfills that have a basal liner. The site is a typical representative of hundreds of landfills of this type that remain as historic deposits in the UK, filled during the 1970s, 1980s, and the early 1990s. Such sites predominantly accepted MSW with commercial and industrial waste, and it was operated and regulated on a co-disposal basis under the Control of Pollution Act (1974), from the first days of waste regulation. Thus, the landfill consists of a complex mixture of organic and inorganic wastes. The site used to be a historical mineral working site, a sand and gravel pit, which was subsequently utilised as a local authority landfill by Norfolk County Council (Figure 6). Norfolk County Council records reveal that there were significant amounts of bulky scrap and car bodies disposed of in the site. Records also indicated that there used to be issues with vermin at the site, which emphasises the presence of heavily putrescible waste. According to Kings Lynn and West Norfolk Borough Council (Grimmer, 2018), there was anecdotal evidence, indicating that improper waste disposal had taken place at Docking I and Docking II out of hours from the landfill site operation.

The present site use encompasses an open field which can be accessed by a road on the southern western boundary of the site along the B1454. To the south, there are industrial areas and beyond that are residential properties. The site consists of a grassy area with a small dome in the centre. Throughout the site's central area, there were several gas monitoring installations. To the north-east of the site, is arable farmland. A residential property and an industrial unit are located to the south-east of the site. Woodland is located to the south-west and west of the B1454 (Fakenham Road).

(a)



(b)

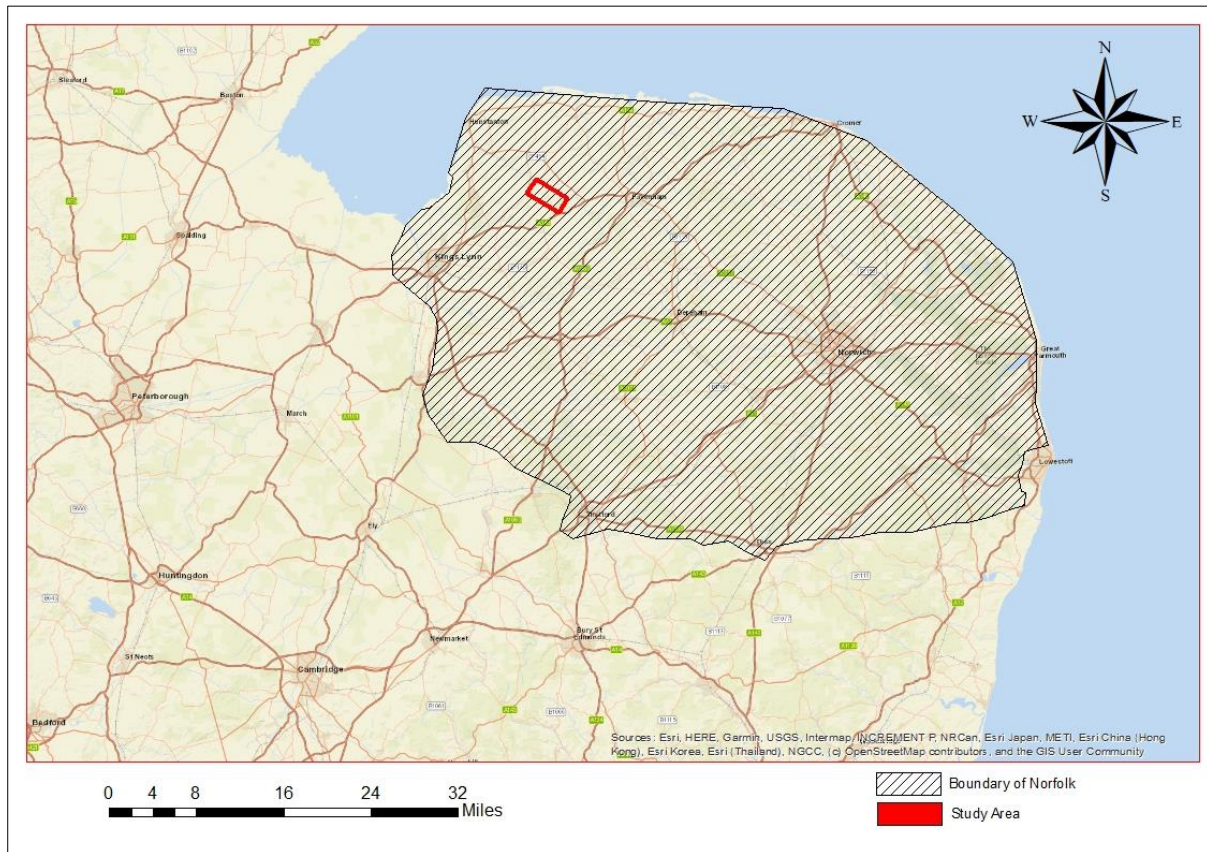


Figure 5. (a) Image showing an aerial photograph of the study area marked in a red boundary. (b) Map of the site location illustrating the boundary of Norfolk and the study area marked with a red boundary, obtained using ArcMap 10.4.1.

The landfill is unlined, and an engineered geo-synthetic clay liner cap was installed in 1998. According to Kings Lynn and West Norfolk Borough Council of (Grimmer, 2018), the site is situated above a main aquifer and there was an identified risk of leachate getting down to groundwater prior to capping at Docking 2. There is a history of landfill gas production and control with intermittent venting and forced gas extraction to atmosphere through a flare stack; a practice no longer permissible due to local air quality and global atmosphere impacts. Additionally, more recent small-scale gas extraction has been via two micro turbines located at the adjacent Docking 2 landfill. The highest level of methane production was recorded in April 1998 with 82% being recorded. There are known ‘hotspots’ of gas production within the waste that were evident as noticeable odour releases during the drilling of wells 1906 and 1907

from which waste samples were recovered during this study. Methane gas has been detected at up to 20% v/v (4.5%) by May 2012 suggesting that the gas source term is declining. There is no evidence of leachate at Docking 1 since the site is on sand and is not engineered at the base; therefore Docking 1 is designated as a typical natural attenuation (dilute and disperse) landfill site, such as processes include sorption (Allen, 2001). It is not known to be impacting on groundwater.

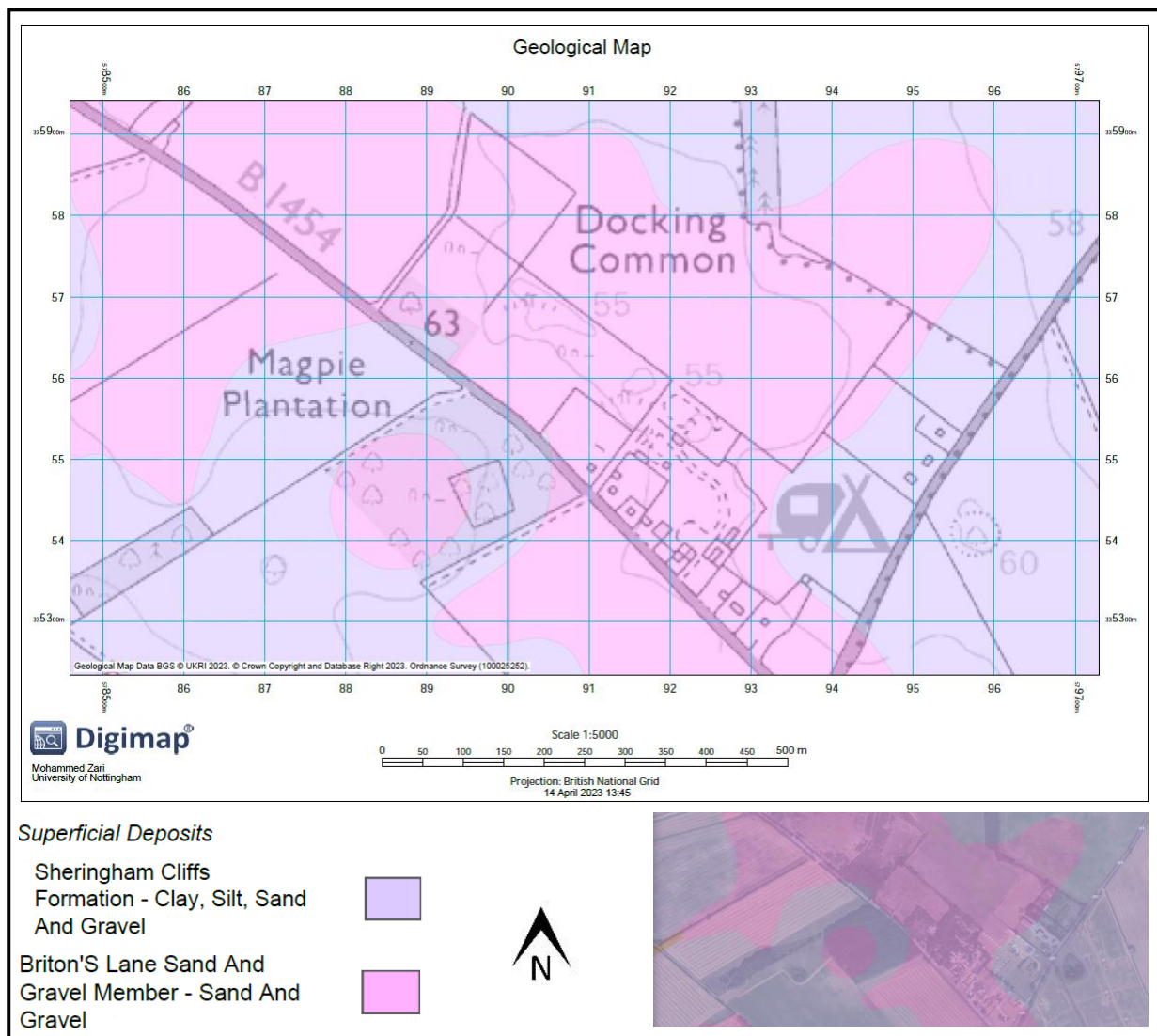


Figure 6. Historic maps of 1880s and 1970s (Edina, 2022b).

3.2 Geology and Hydrogeology

The bedrock geology of the study area is the Lewes Nodular Chalk Formation, Culver Chalk Formation, Newhaven Chalk Formation, and Seaford Chalk Formation. According to the British Geological Survey (BGS), the superficial deposits are recorded as Briton's Lane Sand and Gravel Member - Sand and Gravel (Figure 7 a). The site is classified as a principal aquifer (highly productive aquifer) (Figure 7 b). However, it is not situated within a Source Protection Zone (Grimmer, 2018).

(a)



(b)

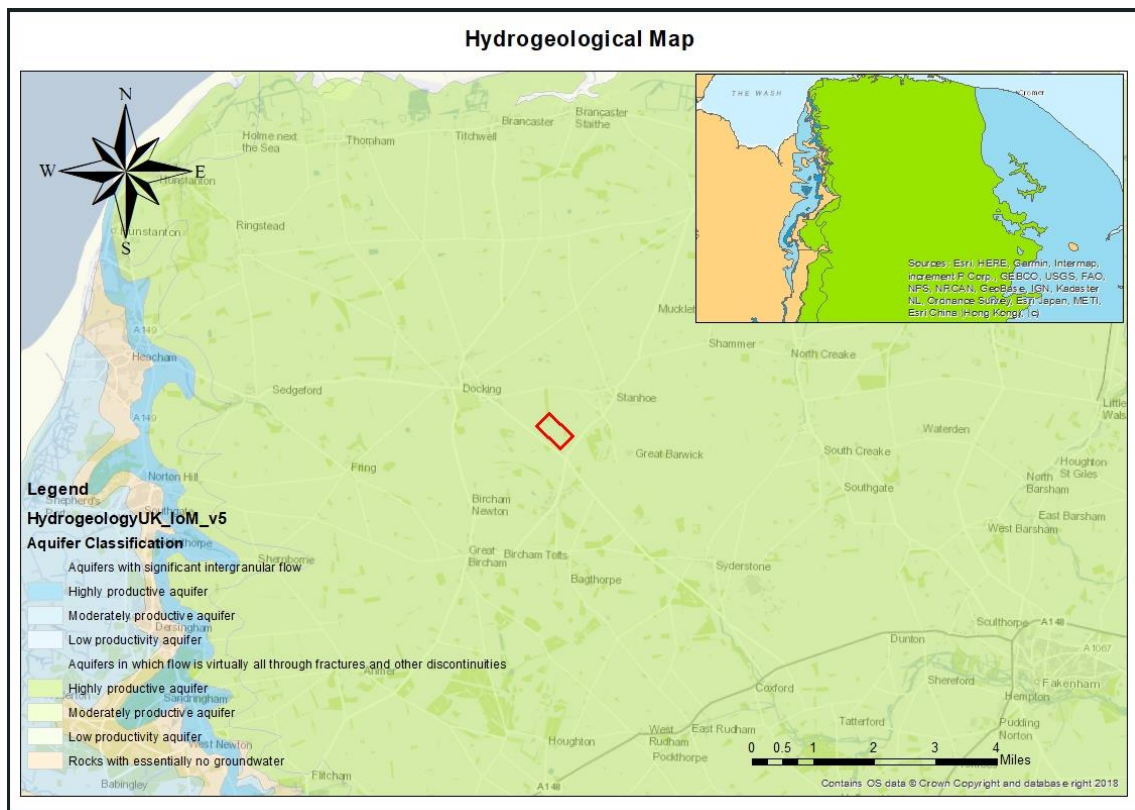


Figure 7. (a) Geological Map of the study site location (Edina, 2019). (b) Map of the Norfolk site location illustrating the hydrogeological settings and the study area marked with a red boundary, obtained using ArcMap 10.4.1.

The principal aquifer includes the Culver Chalk formation, Seaford Chalk formation, Lewes Nodular Chalk formation, and Newhaven Chalk formation. These formations have relatively intermediate permeability and hence components can be potentially migrated. The superficial deposits beneath the site are not classified as being an aquifer. The groundwater at this location has intermediate vulnerability. The geology and hydrogeology of the study area confirmed the design of historical landfill sites in the UK, which directed by the ‘dilute and disperse’ principal.

3.3 Conceptual Site Model

Prior to undertaking a risk assessment, it is important to develop a conceptual model that help in identifying potential contaminants linkage (Defra, 2012). Environmental risk assessment is based on the consideration of three essential elements that constitute a contaminant linkage (Defra, 2012). These key elements are:

- **Source:** this refers to the contaminant;
- **Pathway:** the route through which the contaminant can migrate;
- **Receptor:** this relates to any organism, including people, animals, plants, and properties or controlled water that is likely to be negatively impacted by the contaminant.

In the absence of any one of these elements, on any given site, there is no risk considered (Defra, 2012). The main receptors found within 1.5 km of the studied site are shown in Table 2 with their GPS coordinates. These receptors are most susceptible to the risk of contaminants exposure due to their proximity to the landfill. A preliminary conceptual site model is shown in Table 3 and Figures 8 and 9. The closest water body from the study area is located about 900m west of the site, which is a pond. A land cover map is shown in Figure 10, identifying land uses within 2 km of the landfill site in more details. The Conceptual site model represented the area of concern, contaminant sources, the environmental media that can be affected, and the processes that control the transport of contaminants to potential receptors. Atmospheric transport of contaminants is the pathway considered in this research scope as potential contaminants are directly exposed to the air during LFM activities.

Table 2: Receptor locations around the studied landfill.

Receptor	X (m)	Y (m)
Urban	579097	335489
Suburban	579250	335321
Residential area 1	580126	336486
Residential area 2	577785	336340
Residential area 3	580097	336700
Residential area 4	579445	334439
Arable/horticulture 1	579130	335662
Arable/horticulture 2	578917	335602
Arable/horticulture 3	579098	335438
Pond/freshwater	578031	335753
College	578908	333900

Table 3: Conceptual site model of the studied area.

sources	Excavation Shredding Screening Handling equipment	Receptors		
		Humans	Animals	Controlled waters or agricultural land
Contaminants	Dust (Heavy metals)	Atmospheric transport/deposition → Inhalation of dust or Ingestion of soil and dust through crops	Atmospheric transport/deposition → Inhalation of dust or Ingestion of soil and dust through crops	Atmospheric deposition → Interaction with surface water and agricultural soil
	Dust (Asbestos & Fibres)	Atmospheric transport/deposition → Inhalation of dust or Ingestion of soil and dust through crops	Atmospheric transport/deposition → Inhalation of dust or Ingestion of soil and dust through crops	Atmospheric deposition → Interaction with surface water and agricultural soil
	Landfill Gas	Atmospheric transport or vapor intrusion through soil → Inhalation of vapours	Atmospheric transport or vapor intrusion through soil → Inhalation of vapours	Interaction with atmosphere/surface water → Vegetation damage and acidification
	Gases (Non-methane VOCs)	Atmospheric transport → Inhalation of vapours	Atmospheric transport → Inhalation of vapours	Interaction with atmosphere/surface water → Water and crops harm
	Plastic Bags	Atmospheric transport/deposition → interaction with setting → Ingestion of soil & dust – micro bags	Atmospheric transport/deposition → interaction with setting → Ingestion of soil & dust – micro-bag	Atmospheric deposition → Interaction with surface water → Fish poisoning

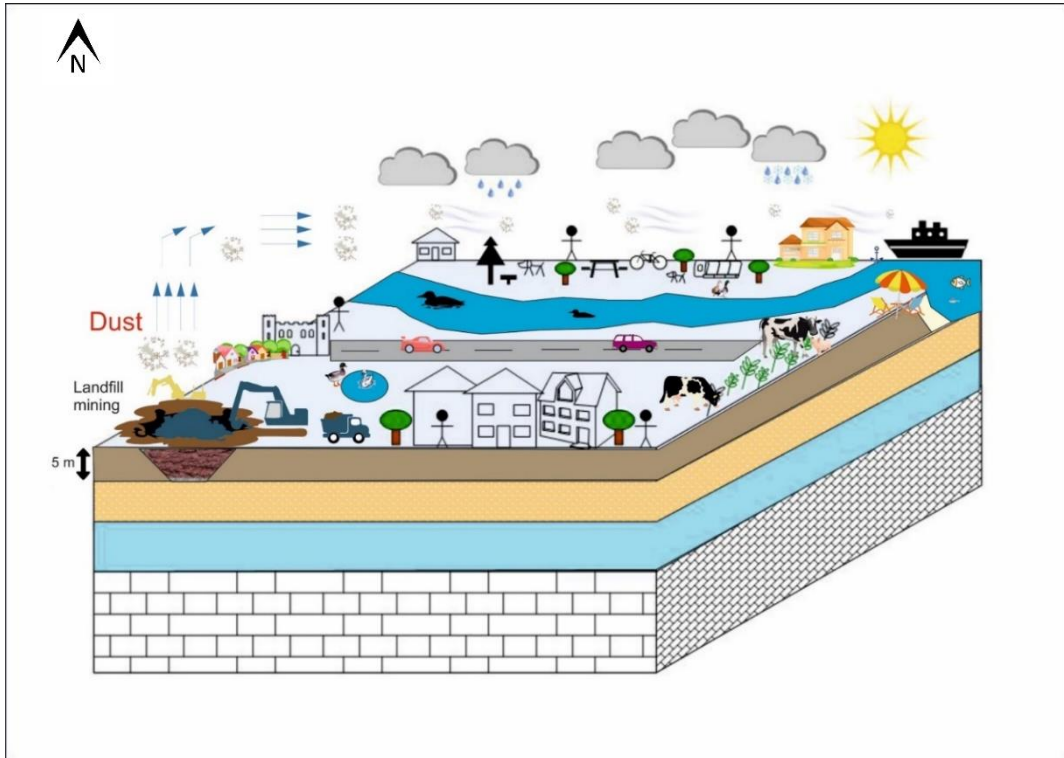


Figure 8. Generic block diagram of the conceptual site model. Produced by using CorelDRAW Software.

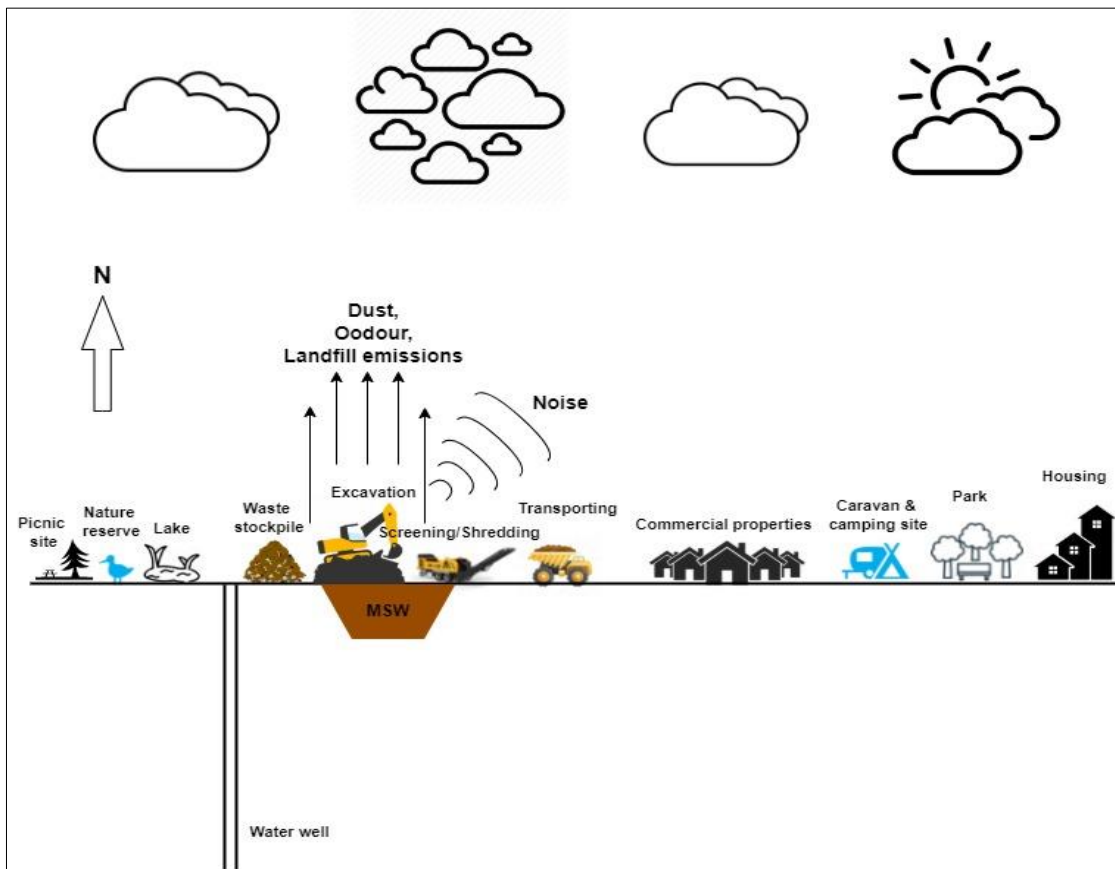


Figure 9. Site-specific SPR conceptual model diagram of the studied area.

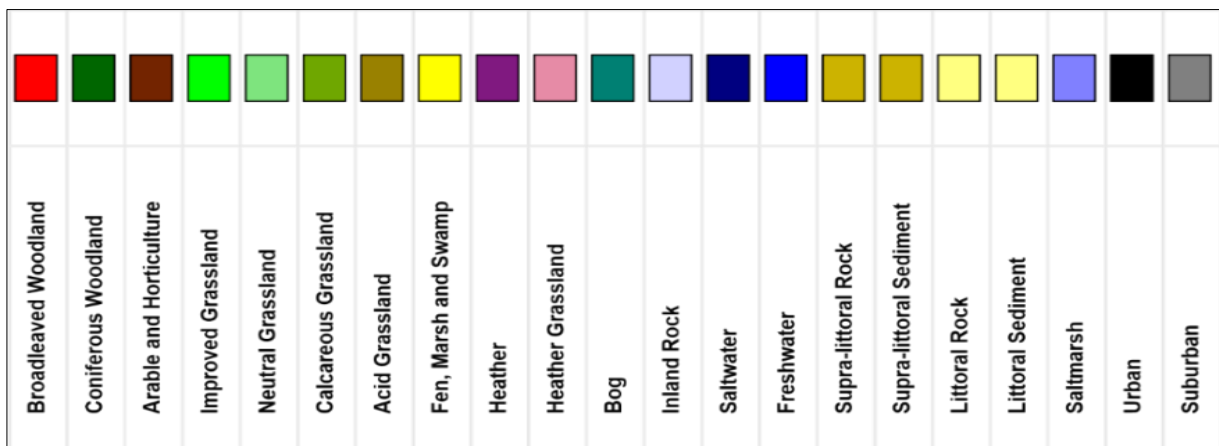
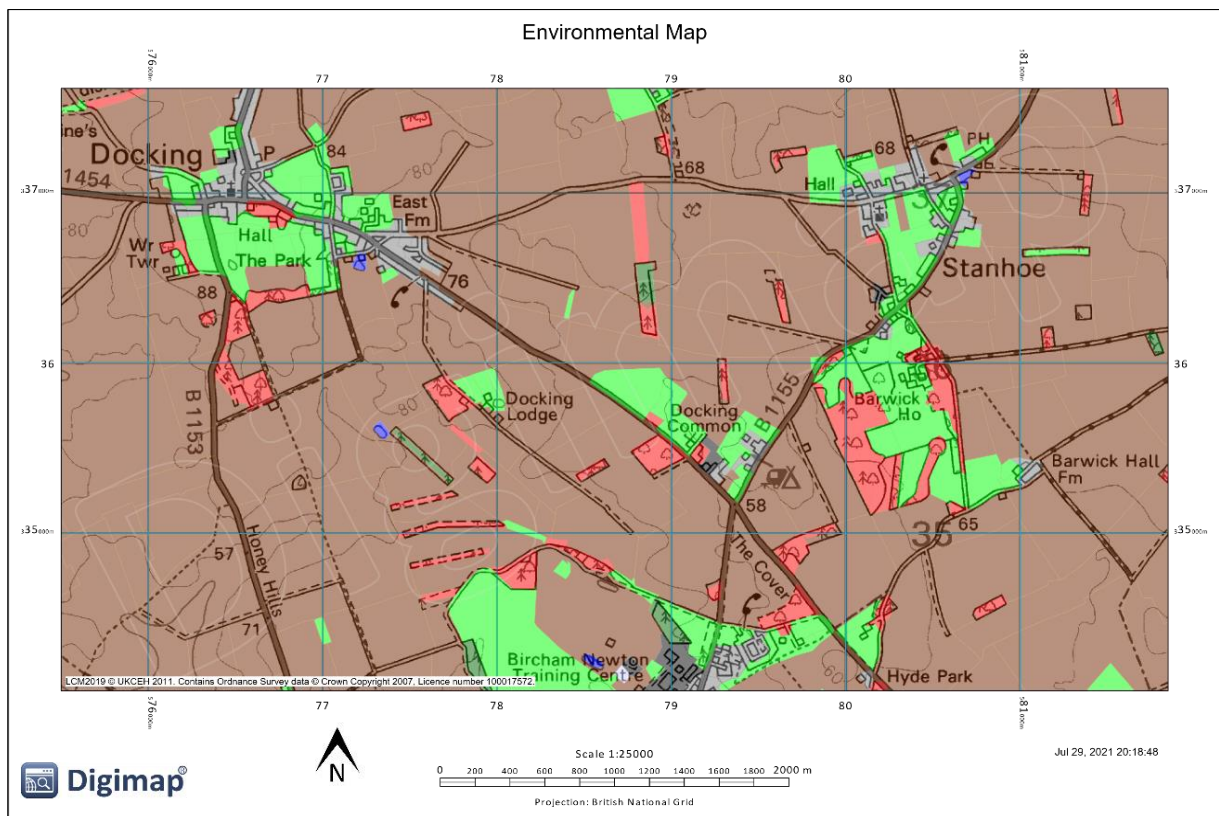


Figure 10. A land cover map showing the land uses within 2 km of the site (Edina, 2022a).

3.4 Sampling Strategy and Location of Samples

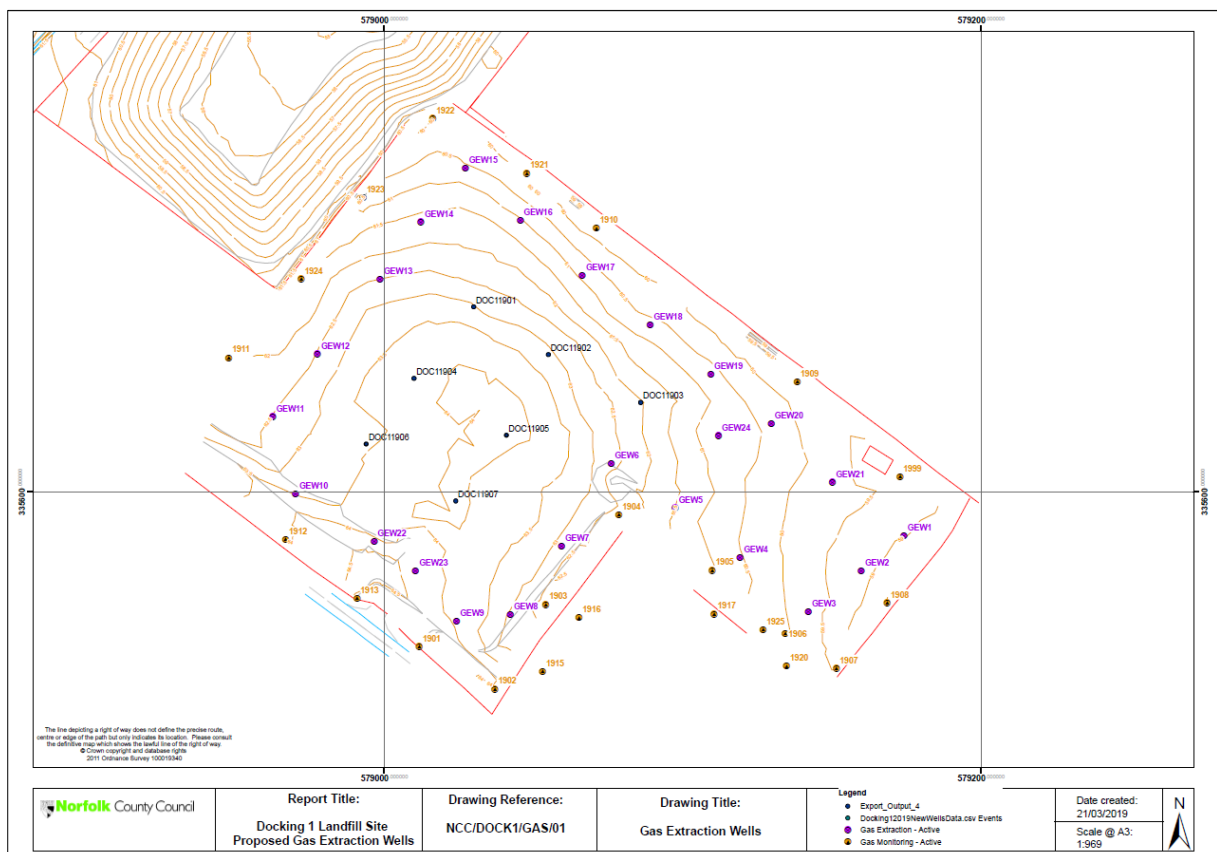
Due to the heterogeneity of waste materials, choosing a method for representative sample is one of the most challenging decisions in waste characterisation analysis (López et al., 2018). Generally, the sampling strategy differs from case to case and is dependent on each study's aim (Singh and Chandel, 2020). Also, the landfill's material composition varies according to the excavation location selected (López et al., 2018; Singh and Chandel, 2020). The sampling

strategy used in this study was based on a planned additional wells drilling programme being implemented by Norfolk County Council for gas extraction as part of the landfill's closure procedure (Figure 11 a). This strategy was in accordance with the study by (Kaartinen et al., 2013). Information on the gas extraction wells level depth is shown in Table 4. The well numbers considered in this study are 1901, 1904, 1906 and 1907 (Figure 11 b).

Table 4: Gas extraction well details for recovered waste samples.

Sample point	Target depth (mAOD)	Ground level (mAOD)	Drill depth (m)	Plain pipe (bglm)	Perforated pipe	Gravel install (m)	Bentonite install (m)	Borehole diameter (mm)	Casing diameter (mm)
1901	56	63.04	7.04	0 - 3.0	0 - 7.04	4.54	2.5	160	63
1904	56	63.79	7.79	0 - 3.0	0 - 7.79	5.29	2.5	160	63
1906	56	63.38	7.38	0 - 3.0	0 - 7.38	4.88	2.5	160	63
1907	56	64.12	8.12	0 - 3.0	0 - 8.12	5.62	2.5	160	63

(a)



(b)

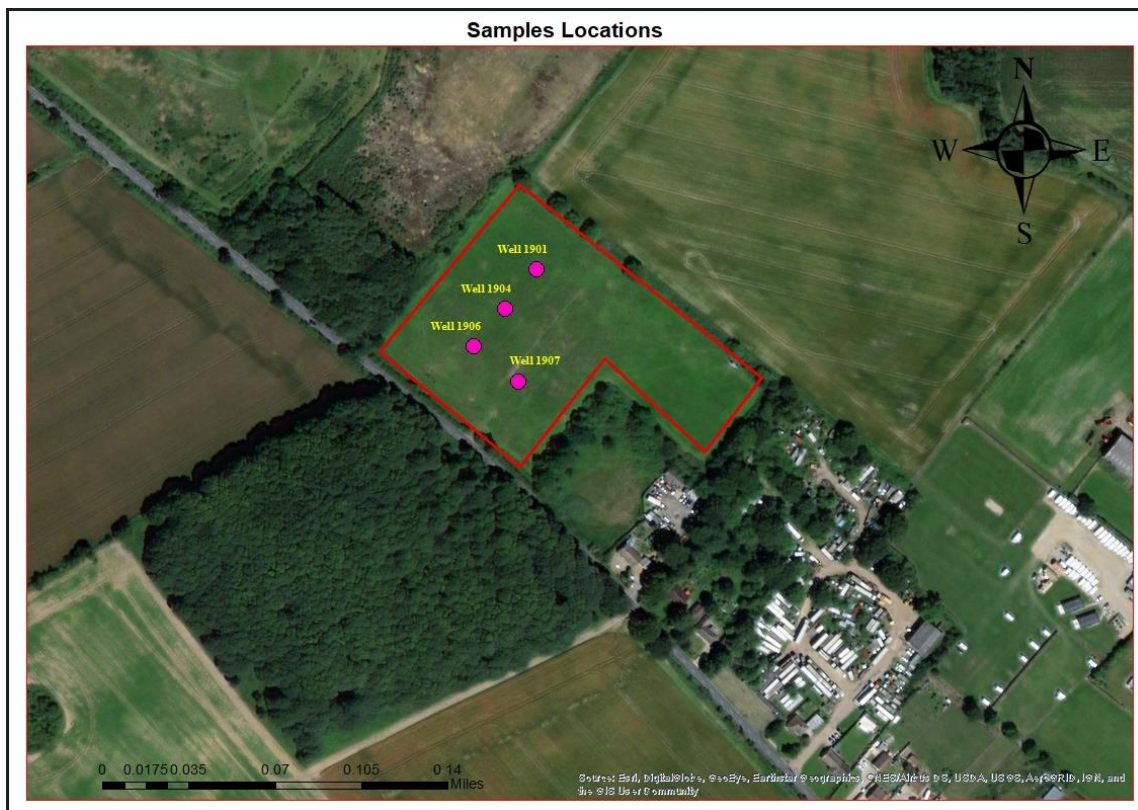


Figure 11. (a) Map showing the gas wells location plan and drill logs by Norfolk County Council. (b) Aerial photograph of the study area marked with a red boundary and sample locations illustrated in purple squares with corresponding well numbers.

3.5 Excavation and Storage

Nearly 40 kg of MSW was collected from four different wells, numbered 1901, 1904, 1906, and 1907 (10 kg each) from within the central waste mass, using a rotary drilling rig with a depth ranging from 7-8 m, mixed and homogenized together. Coordinates of the wells were determined using GPS. The samples were placed in thick-labelled plastic bags and sealed firmly to prevent any loss. The samples were then placed in a rigid plastic box for transfer to the laboratory. The samples were kept in a refrigerator at 4°C until preparation for analysis. The collected volume of wastes was limited due to sample storage constraints at the university laboratory. However, lesser amount of waste excavated for characterization analysis was observed in the study by (Quaghebeur et al., 2013). A photograph of the drilling of each well

to provide a visual indication of the recovered waste is provided in Figure 12. A mixture of solid waste compositions was identified visually within the excavated materials.



Figure 12. Photographs of the recovered wastes from drilling (a) well 1901 (b) well 1904 (c) well 1906 (d) well 1907.

3.6 Sample Processing Methodology

Subsampling was carried out in the laboratory due to unsuitable field conditions. Coning and quartering and a riffle sample splitter (Figure 13 a and b) were used to obtain representative samples, and this method was consistent with previous studies by (Kurian et al., 2003; Masi et al., 2014; Parrodi et al., 2019b; Singh and Chandel, 2020) in their attempt to get representative samples for MSW analysis. Bulky non-biodegradable materials, such as plastic, metal, paper, and textile, were removed from the recovered MSW samples by manual sorting for homogenisation of the samples for subsequent analysis. Coning and quartering was applied four times at first (once for each well). Approximately 20 kg of representative samples were obtained from coning and quartering (5 kg per well). These 5 kilos from each well were further subsampled down to approximately 1 kg each using a riffle sample splitter. All subsamples were kept in nylon plastic bags and sealed firmly. An illustrative flowchart of the sample processing steps is provided in Figure 14.

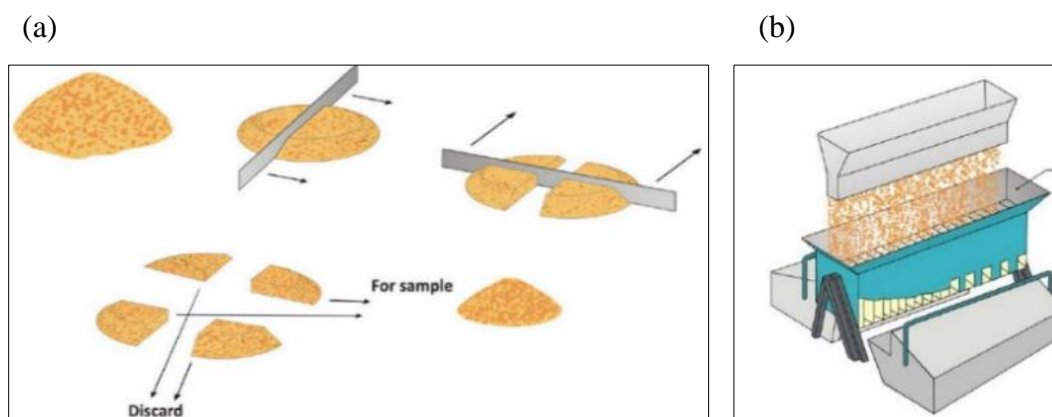


Figure 13. (a) Coning and quartering method was utilized to first split the sample into 4 segments, the diagonally opposite of which are rejected. Quartering was continued till a favourable sample volume is reached. (b) Riffle sample splitter was used to divide the samples into two equal parts. The process of dividing was repeated till a suitable sample size is achieved for analysis (Gerlach et al., 2002).

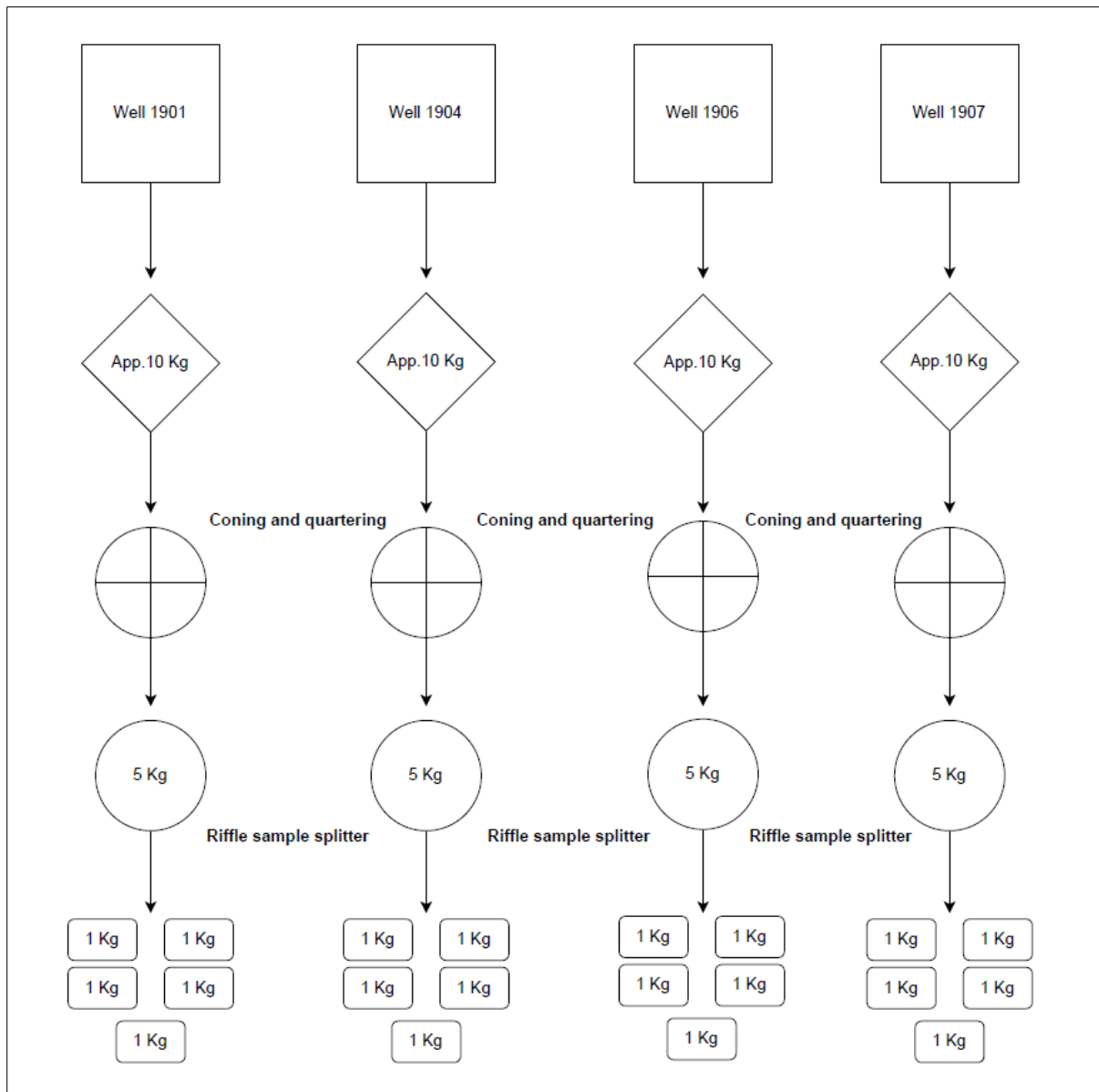


Figure 14. Chart illustrating the sample processing steps followed in the methodology.

3.7 MSW Characterisation and Laboratory Work

Waste composition and biodegradation rate can have a significant influence on the health and the surrounding environment caused by LFM activities (Nguyen et al., 2018; Savage et al., 1993). Different components define different impacts on soil, air, and water (Vergara and Tchobanoglous, 2012). Previous literature has identified the existence of significant amounts of heavy metals and organic/inorganic compounds after the closure of landfills that can pose

potential risks to the environment and human health if released (Cossu et al., 2012; Esakku et al., 2005; Sauve and Van Acker, 2018). According to (Weng et al., 2015), waste composition investigation is significant prior to LFM in order to ensure the effectiveness and the safety of workers during waste utilisation since the composition of waste is not well documented for most landfill sites. Therefore, chemical, physical, and biological characterizations were carried out in this study to identify the waste degradation state and constituents within the waste known for their established health impact. Parameters were selected based on health/environmental impact assessment determination in different environmental compartments. A flowchart diagram of the laboratory work sequence is shown in Figure 15. Justification of the methodologies selected for the lab work analysis is discussed within each analysis section in the next Chapter.

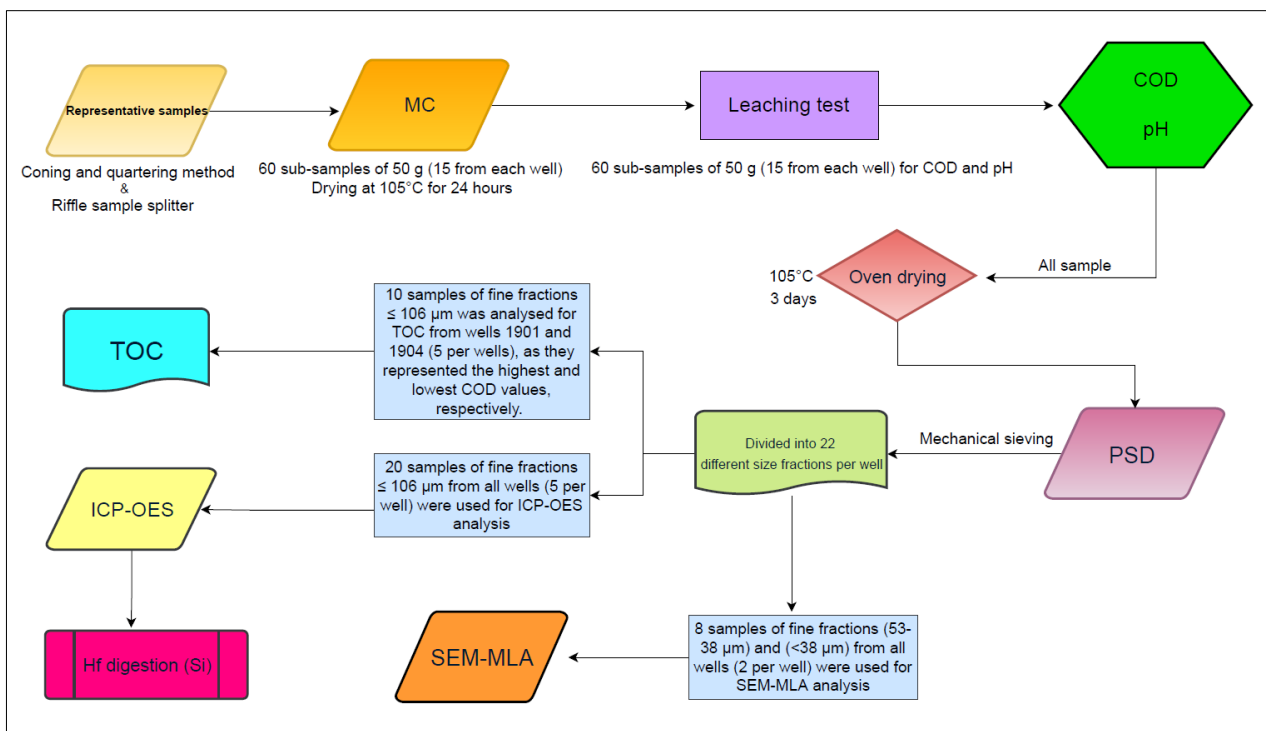


Figure 15. Flowchart diagram of the laboratory sequence.

Chapter 4: Results and Discussion of MSW Characterisation

4.1 Moisture Content (MC)

A total of 60 representative subsamples (15 from each well) of 50 g were used for the determination of MC by using a drying oven at 105°C for 24 hours. An average was calculated from each subsample of 1 kg out of 5 (3 subsamples of each 1 kg). This has led to a total of 20 MC mean samples (5 from each well) as shown in table 5.

Table 5: Mean samples of moisture content.

Well number	Moisture content (%)
1901	24.7
1901	26.7
1901	24.1
1901	24.9
1901	29.0
1904	25.6
1904	20.9
1904	20.4
1904	22.7
1904	25.4
1906	22.0
1906	22.6
1906	26.8
1906	22.4
1906	21.6
1907	24.0
1907	23.2
1907	23.3
1907	21.1
1907	22.5

Degradation of any waste materials is influenced mostly by moisture content (Bäumler and Kögel-Knabner, 2008). Low moisture content can be one of the leading causes for restraining metabolism and microbial function and thereby delaying the biological degradation and stabilization of MSW (Adhikari et al., 2014; Qi et al., 2013). At any landfill, the moisture

content of waste is highly associated with the content of organic materials (Bäumler and Kögel-Knabner, 2008; López et al., 2018) and depth (Pecorini and Iannelli, 2020).

According to (Singh and Chandel, 2020; Wreford et al., 2000), this parameter is crucial for all micro-organisms metabolic processes and thereby enhance degradation of waste materials. However, moisture content can dissolve and carry organic and inorganic pollutants as well as metabolic inhibitors, such as heavy metals (Qi et al., 2013). In this case, it increases the rate of leaching compounds and poses disruption to microbial activities. Low-permeability soil cover can reduce leachate infiltration through waste and minimise the migration rate of toxic contaminants like heavy metals (Albright et al., 2006).

MC was analysed in this study to understand its role in the biodegradation of the recovered waste materials, emission rate estimation, atmospheric pathway mechanism of dust during LFM activities.

According to various researchers, the moisture content of municipal solid waste in the USA and Europe ranges from 20% to 30%; however, that of China ranges from 30% to 60% (Aihong et al., 2012; Hull et al., 2005; López et al., 2018; Sormunen et al., 2008). In China, this disparity occurs as a result of substantial kitchen waste representing 60% of the waste materials (Aihong et al., 2012; López et al., 2018). In a landfill, there are different interconnected parameters determine the moisture content rate. These parameters include the landfill operating systems, climatic conditions, waste composition, waste type and properties, as well as the soil cover layer (Hull et al., 2005; López et al., 2018).

The results of the mean MC showed somewhat similar values over the 4 wells. Well number 1901 relatively represented the highest level of MC, reaching to 25.9 % (Figure 16). Higher level of MC of well no. 1901 was expected owing to visual observation during sample possessing.

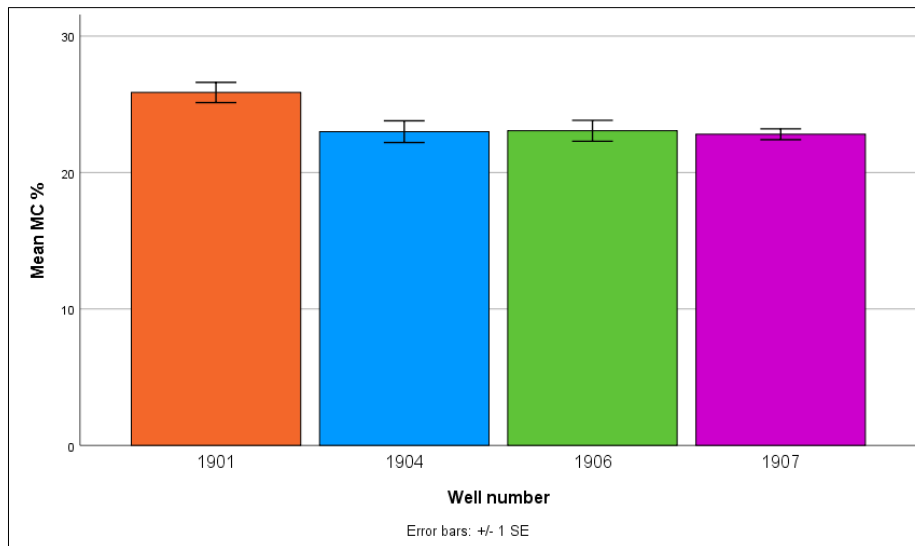


Figure 16. Mean of moisture content from the four wells.

In this study, the moisture content average of all wells was nearly 23.5 %, which is in agreement with that of (Jani et al., 2016) at Högbytorp landfill of similar conditions. The results were also comparable to the study by (Frank et al., 2017) across seven UK landfill sites and that of (Scott et al., 2019) in similar conditions. An engineered Geosynthetic Clay Liner cap was installed in 1998 and therefore the landfill site used to be non-engineered site for 13 years after its closure, so a higher degree of infiltration and likelihood of contaminant flushing is expected within the site.

Rainfall on average falls evenly throughout the year in Norfolk, which is in a relatively dry part of England. The driest month is February and the wettest is October (samples were collected in mid-April). Comparing to the MET office data, the annual actual value precipitation in Norfolk ranges from 600-800 mm which is relatively low for UK conditions (Figure 17). Maps displayed in Figure 17 refer to the years 2018, 2015, 2010 and 2005, respectively. They show that the average rainfall in the study area ranges between 600-800 mm annually. Rainfall maps include all precipitation (rainfall, snow, and hail).

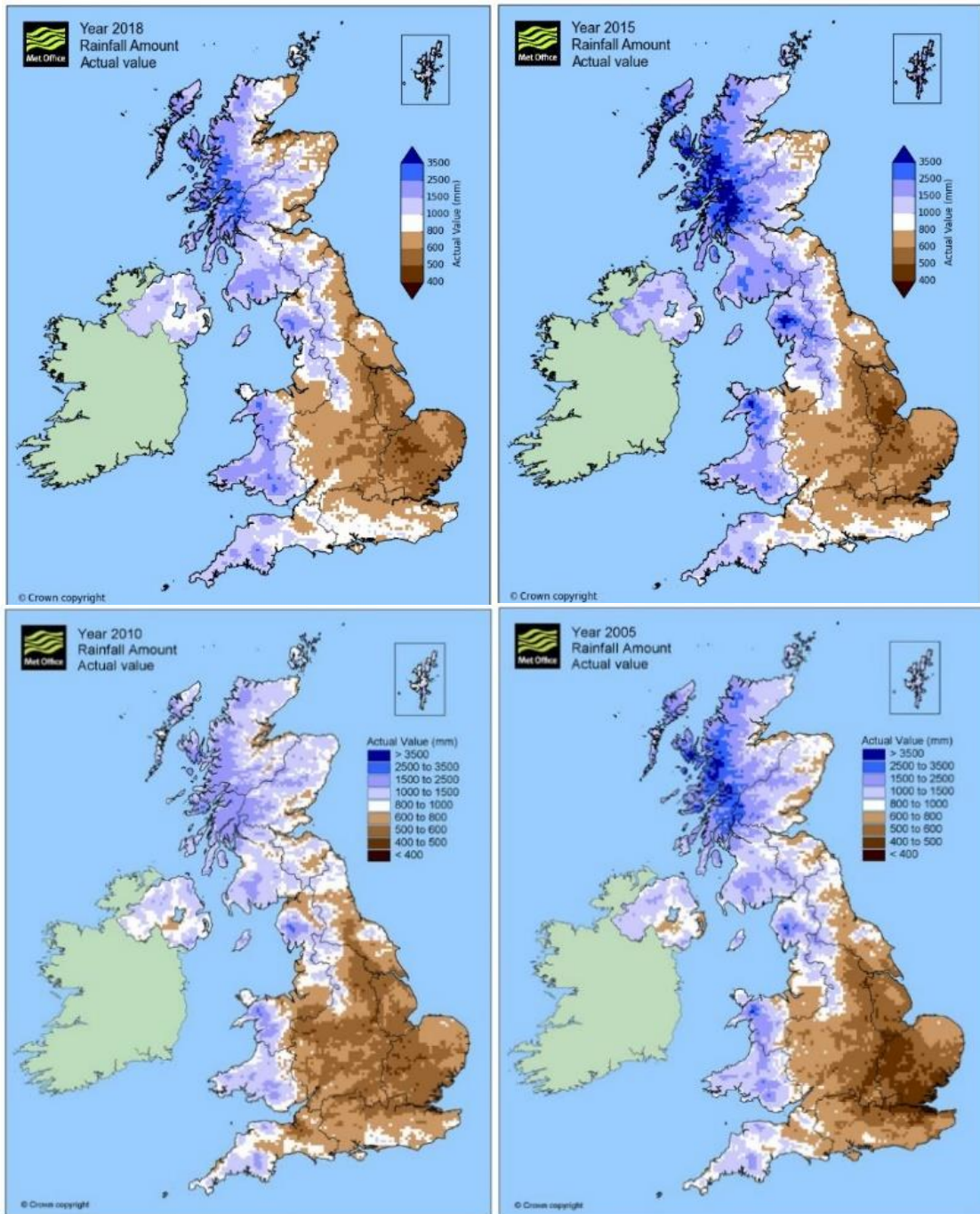


Figure 17. Maps of climate variables in the UK for previous years (Met-Office, 2020).

4.2 Leaching test

The test requires a representative particle size samples below 4 mm as defined in the European Standard for waste material and then brought into contact with water under defined conditions (EN, 2002). Given the fact that the reference is focused on the leaching for inorganic material and allowed drying samples, the landfill samples of the study area are relatively wet and might not be well-sieved and thus they were not sieved. Leaching tests were completed with a liquid/solid (L/S) ratio of 10 because it is expected to promote appropriate contact between the eluent and the waste (Parodi et al., 2011) and represent typical field conditions (Lee et al., 2022b). Furthermore, the waste acceptance criteria of the Environment Agency for England and Wales consider only L: S 10 l/kg leaching test in their Environmental Permitting Regulation (Agency, 2013). Distilled water was used as the eluent for the leaching test.

4.2.1 Procedure of Leaching Test

4.2.1.1 Leaching Step

- 50 g of representative mass of each well subsample (15 per well) was placed in a bottle of 500 ml.
- An amount of leachant (distilled water) establishing a liquid to solid ratio (L/S) = 10l/1kg was added to the 500 ml glass bottles.
- The capped 500 ml bottles were then placed on a roller table.
- Samples in the bottles was then agitated for 24 h.

4.2.1.2 Liquid-solid Separation Step

- The suspended solids were allowed to settle for around 15 min.
- Samples in the bottles were then poured into 50 ml falcon tubes and put in the centrifuge for 10 minutes at 3 000 speeds in g to remove the solids present in the liquid.
- A good solid-liquid separation phase was achieved after centrifuge and then samples were transferred to another 50 ml falcon tubes using pipette.

- Samples' eluate was then stored at 4°C for COD and pH test.

4.3 Chemical Oxygen Demand (COD)

COD was analysed for 60 subsamples (15 per well) to identify the amount of oxygen needed to oxidize the organics present in the leached liquid sample. COD vials of potassium dichromate (potassium dichromate in a 50% sulphuric acid solution) ranging from 0-150 / 0-1000 mg/l were used for COD test. The reagent of COD includes ions of silver and mercury. The silver is used as a catalyst, and the mercury is utilised in order to complex chloride interference (Westwood, 2007). A pipette was used to take the already separated liquid from the centrifuge tube to the COD vials. The first vial was only added with 2 ml of distilled water as a reference and with the liquid leached sample for the rest. The vials were placed on a heated block for 2 hours and then left for approximately an hour to cool down. Once the vials reached about 60°C, they were gently shaken and left out of the heated block for about 10 minutes to reach the room temperature of 20°C. The vials were then placed on a spectrophotometer for obtaining the COD values. The vial of added 2 ml of distilled water was used first as a reference and zeroed. Then, samples were ready for the COD reading test.

COD can be defined as a method of estimating the oxygen level required to oxidize soluble organic/inorganic matter in leachate as a result of chemical oxidation (Abba and Elkiran, 2017). It also evaluates the presence of toxic chemicals and oxidisable pollutants (Hussein et al., 2019). According to (Abu-Daabes et al., 2013), "*The mg/l COD results are defined as the mg of O₂ consumed per litre of sample under the Reactor Digestion Method approved for reporting wastewater*". The COD test is often used as an alternate to BOD due to shorter length of testing time (Kiepper, 2010), and in some cases the ratio of BOD to COD is used to represent the biodegradable fraction (Hussein et al., 2019; Lee et al., 2022a; Meegoda et al., 2018).

Several studies have reported how organic content highly affects the leachate quality, as waste with lower organic content can lead to lower environmental impacts (Wijaya and Soedjono,

2018; Ziyang et al., 2015). In addition, high levels of COD values mean higher oxidation in organic compounds which will lead to a reduction of dissolved oxygen levels (hypoxia), caused by eutrophication process. Subsequently, this reduction can lead to anaerobic condition that is harmful to the aquatic ecosystem (Abba and Elkiran, 2017). Thus, COD levels are significant to quantify, so that its potential impact will have on the oxygen levels of receiving waters (as receptors through atmospheric transport and deposition) can be assessed.

An illustration of the COD mean results is shown in (Figure 18 a). A COD kit ranging from 0-1000 mg/l was used for 20 samples due to the depletion of the COD vials of 0-150 range. Thus, samples resulted higher than 150 mg/l using the 0-1000 mg/l range were fixed to 150 mg/l as shown in Figure 21 a. It can be inferred from the methodology of COD test applied in this study, using a COD kit ranging from 0-1000 mg/l is beneficial to avoid the limitation applied to the COD kit of 150 mg/l.

According to (Legislation, 1994), the standard for effluent discharge regulations of COD is 125 mg/l in the UK. A total of 18 samples out of 60 exceeded the standard limit of the wastewater discharge (Figure 18 b). COD concentrations of young leachate is typically above 20000 mg/l (Abba and Elkiran, 2017; Bhalla et al., 2013).

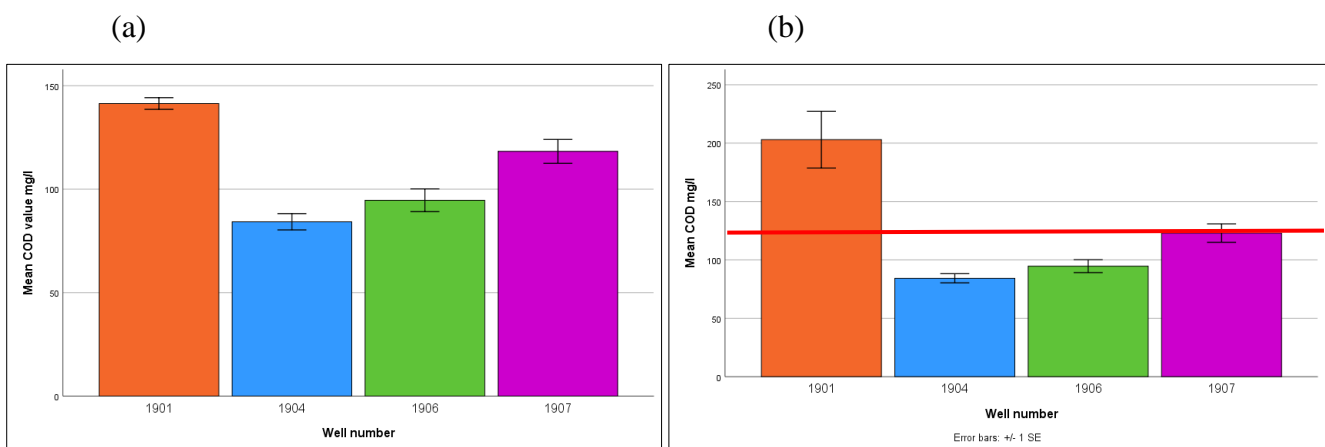


Figure 18. (a) Mean of COD fixed to 150 mg/l as a maximum value with error bars: +/- 1 SE. (b) Mean of COD of both used range kits (0-150 & 0-1000 mg/l) in comparison with the generic acceptance criteria marked with a red line for the effluent discharge regulations.

It can be clearly seen that the mean COD values of well no. 1901 were above 200 mg/l using the 0-1000 mg/l range kit with a heights value reaching to 400 mg/l. Higher COD values of well number 1901 were expected since a stronger smell has been identified during the sample processing.

According to (Hussein et al., 2019; Lee et al., 2010), COD is known as an indicator of the degradation of organic matter, which distinguishes the acetogenic phase from the methanogenic in a landfill. COD results at Docking landfill indicate that the landfill is in a methanogenic state. Literature COD values in comparison with the present COD values are shown in Table 6

Table 6: Literature COD values compared to the present COD values.

Parameter	Present study	(Hogland et al., 2004) Maasalycke, Sweden	(Xiaoli et al., 2007) Shanghai Refuse, China	(Jani et al., 2016) Högbytorp, Sweden	(Kaczala et al., 2017) Kudjape, Estonia	(Frank et al., 2017) 7 landfill sites, UK	(Sormunen et al., 2008) Kujala, Finland	(Yilmaz et al., 2010) Konya, Turkey
Type of waste disposed of	MSW + C&D	MSW	MSW	MSW + C&D	MSW	MSW	MSW	MSW
Age of waste	33 - 41	17 - 22	17	5	5 - 6	35	50	< 5
COD (mg/l)	60.4 – 400	4200 – 9400	1520 – 3270	2390	4924 - 7622	294- 792	367	38200

The COD values of the present study are comparable with the studies by (Frank et al., 2017) and (Sormunen et al., 2008) that investigated landfill site having age >35 years old. The COD of younger landfills presented in table 6 showed higher values which is to be expected since COD decrease with the age of waste (Francois et al., 2006).

4.4 pH

The importance of pH value lies in its responsibility for controlling the solubility and thereby bioavailability of metals in the environment (Lee et al., 2022b; Weiner, 2012). As the pH

decreases which becomes more acidic, the solubility of metals increase (Chuan et al., 1996; Esakku et al., 2003; Kasemodel et al., 2019; Kjeldsen et al., 2002). pH is also a main driver of bacterial activity at various stages of anaerobic waste degradation (Hussein et al., 2019; Parrodi et al., 2018a; Staley et al., 2011). The alkalinity of pH in leachate indicates the biological stabilization of the organic components (Oben et al., 2019). In addition, slightly alkaline and alkaline pH values are closely associated with landfills that already have reached a complete methanogenic phase, with MSW disposed of for more than 5 years (Kaczala et al., 2017). In this regard, the methanogenic stage in landfills is usually characterized by a neutral to slightly alkaline pH values, reflecting the degradation of organic acids to release CH₄ and CO₂ (Femi, 2011; Ziyang et al., 2015). Moreover, research conducted in the Liosia landfill, Greece, reported that the pH values were quite low during the initial stage of decomposition owing to acid formations, while the pH was mostly alkaline during the methanogenic phase (8.07 and 8.63) (Fatta et al., 1999). Therefore, pH is a key parameter for determining waste stabilization condition in landfills and the behaviour of metal solubility and bioavailability when introduced to the surrounding environment of neutral condition.

pH measurements were performed by using pH probe with a value of pH 7.0 of buffer solution. The value of pH was measured for 60 subsamples (15 per well). The pH average of the four wells was approximately between 7.3 and 7.6 (Figure 19). The lowest mean value of the pH was found in well 1901 and the highest in well 1904.

According to the current waste acceptance criteria (threshold) of pH in the UK, it should be >6 for non-hazardous landfills (ALS, 2017). The mean pH across the four wells was between 7.3 and 7.6, indicating that the waste has reached to stabilized conditions (Bhalla et al., 2013). It also denotes that methanogenesis is activated which converts volatile fatty acids (VFAs) into biogas by methanogenic microorganisms (Sormunen et al., 2008). The pH results are quite similar to the study by (Frank et al., 2017) in UK landfills of comparable landfill ages. They

were also found to be in the same pH range (between 7-8) at different landfill sites of similar ages (Francois et al., 2006; Xiaoli et al., 2007). Conversely, lower pH (<6.3). was found in the studies by (Sormunen et al., 2008) and (Mönkäre et al., 2016) of comparable landfills age (>20). This can be concluded by the difference of waste depth being analysed (Parrodi et al., 2018a) or might be due to the difference of waste size fraction selected for the analysis as demonstrated in the study by (Parrodi et al., 2020).

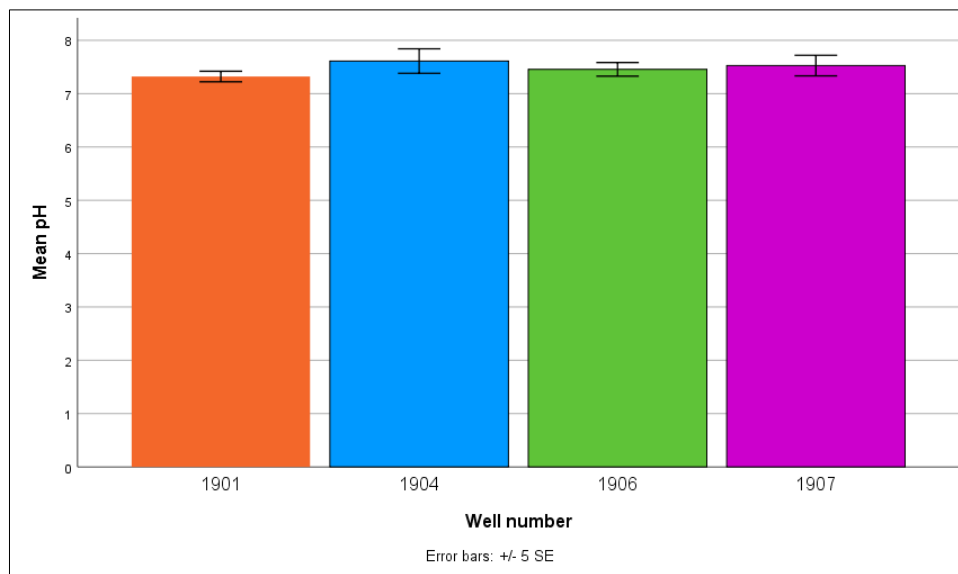


Figure 19. Mean of pH from the four wells.

4.5 Statistical Analysis of (MC, COD, and pH)

Statistical analysis was performed using the Statistical Package for Social Science software (version 27). Descriptive statistics of (COD, pH, and MC) in different wells is shown in Appendix 1. A one-way analysis of variance (ANOVA) was used to compare variances across the means (or average) of different groups. ANOVA analysis demonstrated significant differences among MC, COD and pH values in the four wells ($P < 0.01$), indicating that the data sets were not normally distributed (Appendix 2). Followed by least-significant difference (LSD) tests showed that only well no. 1901 is demonstrated significant differences among MC values of the four wells ($P < 0.01$). COD values of well no. 1901 was significantly higher than that of all other wells ($P < 0.01$). In addition, COD values of well no. 1907 was significantly higher

than that of well no. 1904 and well no. 1906 ($P < 0.01$) (Appendix 3). pH value of well no. 1901 was significantly higher than that of all other wells ($P < 0.01$). The correlation between various physicochemical parameters was also investigated using the Pearson correlation coefficient and linear regression. The Pearson correlation coefficient was used to find trends across different variables. The correlation coefficient, which ranges from -1 to +1, shows whether two parameters are positively or negatively correlated. The statistical significance of the correlation between two parameters is shown by the p-value. pH values were found to be negatively related to COD values using Pearson's correlation (r) 2-tailed analysis which demonstrated significance with COD values of the four wells ($P < 0.01$) (Appendix 4). The inverse correlation was best shown between well 1901 and 1904, as the pH decrease the COD increase (Figure 20). This result is consistent with the study by (Lee et al., 2022a). Additionally, there was a weak significance correlation found between COD and MC values ($P < 0.05$) (Appendix 4). Multiple linear regression analysis was carried out in order to assess the correlation extent between the COD and the other two variables. The analysis demonstrated high significance between COD and both other variables (MC and pH) of the four wells ($P < 0.001$) (Appendix 5).

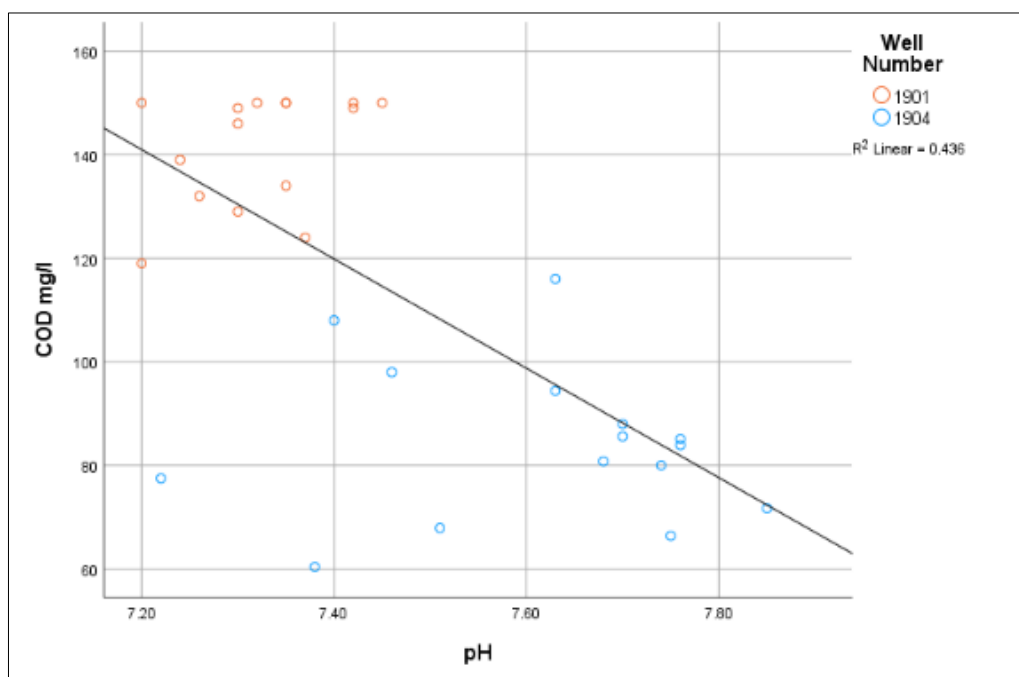


Figure 20. Correlation graph between pH and COD using linear regression line.

4.6 Comparison and Relationship Between the Data of the Studied Site and Seven Other UK Landfill Sites

A recent study by (Frank et al., 2017) who investigated 7 landfill sites in the UK from different ages for compositional and physicochemical changes in MSW materials and biogas production, was compared to the current studied site to identify existing relationships between them. Background information on the previous studied landfill sites 1-7 is shown in Table 7.

Table 7: Characteristics of the previous UK studied landfill sites.

Landfill site	Age of landfill site (as of 2015)	Status of landfills (as of 2015)	Capacity of site (Mt)	Tonnage received per year (kt year ⁻¹)
LFS 1	35	Closed	5.8	200–300
LFS 2	23	Open	6.6	300
LFS 3	22	Open	4.2	200–250
LFS 4	19	Closed	5.0	200–250
LFS 5	8	Open	0.9	100
LFS 6	35	Open	1.4	50
LFS 7	7	Closed	1.1	100–150

4.6.1 Moisture Content

Values of mean moisture content are shown in Figure 21, which range from 24% to approximately 37%. All the landfill sites demonstrated similar trend of moisture content. Variation in moisture content between the sites could be due to different types of capping material used (e.g., high to medium permeability material or a low permeability one), solid waste composition, and the seasonal weather variations (Bhalla et al., 2013).

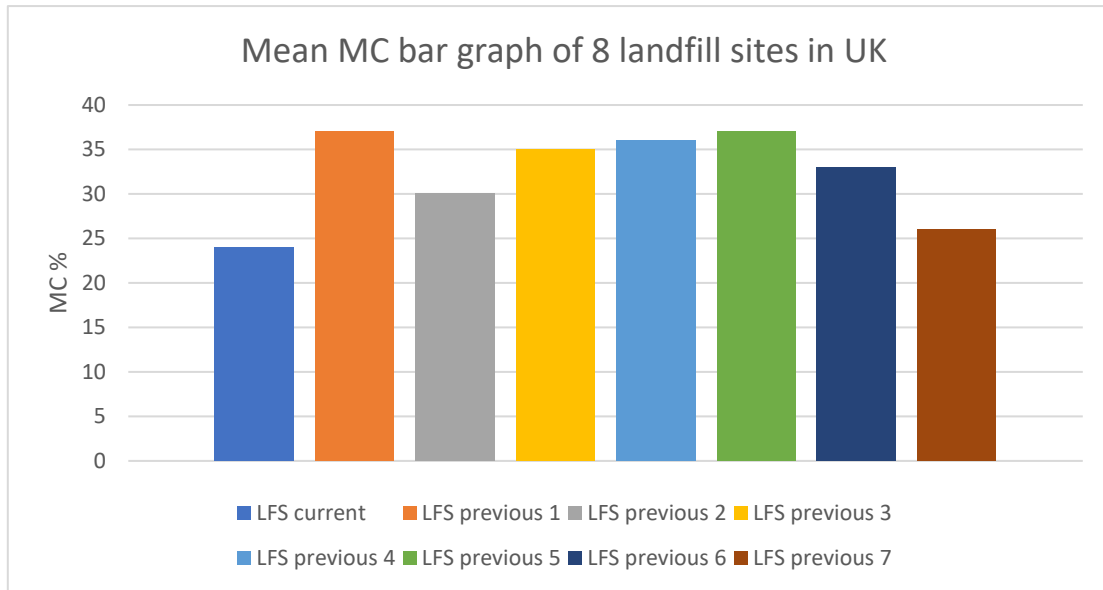


Figure 21. Mean moisture content in the UK landfill sites, including the current site.

4.6.2 Chemical Oxygen Demand (COD)

Values of mean COD are illustrated in Figure 22, which range from 127 mg/l to approximately 1,290 mg/l. LFS 5 and 7 have the highest COD values which they are the youngest landfills. However, COD values equal to or greater than 1,000 mg/l can reflect residual of non-biodegradable organic matter that are refractory to biological degradation such as humic substances (Castrillón et al., 2010; Rodríguez et al., 2004). LFS 1 is relatively comparable with the current site, which share the same landfill conditions. Although LFS 6 is aged the same as the current site, its COD values is higher than the current site and other younger sites like LFS 2,3, and 4. (Reinhart et al., 2002) provides a potential explanation for this by proposing that some conventional landfills were engineered and designed to hinder water from reaching the waste body and thus prevents waste from decomposing over long periods of time. According to (Frank et al., 2017), current landfill managements are the primary reason for wastes to remain non-degraded for a long time. Hence, waste contains high loads of organic matter regardless of landfill age.

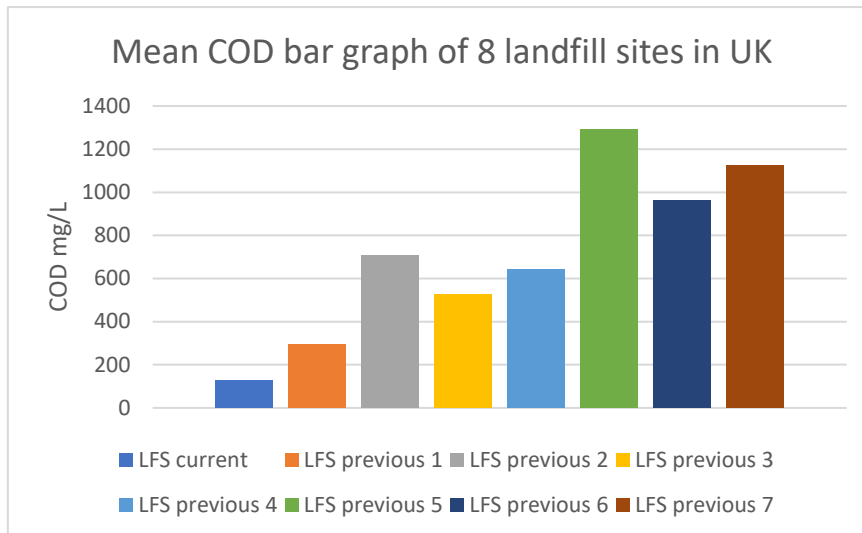


Figure 22. Mean COD in the UK landfill sites, including the current site.

Statistically speaking, no relationships between the different mean variables (MC, pH, and COD) of the studied site and the seven previous landfill sites in the UK was found using Pearson's correlation (2-tailed) analysis. However, there was a weak negative significance relationship noticed between COD and landfill age of the 8 landfill sites (Figure 23) which showed significance ($P < 0.05$) (Appendix 6). These findings confirm the highly heterogeneous nature of landfill material and the site-specific conditions between different landfill sites.

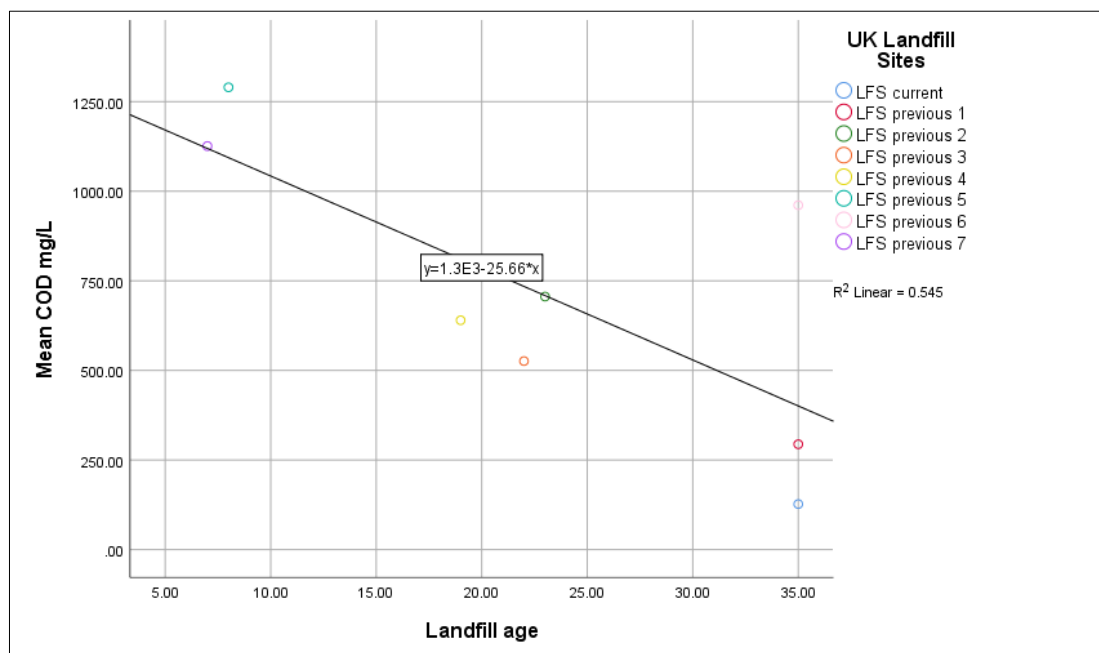


Figure 23. Correlation graph between COD and landfill age using linear regression line.

4.6.3 pH

Values of mean pH are displayed in Figure 24, which range from 7.0 to approximately 7.6. This range of pH values indicate that sites were either in a methanogenic state or in a transition stage towards a methanogenesis (Adhikari et al., 2014). Also, MSW landfills that have pH >7 is deemed as intermediately stable with landfill age greater than 5 years (Adelopo et al., 2017).

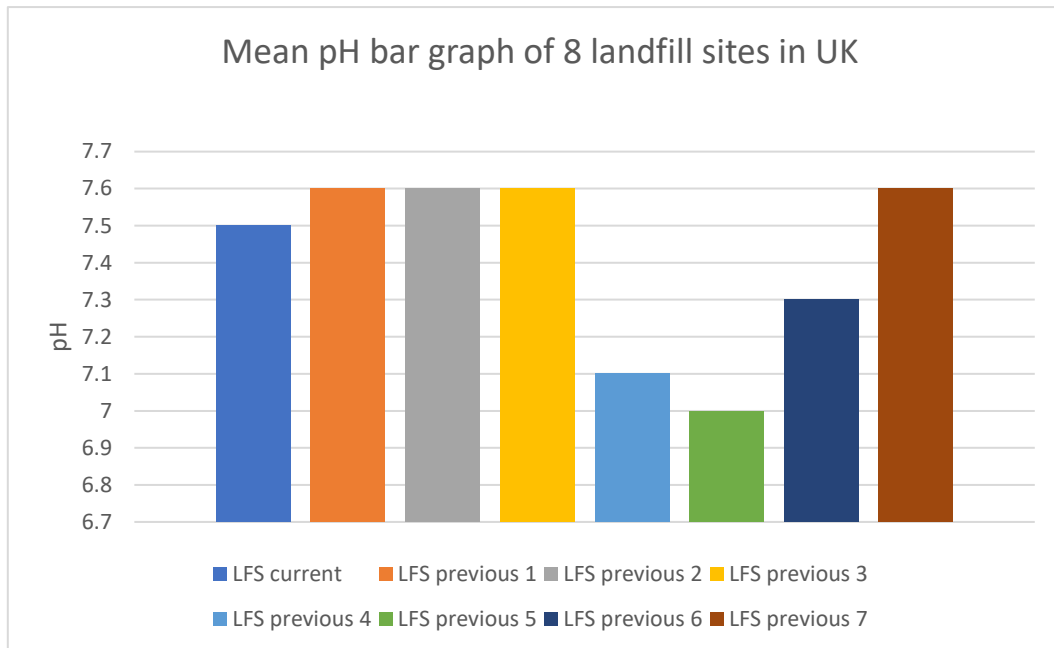


Figure 24. Mean pH in the UK landfill sites, including the current site.

4.7 Oven Drying

All representative samples were oven-dried at 105°C for 3 days for PSD, TOC, ICP-OES, and SEM-MLA analyses.

4.8 Particle Size Distribution (PSD)

A total of around 800 g representative samples of each well was applied for PSD test. Mechanical sieving was used for dividing the samples according to their size fractions for 15 min for each well. The weight and percentage of each sieve was recorded.

The particle size distribution (PSD) test is one of the key parameters in specifying the physical properties of the landfill wastes (Jani et al., 2016). Studying this parameter helps to estimate/model the quantity of the fine fractions that could be dispersed as the form of dust in conjunction with the moisture content during LFM activities. The specific surface area of the waste is affected by particle size (Dino et al., 2018). The larger the specific surface area of a particle, the finer it is.

The fine fractions of waste (soil-like material) make up a considerable proportion of the total amount of MSW disposed of in landfills (60%–70%) from many previous studies, which is resulting from the daily cover of soil, C&D waste, and the humification of organic matter (Parrodi et al., 2018a; Somani et al., 2018). A study by (Francois et al., 2006) in physico-chemical characterisation of landfilled MSW of different ages (3, 8, 20 and 30 years old) at four different sites, pointed out that there is a clear gradual reduction of waste fractions over time (Wang et al., 2021a). A similar trend of particle size reduction was also evidenced in another study by (Singh and Chandel, 2022). This behaviour is attributable to degradation processes of organic materials over time in a landfill (Parrodi et al., 2018a). Thus, it is anticipated that the quantity of fine fractions will be large given the age of the landfill under the study.

The dry sieving results of the waste fractions of the four wells to the particle sizes (>26.5, >22.4, >19, >16, >12.5, >9.5, >6.7, >4.75, >3.35, >2.36, >1.7, >1.18, >0.85, >0.6, >0.425, >0.3, >0.212, >0.15, >0.106, >0.075, >0.053, >0.038, and ≤ 0.038 mm) are illustrated in Figure 25. They demonstrated similar behaviours in all wells. Nearly 70% of the total excavated waste fractions of the four pits passed through a sieve diameter of 4.75 mm, whereas approximately 56% of the particles were ≤ 2.3 mm in size. These fractions were mainly soil-like materials with similar consistency to the soil. MSW fractions of 0.106 mm accounts for 11% of the passings within all wells as an average. Well no. 1901 presented the highest level of fines within

the four wells (2.5% of the analysed waste fractions less than 0.075 mm and higher than or equal to 0.053 mm). Photographs of different size fractions from all wells are shown in Figure 26 (a-d).

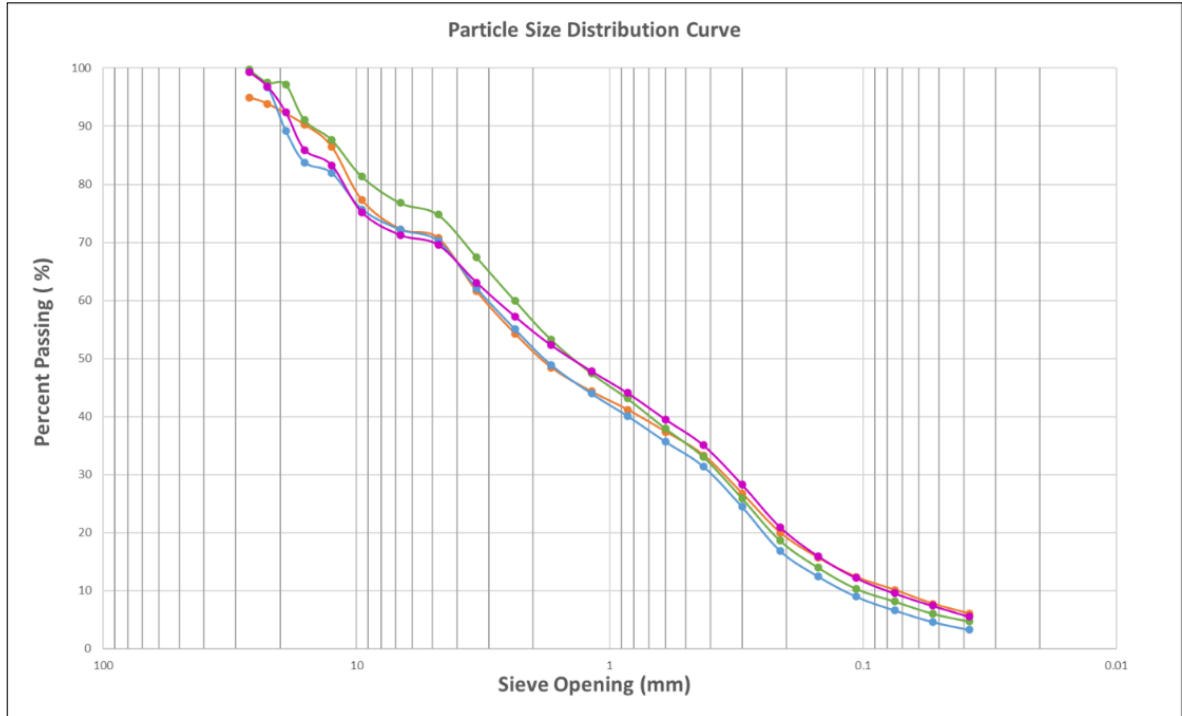


Figure 25. Particle size distribution cumulative passing curve for different sieve sizes of all wells.

a)



b)



c)



d)



Figure 26. Different size fractions of wells. (a) well 1901 (b) well 1904 (c) well 1906 (d) well 1907.

According to visual observation, soil fraction was particularly prevalent within the particle size fraction <4 mm. A complex mixture of waste compositions was observed during sample processing and sieving, as was expected by the heterogeneity and degradation processes associated with landfilled waste. The results of PSD were comparable with that of (Mönkäre et al., 2016) with 70% of the MSW waste fraction (24-40 years old) less than the particle size of 5.6 mm. They were also in agreement to that of (Masi et al., 2014), with approximately 65% of the waste fine fraction (30-60 years old) <4 mm. In contrast, (Prechthai et al., 2008), found that 70% of the MSW fractions of (3-5 years old) >50 mm, while only 18% <25 mm. As stated in the literature, the difference in the results between different studies is particularly owing to the landfilled MSW age.

4.9 Heavy Metals

A total of 20 samples from the four wells (5 from each well) of different size fractions ≤ 0.106 mm were analysed for heavy metals. Analysis was performed using the Agilent 5110 VDV inductively coupled plasma - optical emission spectrometry (ICP-OES) equipped with sea-spray nebuliser and concentric spray chamber and controlled with ICP Expert software. According to (Thermo Fisher Scientific, 2015), ICP-OES has been proven to be more robust for analysing solid waste since samples may contain suspended solids. Approximately 0.5 g mass was used for each sample. The digestion was performed using 9 ml concentration nitric acid and 3 ml hydrochloric acid due to the element suite considered to achieve the highest possible quantity of the extracted metals. Afterward, samples were placed in the microwave leach using concentrated acids as described in EPA 3051A. Then, the leachates were diluted to 100 ml with 18.2 MOhm water and filtered through 0.45 μm filter prior to analysis. The digestion analysis was carried out in two batches through the microwave for ICP-OES analysis. Each batch contained a reagent blank to test for contamination or carryover. Each batch also contained a homogeneous soil sample as an indication of repeatability. Multi-component calibration standards were prepared from Romil single element certified standards diluted in the sample matrix (9% v/v nitric acid, 3% v/v HCl). K, Ca and Na were also added to mimic the ionic strength of the samples. Presence of iron in the samples presented interference to quantification of Cd and Pb so a correction called FACT (Fast Automated Curve-fitting Technique) was used to deconvolute the spectra prior to quantification. Two wavelengths were reported for each element for confirmation purposes. In this study, the following metals were analysed: Pb, Cd, Zn, Cu, Cr, Co, As, Ni, Ba, and Mn, which were selected as being of greatest concern in European and American communities (Abu-Daabes et al., 2013; Cortés et al., 2021). Table 8 presents the heavy metal concentrations of the four wells for different size fractions.

Table 8: Selected heavy metal concentrations of the four wells of various size fractions.

Well number	Particle size (μm)	As (mg/kg)	Ba (mg/kg)	Cd (mg/kg)	Co (mg/kg)	Cr (mg/kg)	Cu (mg/kg)	Mn (mg/kg)	Ni (mg/kg)	Pb (mg/kg)	Zn (mg/kg)
1901	<38	37.1	273.9	2.0	16.5	172.7	514.1	2039.2	51.7	285.1	2205.6
1901	38	28.0	184.4	1.4	12.0	125.0	194.7	1802.9	34.8	191.6	2057.5
1901	53	21.4	158.0	1.2	10.0	104.6	139.8	1648.1	28.7	167.2	1864.3
1901	75	18.5	122.7	1.1	8.0	76.7	126.8	1455.4	22.8	147.9	1645.3
1901	106	17.5	124.1	1.0	7.6	70.2	104.1	1162.1	21.6	146.4	1298.1
1904	<38	42.7	245.9	1.4	17.5	148.5	532.5	766.2	53.7	1356.2	746.7
1904	38	30.0	159.7	0.8	12.9	109.6	215.3	557.3	35.2	1133.5	571.4
1904	53	26.8	128.9	0.8	10.5	88.9	140.6	466.7	29.0	1012.8	477.5
1904	75	22.6	108.7	0.6	9.0	70.5	249.5	390.4	23.9	803.0	415.8
1904	106	16.6	94.3	2.6	7.2	58.3	49.2	318.3	19.4	623.3	315.6
1906	<38	60.4	358.4	2.6	22.2	118.4	695.7	930.8	70.0	304.2	688.9
1906	38	41.5	245.7	1.8	15.9	95.4	212.6	799.6	47.8	213.1	571.7
1906	53	32.4	204.7	1.6	13.3	77.6	136.2	596.7	39.1	173.4	432.0
1906	75	25.7	160.1	1.5	10.3	64.6	81.4	430.7	29.2	140.3	294.2
1906	106	21.8	136.1	0.9	8.5	54.4	72.0	339.0	25.5	147.0	231.9
1907	<38	62.6	580.0	1.2	23.5	107.8	775.8	755.3	79.8	311.8	850.3
1907	38	45.4	385.6	0.2	17.2	82.2	235.0	629.3	57.8	225.9	625.5
1907	53	37.8	313.0	0.2	15.3	65.7	138.1	523.4	47.0	189.6	532.0
1907	75	29.8	237.9	0.1	11.0	52.7	77.0	443.0	34.8	164.2	434.4
1907	106	25.9	201.3	0.1	9.4	40.4	60.1	388.7	29.9	129.2	358.0

To evaluate contamination potentials of excavated waste from a LFM, characterisation of heavy metals is of great importance in terms of environmental and health risks (Adelopo et al., 2018; Esakku et al., 2003; Jain et al., 2005; Sharifi et al., 2016; Xiaoli et al., 2007). Exposure to such heavy metal concentrations may lead to numerous health problems, particularly in susceptible individuals, including the elderly and children (Briki et al., 2017; Dubey et al., 2012; Kamunda et al., 2016; Stewart, 2019). These heavy metals have been reported to stimulate carcinogenesis of organs like kidney, lungs, skin, and bladder (Bhatti et al., 2020; Gujre et al., 2021; Health and Services, 1999; Hussein et al., 2021). Heavy metals are of great concern because, unlike organic pollutants, they remain unaffected during the degradation of waste, thereby having adverse impacts on living organisms (Esakku et al., 2003; Jain et al., 2005; Kirpichtchikova et al., 2006; Mehta et al., 2019; Wuana and Okieimen, 2011).

According to (Adelopo et al., 2018), degradation of waste may reduce landfilled waste weight, but concentration of heavy metals is not always reduced or changed. Heavy metal migration is

limited in comparison to the quantity of metals accumulated in the landfill, especially in the anaerobic processes, and thereby the majority of heavy metals will remain in the landfills (Øygard et al., 2004; Riber et al., 2005). The reason of the slow migration of heavy metals is due to the proneness to strong sorption on soil particles, precipitation that heavy metals undergo under anaerobic conditions, chelation with inorganic and organic ligands in landfills, and the presence of buffering substances in the landfill during the anaerobic process (carbonates) which neutralise pH (Bozkurt et al., 1999; Bozkurt et al., 2000; Xiaoli et al., 2007). It is believed that the presence of toxic heavy metals in soil/waste can significantly inhibit the biodegradation of organic contaminants (Gworek et al., 2016; Hussein et al., 2021; Wuana and Okieimen, 2011). In this regard, heavy metals are problematic owing to their potential complex pathways within the environment and will continue to exist in the waste unless leached out (Jain et al., 2005; Singh and Chandel, 2022). Residual time of heavy metals in an MSW landfill is expected to be approximately 150 years when the metals are leached at a rate of 400 mm/year, which indicates only a small amount of heavy metals content is reflected in the leachate (Adelopo et al., 2018; Hussein et al., 2021). The main heavy metal content is reflected in the solid form of the waste resulting from the interaction between heterogeneous landfilled waste, local landfill management (e.g., top layer), climatic conditions, and degradation activities (Adelopo et al., 2018; Holm et al., 2002). In this regard, some studies have demonstrated that the concentrations of heavy metals in solid waste samples are significantly higher than those in landfill leachates (Øygard et al., 2004; Xiaoli et al., 2007).

During biodegradation, the metal content increase with volume reduction (Esakku et al., 2003). This means that older landfills have higher concentrations of heavy metals than do younger landfills because of transformation processes of fresh MSW over time (Quaghebeur et al., 2013; Singh and Chandel, 2022). It is also due to the redistribution of these metals resulting from waste decomposition and leaching process within the depth of the landfill (Adelopo et al., 2018;

Jain et al., 2005). According to (Singh and Chandel, 2022), sorption, desorption, formation of carbonate bound metals, precipitation of metal sulphides in reducing environment, formation of metal hydroxide and soluble/insoluble metal organic complexes are all examples of transformation process of heavy metals in landfills. Another study investigated the effect of age on heavy metals content of closed and active MSW landfill, and the results showed that the concentrations of heavy metals in closed landfills were significantly higher than those in the active landfill for 11 of 15 heavy metals studied because more degraded components of waste have the ability to adsorb more heavy metals owing to the increased porosity within surface area and the ability to forming a stronger bonding system (Adelopo et al., 2018). The potential of heavy metals propagation into the micro pore of soil and solid waste through co-precipitation and co-flocculation processes is inherent in older landfills (ibid). Therefore, fate and transport of solid waste heavy metals are determined by a number of complexation mechanism with pore water and waste molecules (Singh and Chandel, 2022). On the other hand, in the studies by (Lee et al., 2022a; Lee et al., 2023; Lee et al., 2022b; Ziyang et al., 2009), the accumulation of heavy metals demonstrated an inverse relationship with landfill age. However, this trend is believed to apply to landfill leachate, not to the solid form of waste owing to the high sorption capacity of humic acid in old landfills that enables the retention of metals within the solid waste (Lee et al., 2022a; Lee et al., 2022b) and the decrease in metal solubilization (due to an increase in pH) (Hussein et al., 2019; Lee et al., 2022a). The focus of this study is on the solid waste as it is the form that can be released (become airborne) from landfill sites during LFM activities.

Previous investigations on the characterisation of particle size fractions associated with heavy metals showed that the accumulation of heavy metals is maximal for fine fractions because of the high specific surface area of fine fractions. (Burlakovs et al., 2018; Padoan et al., 2020; Parrodi et al., 2018a; Wolfsberger et al., 2015; Yao et al., 2015). Therefore, the heavy metals

were analysed for fine fraction samples of ≤ 0.106 mm from the four wells. Appendix 7 shows the descriptive statistics of the metals within the four wells. In the fractions, the concentrations of the metals based on average followed the order Zn>Mn>Pb>Cu>Ba>Cr>Ni>As>Co>Cd.

ANOVA analysis showed significant differences for the Pb ($P<0.001$), Zn ($P<0.001$), Mn ($P<0.001$), Cd ($P<0.018$) and Ba ($P<0.026$) values in the four wells, indicating that the data sets were randomly distributed (Appendix 8). The LSD tests (Appendix 9) demonstrated that the Pb concentration in well 1904 was significantly higher than those in wells 1901, 1906, and 1907 ($P<0.001$). The Zn concentration in well 1901 was significantly higher than those in wells 1904, 1906, and 1907 ($P<0.001$). The Mn for well 1901 was significantly higher than those for wells 1904, 1906, and 1907 ($P<0.001$). The Cd concentration in well 1901 was significantly higher than that in well 1907 ($P=0.020$). The Cd concentration in well 1904 was significantly higher than that in well 1907 ($P=0.040$). The Cd concentration in well 1906 was significantly higher than that in well 1907 ($P=0.003$). In addition, the Ba concentration in well 1907 was significantly higher than those in wells 1901 ($P=0.013$) and 1904 ($P=0.006$).

Pearson's correlation analysis (2-tailed) showed significant positive correlations between As and Ba ($r=0.917$, $P<0.001$), As and Ni ($r=0.988$, $P<0.001$), As and Cr ($r=0.466$, $P=0.038$), As and Co ($r=0.987$, $P<0.001$), and As and Cu ($r=0.846$, $P<0.001$). In addition, there were significant positive correlations between Zn and Mn ($r=0.986$, $P<0.001$), Zn and Cr ($r=0.620$, $P=0.004$), Mn and Cr ($r=0.668$, $P=0.001$), Cd and Cr ($r=0.465$, $P=0.039$), Ba and Ni ($r=0.942$, $P<0.001$), Ba and Co ($r=0.903$, $P<0.001$), Ba and Cu ($r=0.743$, $P<0.001$), Ni and Cr ($r=0.529$, $P=0.017$), Ni and Co ($r=0.993$, $P<0.001$), Ni and Cu ($r=0.862$, $P<0.001$), Cr and Co ($r=0.579$, $P=0.008$), Cr and Cu ($r=0.705$, $P=0.001$), and Co and Cu ($r=0.872$, $P<0.001$) (Appendix 10). Some of these correlations are illustrated in Figure 27. The significant correlations between these heavy metals suggest their common origins and sinks in the MSW. They can be subsequently used to

compare different environmental compartments around the landfill site, as the studied landfill has been previously assessed for LFM feasibility.

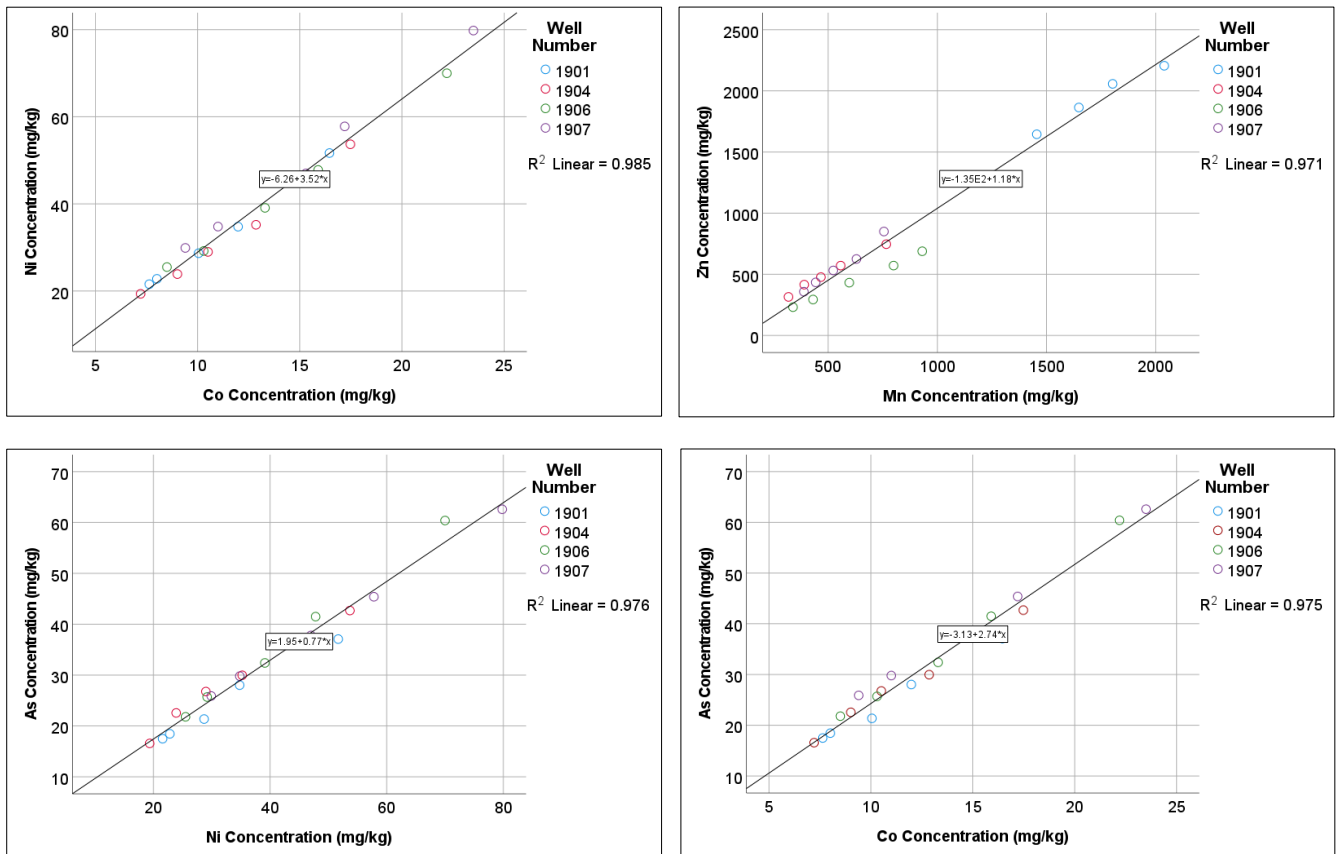


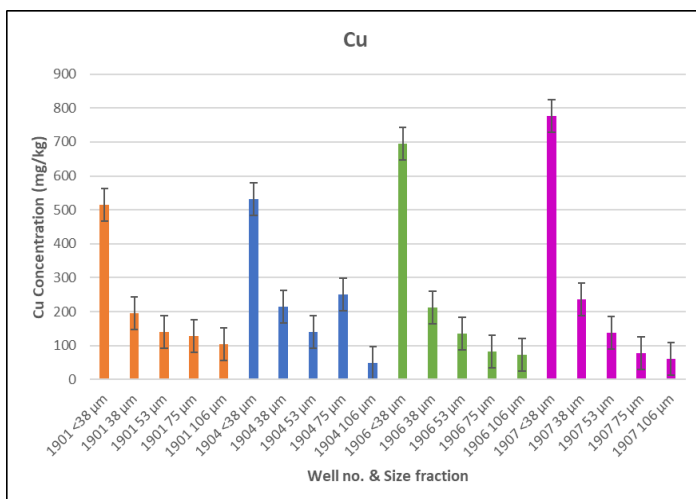
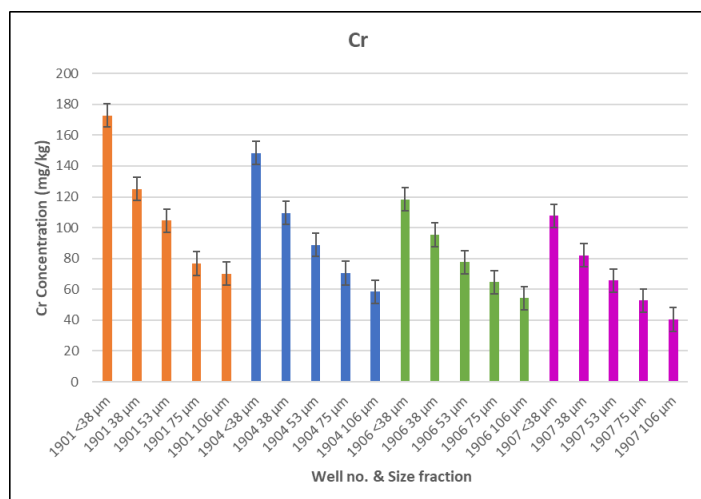
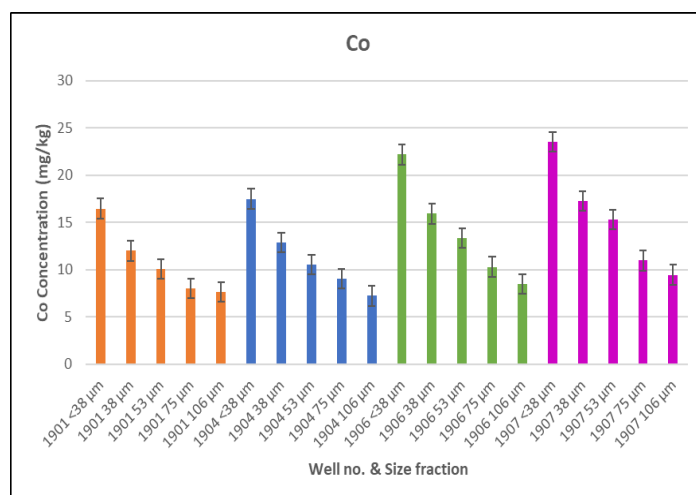
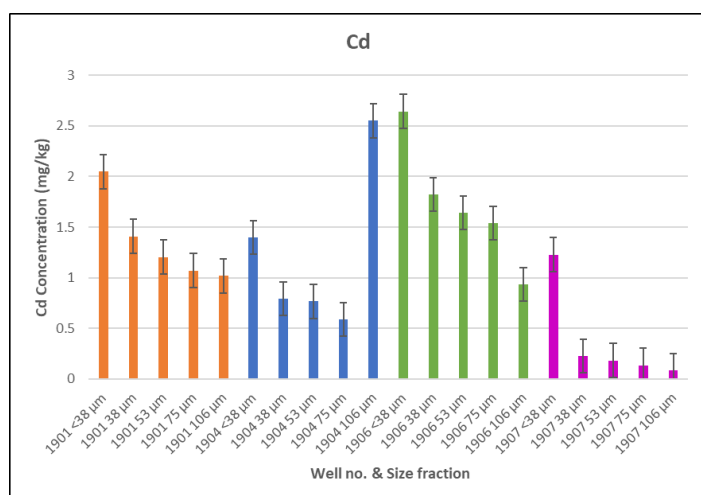
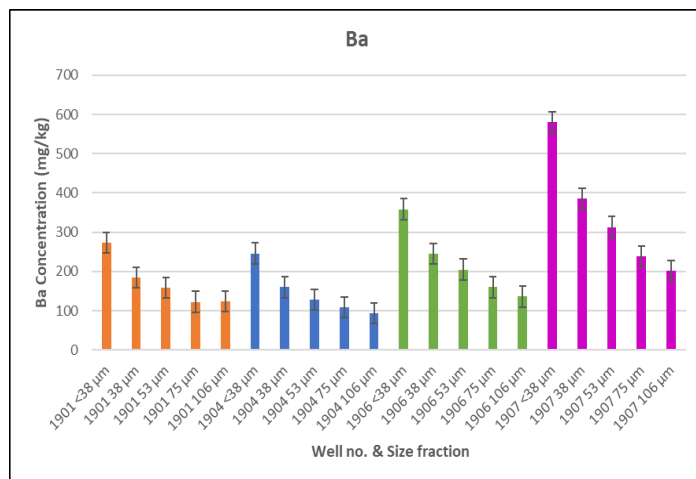
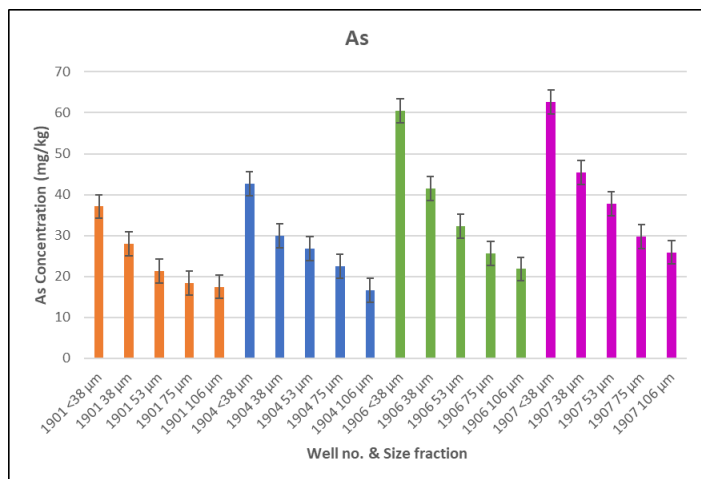
Figure 27. Heavy metals correlated using linear regression.

It was clear that the concentrations of heavy metals increased with a decrease in the size of the waste fractions, with the values for As, Ba, Co, Cr, Cu, and Ni being significant ($P < 0.02$) according to Pearson’s correlation (2-tailed) analysis (Table 9), which supports previous findings. This richness of heavy metals in finer fractions is mainly due to the greater surface adsorption potential of heavy metals and ionic attraction compared to coarse particles, indicating a high specific surface area available for interaction (Filgueiras et al., 2002; Wolfsberger et al., 2015). Individual heavy metal bar graphs of the four different wells with their different size fractions are shown in Figure 28.

Table 9: Correlation analysis between waste size fractions and heavy metals.

Correlation between waste size fractions and various heavy metals

		Size	Pb	As	Ba	Cd	Co	Cr	Cu	Mn	Ni	Zn
Size fractions	Pearson Correlation	1	-.254	-.698	-.561	-.182	-.767	-.756	-.623	-.364	-.715	-.308
	Sig. (2-tailed)		.280	.001	.010	.442	.000	.000	.003	.115	.000	.187
	N	20	20	20	20	20	20	20	20	20	20	20



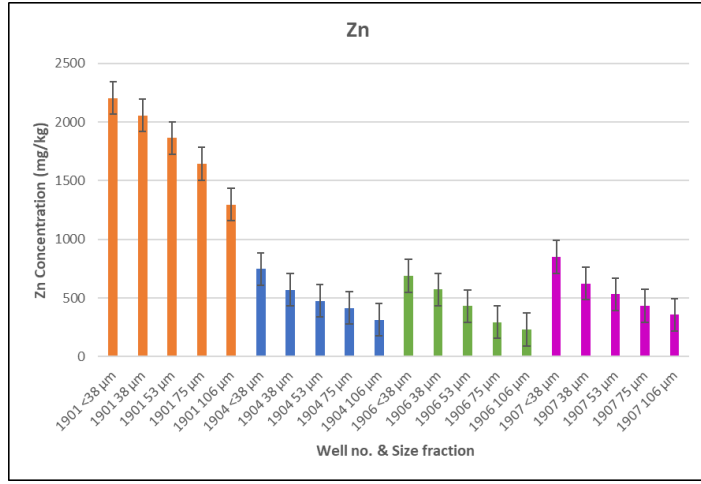
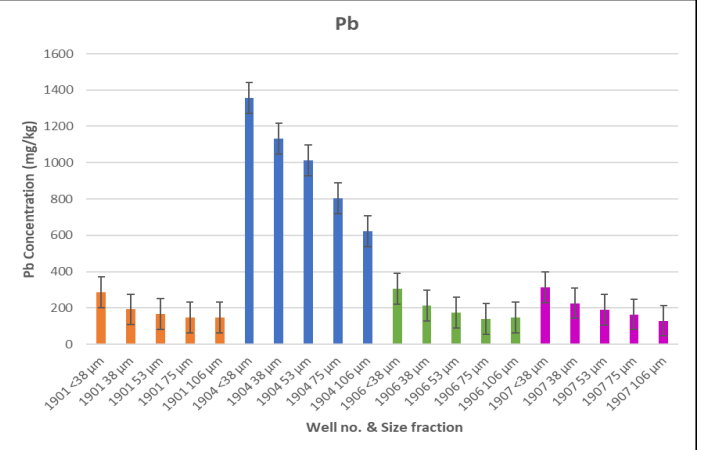
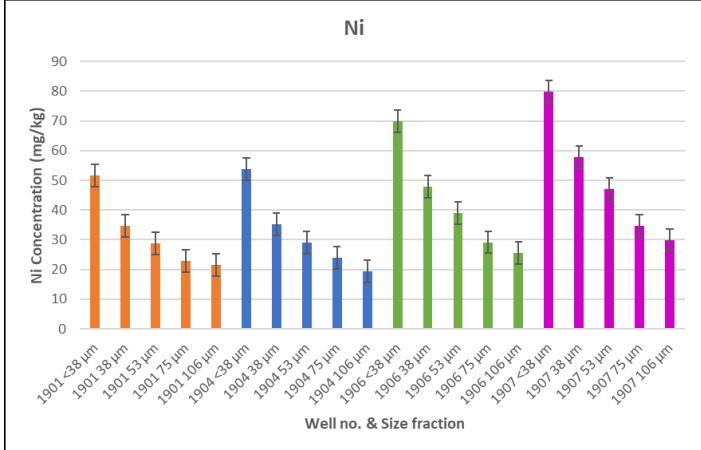
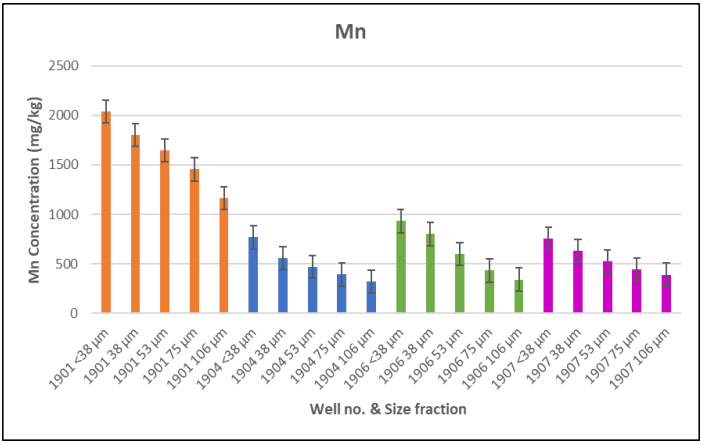
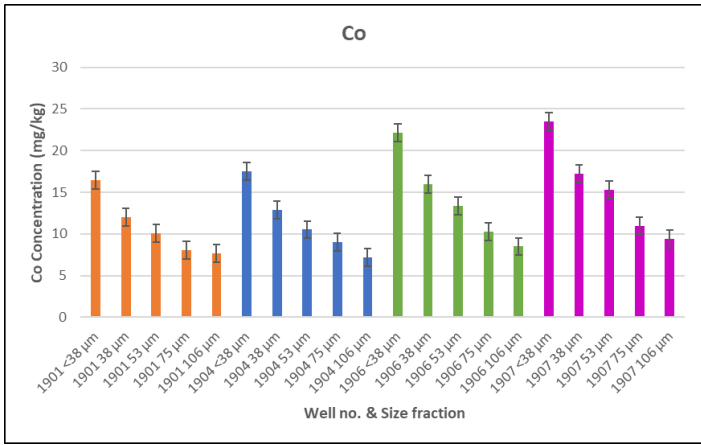
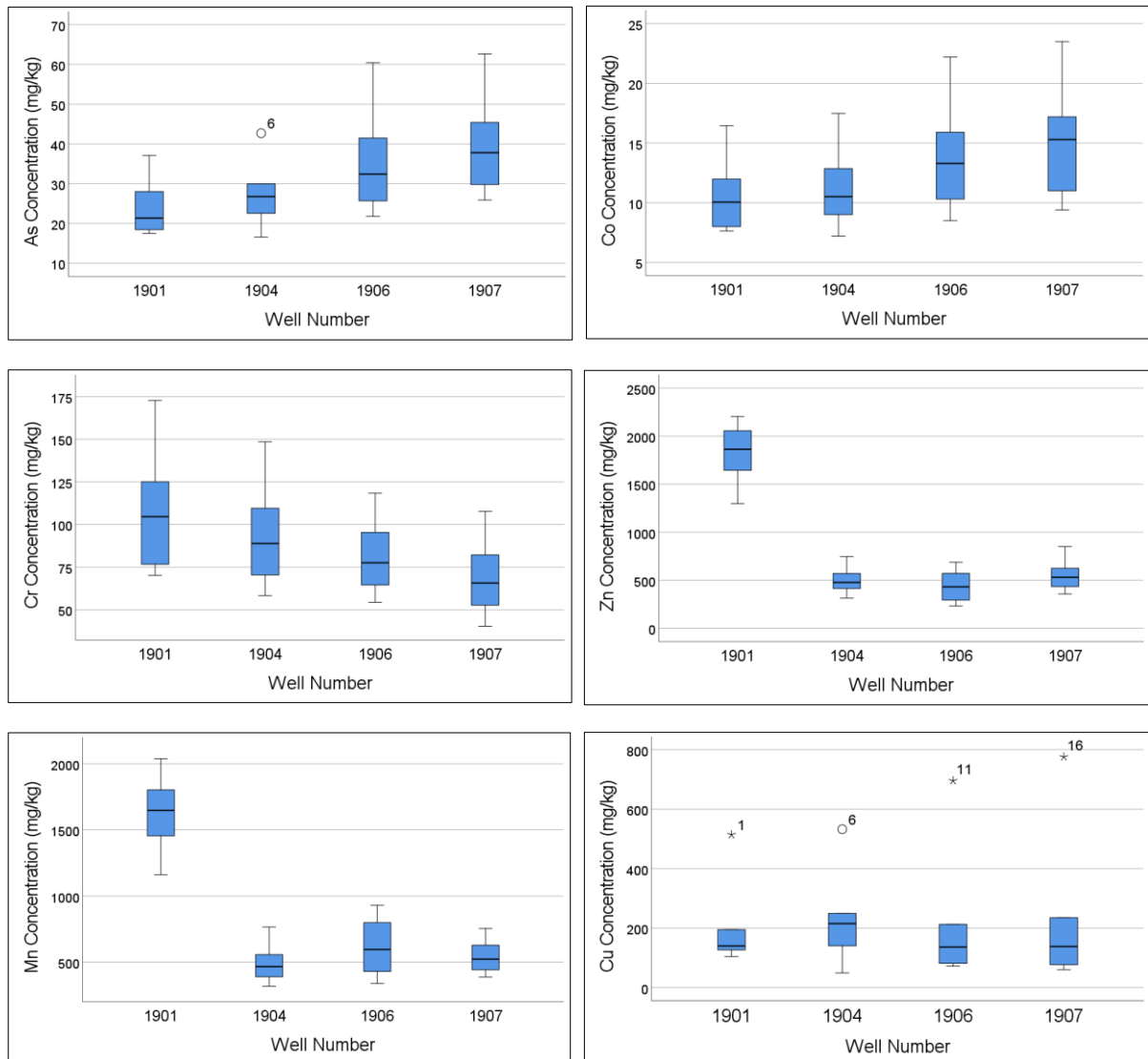


Figure 28. Heavy metals concentration with their different size fractions.

A similar increasing trend is observed in heavy metal content of fine fraction by (Singh and Chandel, 2020) and (Quaghebeur et al., 2013).

The box and whisker plots shown in Figure 29 compare the concentrations of each heavy metal within the four wells of the analysed landfill samples. They present the interquartile range (Q3-Q1), median (Q2, the line within the box), and outliers. The circle indicates that an outlier is present in the data, whereas the asterisk (*) indicates that an extreme outlier is present in the data. The box plots reveal fluctuating heavy metal concentrations within the studied wells, indicating the heterogeneity of the MSW landfills.



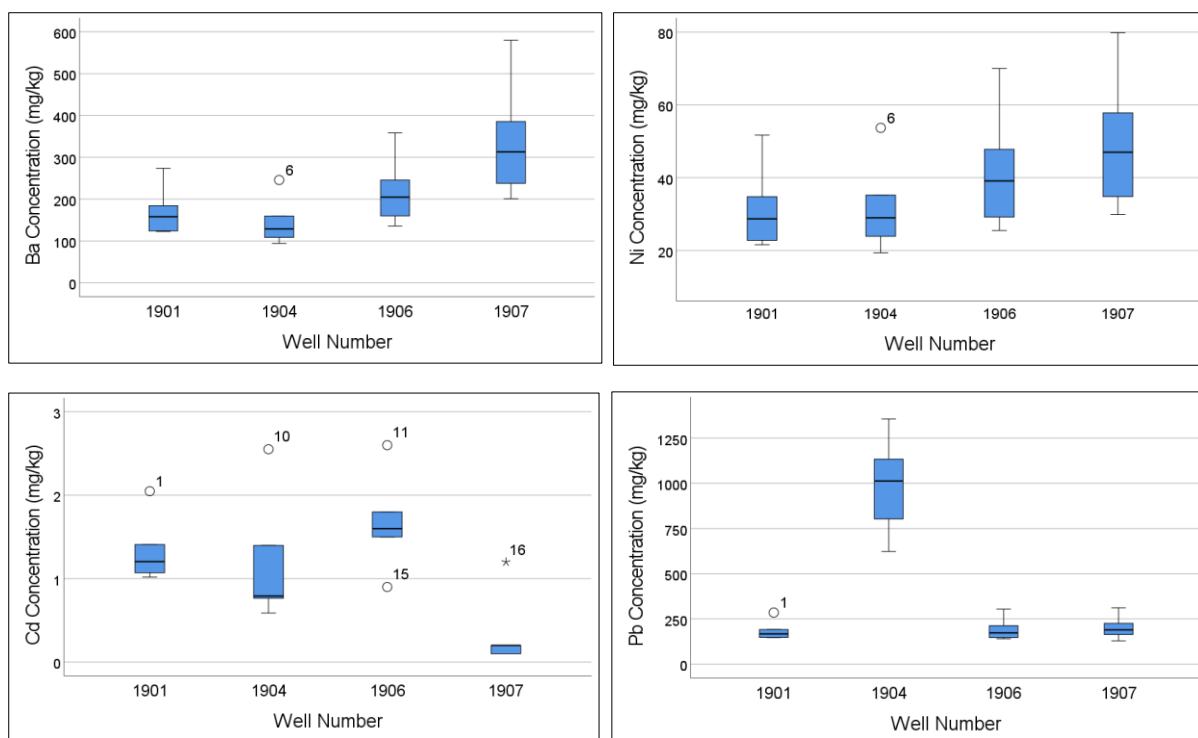


Figure 29. Comparison of heavy metal concentrations from landfill samples recovered from the four wells. The numbers above/below boxplots indicate which observation in the dataset (Table 11) is the outlier (numbers are arranged in descending order).

In terms of heavy metals mobility, many factors control the mobility of trace metals but the key parameters that influence heavy metals leachability is the pH and redox-potential of the surrounding environment (Król et al., 2019; Lee et al., 2023; van der Sloot and van Zomeren, 2012; Zomeren et al., 2014). Generally, the solubility of metals decreases with the increase of pH owing to the precipitation of metal ions at high pH values as insoluble hydroxides (Esakku et al., 2003; Hussein et al., 2021; Lee et al., 2022b). Heavy metals in the waste residues can be a significant environmental issue under low pH and high redox-potential conditions (Xiaoli et al., 2007). The pH results of this study are neutral, indicating that the heavy metals are poorly soluble when comes into contact with water of neutral/normal conditions. At a high pH value, mobilization of heavy metals can be restricted by the presence of oxides or sulphides, or by binding to organic matter (Xiaoli et al., 2007). Hence, the adverse environmental and human effects produced by heavy metals are closely related to their solubility and bioavailability in

the surrounding environment (Ogundiran and Osibanjo, 2009; Singh and Chandel, 2022). However, knowing that heavy metals are insoluble under normal neutral conditions does not necessarily mean that they pose no hazard to the surroundings as environmental conditions are susceptible to change (Mohajan, 2018).

Compared to a previous study by (Wagland et al., 2019) and (Scott et al., 2019) conducted on nine landfill sites and an individual landfill sites, respectively, in the UK, the levels of As, Pb, and Zn were much higher in the current study, whereas the Cd and Cu concentrations were relatively comparable. In contrast, significant accumulation of Cr was observed in their study (Wagland et al., 2019). Similarly, the Cu content in another study (Gutiérrez-Gutiérrez et al., 2015) was considerably higher than that in the current study. These variation of metals between the landfill sites can be attributed to specific solid waste input rich in particular metals (ibid). Batteries, paints, alloys, leather, textiles, and inks in paper and cardboard are all potential sources of heavy metals in MSW (Singh and Chandel, 2020).

Table 10 displays the generic assessment criteria of the UK Soil Guideline Values (SGVs) based on the corresponding land use. SGVs only consider the assessment of human health risks originating from long-term on-site exposure to individual chemicals in soil (Environment Agency, 2004). Compared to recommended maximum allowable limits set by the UK Soil Guideline Values, the highest value of As exceeded the SGVs by 30.6 and 19.6 mg/kg for the residential and allotment land uses, respectively. In addition, the maximum concentrations of Cd and Cr were above the limits for the allotment and residential land uses, respectively, resulting in plant uptake. Similarly, the Cu and Zn levels were beyond the limits set for the allotment land use. The highest Pb concentration was considerably greater than the set limits for all land uses, except for the commercial land use. Concentrations of soil above the guideline levels may cause significant harm to human health (Nathanail et al., 2015).

Table 10: Descriptive statistics of heavy metals according to the generic Assessment Criteria of UK Soil Guideline Values (Defra and Agency, 2009).

Parameter	Range and mean (mg/kg) of analysed heavy metals		Function of Land Use	CLEA Soil Guideline Value (SGV) mg/kg	Reference
As	Max	62.58	Residential	32	CL:AIRE (Environment Agency, 2009b)
	Mean	32.20	Allotment	43	
	Min	16.57	Commercial	640	
Ni	Max	79.80	Residential	130	CL:AIRE (Environment Agency, 2009b)
	Mean	39.07	Allotment	230	
	Min	19.36	Commercial	1800	
Cd	Max	2.64	Residential	10	CL:AIRE (Environment Agency, 2009b)
	Mean	1.16	Allotment	1.8	
	Min	0.09	Commercial	230	
Cr	Max	172.75	Residential with plant uptake	130	ALS (Council, 2003)
	Mean	89.20	Residential without plant uptake	200	
	Min	40.44	Commercial	5000	
Pb	Max	1356.16	Residential with home grown- produce	200	ALS (Council, 2003)
	Mean	393.28	Residential without home grown produce	310	
	Min	129.19	Allotment	80	
Cu	Max	775.82	Commercial	2300	LQM/CIEH S4Uls (Nathanail et al., 2015)
	Mean	237.52	Allotment	520	
	Min	49.18			
Zn	Max	2205.56	Allotment	620	LQM/CIEH S4Uls (Nathanail et al., 2015)
	Mean	830.83			
	Min	231.94			

Compared to globally recommended maximum allowable limits shown in Table 11, a mean of As 32.2 (mg/kg) exceeded the generic acceptance level in all countries on an average rate of 18.5 (mg/kg). Mean of Pb 393.2 (mg/kg) were above the limits of all countries, except for Sweden. Also, a mean of Zn 830.8 (mg/kg) exceeded all permissible limits of all countries without exception. A mean of Cd 1.16 (mg/kg) and Cr 89.2 (mg/kg) were higher than limit value for some countries, such as Germany and Bulgaria. A mean of Cu 237.5 (mg/kg) was considerably greater than the set limits of all countries. Significant accumulation of some metals including As, Pb, Cu, Zn, Cd, Cr, and Cu were observed, and these high concentrations

may be attributed to the disposal of metals-containing wastes of the Norfolk landfill. These metals should be given more attention for future LFM at the study area. They would likely limit the reuse of the residual soils depending on which regulatory threshold serves as a benchmark (Jain et al., 2005).

Table 11: Permissible limit of heavy metal concentrations in soil (mg/kg) for different countries (Jani et al., 2016; Kamunda et al., 2016).

Country	Maximum Allowable Limit of Concentrations of Heavy Metal in Soil (mg/kg) for Different Countries								
	As	Pb	Cd	Cr	Cu	Co	Ni	Zn	Mn
Sweden (EPA)	25	400	15	150	200	35	120	500	n.a.
Germany	50	70	1.0	60	40	n.a.	50	150	n.a.
Poland	n.a.	100	3	100	100	50	100	300	n.a.
Bulgaria	10	26	0.4	65	34	20	46	88	n.a.
EU Guidelines	n.a.	300	3	150	140	n.a.	75	300	n.a.
Australia	20	300	3	50	100	n.a.	60	200	n.a.
Canada	20	200	3	250	150	n.a.	100	500	n.a.
FAO/WHO Guidelines	20	100	3	100	100	50	50	300	n.a.
China	30	80	0.5	200	100	n.a.	50	250	n.a.
South Africa	5.8	20	7.5	6.5	16	300	91	240	n.a.

n.a.: Not available.

4.9.1 Heavy Metals Pollution Assessment

Generally, pollution indicators are the most efficient and suitable tools for the assessment of soil heavy metal pollution (Doležalová Weissmannová et al., 2019; Singh and Chandel, 2022); thus, they were used to assess the data in the current study, as discussed below.

4.9.1.1 Geo-accumulation index

The geo-accumulation index (I_{geo}) was used to examine the contamination level of landfill precursors affected by metals. It is a geochemical criterion (unitless) coined by (Muller, 1969) and has been widely employed in European research on trace metals (Li et al., 2014). It can be calculated using the following equation:

$$I_{geo} = \text{Log}_2 \left(\frac{C_n}{1.5B_n} \right)$$

where C_n is the measured concentration of heavy metal analysed in the landfill precursors and B_n is the normal background concentration in English soils, as reported by the BGS (Johnson et al., 2012). A constant of 1.5 was introduced to minimise potential variations in background values, referred to as lithogenic variations (Aiman et al., 2016; Hassaan et al., 2016). Classification of the I_{geo} pollution levels is presented in Table 12 (Muller, 1969; Rahman et al., 2012; Tang et al., 2015).

Table 12: Classification levels of geoaccumulation index (I_{geo}).

Geoaccumulation index (I_{geo})		
Class	Value	Classification
0	<0	Uncontaminated
1	0-1	Uncontaminated to moderately contaminated
2	1-2	Moderately contaminated
3	2-3	Moderately to strongly contaminated
4	3-4	Strongly contaminated
5	4-5	Strongly to extremely contaminated
6	>5	Extremely contaminated

Only five of the ten heavy metals were considered for the geo-accumulation index calculations because of the availability of normal background concentration data for English soils. Table 13 shows the class distribution of the geo-accumulation index of the heavy metals.

Table 13: Results of the geo-accumulation index of heavy metals.

Descriptive statistics (20 samples)	As	Cd	Cu	Ni	Pb
Geo-accumulation index (I_{geo})					
Max.	0.39	0.53	2.51	0.38	1.51
Mean	0.20	0.23	0.77	0.19	0.44
Min.	0.10	0.02	0.16	0.12	0.14

Numbers displayed in red indicate potential risks of contamination with different level ($1 < I_{geo} < 3$).

Three of the heavy metals evaluated (As, Cd, and Ni) had geo-accumulation indices between zero and one, indicating no contamination to moderate contamination. The maximum value of Cu was above two ($I_{geo} > 2$, indicating moderate to strong contamination), while its mean was 0.77, suggesting that some wells have a higher pollution potential than others, that is, contaminants are not uniformly distributed, as expected. Similarly, the maximum value of Pb was > 1 , which indicates moderate contamination based on the classification level.

4.9.1.2 Contamination factor (CF)

The contamination factor indicator represents the anthropogenic contribution of heavy metal pollution and is commonly used as a measure for landfill precursor pollution assessment (Adelopo et al., 2018; Pandey et al., 2016). The CF was obtained by dividing the concentration of heavy metals in the waste samples by their background concentrations (Chen et al., 2015).

The reference concentrations considered were obtained from the BGS (Johnson et al., 2012).

The CF (unitless) was calculated according to the following equation (Hakanson, 1980):

$$CF = \frac{C_i}{B_i}$$

where C_i is the concentration of the analysed heavy metal and B_i is the geochemical background value of that metal. The pollution levels of the CF were divided into seven classes, numbered 0 through to 6 (Table 14) (Doležalová Weissmannová et al., 2019; Pandey et al., 2016; Rahman et al., 2012).

Table 14: Classification levels of contamination factor (CF).

Contamination factor (CF)		
Level	Value	Categorisation
0	0	None
1	1	None to medium
2	2	Moderate
3	3	Moderate to strong,
4	4	Strongly polluted
5	5	Strong to very strong
6	≥ 6	Very strong

Only five of the ten heavy metals were considered for the CF calculations because of the availability of normal background concentration data for English soils. Table 15 shows the class distribution of the CFs of the heavy metals. Figure 30 illustrates the distribution pattern of the CF values within the four wells.

Table 15: Results of the contamination factor of the heavy metals.

Descriptive statistics (20 samples)	As	Cd	Cu	Ni	Pb
Contamination factor (CF)					
Max.	1.96	2.64	12.51	1.67	7.53
Mean	1.01	1.16	3.83	0.93	2.18
Min.	0.52	0.09	0.97	0.46	0.72

Numbers displayed in red indicate potential risks with different level of contamination ($1 < CF \leq 6$).

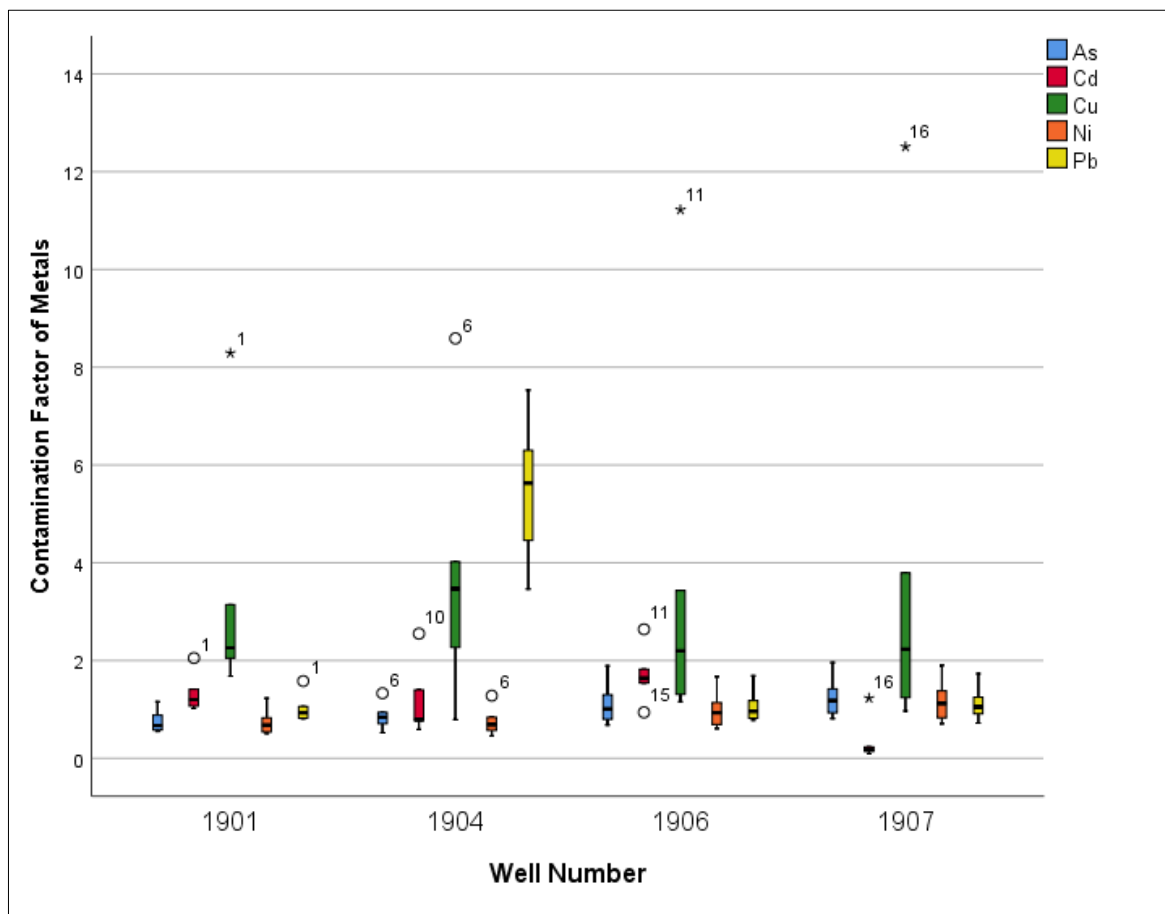


Figure 30. Boxplots of the contamination factor values of five heavy metals within the four wells.

The results of the CF revealed that the values followed a similar trend to the geo-accumulation index values, but with higher values owing to the direct calculation of the risk, which is different to how the geo-accumulation index was calculated. The CF values for As, Cd, and Ni fell between the categories of none-to-medium and moderate-to-strong. A significant concern was observed regarding the maximum CF values for Cu and Pb, with their pollution levels being classified as very strong (CF >6). The mean CF values for Cu and Pb fell within the moderate-to-strong degree of contamination.

4.9.1.3 Pollution load index (PLI)

To assess the overall pollution, the pollution load index provides a proven approach for calculating the accumulation of heavy metals in samples (Kowalska et al., 2018; Wang et al., 2020). The PLI (unitless) can be obtained by calculating the geometric mean of the CFs of each element analysed (Tomlinson et al., 1980), as follows:

$$PLI = (CF_1 \times CF_2 \times CF_3 \times \dots \times CF_n)^{1/n}$$

where n is the number of analysed heavy metals and CF is the contamination factor of each metal. A PLI value >1 indicates the presence of pollution, whereas no pollution load is indicated by a value <1 (Pandey et al., 2016; Tomlinson et al., 1980).

PLI index calculation was equal to 1.55. The PLI value of 1.55 indicates that there is a pollution load within the site, which reflects the pollution of metals in waste materials. The nature of contamination found in the current study based on the three calculated indices is comparable to the results of previous investigations (Adelopo et al., 2018; Kolawole et al., 2018; Somani et al., 2020).

4.9.2 Health Risk Assessment

A human health risk assessment is used to assess the potential impacts of chemical exposure in contaminated environmental media on human health (Li et al., 2014; Reyes et al., 2021). They were used to assess the data in the current study, as discussed below.

4.9.2.1 Non-carcinogenic (HQ) health hazard characterization

A human health risk assessment is extensively used for estimating the health effects of heavy metals as a result of exposure to these chemicals (Doležalová Weissmannová et al., 2019). Quantification of heavy metals has been categorised by the (USEPA, 2002) as being non-carcinogenic or carcinogenic in human health risk assessments (Kamunda et al., 2016). The exposure of humans to heavy metals from soil is estimated through three main exposure routes: ingestion of substrate dust particles, inhalation of suspended dust particles through mouth/nose, and dermal contact/absorption of heavy metals in particles adhered to exposed skin, according to the recommendations and methodology of the USEPA (Adelopo et al., 2018; USEPA, 2002). The non-carcinogenic risk effect is typically characterised by the hazard quotient (HQ), which is defined as the ratio of the average daily intake to the toxicity threshold value (also referred to as the reference dose) of a chemical for the same exposure. It is also characterised by the hazard index (HI), which estimates the overall potential for non-carcinogenic effects. Both the HQ and HI are unitless, expressed as an individual's likelihood of experiencing adverse effects. The equation used in this study was based on the recommendations provided by the Environment Agency (2009) (Hosford, 2009). In practice, when soil guideline values (SGVs) exist for a metal, the HQ and HI can be estimated by dividing the soil concentration of each contaminant by its SGVs and summing the results (Hosford, 2009). The derivation of SGVs was calculated based on all the exposure routes, considering four steps of hazard identification using the Contaminated land exposure assessment (CLEA) model (Sun et al., 2020). The HQ of each chemical was determined using the following equation:

$$HQ (non - carcinogenic) = \frac{C_c}{SGV}$$

where C_c is the contaminant concentration of each element and SGV is the soil guideline for the corresponding element. The HQ represents the non-carcinogenic risk from individual heavy metals, whereas the HI is the sum of the hazard quotient and indicates the cumulative non-carcinogenic risk. The HI was determined according to equation the following equation:

$$HI (non - carcinogenic) = \sum HQ$$

HQ and HI values <1 indicate a lack of adverse non-carcinogenic effects on health, whereas if HQ and $HI >1$, non-carcinogenic adverse health effects may occur (USEPA, 2002), and the likelihood of effects increases as the HQ/HI value increases.

The calculation of the HQ was based on the individual land use, as $SGVs$ are derived from different generic land use scenarios, which are described in detail in (Environment Agency, 2009a). A total of seven out of ten heavy metals were considered in the non-carcinogenic assessment because Ba and Co do not yet have published $SGVs$. The results of the HQ calculations are presented in Table 16. Following the results of the non-carcinogenic health risk assessment, the hazard index (HI) values are displayed in Table 17, with the categorised risk levels (Tenebe et al., 2018).

Table 16: Potential human health non-carcinogenic risk assessment index (HQ) of heavy metals categorised by intended future land use.

Statistics (20 sample)	Hazard quotient (HQ)						
	As	Ni	Cd	Cr	Pb	Cu	Zn
Allotment							
Maximum	1.46	0.35	1.47		16.95	1.49	3.56
Mean	0.75	0.17	0.65		4.92	0.46	1.34
Minimum	0.39	0.08	0.05		1.61	0.09	0.37
Commercial							
Maximum	0.10	0.04	0.01	0.03	0.59		
Mean	0.05	0.02	0.01	0.02	0.17		
Minimum	0.03	0.01	0.00	0.01	0.06		
Residential							
Maximum	1.96	0.61	0.26				
Mean	1.01	0.30	0.12				
Minimum	0.52	0.15	0.01				
Residential with plant uptake / Residential without plant uptake							
Maximum				1.33/0.86			
Mean				0.69/0.45			
Minimum				0.31/0.20			
Residential with home grown-produce / Residential without home grown-produce							
Maximum					6.78/4.73		
Mean					1.97/1.27		
Minimum					0.65/0.42		

Numbers displayed in red indicate potential risks (HQ >1)

Table 17: Overall potential for non-carcinogenic (HI) effects of heavy metals and the associated risk-level categories.

Descriptive	Hazard index (HI) mean values for non-carcinogenic risk	Level of risk
Allotment	8.28	High
Commercial	0.27	Low
Residential of all different uses	7.21	High

Numbers displayed in red indicate potential risks (HI >1)

The highest HQ for As was 1.96 for the residential land use, followed by a value of 1.46 for the allotment land use. The mean for Pb was 4.92, with a maximum value of 16.95 for the allotment land use. The mean Zn value was greater than one for allotment land use. The HQ for Ni was the only metal within the acceptable limit (HQ <1) for all land-use scenarios. High HQ values were observed, indicating heavy metal pollution that might pose non-cancer health risks to surrounding populations. Compared to the equations provided by the USEPA for the health risk assessment, the equation of HQ applied in this study is more suitable for this study because it uses the UK-based Soil Guideline Values (SGVs) for different land uses.

The HI denotes the cumulative non-carcinogenic health risk index, and the highest mean value of HI was found for the allotment land use, followed by the residential land use. The heavy metal Pb was found to be the greatest contributor to non-carcinogenic risk.

4.9.2.2 Carcinogenic (CR) health risk analysis

The carcinogenic risk (CR) and lifetime cancer risk (LCR) were calculated using the following equations, respectively, which express the likelihood of developing cancer in a lifetime due to potential carcinogen exposure (unitless).

$$CR \text{ (carcinogenic risk)} = Cc \times SF$$

$$LCR = \sum CR$$

where Cc is the contaminant concentration of each element analysed and SF is the cancer slope factor identified by (USEPA, 2002). The values for As, Cd, Pb, Cr, and Ni are 20.26, 6.3, 0.0085, 42, and 0.84 mg/(kg·day), respectively (Adimalla and Wang, 2018; Chen et al., 2015; Ferreira-Baptista and De Miguel, 2005; USEPA, 2002). The cancer SF directly converts the estimated daily intake of an average toxin over a lifetime of exposure to the incremental risk

of developing cancer (Li et al., 2014). The LCR is the summation of CR values and indicates the overall risk. Values above 1×10^{-4} are considered unacceptable and indicate significant health effects, whereas values below 1×10^{-6} indicate nonsignificant health effects. Values ranging from 1×10^{-4} to 1×10^{-6} are generally considered tolerable (Fryer et al., 2006; Hu et al., 2012; Li et al., 2014; Tenebe et al., 2018).

Owing to the lack of carcinogenic slope factors for Cu, Mn, Co, and Zn, only the cancer risks for the other five metals (As, Cd, Pb, Cr, and Ni) were estimated. The cancer risk values of the heavy metals are illustrated in Figure 31, which presents a comparison between the elements.

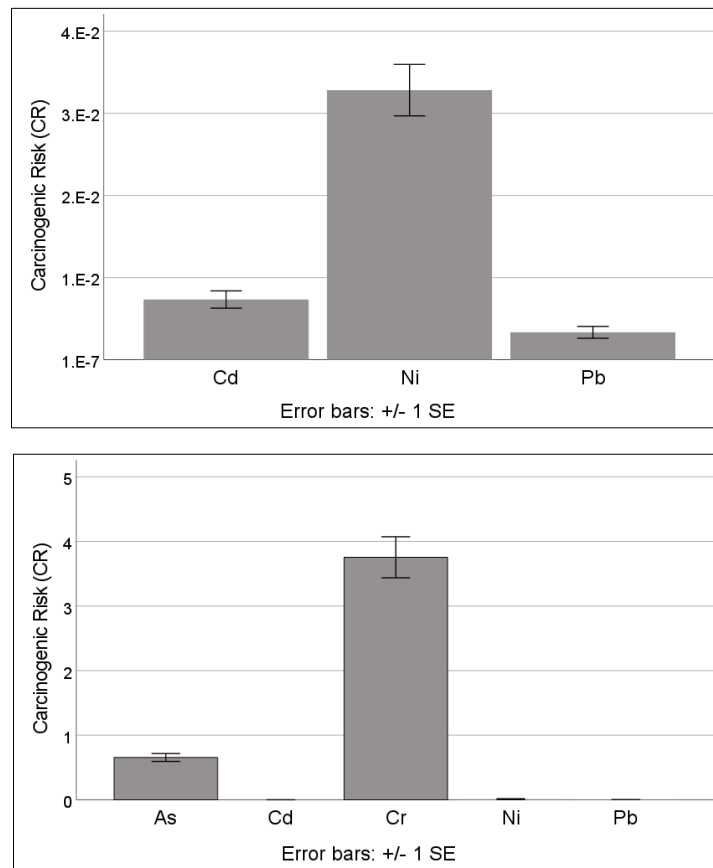


Figure 31. Cancer risk (CR) values of heavy metals.

Overall, the CR values calculated to assess the carcinogenic health risk of metal(loid)s were found to be significantly higher than the acceptable range of 1.0×10^{-6} to 1.0×10^{-4} . The CR factors from all routes implied that Cr and As were the most potent health risk hazards. The

risk potential of the metals was in the order Cr>As>Cd>Pb>Ni, and the mean total LCR value was 4.44. Elevated values of cancer risk suggest that more attention should be paid to heavy metal concentrations prior to LFM, since heavy metals, including Cr, As, Cd, and Pb, are classified as metals with carcinogenic health risks (Doležalová Weissmannová et al., 2019). It is evident that, with respect to the carcinogenic risk levels and required standards, the values obtained indicate a risk to human health, especially in the case of Cr. Compared to the current study, a recent study by (Wagland et al., 2019) showed significantly greater levels of chromium (834 mg/kg) within waste materials, suggesting the necessity to consider the human health risks posed by Cr in its enhanced LFM framework. The source of Chromium is believed to be resulting from potentially hazardous substances such as paints, batteries, and chemical or industrial wastes (Wagland et al., 2019).

4.10 Total Organic Carbon (TOC)

TOC was analysed for ten samples of the fine fraction ≤ 0.106 mm for wells 1901 and 1904 only (5 per well), as they represented the highest and lowest COD values. The test was performed using LECO CHN628 TOC analyser. TOC values were obtained by high temperature combustion. The organic carbon was oxidized to CO₂ and detected by an infrared analyser. Approximately 70 mg dry sample was used in the analysis for each sample. TOC is the total amount of organic carbon, that is, the total carbon present as organic molecules (Standard, 1997). Knowing the TOC helps determine the state of degradation of landfilled waste (Singh and Chandel, 2020) and ensure the safety of a workplace by quantifying the level of methane that can be airborne during LFM, which is crucial for determining the suitability of a site for LFM (Pecorini and Iannelli, 2020). Thus, TOC was analysed in this study, which refers to the total amount of carbon that is organic in origin, including VOCs (Bisutti et al.,

2004; MacKinnon, 1979). TOC is a more direct expression of the total organic content compared to other similar parameters. (Abu-Daabes et al., 2013).

A more significant amount of organic content is likely within the fine fractions of the excavated waste material, as degradation processes of organic waste decrease grain size fractions with the progression of time in landfills (Parrodi et al., 2018a; Pecorini and Iannelli, 2020; Somani et al., 2018; Wei et al., 2015), depending on site-specific conditions. Hence, the TOC was analysed for fine fraction samples ≤ 0.106 mm.

TOC results are shown in Table 18, which were approximately ranging from 2-6 % with the highest value being in well 1901 of the sample <38 microns (Figure 32).

Table 18: TOC values of different waste size fractions.

Well number	Size (μm)	TOC (%)
1901	<38	6.15
1901	38	4.71
1901	53	3.94
1901	75	3.64
1901	106	2.91
1904	<38	5.29
1904	38	3.96
1904	53	3.19
1904	75	2.75
1904	106	2.05

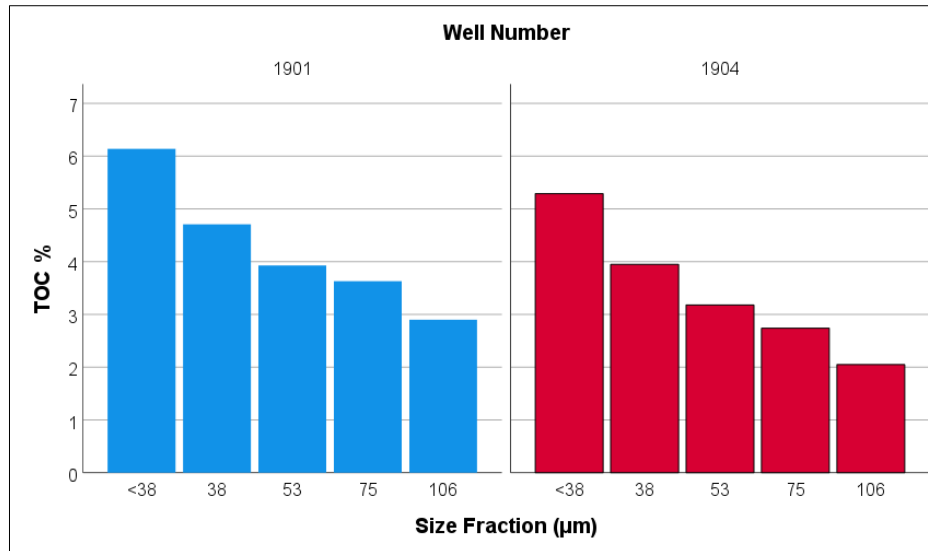


Figure 32. TOC values of different size fractions from wells 1901 and 1904.

Literature TOC values in comparison with the present TOC results is shown in Table 19. Previous studies displayed in table 17 have relatively demonstrated a significantly higher content of organic matter and also the studies by (Frank et al., 2017; García et al., 2016), which is explained by the difference in landfill management and status (Frank et al., 2017; Reinhart et al., 2002). Conversely, TOC results were in agreement with the study by (Scott et al., 2019) that investigated a historic landfill site in the UK of similar conditions to the current study area.

Table 19: Literature TOC values from different landfills.

Parameter	Present study	(Mönkäre et al., 2016) Lohja, Finland	(Kurian et al., 2003) Filborna, Sweden	(Kaartin en et al., 2013) Kuopio, Finland	(Prechthai et al., 2008) Nonthaburi, Thailand	(Jani et al., 2016) Högbytorp, Sweden	(Oettle et al., 2010) southern California, USA	(Quaghebeur et al., 2013) Remo, Belgium	(Mönkäre et al., 2016) Kuopio, Finland
Type of waste disposed of	MSW + C&D	MSW + C&D + Soil	MSW	MSW	MSW	MSW + C&D	MSW	MSW	MSW + C&D + Soil
Age of waste	33 - 41	24 - 40	10	5 - 10	3 - 5	5	60	14 - 29	1 - 10
TOC (%)	2-6	4.9 ± 0.4 - 14.3 ± 0.8	13	4.7 ± 0.8 - 5.8 ± 1.6	15.6 ± 1.9 - 21.0 ± 5.7	5.6	5.6 - 12.4	7.6 - 12.4	4.7 - 5.6

Several studies have revealed a positive relation trend between organic and moisture contents, such studies by (Chandana et al., 2020; Hull et al., 2005; Song et al., 2003; Zornberg et al., 1999), which high levels of moisture content were correlated to a high percentage of organic contents. On the other hand, the organic content decreased with the increase of the moisture content in the studies by (Adelopo et al., 2017; Jani et al., 2016; Pecorini and Iannelli, 2020), which low levels of organic content were related to a high percentage of moisture content, indicating a negative relationship (Pecorini and Iannelli, 2020). The different relationships between these studies are believed due to the activity of bacteria responsible for the waste degradation, waste composition, seasonal variations, landfill age, and the studied particle sizes (Jani et al., 2016; Pecorini and Iannelli, 2020). In this study, correlation found to be positive between organics and MC because there was a weak significance correlation found between COD and MC values ($r=0.263$, $P=0.042$). TOC values cannot be statistically compared to MC values since TOC was analysed for 10 samples only from wells 1901 and 1904 (5 per well). An illustrative bar graph for MC and TOC for wells 1901 and 1904 is shown in Figure 33. An average of each 3 samples out of 15 from wells 1901 and 1904 was calculated for MC to be used in the figure below.

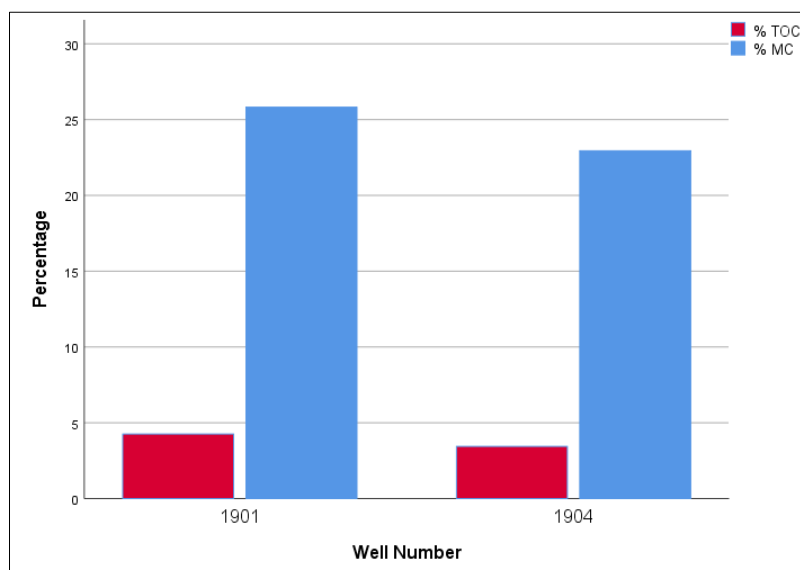


Figure 33. TOC and MC values of wells 1901 and 1904.

In order to avoid errors caused by the presence of inorganic carbon represented in the carbonate, bicarbonate, and dissolved carbon dioxide, it is necessary to acidify and aerate the sample prior to performing the TOC analysis (Bisutti et al., 2004; Singh and Chandel, 2020). However, some organic molecules cannot be totally oxidized (Masi et al., 2014). As a result, the TOC values determined in this analysis might be slightly less than what is actually present in the samples. In contrast, since samples were dried at 105°C, it is believed that some volatile fractions are evaporated at this temperature (López et al., 2018; Parrodi et al., 2019b).

The waste acceptance criterion (threshold) of TOC is 5% for non-hazardous landfills in the UK (Council, 2003). This categorises the Norfolk landfill with an average TOC of 1.5%, indicating that it is in an advanced methanogenic state. In terms of the safe exposure limit for methane, the National Institute for Occupational Safety and Health's maximum recommended safe methane concentration for workers during an 8-hour period is 1,000 ppm (a level of 0.1 %) (Atia, 2004). Methane can explode when sufficient quantities accumulate (5 – 15% by volume) and form a highly explosive gas within a mixture of air (ibid). Therefore, methane needs to be routinely monitored at the working face of a LFM site due to its potential risk for ignition (Scott et al., 2019).

Pearson's correlation (2-tailed) showed a significant negative correlation between the size of waste fractions and TOC values ($P < 0.01$) (Table 20). This association is mainly due to the reduction in organic waste material particle size over time, which is promoted by biodegradation and weathering effects (Parrodi et al., 2018a). Nevertheless, it is important to mention that fine fractions within the landfill may also result from vertical transport in deeper layers, such as downward migration due to gravitational force (ibid).

Table 20: Correlation analysis between waste size fractions and TOC values.

Correlation between waste size fractions and TOC			
		Size	C
Size fractions	Pearson Correlation	1	-.823**
	Sig. (2-tailed)		.003
	N	10	10
TOC	Pearson Correlation	-.823**	1
	Sig. (2-tailed)	.003	
	N	10	10

** . Correlation is significant at the 0.01 level (2-tailed).

Pearson’s correlation (2-tailed) also showed significant positive correlations between TOC and Ba ($r=0.971$, $P<0.001$), TOC and Cr ($r=0.978$, $P<0.001$), TOC and Ni ($r=0.919$, $P<0.001$), TOC and Co ($r=0.896$, $P<0.001$), TOC and As ($r=0.838$, $P<0.003$), and TOC and Cu ($r=0.834$, $P<0.004$) (Appendix 11). Some of these correlations are shown in Figure 34.

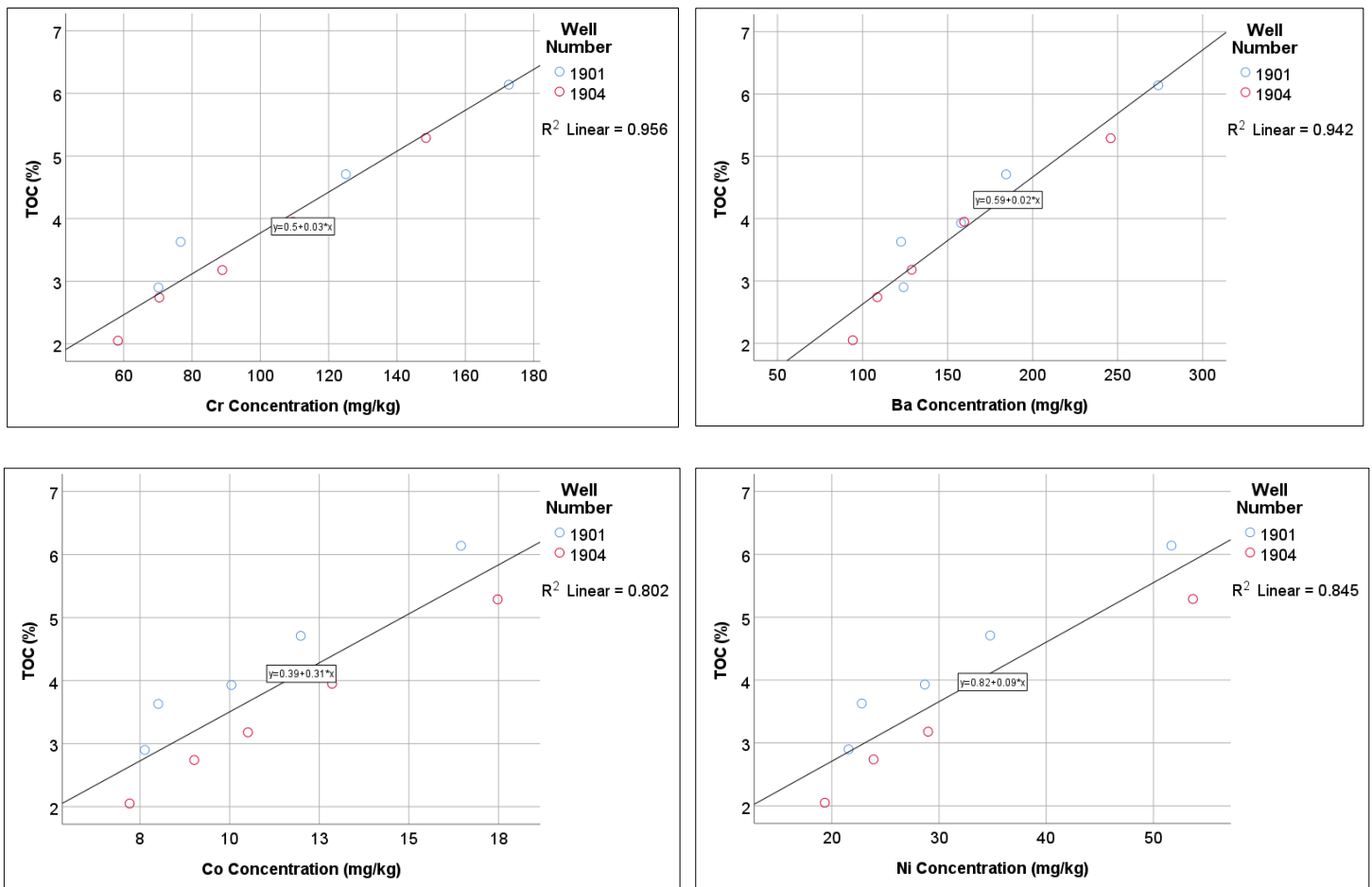


Figure 34. Correlation graph between TOC and various heavy metals using linear regression

line.

The scientific reason behind the close association between organics and metals is that metals are likely to have been immobilised during waste degradation through a variety of processes including sorption to soil particles and organic matter in the waste (Brand et al., 2018). According to (Pandey et al., 2016; Wagland et al., 2019), organic carbon is considered an essential elemental adsorbent in landfilled waste. Both humic and fulvic acids are the main components of organic materials and have a robust complexation capacity with heavy metals (Lee et al., 2022b; Tang et al., 2014). Hence, more TOC is found within waste particles, and more heavy metals are adsorbed, thereby slowing the migration of heavy metals (Wei et al., 2015).

4.11 Waste Degradation Stages in Landfills

Waste degradation and stabilization in landfills are contingent on metabolism of various microorganisms like bacteria and methanogenic archaea to a large extent, and directly related to the structure of the microbial community and functional organisation (Qi et al., 2013). These processes inside landfills are complex due to several environmental factors, such as moisture content, toxic inorganic metals, and landfill design and management (e.g., material type of daily cover) and consequently impact the functional structure of microbial communities and the decomposition of organic matter (ibid). Generally, landfills have usually between 5 to 8 stages of waste degradation, landfill gas and leachate generation, which are represented in stages I-IV following stages of landfill completion from V-VIII (Figure 35 a) (Brown et al., 2018; Kjeldsen et al., 2002). Theoretical waste degradation processes, without timescales, are illustrated in Figure 35 b. The first stage of the landfill is characterized by aerobic degradation of waste, which consumes the available oxygen in its surroundings and emits carbon dioxide. Stage II commences after the oxygen consumption in the landfill which is the onset of the degradation of acidogenic waste. Acidogenic bacteria use soluble organic materials to generate

VFAs through acidification (Zhao et al., 2020). The main products of this process are carbon dioxide and hydrogen.

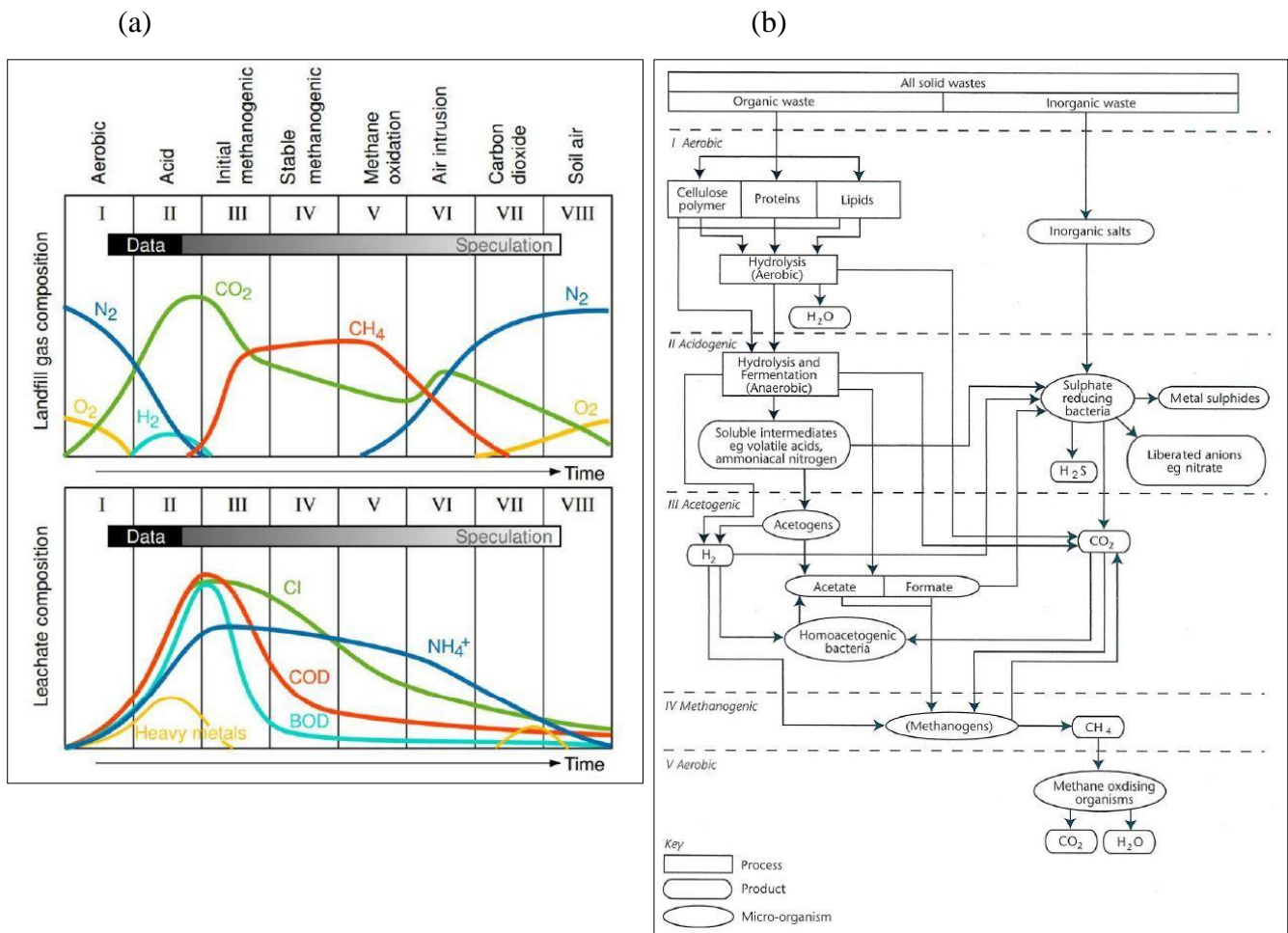


Figure 35. (a) Theoretical MSW landfill gas and leachate evolution (b) waste degradation stages (Brown et al., 2018).

Stage III is recognized as the acetogenic phase, which is the initial of methanogenic phase when methane starts to build-up. Methane production peaks at the IV stage, which is the methanogenic phase. Stable methanogenesis is reached at the final phase of the anaerobic waste decomposition by bacteria known as methanogens. The approximate time from stages I-III is generally 6 months (Barry et al., 2004). The period time of the IV stage is based on the cellulose hydrolysis rate and landfilling years number. Air is expected to infiltrate towards waste mass during methane oxidation phase (V), which is the stage considered to be the time when a

landfill stops receiving waste and starts the post-closure management. A significant amount of methane is oxidized during the air intrusion phase (VI), that resulted from residual anaerobic degradation. The remaining organic matter is degraded during the carbon dioxide phase (VII), which is the transitional phase from anaerobic back to aerobic conditions in landfills. When the composition of the landfill gas and soil air are the same, the last stage can be achieved, known as the soil air phase (VIII). Typical changes of leachate composition are displayed in Table 21.

Table 21: Development of acetogenic to methanogenic leachate quality in a landfill (Brown et al., 2018).

Constituent	Period since initial waste deposition (months)		
	14 months	22 months	30 months
pH	5.6	6.9	7.6
COD	76000	18000	2600
TOC	24600	5900	850
Total fatty acids (as C)	21220	5054	127

Note: All units are expressed in mg/l except pH.

Data shown in the table above are general methanogenic conditions for most landfill sites received household waste. Quantifying COD as measure of organic matter and for the determination of waste stabilisation state/stage is not adequate (Francois et al., 2006) because many inorganic substances can represent one-third of COD results by interfering with COD values (Kjeldsen et al., 2002; Kylefors et al., 2003). Therefore, it can be inferred from the data generated in this research that the studied landfill in Norfolk is in advanced state of degradation, which can be anticipated between the air intrusion phase (VI) and the carbon dioxide phase (VII) since there are still some non-degraded residuals found within the studied wells. However,

according to (Brown et al., 2018), the duration between stages V-VIII is very difficult to quantify and can take up to 1000 years, depending on the site conditions.

In regard to relationship between landfill gas and leachate, higher organic matter represented in COD and BOD parameters indicate higher landfill gas within the waste (CH₄ and CO₂). The soluble organic matter of the environment is represented in the soluble COD and VFAs, which are the substrates for the methanogenesis, transformed into methane and carbon dioxide (Bhalla et al., 2013; Schirmer et al., 2014; Zhao et al., 2020). Regarding relationship between CH₄ and COD, a study showed that 83% of the COD removed from leachate using anaerobic treatment was converted to CH₄ (Timur and Öztürk, 1999). In contrast, the study by (Frank et al., 2017) demonstrated no correlation found between CH₄ and COD using the same analytical analysis. This indicates the presence of inorganic components (Kylefors et al., 2003) or refractory substances (organic compounds that show up in the COD tests as being chemically oxidizable but are not readily biodegradable especially at the late stage of landfills) within some COD tests of leachates (Bhalla et al., 2013). Hence, the relation between CH₄ and COD is not always steady since it is site dependant.

4.12 Mineral Composition

A total of 8 samples from the four wells (2 from each well) of two different size fractions: (53-38 µm) and (<38 µm) were analysed. Analysis was carried out using Scanning Electron Microscopy (SEM) technique (quantitative), which comprises an FEI Quanta 600 MLA. SEM was applied with the use of mineral liberation analyser (MLA) measurements that can offer a wide range of mineralogical classification, including mineral abundance and imaging, grain size distribution and morphology, elemental distribution, and mineral association/locking (Zhang et al., 2021). The MLA is equipped with EDS software that allows automated large area analysis of polished specimens to identify and quantify mineral composition and distribution (Gu, 2003). Approximately 10 g of dried samples were first placed in rounded

cylindrical rubber. Epofix resin was then added to the samples which is a suitable media for embedding for electron microscopy. Then, they were mixed with epofix hardener and stirred, and were let to rest at room atmosphere. Samples were then oven dried for an overnight. Afterward, samples were polished in several steps and carbon coated prior to MLA performance.

Minerals and natural inorganic fibres can result from LFM activities aiming to recover energy and raw materials and thus, can create localised environmental and health impacts (Smart-Ground, 2018; Warren and Read, 2014). Some of these materials can cause harm to human health while breathing at high doses such as asbestos, crystalline silica, and quartz dust (Gautam et al., 2018; Smart-Ground, 2018). Therefore, their possible existence in the atmosphere should be evaluated prior to initiation of LFM activities (Smart-Ground, 2018). SEM technique has been widely used in many environmental applications for respirable inorganic fibers quantification (Capella et al., 2020; Smart-Ground, 2017), especially at very low concentrations (Yang et al., 2020).

Asbestos, as a group of six minerals, is among the toxic inorganic fibers (Capella et al., 2020; Peña-Castro et al., 2023). High-dose asbestos exposure has been linked to a variety of illnesses, including asbestosis, pleural mesothelioma, and lung cancer (Huang et al., 2011; Osinubi et al., 2000; Oury et al., 2014; Toyokuni, 2009). In addition, among crustal components, silica also known as silicon dioxide (SiO_2) has been proved to be harmful when inhaled for long periods of time (occupational exposure) and is a well-known cause of lung disorders, such as silicosis and silico-tuberculosis (Brown, 2009; Huertas et al., 2012b). However, there is currently no evidence that low quantities of breathing crystalline silica in the air cause health problems (Smart-Ground, 2018). According to (Patra et al., 2016), numerous reviews demonstrates that negative health effects of PM inhalation are common during surface mining activities, regardless of the mineral types resulting from mining activities.

Apart from asbestos and silica, several additional natural and man-made (synthetic) airborne mineral dusts are also identified as potential health hazards, such as carbonaceous dust, glasswool, and rockwool (Amin et al., 2023; Fubini and Arean, 1999; Lippmann, 2014; Park, 2018). These materials can be found in both the workplace and the general environment, and their health effect should be proportional to the total number of particles inhaled, considering that different types of particulates might function not just additively but also synergistically (Fubini and Arean, 1999).

Particles/minerals were categorised by aerodynamic diameter into two categories based on the predicted penetration capacity into the lung: PM₁₀ and PM_{2.5} (Elmes and Gasparon, 2017; Kampa and Castanas, 2008; Kappos et al., 2004; Patra et al., 2016; Rodriguez et al., 2019). Fine particulate matter (PM_{2.5}) poses the highest risk to the health (Amoatey et al., 2018; Kampa and Castanas, 2008). These fine particles may penetrate deep into the lungs, and some may even get absorbed directly into the bloodstream (Davidson et al., 2005; Elmes and Gasparon, 2017; Manisalidis et al., 2020; Rodriguez et al., 2019). The size and shape of particles entering the pulmonary system determine relevant aerodynamic properties, which govern how they behave (Kampa and Castanas, 2008; Losacco and Perillo, 2018; Patra et al., 2016; Rodriguez et al., 2019). Only particles with a diameter of less than 5-1 µm are probable to reach the alveoli when they have a more or less spherical shape (Costa and Orriols, 2012; Fubini and Arean, 1999; Kampa and Castanas, 2008; Utell and Maxim, 2018). Larger particles are deposited mainly in the upper air passages and eliminated by the mucociliary escalator (Costa and Orriols, 2012; Elmes and Gasparon, 2017; Fubini and Arean, 1999; Kampa and Castanas, 2008). Fibres are a more complicated case because their aerodynamic behaviour varies depending on their length and diameter (Fubini and Arean, 1999). The majority of airborne mineral fibres are characteristic by a diameter of a few tenths of a micrometre and lengths ranging from a few micrometres to several hundreds of micrometres (ibid). According

to (Costa and Orriols, 2012). fibres can be defined as a long particle characteristic by its length, which is several times more than its diameter. Despite pathological examinations of lung tissue that have revealed fibres are as long as 200 μm , the vast majority are shorter than 50 μm . The relative dimensions of mineral fibres may have a differential influence on pathogenicity, in addition to affecting lung clearance rates (Fubini and Arean, 1999). Fine and long fibres having diameter less than 0.25 μm and length longer than 8 μm are thought to be more carcinogenic than short, thick fibres (Fubini and Arean, 1999; Park, 2018).

Inhaled mineral dusts/fibers toxicity is caused by a number of interconnected factors (mainly physical and chemical parameters) (Park, 2018; Patra et al., 2016), which in turn making the assessment of each process complicated to a large degree (Fubini and Arean, 1999). Particle size and shape are among the physical parameters which determine the deposition rate of airborne particles and clearance from the lungs (Fubini and Arean, 1999; Gautam et al., 2018; Kampa and Castanas, 2008). Surface roughness and area of particles may influence inflammatory processes as well as chemical behaviour and dissolving rate (Fubini and Arean, 1999; Rodriguez et al., 2019). Chemical factors are linked to composition (Elmes and Gasparon, 2017) and processes that take place at the mineral particle-pulmonary tissue contact (Fubini and Arean, 1999; Kampa and Castanas, 2008). It is important to note that a single physical or chemical factor is unlikely to be the sole pathogenic determinant for any particle (ibid).

Different types of asbestos and crystalline silica have been significantly reported in fine fractions. For example, thirteen inorganic fibres having a respirable size (length $>5 \mu\text{m}$, width $<3 \mu\text{m}$, aspect ratio greater than or equal to $\geq 3:1$; WHO 1986) were detected in a C&D landfill in Italy (Smart-Ground, 2018). In order to identify content of inorganic fibres and potential harmful minerals that might be potentially air-dispersed and respired during LFM activities, fine fraction samples of $\leq 38 \mu\text{m}$ (returned in the pan from the PSD analysis of the current

study) were analysed for the four wells. Classification of the mineral compositions of the waste fractions from the four wells are illustrated in Figure 36.

Approximately, the most abundant detected particles among the four wells were SiO₂ (40%), ferroan clay (30%), and other silicate minerals (23%). The other species were each in percentage less than 6%. Synthetic glasses were identified through the four wells as sodic and fiber glass. Old battery ZnMn was also identified within the four wells. These found materials indicated the presence of industrial wastes within the Docking Common landfill. SEM-MLA analysis revealed significant variation in terms of abundance, morphology, size, and composition of particles within the waste materials. MLA Modals mineralogy of samples of the four wells are shown in Tables 22-29.

Among potential toxic minerals, glass fibers and silica (found as quartz) were detected in the mean percentage of 0.6% and 40%, respectively. According to Washington State Department of Health (WSDH), fiberglass can be introduced to the environment by the disposal of fiberglass-containing materials, which in turn can be released into the air when disturbed. Fiberglass in the air may eventually become settled as dust with other airborne particles, which can be clearly seen in the analysed samples (Figure 37). Synthetic fibers have been widely used with the aim of reducing the health concerns associated with asbestos (Sripaiboonkij et al., 2009). However, their exposure via inhalation and direct contact with skin has been evidenced to increase the likelihood of respiratory and skin symptoms, wheezing and asthma, and minor decrements in lung function (Camacho et al., 2019; Kilburn et al., 1992; Sripaiboonkij et al., 2009; Utell and Maxim, 2018). They also can give rise to genetic damage and neoplastic transformation (Costa and Orriols, 2012). The toxicity of synthetic inorganic fibers is closely associated to their length according to cell culture research (ibid).

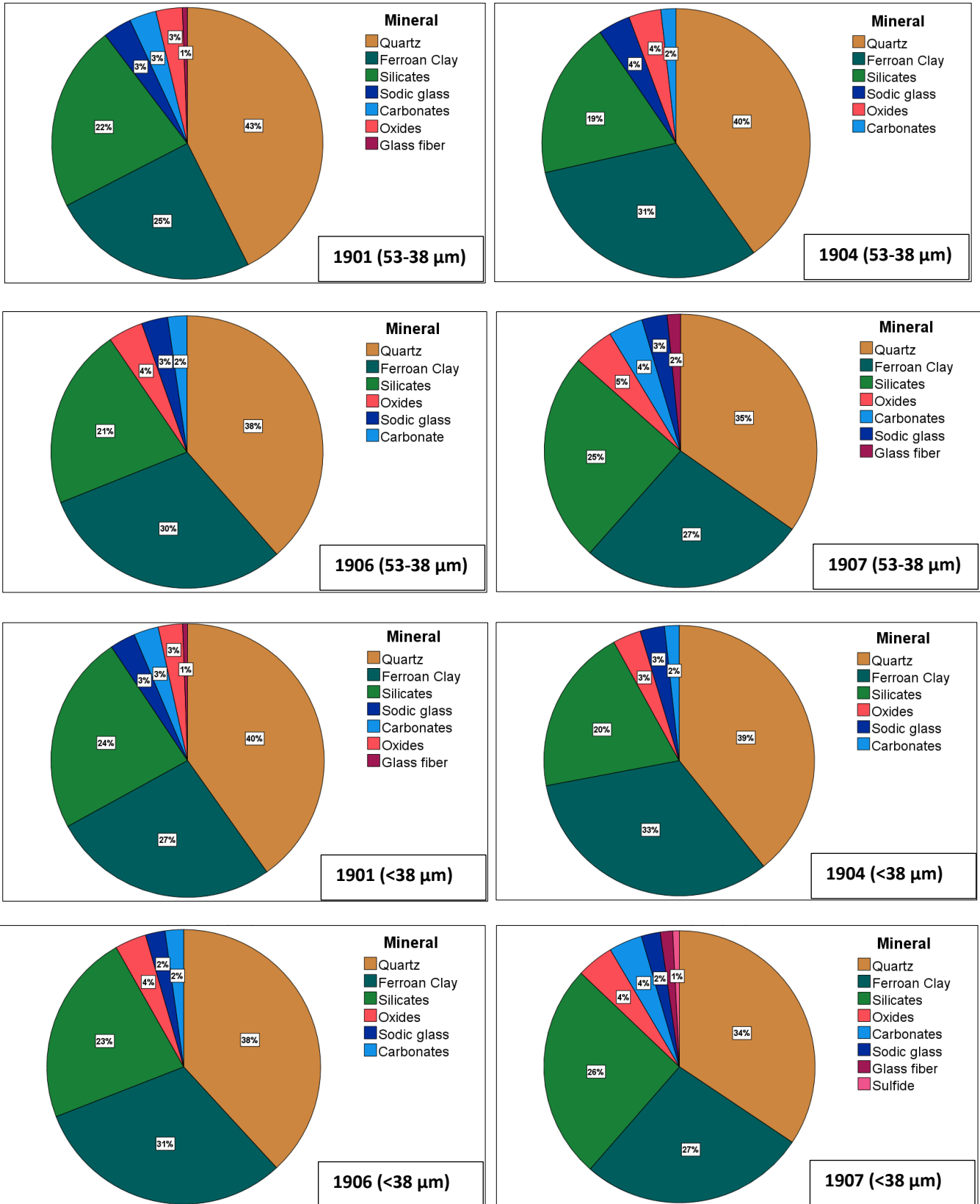


Figure 36. Pie diagrams of minerals found in two different waste size fractions.

Table 22: Modals mineralogy of samples 53-38 μm of well 1901.

Name	Pixels	Particles	Area %	Weight %	Area Microns
Quartz	16741813	57732	42.30%	42.59%	48056466.63
Stilpnomelane	716324	15592	1.81%	1.99%	2056169.21
Hematite	457461	7914	1.16%	2.35%	1313117.00
Calcite	759608	7629	1.92%	2.00%	2180413.58
Orthoclase	2317449	13996	5.85%	5.75%	6652111.72
Muscovite	667915	6104	1.69%	1.83%	1917213.80
Chamosite	91215	1829	0.23%	0.28%	261827.71
Old battery ZnMn	76521	586	0.19%	0.42%	219649.38
Ferroan Clay	9383221	81185	23.71%	24.83%	26934027.21
Zircon	26205	173	0.07%	0.12%	75220.03
Epidote	1989834	19080	5.03%	6.65%	5711710.63
Sodic glass	2213677	28879	5.59%	3.41%	6354239.82
Albite	1989069	11103	5.03%	5.05%	5709514.74
Dolomite	98075	578	0.25%	0.27%	281518.97
Bixbyite	42802	359	0.11%	0.21%	122860.82
Lead or Galena	2434	54	0.01%	0.03%	6986.67
Ankerite	312923	4720	0.79%	0.93%	898228.51
Fe TiCr oxide	11035	122	0.03%	0.06%	31675.37
Glass fibres	380934	5158	0.96%	0.59%	1093450.40
Rutile	61960	742	0.16%	0.26%	177852.82
Hornblende	116608	1039	0.29%	0.33%	334716.94
Cu oxide	7465	32	0.02%	0.06%	21427.88

Table 23: Modals mineralogy of samples 53-38 μm of well 1904.

	Name	Pixels	Particles	Area %	Weight %	Area Microns
	Quartz	17502327	59526	40.14%	39.95%	50239480.84
	Stilpnomelane	909588	22066	2.09%	2.27%	2610923.04
	Hematite	644696	10436	1.48%	2.97%	1850564.92
	Calcite	462156	4380	1.06%	1.09%	1326593.74
	Orthoclase	2524531	16513	5.79%	5.62%	7246529.38
	Muscovite	569692	5568	1.31%	1.40%	1635270.00
	Chamosite	145366	3068	0.33%	0,40%	417265.22
	Old battery ZnMn	10250	79	0.02%	0.05%	29422.07
	Ferroan Clay	13130095	96944	30.12%	31.17%	37689225.90
	Zircon	61018	310	0.14%	0.25%	175148.86
	Epidote	1059621	10380	2.43%	3.18%	3041584.64
	Sodic glass	2795297	31630	6.41%	3.87%	8023748.50
	Albite	2396623	13690	5.50%	5.46%	6879376.40
	Dolomite	37008	227	0.08%	0.09%	106229.46
	Bixbyite	7905	54	0.02%	0.03%	22690.87
	Lead or Galena	29506	139	0.07%	0.29%	84695.37
	Ankerite	239332	3862	0.55%	0.63%	686989.53
	Fe TiCr oxide	14436	152	0.03%	0.07%	41437.76
	Glass fibres	149441	2113	0.34%	0.21%	428962.29
	Rutile	97608	897	0.22%	0.36%	280178.47
	Hornblende	84823	749	0.19%	0,21%	243479.82
	Cu oxide	60407	35	0.14%	0,41%	173395.02

Table 24: Modals mineralogy of samples 53-38 μm of well 1906.

Name	Pixels	Particles	Area %	Weight %	Area Microns
Quartz	16250095	52390	38.70%	38.40%	46645016.77
Stilpnomelane	1212074	26673	2.89%	3.13%	3479192.71
Hematite	700085	11340	1.67%	3.34%	2009556.04
Calcite	539440	5328	1.28%	1.32%	1548433.28
Orthoclase	2262324	14124	5.39%	5.21%	6493878.40
Muscovite	1190491	9102	2.84%	3.03%	3417239.88
Chamosite	99375	2207	0.24%	0.29%	285250.55
Old battery ZnMn	17200	94	0.04%	0.09%	49371.67
Ferroan Clay	12346500	96489	29.41%	30.34%	35439958.94
Zircon	50963	243	0.12%	0.21%	146286.53
Epidote	1502368	14954	3.58%	4.67%	4312465.90
Sodic glass	2170339	23218	5.17%	3.11%	6229840.44
Albite	1933554	10527	4.61%	4.56%	5550161.94
Dolomite	34549	153	0.08%	0.09%	99171.03
Bixbyite	4730	34	0.01%	0.02%	13577.21
Lead or Galena	7481	93	0.02%	0.08%	21473.80
Ankerite	311885	5344	0.74%	0.86%	895248.98
Fe TiCr oxide	11638	146	0.03%	0.06%	33406.25
Glass fibres	176086	2538	0.42%	0.26%	505445.32
Rutile	86026	857	0.20%	0.33%	246932.97
Hornblende	120834	1103	0.29%	0.32%	346847.45
Cu oxide	44326	26	0.11%	0.31%	127235.38

Table 25: Modals mineralogy of samples 53-38 μm of well 1907.

Name	Pixels	Particles	Area %	Weight %	Area Microns
Quartz	14029460	47048	34.99%	34.67%	40270804.38
Stilpnomelane	1237185	23998	3.09%	3.34%	3551272.47
Hematite	790630	9624	1.97%	3.94%	2269460.55
Calcite	1099707	9677	2.74%	2.81%	3156649.33
Orthoclase	2035988	12093	5.08%	4.91%	5844193.18
Muscovite	1384628	10580	3.45%	3.68%	3974499.61
Chamosite	85216	1502	0.21%	0.26%	244607.91
Old battery ZnMn	3696	37	0.01%	0.02%	10609.17
Ferroan Clay	10426626	80779	26.01%	26.80%	29929064.70
Zircon	32303	209	0.08%	0.14%	92724.01
Epidote	2415238	21596	6.02%	7.84%	6932809.75
Sodic glass	1994717	20880	4.98%	2.99%	5725727.01
Albite	1788090	9757	4.46%	4.41%	5132615.41
Dolomite	36014	187	0.09%	0.10%	103376.23
Bixbyite	569	4	0.00%	0.00%	1633.28
Lead or Galena	19078	239	0.05%	0,20%	54762.36
Ankerite	408688	5328	1.02%	1.17%	1173116.75
Fe TiCr oxide	15830	140	0.04%	0.09%	45439.16
Glass fibres	1042916	10645	2.60%	1.58%	2993633.84
Rutile	71862	707	0.18%	0,29%	206275.98
Hornblende	117918	914	0.29%	0.32%	338477.23
Cu oxide	60851	34	0.15%	0.45%	174669.50

Table 26: Modals mineralogy of samples <38 µm of well 1901.

	Name	Pixels	Particles	Area %	Weight %	Area Microns
	Quartz	15343242	61791	39.79%	40.09%	50506948.99
	Stilpnomelane	893863	18868	2.32%	2.55%	2942422.01
	Hematite	410999	7914	1.07%	2.17%	1352928.25
	Calcite	652809	7554	1.69%	1.76%	2148919.43
	Orthoclase	2069526	14136	5.37%	5.27%	6812474.45
	Muscovite	613035	6708	1.59%	1.72%	2017991.21
	Chamosite	191489	4037	0.50%	0.61%	630344.30
	Old battery ZnMn	69898	639	0.18%	0.40%	230090.53
	Ferroan Clay	9867869	85482	25.59%	26.81%	32483092.96
	Zircon	23527	171	0.06%	0.11%	77446.28
	Epidote	2265173	21922	5.87%	7.78%	7456506.07
	Sodic glass	1902859	29924	4.93%	3.01%	6263839.31
	Albite	1915053	12924	4.97%	4.99%	6303979.58
	Dolomite	86149	594	0.22%	0.24%	283585.64
	Bixbyite	39436	342	0.10%	0.19%	129815.59
	Lead or Galena	12064	111	0.03%	0.14%	39712.33
	Ankerite	303436	5018	0.79%	0.92%	998851.91
	Fe TiCn oxide	10780	136	0.03%	0.06%	35485.65
	Glass fibres	363671	5322	0.94%	0.58%	1197133.74
	Rutile	57172	772	0.15%	0,24%	188199.03
	Hornblende	118171	1266	0.31%	0.34%	388995.80
	Cu oxide	103	7	0.00%	0.00%	339.06























Table 27: Modals mineralogy of samples <38 µm of well 1904.

	Name	Pixels	Particles	Area %	Weight %	Area Microns
	Quartz	14888998	59575	39.23%	39.04%	49011640.04
	Stilpnomelane	937155	23712	2.47%	2.68%	3084929.12
	Hematite	521850	9808	1.37%	2.76%	1717827.11
	Calcite	364158	3990	0.96%	0.99%	1198736.20
	Orthoclase	2055529	15329	5.42%	5.26%	6766395.39
	Muscovite	514123	6000	1.35%	1.45%	1692391.35
	Chamosite	283758	6347	0.75%	0.91%	934075.28
	Old battery ZnMn	8692	66	0.02%	0.05%	28612.35
	Ferroan Clay	11949022	100460	31.48%	32.58%	39333819.85
	Zircon	49687	268	0.13%	0.23%	163559.79
	Epidote	1031991	11487	2.72%	3.56%	3397110.50
	Sodic glass	1828738	27621	4.82%	2.90%	6019844.22
	Albite	2098799	14927	5.53%	5.49%	6908831.68
	Dolomite	35436	220	0.09%	0.10%	116648.31
	Bixbyite	5537	42	0.01%	0.03%	18226.71
	Lead or Galena	32041	160	0.08%	0.36%	105472.64
	Ankerite	211297	3716	0.56%	0.64%	695547.98
	Fe TiCr oxide	11545	141	0.03%	0.07%	38003.86
	Glass fibres	131406	2086	0.35%	0.21%	432562.59
	Rutile	71373	855	0.19%	0.30%	234945.82
	Hornblende	77835	817	0.21%	0.23%	256217.44
	Cu oxide	20116	494	0.05%	0.16%	66217.90

Table 28: Modals mineralogy of samples <38 µm of well 1906.

	Name	Pixels	Particles	Area %	Weight %	Area Microns
	Quartz	13920016	53721	38.30%	37.89%	45821942.72
	Stilpnomelane	1205779	27513	3.32%	3.58%	3969186.26
	Hematite	580440	11002	1.60%	3.19%	1910693.81
	Calcite	432856	5015	1.19%	1.22%	1424876.44
	Orthoclase	1881597	13533	5.18%	4.99%	6193845.61
	Muscovite	1011535	9732	2.78%	2.96%	3329773.39
	Chamosite	211556	5002	0.58%	0.70%	696400.56
	Old battery ZnMn	13888	92	0.04%	0.08%	45716.55
	Ferroan Clay	10865895	96566	29.89%	30.76%	35768379.74
	Zircon	42842	252	0.12%	0.21%	141027.40
	Epidote	1447800	16164	3.98%	5.18%	4765871.58
	Sodic glass	1392599	19745	3.83%	2.30%	4584160.79
	Albite	1693034	11622	4.66%	4.60%	5573133.46
	Dolomite	32260	154	0.09%	0.10%	106193.55
	Bixbyite	3280	33	0.01%	0.02%	10797.11
	Lead or Galena	34801	311	0.10%	0,41%	114558.02
	Ankerite	269345	5034	0.74%	0.85%	886630.53
	Fe TiCr oxide	12174	118	0.03%	0.07%	40074.40
	Glass fibres	143906	2440	0.40%	0.24%	473710.12
	Rutile	64446	795	0.18%	0.28%	212143.50
	Hornblende	98743	1077	0.27%	0.30%	325042.45
	Cu oxide	8438	221	0.02%	0.07%	27776.23

Table 29: Modals mineralogy of samples <38 µm of well 1907.

	Name	Pixels	Particles	Area %	Weight %	Area Microns
	Quartz	12669401	50925	34.74%	34.37%	41705187.87
	Stilpnomelane	1224803	24800	3.36%	3.63%	4031811.70
	Hematite	675977	9925	1.85%	3.70%	2225183.95
	Calcite	957932	9513	2.63%	2.68%	3153324.61
	Orthoclase	1771141	12012	4.86%	4.69%	5830249.44
	Muscovite	1303974	11842	3.58%	3.81%	4292427.14
	Chamosite	143026	3140	0.39%	0.47%	470813.59
	Old battery ZnMn	4812	49	0.01%	0.03%	15840.16
	Ferroan Clay	9595195	86564	26.31%	27.07%	31585503.54
	Zircon	30231	209	0.08%	0.15%	99514.53
	Epidote	2302680	23368	6.31%	8.21%	7579971.78
	Sodic glass	1369890	19031	3.76%	2.25%	4509409.70
	Albite	1617566	10912	4.44%	4.38%	5324710.61
	Dolomite	32404	208	0.09%	0.10%	106667.62
	Bixbyite	29	4	0.00%	0.00%	95.46
	Lead or Galena	68028	561	0.19%	0.80%	223934.86
	Ankerite	382079	5490	1.05%	1.20%	1257729.27
	Fe TiCn oxide	13469	147	0.04%	0.08%	44337.31
	Glass fibres	887646	10341	2.43%	1.48%	2921956.86
	Rutile	59187	737	0.16%	0.26%	194832.02
	Hornblende	101230	1031	0.28%	0.30%	333229.34
	Cu oxide	42330	778	0.12%	0.34%	139342.07

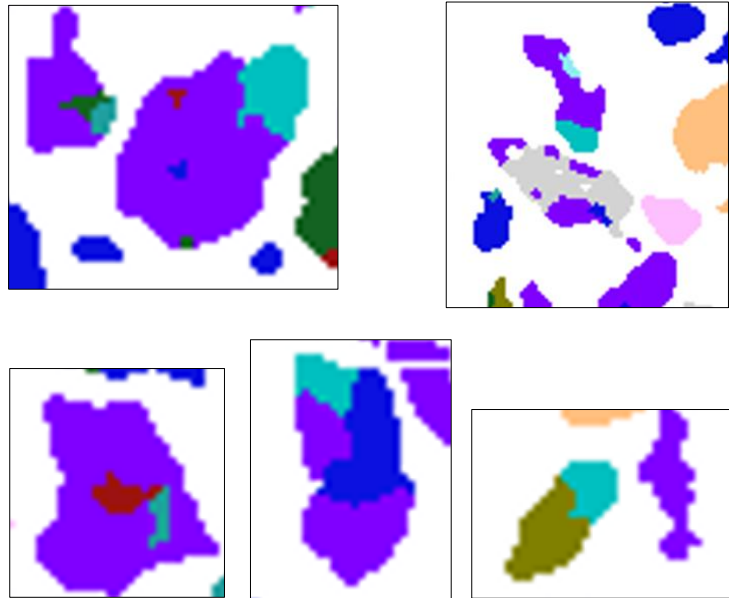


Figure 37. Photos of selected mineral phases showing fiberglass particles in light blue colour adhered on the top of other particles using SEM-MLA analysis.

According to (Park, 2018), the size, biopersistence, and physicochemical characteristics of the fiber are the main determinants of the risks associated with synthetic fibers. Synthetic fibers have a range of risks; those with biopersistence were shown to be highly hazardous, while other materials were determined to be less hazardous (ibid).

Fiber glass and asbestos fibers have some similarities in regard with aerodynamic properties. fibre glass is divided transversally to a large degree which produce shorter and shorter particles that can be eliminated more effectively through the phagocytic system, whereas asbestos fibers generally break up longitudinally, which lead to long fibers that become thinner and thinner and can remain in the lungs over time (Costa and Orriols, 2012). Synthetic fibers can have a vitreous or crystalline structure and the vitreous (amorphous) is found in the most prevalent man-made mineral fibers (ibid). Fibres glass in the studied sample revealed relatively amorphous structures within all the analysed samples. However, some fibres glass particles of both samples in well 1907 seemed to have crystalline structures (Figure 38). These particles

were only noticed in well 1907, confirming the heterogeneity of waste components. Asbestos was not detected in the analysed samples of the four wells. However, this does not mean that asbestos is not contained in the landfilled waste and thus, additional extensive systematic sampling regimes might confirm its presence within the landfill site.

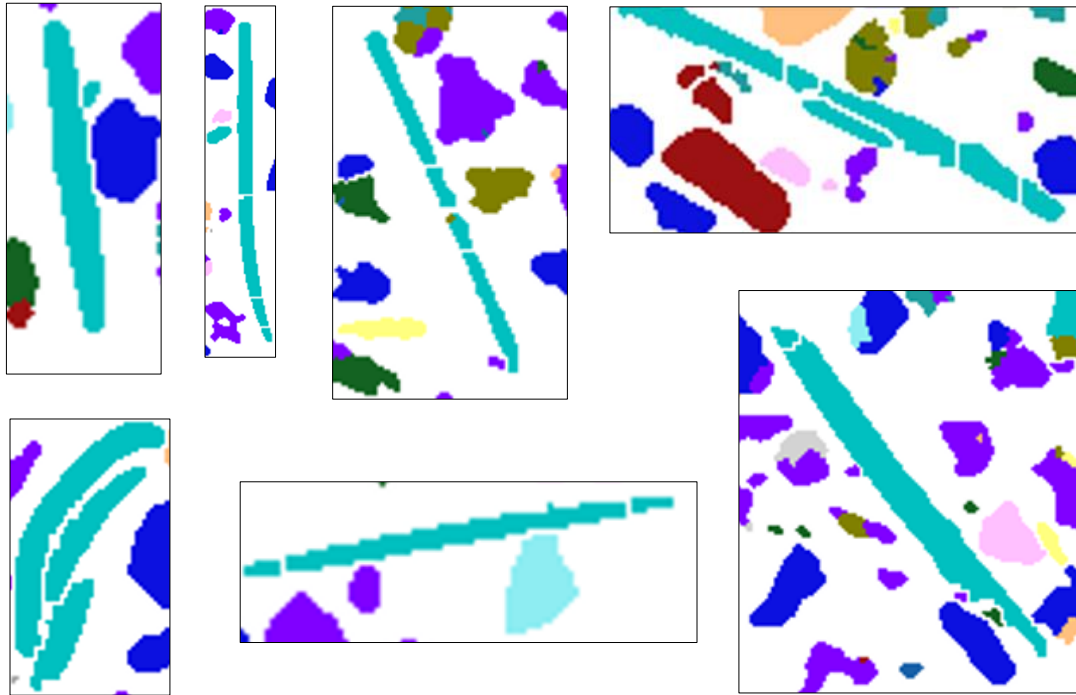
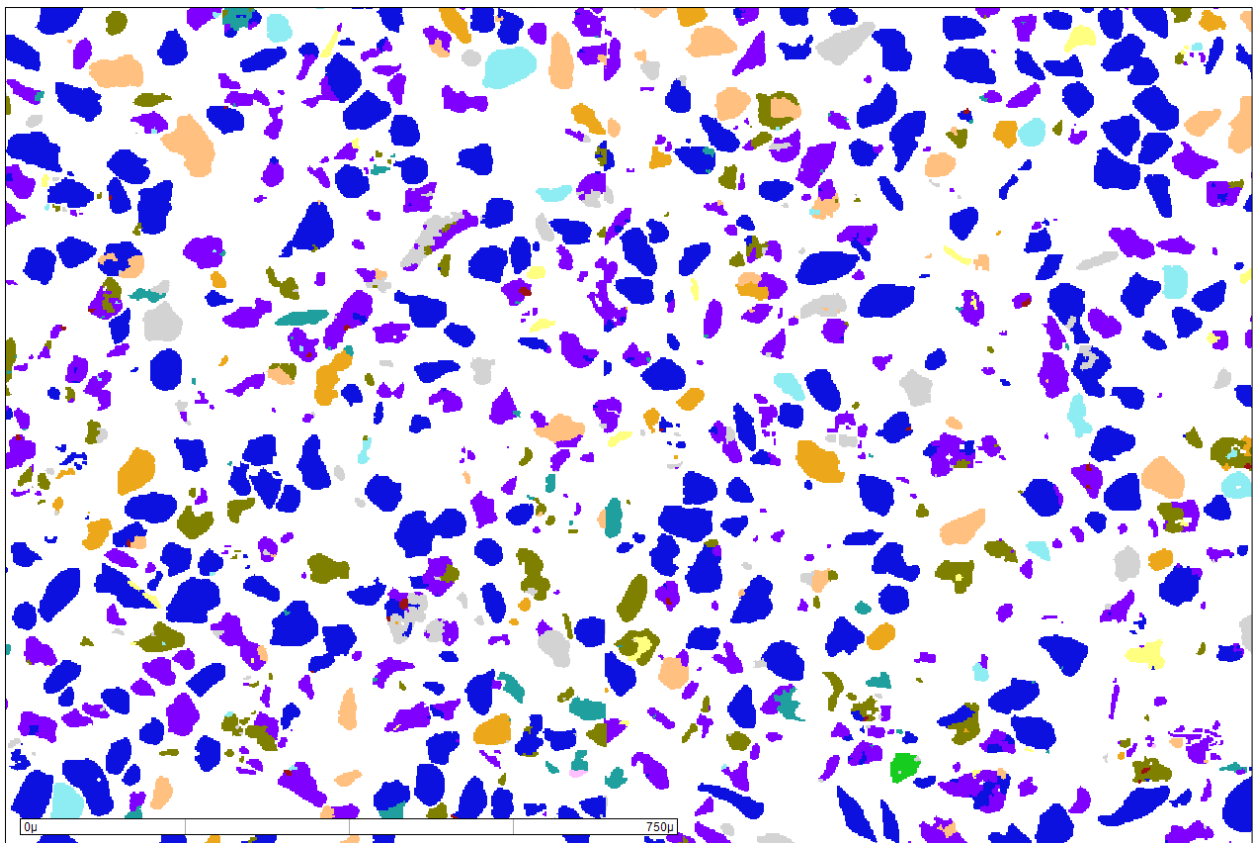


Figure 38. Glass noodle and rod-like fibre particles of well 1907 in blue light colours.

Amorphous quartz was the most prominent minerals by weight within all analysed samples which was in agreement with other LFM studies (Parrodi et al., 2018b). Its abundance within the landfilled waste suggests the past deposition of SiO₂-enriched materials, e.g., building sand (Vollprecht et al., 2020). More detailed investigations are important to quantify its amount in mg/m³ for determination whether the identified amount is potentially harmful to the human health (Smart-Ground, 2018). In contrast, its abundance in landfilled waste can be of interest to stockholders for reuse in different applications (Lesovik et al., 2021).

The high amount of ferroan clay is expected since the studied landfill site is capped with bentonite clay. The name of ferroan describe minerals containing ferrous iron. The presence of

ferroan clay within the analysed samples indicate that the landfill was capped with the addition of iron oxide rich to its material since it has been shown to increase removal efficiency (Adsorption) of heavy metals in municipal solid waste (Cheriyana and Chandrakaran, 2021). In turn, the clay particles become rich in heavy metals, increasing the potential risk of dust (pollutants) exposure and toxicity in the application of LFM activities. It was observed that ferroan clay particles were the most mineral having mineral locking behaviour (Figure 39), which can be interpreted due to its high specific surface area and ion exchange capacities (Al-Ani and Sarapää, 2008).



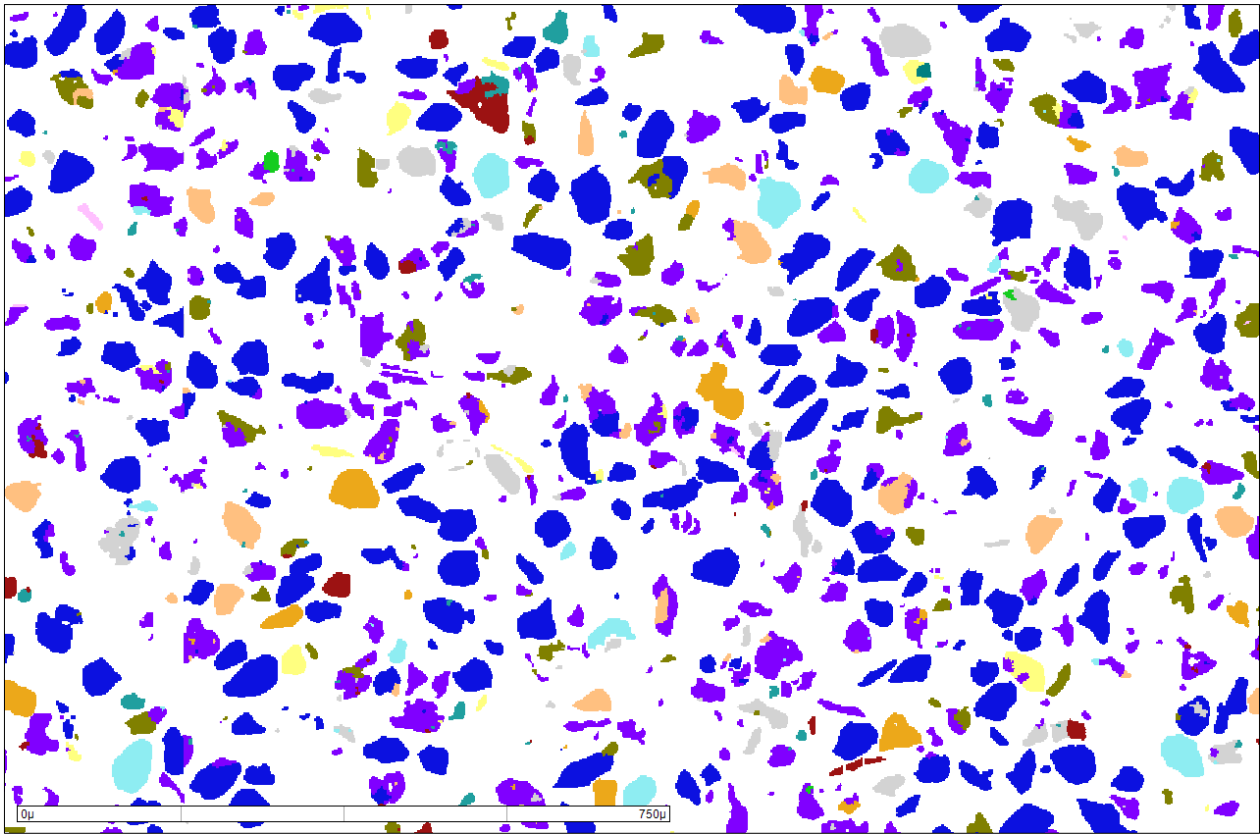


Figure 39. Photomicrographs displaying fine-grained and heterogeneously composed parts in intergrowth with ferroan clay in purple colour.

Carbonaceous dust in the studied samples were present as calcite, dolomite, and ankerite minerals. Several studies have linked long term exposure to carbonaceous aerosols to be more likely associated with respiratory symptoms, (Li et al., 2018; Neghab et al., 2012), especially in ultrafine particles (Amin et al., 2023). Carbonates mineral group represented around 3 percent within the analysed samples.

Literature reviews regarding the exposure to iron oxide dust have reported no acute changes in the health parameters measured (Bourgakard et al., 2009; Lewinski et al., 2013). Oxide minerals group were found in the percentage of 4 within the analysed samples, mostly as hematite mineral.

MLA analysis of particles size distribution of well 1901 showed that PM10 represent around 1% of the total sample of ($\leq 38 \mu\text{m}$), which approx. represent 0.034 from the total sample of 1901 of all size fractions (considering previous mechanical particle size distribution). PM2.5 was not present in the studied well of 1901 and additional classifications of other wells or extensive systematic sampling regimes might confirm its presence within the landfill site. MLA analysis of particles size distribution of well 1901 is demonstrated in Table 30.

Table 30: MLA particles size distribution.

Sieve Size (μm)	Retained Wt%	Cum. Retained Wt%	Cum. Passing Wt%
125	0.00	0.00	100.00
106	0.03	0.03	99.97
90	0.03	0.06	99.94
75	0.19	0.25	99.75
63	1.13	1.37	98.63
53	5.70	7.07	92.93
45	16.08	23.15	76.85
38	24.39	47.54	52.46
32	20.97	68.51	31.49
27	12.53	81.05	18.95
22	7.96	89.00	11.00
19	3.31	92.32	7.68
16	2.51	94.83	5.17
13.5	1.81	96.63	3.37
11.4	1.14	97.78	2.22
9.6	0.81	98.59	1.41
8.1	0.65	99.24	0.76
6.8	0.42	99.66	0.34
5.7	0.28	99.94	0.06
4.8	0.04	99.98	0.02
4.1	0.01	99.99	0.01
3.4	0.01	100.00	0.00
2.9	0.00	100.00	0.00
2.4	0.00	100.00	0.00
2	0.00	100.00	0.00
1.75	0.00	100.00	0.00
1.45	0.00	100.00	0.00

Appendix 12 demonstrates descriptive statistics of minerals within the four different wells. ANOVA analysis shows significant differences for Calcite ($P < 0.001$), Muscovite ($P < 0.001$), Old battery ZnMn ($P < 0.001$), Zircon ($P < 0.001$), Albite ($P < 0.001$), Dolomite ($P < 0.001$),

Bixbyite ($P < 0.001$), Ankerite ($P < 0.001$), Glass fibres ($P < 0.001$), Hematite ($P < 0.003$), Epidote ($P < 0.003$), Hornblende ($P < 0.004$), Ferroan Clay ($P < 0.007$), Quartz ($P = 0.009$) values in the four different wells, confirming that the data sets were randomly distributed (Appendix 13).

A method for evaluating type and concentration of minerals/inorganic fibers (not only asbestos classified) that can be airborne from landfills and cause potential harm to humans was represented in this research. Inorganic fibres potentially harmful to the human health were detected in the site under the study. Additionally, waste size fractions ≤ 10 and > 3 microns were also found in the studied site. Hence, care should be taken when handling with the waste materials during a LFM project.

Chapter 5: ADMS Methods and Modelling

5.1 Introduction to Air Dispersion Modelling

The air, water, soils, and biota are the main transport routes for pollutants in the environment (Csavina et al., 2012). Contaminants in the form of dust can be transported by air in two ways: as volatilized species and then converted to solid (liquid-solid) or directly as particles (ibid). The indirect transport of contaminants as volatilized species come from gaseous precursors (Kim et al., 2015), such as ammonia, oxides of nitrogen, sulphur dioxide, and non-methane volatile organic compounds that are released from anthropogenic sources (Kampa and Castanas, 2008; Kim et al., 2015; Rodriguez et al., 2019). Atmospheric particles (dust), typically within the particle size range $<60 \mu\text{m}$ can play a significant role in the transport of contaminants into the environment (Csavina et al., 2012; Omrani et al., 2017). They become particularly important when are characterised by low volatility and low aqueous solubility, and thus remaining attached to particles of soil (ibid). Because air mass moves at a considerably faster rate than other environmental media, atmospheric particles have the greatest potential to transfer pollutants through the environment in the short-term (hours to days) (Csavina et al., 2012; Manisalidis et al., 2020). Due to the increase of human activities and projected climate change, the transport of atmospheric particulates is potentially to become more significant in the future (Afzali et al., 2017; Csavina et al., 2012; Pelletier, 2006). Contaminant transport by air is likely to be the most significant among all the major transport pathways in terms of their potential risk to human health and the environment, owing to the potential distance, speed, and aerial extent with which contaminants can be transported in the environment (Csavina et al., 2012; Elmes and Gasparon, 2017; Kim et al., 2015; Liu et al., 2023). Hence, policy-makers have integrated air pollution control methods as an intrinsic aspect of urban planning (Afzali et al., 2017). Mining operations offer the largest potential adverse effect to human health and the environment, which can degrade vegetation cover and diversity of flora and fauna, despite

the fact that there are several natural and anthropogenic sources of air particles (Csavina et al., 2012; Wang et al., 2022a). They are also one of the most significant sources of particulate emissions (Gautam et al., 2016; Richardson et al., 2019; Wang et al., 2021b; Wang et al., 2022b). Thus, it is critical to understand the influence of LFM activities on air quality.

Because regular monitoring of pollutants through monitoring networks is costly and not always feasible/available (Abril et al., 2016; Afzali et al., 2017). Instead, air dispersion modelling provides more reliable information on air quality above and beyond monitoring sites (Richardson et al., 2019; Zou et al., 2010), and is used for the design/implementation of emission reduction and control measures as well as supporting environmental impact assessments (Abril et al., 2016; Joseph et al., 2018). Atmospheric dispersion modelling has been extensively utilized to predict dust concentrations and dispersion (Abril et al., 2016; Appleton et al., 2006; El-Fadel and Abi-Esber, 2012; Kartal and Özer, 1998; Leelőssy et al., 2014). Modelling uses mathematical equations to calculate concentrations at various receptors as a result of a pollutant released from sources of a given geometry, which describe the atmospheric physical and chemical processes of dispersion (Afzali et al., 2017; Douglas et al., 2017; Holmes and Morawska, 2006; Sairanen and Pursio, 2020). In other words, it is a computer programme used to solve mathematical equations and algorithms that simulate air pollutant dispersion (Douglas et al., 2017; El-Harbawi and Rashid, 2008; Leelőssy et al., 2014).

5.2 Factors Affecting Dispersion of Pollutants in the Atmosphere

Several factors can affect pollutant dispersion in the atmosphere. These factors include, but are not limited to, meteorology, topography, surface roughness and buildings (Leroy et al., 2010).

5.2.1 Meteorology

Meteorological data is an inevitable element of air dispersion modelling in the mining sector because it influences the atmosphere's diluting effects (Chaulya et al., 2022; Chaulya et al.,

2019; EPA, 2005; Huertas et al., 2014; Mishra et al., 2016; Neshuku, 2012; Pandey et al., 2014; Piras et al., 2014; Sahu et al., 2018; Seaman, 2000; Srivastava et al., 2021; Tian et al., 2014; Wang et al., 2022a). Additionally, it can play an important role for substance concentration thresholds to be reached in the presence of certain meteorological conditions, and not only by the increase in emissions from different sources (Luo et al., 2021; Pérez et al., 2020). Pollutant dispersion, transformation, and removal in the atmosphere are all influenced by the meteorological conditions within a site (Huertas et al., 2012b; Meng et al., 2019b; Wang et al., 2016; Wang et al., 2022a; Wu et al., 2018). As a result, in order to get the best results from modelling, adequate meteorological data, ideally from a weather station within the area of interest, is required (CERC, 2016). A detailed description of the role of each meteorological parameter in pollutant dispersion effect is provided below.

5.2.1.1 Wind speed

In air dispersion modelling, wind speed is one of the most significant meteorological parameters (Du et al., 2022; Pandey et al., 2014; Seaman, 2000; Tian et al., 2014). According to (Csavina et al., 2014), wind speed is regarded the main driver in predicting dust concentrations. The initial dilution of a plume leaving a source is influenced by wind speed; consequently, the stronger the wind speed, the faster the dilution of the pollutants and thereby the lower the ground level concentrations (Thomas, 2009). In contrast, low and calm winds are the most important meteorological conditions responsible for the highest pollutant concentration values at ground level (Cuculeanu et al., 2019; Zhang et al., 2013).

5.2.1.2 Wind direction

The direction in which pollutants emitted into the atmosphere is determined by wind direction (Meng et al., 2019a; Tian et al., 2014; Turner, 2020). The dispersion of pollutants can be assumed to occur with the prevailing wind directions (El-Fadel and Abi-Esber, 2012). Therefore, it has a significant influence on dust dispersion as it determines the direction of

vulnerable receptors (Mishra et al., 2016; Sairanen and Pursio, 2020; Tian et al., 2014). The concentration of dust measured in upwind direction can be used to represent background concentration (Lal and Tripathy, 2012; Piras et al., 2014).

5.2.1.3 Air temperature

Ambient temperature is a variable that can affect the dust concentrations particularly in the presence of temperature inversions (a layer that is classified when the lapse rate is greater than zero) (Al-Hemoud et al., 2019; Lang et al., 2013; Meng et al., 2019a; Trinh et al., 2019), which hampers the diffusion and dilution of pollutants (Meng et al., 2019b; Wu et al., 2018) and sometimes makes the pollutants restricted at low levels (referred to as mixing height), near to the surface especially in winter (EPA, 2005; Meng et al., 2019a; Pandey et al., 2014; Sánchez-Ccoyllo and de Fatima Andrade, 2002). Hence, temperature is considered a pollution control parameter (Kartal and Özer, 1998). Furthermore, the lowest plume rise of particulates occurs as a result of higher ambient temperatures and thus is responsible for the largest impacts (EPA, 2005).

5.2.1.4 Topography

Terrain features can have a significant impact on concentration distributions of pollutants (Appleton et al., 2006; CERC, 2016; Joseph et al., 2018; Kakosimos et al., 2011; Meng et al., 2019a; Pandey et al., 2014; Piras et al., 2014; Triantafyllou, 2001; Triantafyllou and Kassomenos, 2002). For example, for moderate gradients, the flow of a pollutant follows hills with little deviation and thus there will be a slight change in concentrations between the terrain and no terrain model concentrations (CERC, 2016). Topographical features such as surface roughness, hills, buildings, trees, and barriers can all influence pollutant dispersion in the atmosphere (Neshuku, 2012). Surface roughness has an impact on the wind vertical profiles and temperature, as well as the dispersion rates in the surface layer, and is an important factor to consider when evaluating dispersion at receptor locations (Asif et al., 2018).

5.2.1.5 Relative humidity

The relative humidity is also a significant influencing factor on particulate pollution dispersion (Meng et al., 2019a; Wang et al., 2022a). It has a negative relationship with dust suspension concentrations (Oguntoke et al., 2013; Pandey et al., 2014; Sairanen and Pursio, 2020; Wu et al., 2018) because it controls the rate at which contaminants/particles are absorbed making them too heavy to travel through the air (Kartal and Özer, 1998; Wu et al., 2018), and thus reduces the amount of suspended dust/increases particle deposition rate (Sánchez-Ccoyllo and de Fatima Andrade, 2002; Wu et al., 2018). In this case, the deposited dust is considered as a result of wet deposition rather than dry deposition.

5.3 Air Dispersion Models

There are many types of models that have been previously developed to be used for the prediction of air quality for mining application (Asif et al., 2018), the most important of which are Box models, Gaussian model, Eulerian, and Lagrangian model (Douglas et al., 2017; El-Fadel and Abi-Esber, 2012; Lilic et al., 2018; Reed et al., 2002). These models differ from each other in terms of the pollutant chosen and the kind of activity of pollution source (Reed and Control, 2005; Xu et al., 2020). The most widespread dispersion models utilized in atmospheric dispersion modelling are Gaussian type models (Brusca et al., 2016; Douglas et al., 2017; El-Fadel and Abi-Esber, 2012). However, older Gaussian plume models using the Pasquill-Gifford (P-G) stability class scheme had some limitations when used in particle dispersion analysis (El-Fadel and Abi-Esber, 2012; Kim et al., 2013; Leroy et al., 2010; Neshuku, 2012). These limitations arose from the inability to account for changes in boundary layer parameters as a function of height, the use of steady state estimates that do not account for the time it takes for the pollutant to reach to the receptor, and the vertical particle movement caused by gravity during that period (El-Fadel and Abi-Esber, 2012; Holmes and Morawska, 2006; Kim et al., 2013). Advanced Gaussian models had been developed in the following years to resolve most

of the limitations of earlier Gaussian models (El-Fadel and Abi-Esber, 2012; Neshuku, 2012). In this context, the new generation models of American Meteorological Society/Environmental Protection Agency Regulatory Model (AERMOD) and Advanced Dispersion Modelling System (ADMS) were designed with enhanced algorithms to address the limitations of early Gaussian models (Asif et al., 2018; Hanna et al., 2001; Joseph et al., 2018; Leelőssy et al., 2014; Neshuku, 2012), which allow meteorological parameters and turbulence fluctuations to vary with height, resulting in a more physically realistic representation of the atmosphere (El-Fadel and Abi-Esber, 2012; Joseph et al., 2018; Leelőssy et al., 2014; Leroy et al., 2010).

AERMOD is based on a steady-state plume (Gaussian algorithm) (Abril et al., 2016; Joseph et al., 2018; Kim et al., 2013; Leelőssy et al., 2014; Tartakovsky et al., 2013), and can estimate pollution concentrations up to 50 km away from the source (Tartakovsky et al., 2016). Published investigations demonstrated, however, that AERMOD is not ideal for calm conditions or low wind speeds and the performance of ADMS is superior to that of AERMOD in predicting air particulate matter (Asif et al., 2018; Hanna et al., 2001; Neshuku, 2012). Therefore, ADMS is the model chosen for the dust dispersion analysis in this study and also due to the fact that it is capable of modelling dispersion from multiple sources (El-Fadel and Abi-Esber, 2012; Kim et al., 2013; Vardoulakis et al., 2007). ADMS is also the model preference for UK regulators (Holmes and Morawska, 2006).

A developed methodology for modelling atmospheric dust dispersion using ADMS 5 was investigated and utilised as the latest available version. Inputs used in the analysis were based on the present studied site-specific settings. The aim of this investigation is to define the contribution of the LFM operation towards air pollution. Different scenarios were considered based on studied site meteorological changes.

5.4 ADMS

The ADMS is an advanced steady-state Gaussian dispersion model, capable of simulating dispersion of different industrial and traffic releases in the atmosphere (Appleton et al., 2006; Carruthers et al., 1994; Leroy et al., 2010). “It is a “new generation” dispersion model which uses two parameters to describe the atmospheric boundary layer, namely the boundary layer height h and the Monin-Obukhov length L_{MO} , and a skewed Gaussian concentration distribution to calculate dispersion under convective conditions” (CERC, 2016). It has been widely validated against field datasets (CERC, 2016; Riddle et al., 2004). The model can be used to about 60 km downwind from the source and is useful for distances reaching to 100 km (CERC, 2016; Davies, 1996). ADMS is jointly developed by the Cambridge Environmental Research Consultants (CERC) in the UK, National Power and the U.K. Met. Office (Athanassiadou et al., 2010; El-Fadel and Abi-Esber, 2012; Hanna et al., 2001). The Environment Agency for England and Wales has certified ADMS for use in assessments that support pollution prevention and control applications, determining appropriate discharge conditions such as stack height, and requirements for pollution control systems and safety planning (Appleton et al., 2006). The term ‘stability’ in ADMS is detailed in Table 31.

Table 31: Stability categories in ADMS (CERC, 2016).

Stable	$h/L_{MO} > 1$
Neutral	$-0.3 \leq h/L_{MO} \leq 1$
Convective	$h/L_{MO} < -0.3$

The Monin–Obukhov length is a depth measure of the near-surface layer where wind shear effect is probable to be significant through any stability condition (CERC, 2016). In ADMS 5, the boundary layer is characterised by the boundary layer height h and the Monin-Obukhov length L_{MO} and not by a Pasquill-Gifford stability category (A to G) and it can be defined as:

$$L_{MO} = \frac{-u_*^3}{\left(\frac{\kappa g F_{\theta 0}}{\rho c_p T_0}\right)}$$

where u_* is the friction velocity at the Earth’s surface, κ is the von Karman constant (0.4), g is the acceleration due to gravity, $F_{\theta 0}$ is the surface sensible heat flux, ρ and c_p are, respectively, the density and specific heat capacity of air and T_0 is the near-surface temperature.

The Monin-Obukhov length is negative in unstable or convective conditions, and it is defined as the height above which thermal turbulence dominates over mechanical turbulence in causing turbulent motions. The Monin-Obukhov length is positive in stable conditions, and it is quantified as the height above which stable stratification prevents vertical turbulent motion (CERC, 2016).

The ADMS model includes a meteorological pre-processor developed by the UK Met Office, which uses the input of meteorological data for the calculation of the boundary layer height (h) and the Monin-Obukhov length (L_{MO}) to define the wind and turbulence vertical profiles in the boundary-layer (El-Fadel and Abi-Esber, 2012; Joseph et al., 2018). It also includes an integrated mapping tool ‘Mapper’ which allows users to visualize model setup as well as construct and change sources, receptors, and buildings (CERC, 2016).

Inputs required for the air dust modelling are source emissions rate (emission inventory), geometry of a source, topography of the study area (DP and TR, 2015; El-Fadel and Abi-Esber, 2012; Kumar et al., 2016), meteorological variables, such as wind speed and direction, and total precipitation and daily temperature, together with solar radiation and humidity (Asif et al.,

2018; Kumar et al., 2016). The software output is pollutant concentrations contour plots in $\mu\text{g}/\text{m}^3$ underlain by a map to show receptor locations for a specific time period (Kumar et al., 2016). The contour plots are useful for visually showing how concentrations vary with distance from the source and the variation in the long-term averages coupled with direction. The first step in analysing any potential impact on human health or the environment is to model dust concentrations at receptors in a proximity to the emission sources (DP and TR, 2015). A user-friendly model interface or modifying input files (.apl files) can be used to enter model input parameters into ADMS (Douglas et al., 2016). Figure 40 illustrates a schematic representation of the input-output of an air dispersion model.

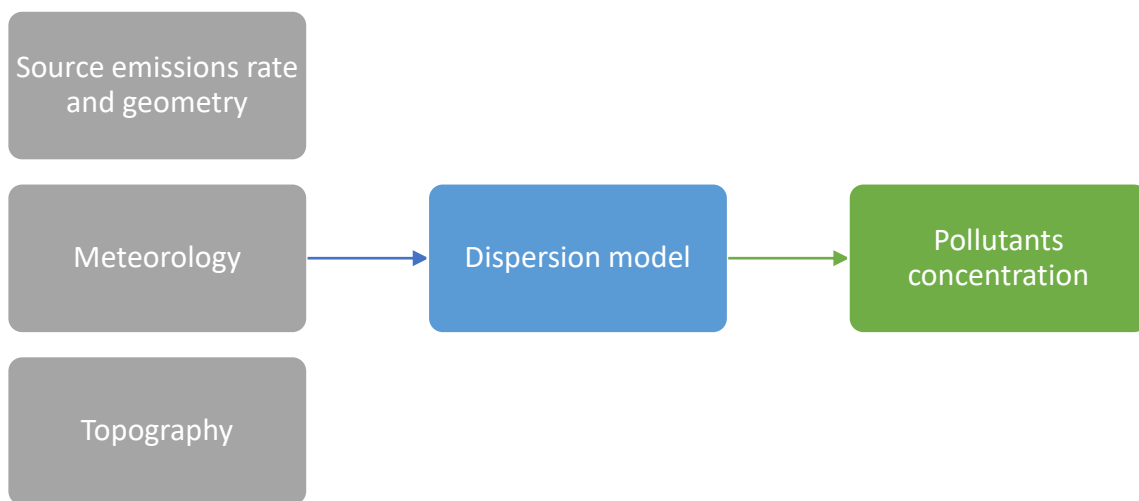


Figure 40. A simplified schematic representation of the input-output of the air dispersion model.

5.5 ADMS Modelling Methodology

There are two types of distinct deposition of pollutants onto the surface: dry deposition and wet deposition (Chu et al., 2008; Leelössy et al., 2014; Wu et al., 2018). Pollutants are removed from the air in a dry deposition process owing to the gravitational effect at varying rates, which depend on the size fraction and density of a particle (Asif et al., 2018; Mariraj Mohan, 2016; Parsa et al., 2019). However, in wet deposition, pollutants are eliminated from the atmosphere

by rain or snow, or fog (Asif et al., 2018; CERC, 2016; Leelössy et al., 2014). The dry deposition model option was used in this study to account for the direct delivery of pollutants from the atmosphere to the surface (Giardina and Buffa, 2018; Parsa et al., 2019; Wu et al., 2018) through all exposure routes to which a human being is normally exposed, thus having the greatest potential impact on human health and the environment (Emerson et al., 2020; Mariraj Mohan, 2016; Wang et al., 2014). Additionally, the results are more precise and closer to the field observations values by applying the dry deposition model (Asif et al., 2018; Costa et al., 2006; Mariraj Mohan, 2016; Moreira et al., 2005). Dry deposition happens when material from the plume (dust) is lost at the ground surface (Mariraj Mohan, 2016; Tartakovsky et al., 2016) and is treated as a first-order removal mechanism from atmosphere (Aksoyoglu and Prévôt, 2018). It affects the airborne concentration of dust in comparison with the scenario of no deposition through the depletion of the plume concentration with the increase of distance downstream from the source (CERC, 2016). Modelling of dry deposition effects in ADMS 5 requires some deposition parameters to be defined, such as particle diameter and density in order to be used in the estimation of deposition velocity and/or terminal velocity for particulates dispersion (Appleton et al., 2006; CERC, 2016; Mariraj Mohan, 2016). The dry deposition rate is thought to be proportional to the concentration at the near-surface and is calculated in ADMS through the following equation (CERC, 2016; Mariraj Mohan, 2016; Piras et al., 2014):

$$F = v_d C(x, y, 0)$$

where F is the rate of deposition per unit area per unit time, v_d is the deposition velocity, and C is the predicted airborne concentration at the position, ground level for this study (x, y, 0).

5.6 Emission Estimation

An estimate of dust generation is required in mine planning to determine the expected degree of air pollution in the mining region (Triantafyllou et al., 2021). Additionally, Data of dust

emissions inventories is critical for environmental risk assessment and provides the foundation for analysing the environmental fate of these emissions (EPA, 2005; Richardson et al., 2019). An emission inventory must be created in air quality models to account for the predicted amount of dust released into the atmosphere (Kumar et al., 2016; Triantafyllou et al., 2021). For estimating a source's emissions, data from source-specific emission tests or continuous emission monitors are typically chosen because they provide the most accurate representation of the tested source (Abril et al., 2016). However, because neither emission monitoring data nor emission field tests (samplers) were available in the study area, emission factors had to be approximated using prediction-type equations for the development of emission factors (EPA, 2005). Emissions estimation from different sources is generated by emission factors (Neshuku, 2012). An emissions factor is “*a representative value that attempts to relate the quantity of a pollutant released to the atmosphere with an activity associated with the release of that pollutant*” (Abril et al., 2016; USEPA, 1995). In other words, it is a calculation of the estimated degree of emissions released into the atmosphere with an activity associated with that release in a certain area (Abril et al., 2016; EPA, 2005). It should include evaluations for all significant sources of dust, as well as a range of suspended dust emissions rate (Chaulya et al., 2002). These variables are commonly stated as the weight of the pollutant divided by the unit weight, distance, volume, or the duration of the pollutant-emitting activity (Abril et al., 2016). Dust emissions are influenced by a variety of factors in the mining sector, including weather conditions, heavy equipment dimensions, emission control efficacy, and physical characteristics of material (Chaulya et al., 2019; Neshuku, 2012). The general equation for emissions estimation is the following (Abril et al., 2016; Appleton et al., 2006; Kim et al., 2020):

$$E = A \times EF \times \left(\frac{1 - ER}{100} \right)$$

where E is the total emissions rate (e.g., kilograms of dust released per day), and A is the activity rate (e.g., tonnes of waste handled per day). EF represents the emission factor (e.g., kilograms of dust released per tonne of waste handled), and ER the overall emission reduction efficiency (%) (Kim et al., 2020). The emission reduction only applies if there are any emission-controlling methods used (Abril et al., 2016). Dust from surface mining activities is produced from a variety of activity sources, similar to those considerably used in LFM activities. An equation for estimating emissions has been developed for each source of activity in the mining sector (Neshuku, 2012). The United States Environmental Protection Agency (USEPA) and Central Mining Research Institute in India has carried out a lot of work developing emission estimating formulas for these activities (Chakraborty et al., 2002; Chaulya et al., 2003; Chaulya et al., 2019; Lal and Tripathy, 2012; Neshuku, 2012; Richardson et al., 2019). A set of field observations of dust generation from all individual activities was validated against these expressions (Lal and Tripathy, 2012). The equations employed in this research were adopted from surface mining operations by (Chaulya, 2006) (Table 32) because the focus of those studies was based on surface mining and allowed for a more accurate prediction of dust formation (Triantafyllou et al., 2021). (Chaulya, 2006) has performed extensive work on the development and validation of a series of Gaussian dispersion equations for calculating the emission rate by considering ground level, vertical, and horizontal dispersion coefficients from various surface mining operations. Each activity's formula is based on a field investigation of three surface mines and an average of three data at each monitoring station. The accuracy of the validation study was found to be between 92% and 97% of actual field measurement data (Lilic et al., 2018; Patra et al., 2016). These equations have considered the major influencing parameters for each individual activity (Chaulya, 2006).

A range of each formula component was given for modelling emission rate variability in this study to predict maximum and minimum emission values. Parameters identified in the

equations were adjusted to LFM applications and for local weather conditions. MC and silt contents of the recovered waste analysed in this study were used in the emission rate calculation. MC values ranged from (22.8% - 25.8%) of all different sampling locations. The passing waste size fractions of 0.053 mm sieve obtained previously in this study from the entire recovered MSW was considered as the silt content range (4.6% - 7.7%) in the emission rate calculation because fractions between 0.002 to 0.06 mm are classified as silt content (Abril et al., 2016; Neshuku, 2012; Pimolthai and Wagner, 2014) and airborne particular matter (TSP) (Patra et al., 2016; Ronowijoyo et al., 2020; Sahu et al., 2018). It is also believed that particles $>50 \mu\text{m}$ cannot enter the respiratory tract (Araújo et al., 2014) and is considered a criteria pollutant in air quality standards (Huertas et al., 2014).

Wind speed was calculated for a range of 0 to 30 m/s to account for the best- and worst-case scenarios. Required components of the equations regarding heavy equipment dimensions and average vehicle speed range have been estimated from literature of LFM case studies and landfill operation reports (CAT, 2008; ISWA, 2019; Jain et al., 2013; LLC, 2009; Parrodi et al., 2019b). Loader sizes range from 1-2.5 m³ was used for loading activities (e.g., Caterpillar 320, Hitachi 250LC, and Liebherr 934). For unloading activities, the range was also 1-2.5 m³ if waste directly unloads to screening plant or 22-35 t in the case of using an unloader truck for waste delivery to the screening plant in large areas. As the direct delivery of waste to the screening plant was the considered method in this study and the capacity of unloader in the equation was given per t, a range of 0.5-1.5 tonne was used in the emission rate calculation for unloading activities, which can approximately fill the bucket size of 1-2.5 m³ used. The direct fed of waste materials into screening plant is the process undertaken for the majority of LFM investigations and projects (Hogland et al., 2014; Jain et al., 2013; LLC, 2009; Lopez et al., 2019; Lucas et al., 2019a; Parrodi et al., 2020). Hence, it is the scenario considered in this study.

Table 32: Emission inventory and mathematical expressions for emission rate.

Activity	Source type	Parameter			Equation
		Symbol	Name	Unit	
Cover removal loading	Point	m	Moisture content of waste	%	$E = \left[0.0081 \left\{ \frac{(100 - m)}{m} \right\}^{1.4} \left\{ \frac{s}{(100 - s)} \right\}^{0.3} (u)^{1.1} (h * f * l)^{0.1} \right]$
		s	Silt content of loading waste material	%	
		u	Wind speed	m s ⁻¹	
		h	Drop height	m	
		l	Size of loader	m ³	
		f	Frequency of loading	no. h ⁻¹	
		E	Emission rate	g s ⁻¹	
Recovered waste loading	Point	m	Moisture content of waste	%	$E = \left[h \left\{ \frac{(100 - m)}{m} \right\}^{0.4} \left\{ \frac{0.555 * s}{(100 - s)} \right\} (u^2 * f * l)^{0.1} \right]$
		s	Silt content of loading waste material	%	
		u	Wind speed	m s ⁻¹	
		h	Drop height	m	
		l	Size of loader	m ³	
		f	Frequency of loading	no. h ⁻¹	
		E	Emission rate	g s ⁻¹	
Haul road	Line	m	Moisture content of haul road dust	%	$E = \left[\left\{ \frac{(100 - m)}{m} \right\}^{0.7} \left\{ \frac{u * S}{(100 - s)} \right\}^{0.1} (41.6 + 0.03 * f * c + 108 * v) 10^{-5} \right]$
		s	Silt content of haul road dust	%	
		u	Wind speed	m s ⁻¹	
		v	Average vehicle speed	m s ⁻¹	
		f	Frequency of vehicle movement	no. h ⁻¹	
		c	Capacity of dumpers	t	
		E	Emission rate	g s ⁻¹ m ⁻¹	
Transport road	Line	m	Moisture content of road dust	%	$E = \left[\left\{ \frac{(100 - m)}{m} \right\}^{0.35} \left\{ \frac{u * s}{(100 - s)} \right\}^{0.7} \{0.5 + 0.1(f + 0.42 * v)\} 10^{-3} \right]$
		s	Silt content of transport road dust	%	
		u	Wind speed	m s ⁻¹	
		v	Average vehicle speed	m s ⁻¹	
		f	Frequency of vehicle movement	no. h ⁻¹	
		E	Emission rate	g s ⁻¹ m ⁻¹	

Cover removal unloading	Point	m	Moisture content of waste	%	$E = \left[0.33 \left\{ u * h \frac{(100 - m)}{m} \right\}^{0.1} \left\{ \frac{s}{(100 - s)} \right\}^{0.3} (f * c)^{0.15} \right]$
		s	Silt content of unloading waste material	%	
		u	Wind speed	m s ⁻¹	
		h	Drop height	m	
		c	Capacity of unloader	t	
		f	Frequency of unloading	no. h ⁻¹	
		E	Emission rate	g s ⁻¹	
Recovered waste unloading	Point	m	Moisture content of waste	%	$E = 0.156 * h^{0.6} \left[\left\{ \frac{(100 - m) * s * u * c * f}{m(100 - s)} \right\}^{0.1} \right]$
		s	Silt content of unloading waste material	%	
		u	Wind speed	m s ⁻¹	
		h	Drop height	m	
		c	Capacity of unloader	t	
		f	Frequency of unloading	no. h ⁻¹	
		E	Emission rate	g s ⁻¹	
Exposed cover removal waste	Area	m	Moisture content of exposed material	%	$E = \left[\left\{ \frac{(100 - m)}{m} \right\}^{0.1} \left\{ \frac{s}{(100 - s)} \right\}^{0.6} \left\{ \frac{u}{(19 + 0.01 * u)} \right\} \left\{ \frac{a}{(6 + 256 * a)} \right\} \right]$
		s	Silt content of exposed material	%	
		u	Wind speed	m s ⁻¹	
		a	Area of active dump	km ²	
		E	Emission rate	g s ⁻¹ m ⁻²	
Screening plant	Area	m	Moisture content of waste	%	$E = \left[\left\{ \frac{(100 - m)}{m} \right\}^{0.5} \left\{ \frac{s * a}{(100 - s)} \right\}^{0.1} \left\{ \frac{u}{(20 + 3300 * u)} \right\} \right]$
		s	Silt content of screening material	%	
		u	Wind speed	m s ⁻¹	
		a	Area	km ²	
		E	Emission rate	g s ⁻¹ m ⁻²	
Exposed pit surface	Area	m	Moisture content of surface material	%	$E = \left[\left\{ \frac{(100 - m)}{m} \right\}^{0.1} \left\{ \frac{s}{(100 - s)} \right\}^{0.3} a^{1.6} \left\{ \frac{u}{(10 + 125 * u)} \right\} \right]$
		s	Silt content surface material	%	
		u	Wind speed	m s ⁻¹	
		a	Area	km ²	
		E	Emission rate	g s ⁻¹ m ⁻²	

Area units from the existing landfill were used in the equations whose source type is area (1 phase = 0.0044 km²). Average vehicle speed of 2.6 m/s for haul road and 11 m/s for transport road were used in the calculation of emission rate. The silt content of haul and transport road dust range were estimated a little higher than the silt content of waste materials (15-25, 10-20 %), respectively. The estimated area used for the screening plant activity was 0.0009 km². Drop height values used in the formulas were ranging between 1-3 m for loading/unloading activities. Frequency of loading values in the equations were estimated based on the computed volume of the landfill waste under the study.

ADMS has the function to add time varying emissions source data that could help to address the intermittent nature of LFM activities, such as excavation, shredding, and screening (Douglas et al., 2017). This feature is applied to the modelling analysis as some sources are not constant.

5.7 Meteorological and Terrain Data

Meteorological data were obtained from UK Met Office platform at Marham station, 573813 easting, 309014 northing (latitude = 52:65N, longitude = 00:57E) with an elevation of 21 m above mean sea level, which is the nearest weather station to the Docking landfill site - 28 km from the study area. The data obtained were recorded at a series of hourly sequential intervals from 2016-2019 for 24 h throughout the years. Sequential data comprising continuous hour-by-hour measurements are a better representation of meteorological conditions than statistically-averaged data (CERC, 2016). Meteorological input data required for the dry deposition model are the following parameters:

- Year.
- Julian day number (e.g., Dec 31 =365 or 366).
- Local time (0-24).

- Wind speed (m/s).
- Wind direction (degree).
- Solar radiation (W/m²)
- Cloud amount (oktas).
- Temperature (°C).

In order to estimate the boundary layer height by ADMS, solar radiation and cloud cover alongside the year, day and hour, and the latitude input to the interface are required in the absence of sensible surface heat flux values (CERC, 2016). The boundary layer meteorological parameters required by the dispersion model are calculated by the meteorological input module using standard algorithms defining the boundary conditions of an analysed site used by the model. (Holtslag and Van Ulden, 1983) provide comprehensive information for these calculations.

Solar hourly radiation dataset was acquired at Holbeach No 2 weather station (33.1 km from the study area), 5440E 3327N (Latitude: 52.8729, Longitude: 14021) with an elevation of 3 m above mean sea level. Dry deposition model does not require precipitation parameters within its analysis since it only considers deposition due to grounding of the plume (CERC, 2016). Terrain data file (ter.) of the study area was created using the utility tool in the ADMS 5 interface that is linked to commonly available data formats, such as Ordnance Survey (OS Terrain 50).

5.8 LFM Assumed Process Plan

The study area was divided into 5 phases according to its unit area (Figure 41). LFM process plan and the subsequent air dispersion modelling was carried out on the basis of 1 phase out of 5 which approximately accounts for 0.48 hectares. The landfill is assumed to be mined on a phased basis as shown in Figure 41 and the phase no.4 was used in the ADMS modelling. Area

and line sources related activity geometry with X and Y coordinates were approximately determined over a horizontal convex polygon with 4 vertices and a straight line joining two vertices, respectively.



Figure 41. Assumed plan of LFM phases.

The total assumed waste volume range of one phase was achieved by calculating the length*width*depth (6-7 m, respectively) of the studied landfill site. Furthermore, in order to specify periods for meteorological data to be applied in the ADMS modelling, a timeframe of a LFM project should be estimated. The following equation has been established to be used for the determination of time taken for a LFM project to be completed:

$$T = \left(\frac{\text{Waste volume (m}^3\text{)}}{\text{Loader dimension (m}^3\text{)} * \text{Loading frequencies (no./hour)} * \text{Working hours (no. hour/day)}} \right)$$

where T is the timeframe of a LFM project. The loading frequencies refer to the total number of repetitions per day in a LFM project. A LFM assumed processes plan flowsheet will be developed based on the empirical formulas used in the emission rates calculation and the waste volume range that will be assumed so as to visualise the processes and define volumetric throughput ranges for each unit operation. Line source of transport road is not considered in the LFM assumed processes plan.

5.9 Selection of Scenarios

In order to form a specific number of scenarios for weather conditions, an extensive statistical analysis of the study site's real-recorded meteorological data for the years from 2016 to 2019 was conducted. As wind speed is the main factor in controlling the transfer of pollution (dust) from a landfill site to nearby receptors (Csavina et al., 2014; Kakosimos et al., 2011; Richardson et al., 2019; Wu et al., 2018), three different scenarios were established on the basis of wind speed data variations of the landfill site. Figure 42 below shows a boxplot chart of wind speed data from 2016 to 2019. Lower and upper quartile numbers from the chart were used as low and high wind speed conditions (2.5, 6.5 m/s), respectively. The maximum value in the data chart illustrated as an outlier (21 m/s) was used as an extreme condition.

The mean temperature ($^{\circ}10$) was used in the modelling for all scenarios (Figure 43). These three different scenarios were applied to all sources of activities (individually and in combination) in the modelling analysis for the minimum and maximum emission rate values to see under what scenario is dispersion an environmental/health risk and under what meteorological conditions is dispersion worst/best.

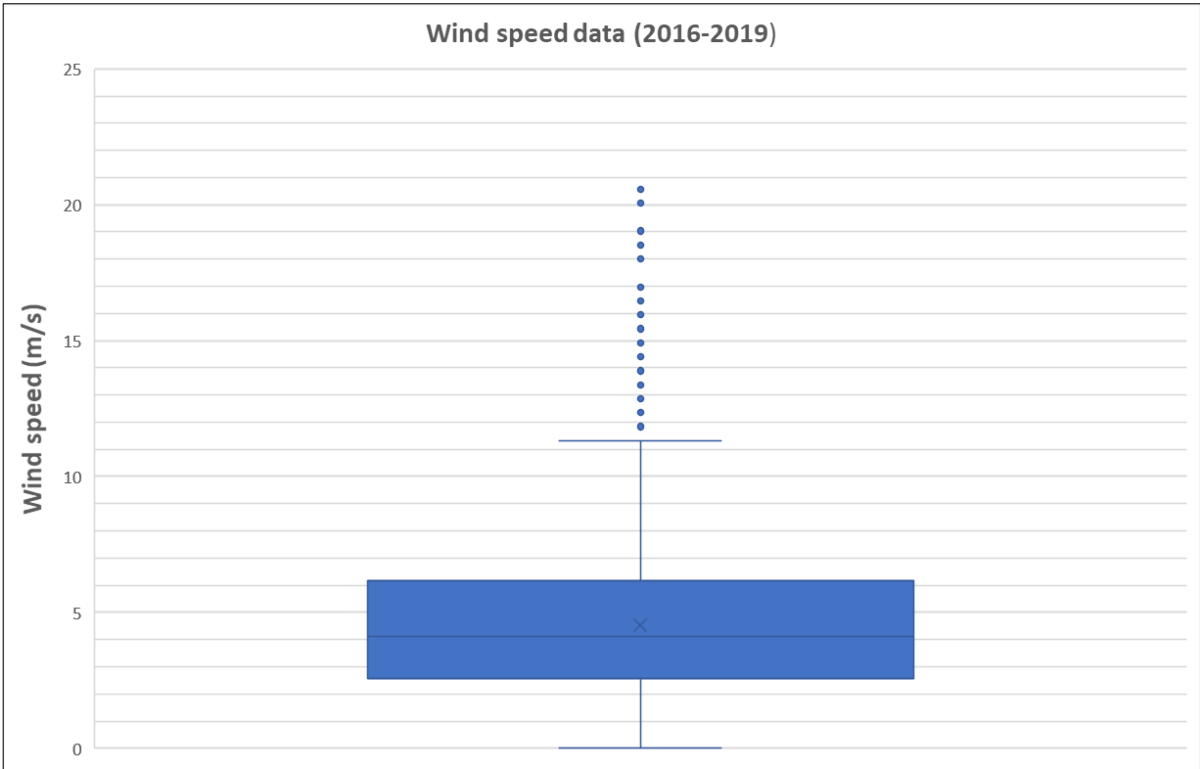


Figure 42. Boxplots of the real-recorded wind speed data from 2016 to 2019.

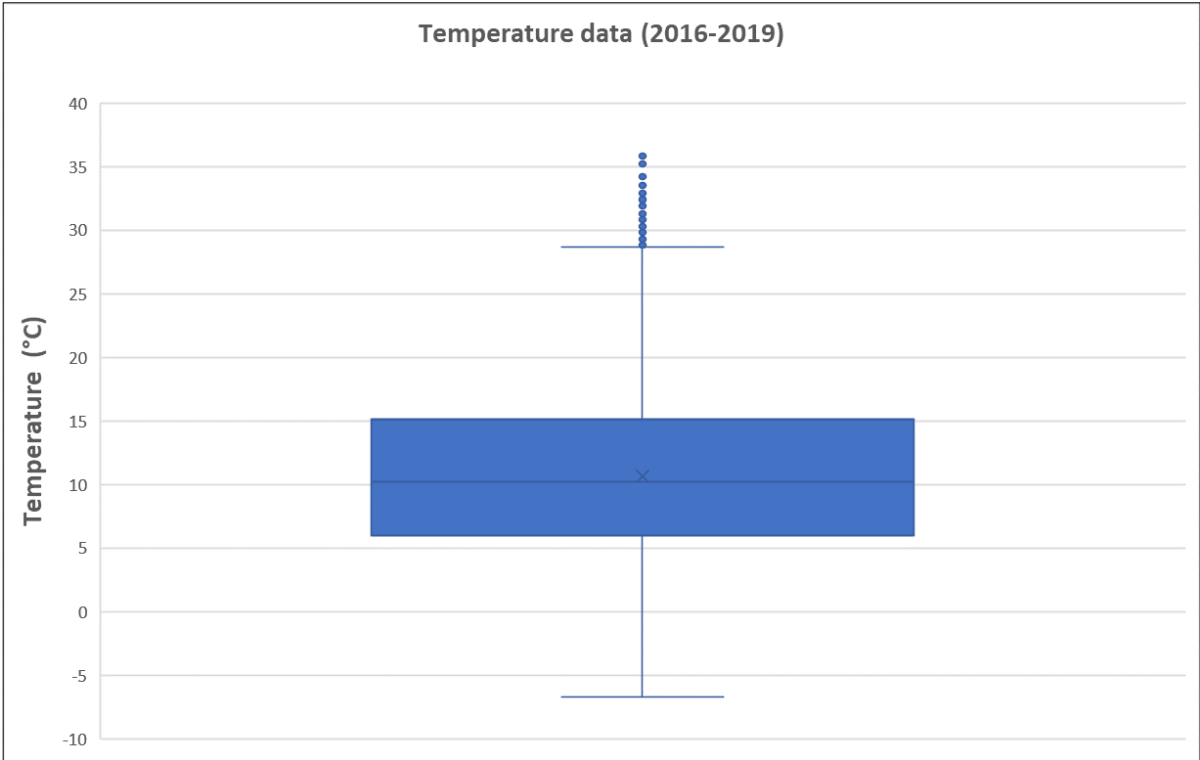


Figure 43. Boxplots of the real-recorded temperature data from 2016 to 2019.

5.10 Formatting Input Data to ADMS Format

Meteorological data (.met) and time-varying sources data (.var) files extension were initially prepared in Microsoft Excel and then had to be saved in comma-separated format (.csv) and (.txt), respectively, to meet the ADMS format and be ready for the modelling analysis. This required to change arrangement of the met office data cells, parameter names, and some parameter units to match with the ADMS format. Full details about the ADMS format of the meteorological data (.met) file and entering time-varying emissions (.var) file can be found in ADMS 5 User Guide (CERC, 2016).

5.11 Inputs of Dry Deposition Modelling

When setting up a modelling problem in ADMS, it requires the user to provide information defining the site is being modelled, such inputs relating to the types of pollutants, types of sources and their dimensions, meteorological and release conditions, and details of the output required (CERC, 2016). There are six basic input screens associated with an ADMS 5 model run as shown in Figure 44, namely Setup, Source, Meteorology, Background, Grids and Output (CERC, 2016). Input information used in this study for the dry deposition modelling of all different sources is presented in Table 33 with justification.

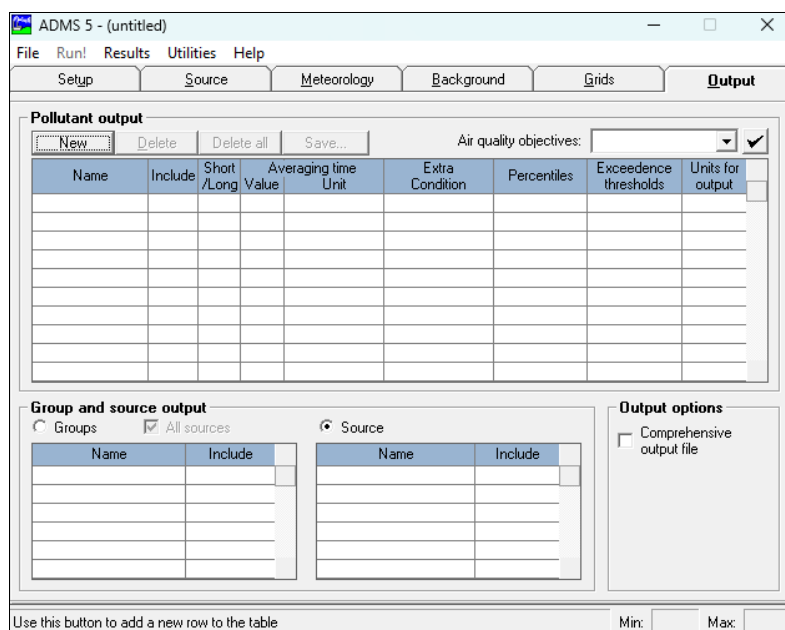


Figure 44. The ADMS interface.

In the source section, there are three different ways of using time-varying source data in ADMS 5 interface; source data from *.var file, emission factors from *.fac file, and emission factors from screen as shown in Figure 45. For each individual activity run of all scenarios, emission factors from screen option were used. Using the on-screen time varying factors simply takes the emission rate defined on the source emissions screen and multiplies it by the appropriate time varying factor (emission factor). It does this on a regular weekly pattern. Therefore, this way is much more convenient and straightforward. The sources were entered to operate during typical working hours, 9am to 5pm, and so the values (1) had to be entered at weekdays at the corresponding hours (9-17 local time hours). For all sources analysis (in combination), a .var file was used to ensure the accuracy of the inputs since time variation of source parameters is entered by hourly basis of each day. However, emission factors from screen option is applicable to be applied to all sources. Using a .var file applies hourly emission rates and other parameters for every hour of the modelling period and it does not need to follow a regular pattern.

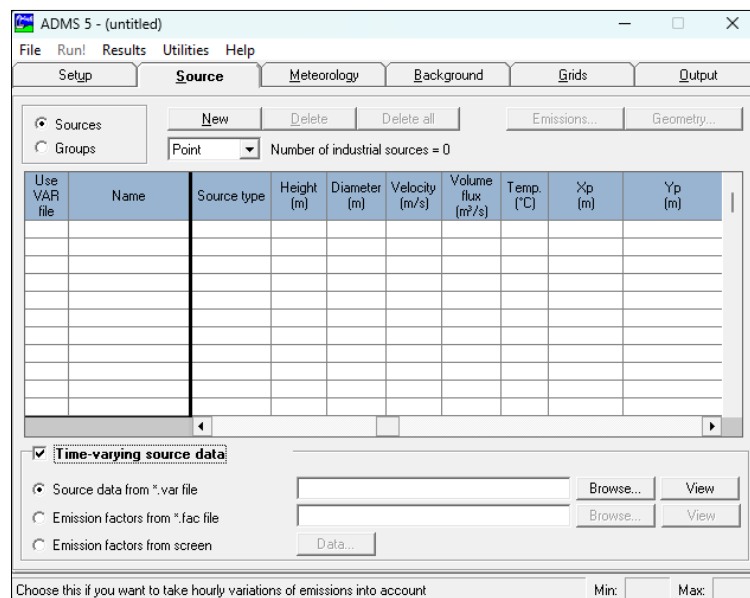


Figure 45. The Source screen.

Table 33: Inputs of the dry deposition model.

Parameter/Selection	Value/Name/Description	Reference/Justification

Setup		
Pollutant	Dust	Environmental and health impact of LFM dust emission
Particle diameter (m)	0.0265 0.0224 0.016 0.0125 0.0095 0.0067 0.00475 0.00335 0.00236 0.0017 0.00118 0.00085 0.0006 0.000425 0.0003 0.000212 0.00015 0.000106 0.000175 0.000053 0.000038 0.00002 0.00001	Consistent with the analysed particulate size distribution of the study area
Particle density (kg/m ³)	2583 560 1837 1948 4713 2567 787 4681 3755 2979 2119 1595 1954 2071 3347 3476 2227 1701 1133 1220 877 1933 1160	Assumption $\frac{\text{mass of returned (g) (from PSD)}}{\text{volume (15 cm}^3\text{)} \times 1000}$
Mass fraction	0.050 0.011 0.036	Must be 1 (± 0.05), consistent with the analysed particulate

	0.038 0.092 0.050 0.015 0.091 0.073 0.058 0.041 0.031 0.038 0.040 0.065 0.068 0.043 0.033 0.022 0.024 0.017 0.038 0.023	size distribution of all fractions in this study
Model option	Dry deposition	The focus of research since it is more significant for all exposure routes, and thereby has the greatest potential impact on the human health and the environment
Source		
Source type	Point/line/area	Activity-based
Height of the source (m)	0 (ground-level)	Height of source above the ground
Diameter of the source (m)	30	Internal diameter of the source (1 phase)
Efflux	Exit velocity	Default
Velocity of source release (m/s)	2.5/6.5/21	Consistent with the wind speed used in .met file
Coordinates (Xp,Yp) /geometry (m)	Point sources 579032 335597 Line source 579010 335573 (Haul road) 579065 335622	Coordinates of the analysed sources within phase no. 4
Cp (J ⁰ C/kg)	1012	Default (typical value for air)
Mol. Mass (g)	28.966	Default (typical value for air)
T, RHO or Ambient	Ambient	Release is at ambient temperature and density
Actual or NTP	Actual	Default (at actual release temperature and pressure)
Time varying emission factors	(1) for 8 hours on weekdays	Most emissions are not constant

Meteorology		
Latitude (°)	52.8	Latitude of northern England
Surface roughness (m)	0.3	Agricultural area max. value based on the site settings
Height of recorded wind (m)	21	Met office (MARHAM station)
Met. data	3 months hourly sequential	Met office
Met. data are hourly sequential	Yes	Met office data based on an hourly basis
Background		
Background concentration	None	Only contributed air concentration from the sources is considered
Grids		
Coordinate system	Cartesian coordinate system	Specified points
Receptor type	Grided	Coordinates of receptors were identified
Spacing	Regular	User-defined in Mapper interface
Number of output points	500 in each direction (x and y axis) from the proposed LFM site	Adequate resolution for capturing the areas of high concentration
Output		
Short/long	Long	To calculate the average of dust concentrations and to compare with UK standards
Averaging time unit	Hour	UK air quality limits and guidelines of PM10 (24-hour mean)
Averaging time value	24	UK air quality limits and guidelines of PM10 (24-hour mean)
Extra condition	None	Long term average concentration and deposition values are always calculated using all averaging periods
percentiles	90.4	UK air quality limits and guidelines of PM10 (as max. no. of exceedances allowed: 35 times a year)
Exceedance threshold ($\mu\text{g}/\text{m}^3$)	50	UK air quality limits and guidelines for PM10
Units for output	$\mu\text{g}/\text{m}^3$	Used protocol for air quality standards

Chapter 6: Results and Discussion of Air Dispersion Models

6.1 Emission Estimation

Nine empirical formulas were adopted from surface mining activities to compute the suspended emission rate for each activity of LFM. The calculated range of emission rates are shown in Table 34 with their statistics descriptive. Parameters of the formulas were described previously in the methods section in Table 32. Components of these formulas presented earlier, such as wind speed, moisture and silt contents represent the most key influencing parameters for emission rate (Chakraborty et al., 2002; Chaulya, 2006; Kim et al., 2020; Richardson et al., 2019). This is also valid in this study for all LFM activity sources with the exclusion of wind speed and the inclusion of the drop height parameter as a main driver, especially in the recovered waste loading and unloading activities' emissions. It was observed from the emission results as shown in Figure 46 that point source activities are the major sources of emission in this study. These results are in agreement with studies by (Chakraborty et al., 2002; Chaulya, 2006).

The order of the factors influencing dust emission rate of point source activities was determined as the significant emissions. For cover removal loading, the order of the factors influencing dust emission rate was as follows: moisture content > drop height > silt content > size loader > wind speed > loading frequency. For recovered waste loading, the order of the factors influencing dust emission rate was as follows: drop height > silt content > size loader > moisture content > wind speed > loading frequency. For cover removal unloading, the order of the factors influencing dust emission rate was as follows: silt content > unloading frequency > drop height > moisture content > capacity of unloader > wind speed. For recovered waste unloading, the order of the factors influencing dust emission rate was as follows: drop height > silt content > moisture content > unloading frequency > capacity of unloader > wind speed.

Table 34: Descriptive statistics results of emission estimation of 9 different LFM activities.

Activity	Source type	Emission rate calculation	Unit	Equation
Cover removal loading				$E = \left[0.0081 \left\{ \frac{(100 - m)}{m} \right\}^{1.4} \left\{ \frac{s}{(100 - s)} \right\}^{0.3} (u)^{1.1} (h * f * l)^{0.1} \right]$
Min.	Point	0.02	g s ⁻¹	
Mean		0.45		
Max.		1.11		
Recovered waste loading				$E = \left[h \left\{ \frac{(100 - m)}{m} \right\}^{0.4} \left\{ \frac{0.555 * s}{(100 - s)} \right\} (u^2 * f * l)^{0.1} \right]$
Min.	Point	0.06	g s ⁻¹	
Mean		0.13		
Max.		0.19		
Haul road				$E = \left[\left\{ \frac{(100 - m)}{m} \right\}^{0.7} \left\{ \frac{u * S}{(100 - s)} \right\}^{0.1} (41.6 + 0.03 * f * c + 108 * v) 10^{-5} \right]$
Min.	Line	0.006	g s ⁻¹ m ⁻¹	
Mean		0.008		
Max.		0.010		
Transport road				$E = \left[\left\{ \frac{(100 - m)}{m} \right\}^{0.35} \left\{ \frac{u * s}{(100 - s)} \right\}^{0.7} \{0.5 + 0.1(f + 0.42 * v)\} 10^{-3} \right]$
Min.	Line	0.002	g s ⁻¹ m ⁻¹	
Mean		0.01		
Max.		0.04		
Cover removal unloading				$E = \left[0.33 \left\{ u * h \frac{(100 - m)}{m} \right\}^{0.1} \left\{ \frac{s}{(100 - s)} \right\}^{0.3} (f * c)^{0.15} \right]$
Min.	Point	0.31	g s ⁻¹	
Mean		0.43		
Max.		0.52		
Recovered waste unloading				$E = 0.156 * h^{0.6} \left[\left\{ \frac{(100 - m) * s * u * c * f}{m(100 - s)} \right\}^{0.1} \right]$
Min.	Point	0.45	g s ⁻¹	
Mean		0.58		
Max.		0.66		
Exposed cover removal waste				$E = \left[\left\{ \frac{(100 - m)}{m} \right\}^{0.1} \left\{ \frac{s}{(100 - s)} \right\}^{0.6} \left\{ \frac{u}{(19 + 0.01 * u)} \right\} \left\{ \frac{a}{(6 + 256 * a)} \right\} \right]$
Min.	Area	0.00001	g s ⁻¹ m ⁻²	
Mean		0.0001		
Max.		0.0002		
Screening plant				$E = \left[\left\{ \frac{(100 - m)}{m} \right\}^{0.5} \left\{ \frac{s * a}{(100 - s)} \right\}^{0.1} \left\{ \frac{u}{(20 + 3300 * u)} \right\} \right]$
Min.	Area	0.00020	g s ⁻¹ m ⁻²	
Mean		0.00021		
Max.		0.00022		
Exposed pit surface				$E = \left[\left\{ \frac{(100 - m)}{m} \right\}^{0.1} \left\{ \frac{s}{(100 - s)} \right\}^{0.3} a^{1.6} \left\{ \frac{u}{(10 + 125 * u)} \right\} \right]$
Min.	Area	0.00000057	g s ⁻¹ m ⁻²	
Mean		0.00000067		
Max.		0.00000073		

Overall, the results of the calculated emission rates revealed a higher emission rate with an increase in wind speed, silt content, drop height, size loader/unloader, loading/unloading frequency, and a decrease in moisture content. This is also consistent with comparisons of emission rates of the existing research current approaches (Kim et al., 2020; Richardson et al., 2019; Wang et al., 2022a).

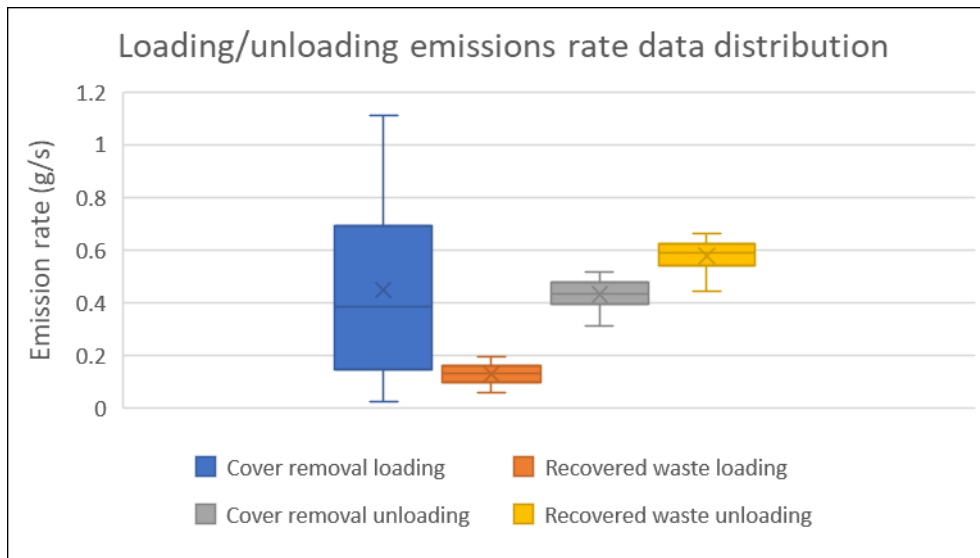


Figure 46. Box and whisker plot showing the point source activities emission rates.

The highest calculated emission rate of 1.11 g/s was for the cover removal loading activity. For this source, moisture content appeared to be the major influencing driver of high/low emission rate. This highlights the importance of low moisture content in the production of dust during LFM activities. Therefore, mitigation or suppression measures, such as using tankers or bowsers to spray water around the mining area should be considered against high emissions related activity. In order to reduce dust emissions in the LFM area further, a lower drop height and smaller size loader should be considered. The overall maximum/average/minimum point sources emission rate is 2.5 g/s or 9 kg/hr /1.6 g/s or 5.76 kg/hr / 0.8 g/s or 2.88 kg/hr, respectively. However, line sources maximum/average/minimum emission rates were only responsible for producing 0.05/ 0.02/ 0.01 g/s/m or 0.18/ 0.072/ 0.036 kg/hr/m, respectively. The total emissions rate of area sources revealed negligible rate of emissions.

According to (Holnicki and Nahorski, 2015; Joseph et al., 2018; Ni et al., 2018; Srivastava et al., 2021), emission inventory input data is regarded as a factor influencing the particulates dispersion model. Therefore, it is important to note that the used formulas in this study were originally developed based on emission inventory for winter season to predict the (worst possible) maximum concentration of total suspended particular matter around mining activities in a different region with a larger leasehold mining area (Chaulya, 2006; Chaulya et al., 2019). Thus, these factors can lead to results with overestimation (Huertas et al., 2012a). Moreover, the emission estimation method used may carry large uncertainties due to differences in the site practices, nature of mining, mitigation measures, as well as climatic and geological conditions (Chakraborty et al., 2002; Holnicki and Nahorski, 2015; Richardson et al., 2019). This was evidenced in the application of the U.S. emission estimation methods to other regions (Triantafyllou et al., 2021). As a result, for a reliable calculation of fugitive dust emissions, experimentally based derivation of emission factors relevant to the area and activities under study is necessary to avoid over- or under-estimation of emissions (Chaulya et al., 2022; Richardson et al., 2019), as clearly seen in the screening plant activity results of this study, which is very low, and thus the reasons for this requiring further research.

6.2 Meteorological and Terrain Data

The observed meteorological data were collected at 21 m height at Marham station, UK by the Met Office platform. The assumed LFM project will take around 3 months to complete per phase based on the computed volume of waste and considering 8 working hours during weekdays. Hence, meteorological data was generated for the period from 1st January 2019 to 31st March 2019. This particular period of the year was selected since earlier studies reported that the highest PM10 concentration levels were found in the winter season (Abril et al., 2016; Chaulya et al., 2022; Chaulya et al., 2019; Feng et al., 2022; Kumar et al., 2016; Luo et al., 2021; Pandey et al., 2014; Srivastava et al., 2021; Tian et al., 2014; Wang et al., 2014; Wang

et al., 2022a; Zhao et al., 2018) due to lower temperature, wind speed, and planetary boundary layer (Abril et al., 2016; Pandey et al., 2014; Zhao et al., 2018), leading to lower mixing height and poor dispersion conditions in the presence of an inversion layer phenomena (CERC, 2016; Pandey et al., 2014). It also due to foggy and wet conditions accompanied by low wind speed preventing particulate dispersion (Luo et al., 2021). The ADMS models take account of the temperature inversions from information of the estimated boundary layer height (calculated from wind speed, cloud cover, and solar radiation values in the met. data file) (CERC, 2016).

The station recorded the following parameters: temperature, wind speed, wind directions, solar radiation, cloud cover, rainfall, and relative humidity. Temperature in the area during the analysed period ranged from -4 to 17°C with an average of 6.1°C, while the relative humidity varied between 55 and 100% with an average of 82.5%. The wind speed during the analysed period was in the range between 0.5 to 12.8 m/s. The average wind speed was observed to be 5 m/s during the analysed period. Wind rose diagram for the period considered in the models is depicted in Figure 47. The analysis of wind patterns showed that the predominant wind direction was blowing from SW and W followed by North-West and South-East. The receptors in the downwind directions from the dust-generating sources (north-east and east), will be the most affected form pollutant concentration (dust). Precipitation rate was almost 0 mm/h for the analysed periods. As discussed earlier, total rainfall and relative humidity parameters are not considered in this study since dry deposition model only considers deposition due to grounding of the plume and not washout.

The site has an elevation of around 65 m above sea level (Figure 48). Norfolk is low-lying, with the Rivers Wensum, Yare and Bure, and their tributaries, draining it into the North Sea. The River Ouse drains the northwest corner of the county into The Wash, which is a shallow North Sea inlet.

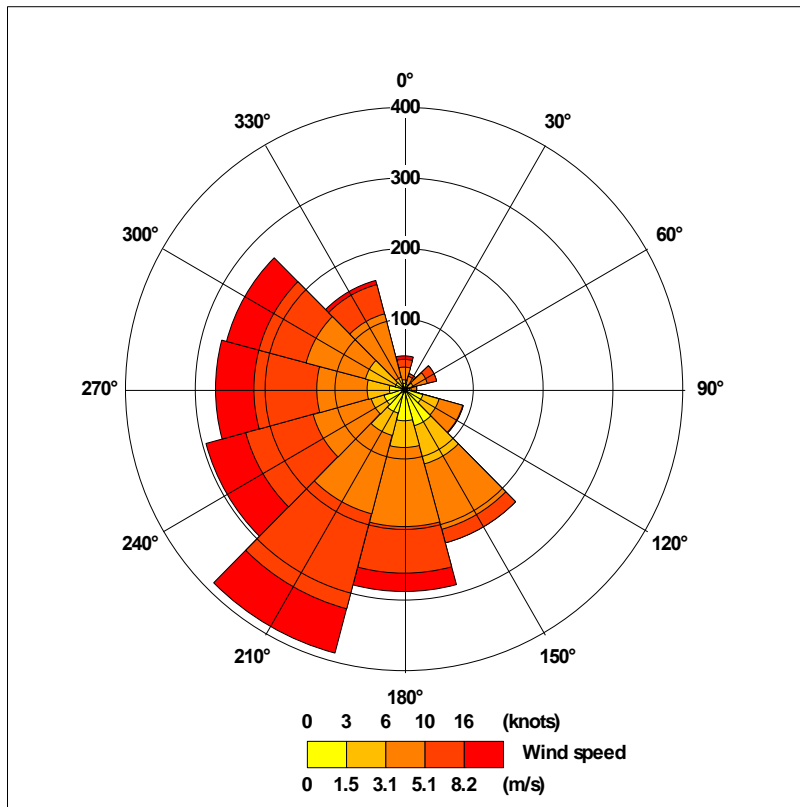


Figure 47. Wind rose diagram of the study area.

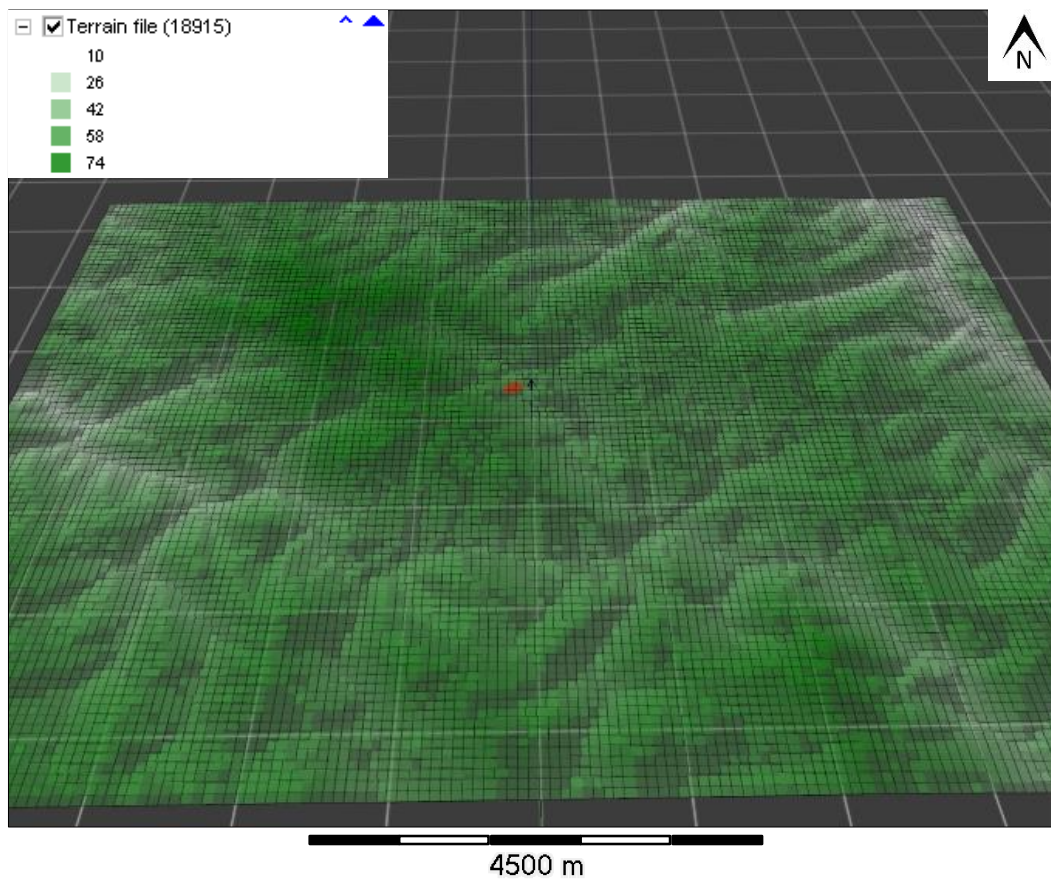


Figure 48. Topography 3D view of the upper part of Norfolk showing the land height above sea level in m with a red circle showing the study area. Produced by using Mapper Software.

6.3 LFM Process Plan

The first unit operation in LFM activities is the cover removal loading (López et al., 2018; Parrodi et al., 2019b; Parrodi et al., 2020). Overlying soils (capping) are removed in order to expose the waste during this procedure (Scott et al., 2019). During the removal and transportation of the overburden materials, air pollution is a key concern in surface mining (Patra et al., 2016). Similarly, the final cover (capping) of a landfill site may contain materials help to increase removal efficiency of heavy metals as inferred in the present study, which increase the potential risk of dust exposure and air pollution during LFM projects. These particles become airborne depending on air velocity, particle diameter, and drop height (Patra et al., 2016). Subsequent mining activity processes have also been concluded to be major sources of airborne particle (Chaulya, 2006; Ghose and Majee, 2000; Onder and Yigit, 2009). The total assumed volume range of waste according to 1 phase out of 5 calculated to app.= 22,400 m³ (if the landfill depth= 6 m) to 26,880 m³ (if the landfill depth= 7 m). The LFM project is calculated in this study to approximately last for 3 months with the exclusion of weekend days for each phase. A LFM flowsheet processes plan produced based on 1-day typical working hours (8 hours) is shown in Figure 49 so as to visualise the processes and define volumetric throughput/number of loading frequencies/timeframe ranges for each unit operation with their respective emission rate.

The total number of loading frequencies ranged from 20 to 24 per hour in the flowsheet, based on the estimated volume range of landfilled waste under the study using a size loader of 2 m³ operating for 8 hours per day. These numbers were distributed to cover and waste removal loadings/unloadings and adapted to the nature of LFM activities as shown in the below flowsheet diagram. As a landfill cover/capping is around 1-2 m in thickness (Hölzle, 2017), the majority of loading numbers were in favour of waste recovery. Timeframe for each individual activity was given in the diagram based on its no. of loading frequencies.

In terms of screening plant operation that separates the fractions into different sizes, only recovered waste was assumed to be introduced to it, which is in accordance with the study by (Lopez et al., 2019; Parrodi et al., 2019b), and therefore its volumetric throughput was in the range of 36-42 (m³/hour). The screening plant heavy machinery meant to be used in the assumed plan has a capacity of 49.7 (m³/hour) (TR510). Stockpiled exposed cover removal of waste volumetric throughput ranges were assumed to include the reclaimed soil from the screening plant activity, which estimated to be 100 (m³/day) out of the 288-336 range (m³/day) as illustrated in the flowsheet below. Exposed pit surface volumetric throughput ranges were estimated based on both cover and waste removal volume per day. Screened waste is assumed to be loaded on to an articulated dump truck for off-site transportation at the end of each day (Parrodi et al., 2019b). The screened waste volumetric throughput ranges meant to be transferred off-site were assumed to be 23.5-29.5 (m³/hour) since the reclaimed soil from the screening plant was estimated to be 12.5 (m³/hour). Reclaimed soil is meant to remain on site until completion of a LFM operation. Haul road number of loading frequencies per hour was calculated based on articulated dump trucks capacity of 13.7 (m³) (Caterpillar 725).

The one phase cumulative for the maximum/average/minimum point sources emissions over the lifetime of the LFM operation are approximately 5.04 tonnes (t) / 3.23 (t) / 1.61 (t), respectively. However, the one phase cumulative for the maximum/average/minimum line sources emissions over the lifetime of the LFM operation are approximately 100.8 (kg/m) / 40.32 (kg/m) / 20.16 (kg/m), respectively. These cumulative emissions are based on the assumed waste volume range of 22,400 m³ to 26,880 m³.



Figure 49. Flowsheet illustrating the LFM processes and defining volumetric throughput/number of loading frequencies/timeframe ranges for each unit operation with their respective emission rate.

6.4 ADMS Modelling

The ADMS modelling results of each source of activity and all sources (in combination) considering the three different scenarios of wind speed were compared to the Air Quality Strategy for England (AQS) of pollutant concentrations, which is published by the Department for Environment, Food and Rural Affairs (Defra, 2007). Many of the air quality limits are stated in terms of “*not more than N exceedances of a threshold value per year*”, where N is an integer (CERC, 2016). The limits can be restated in terms of percentiles by calculating the appropriate percentile from the maximum number of exceedances N. Results in ADMS 5 can be calculated in terms of exceedances (where the user specifies the threshold values on the Output screen) and/or percentiles (where the user specifies the percentiles to be calculated on the Output screen) (CERC, 2016). When using the percentiles option in the output tab, the output from the model is given as a concentration, which represents the concentration after the allowed exceedances have been taken into account. When using the exceedances option, the model output provides the number of exceedances occurring at each output point. Both options can only be used for long-term averages, where the averaging times should represent the air quality objective (CERC, 2016). The UK AQS limit of PM10 limit is “not more than 35 exceedances per year of 50 µg/m³ as a 24-hour average”. This means that 35 exceedances are acceptable and 36 are not. The corresponding percentile to be calculated is therefore:

$$\frac{365 - 35}{365} \times 100 = 90.41^{th} \text{ percentile}$$

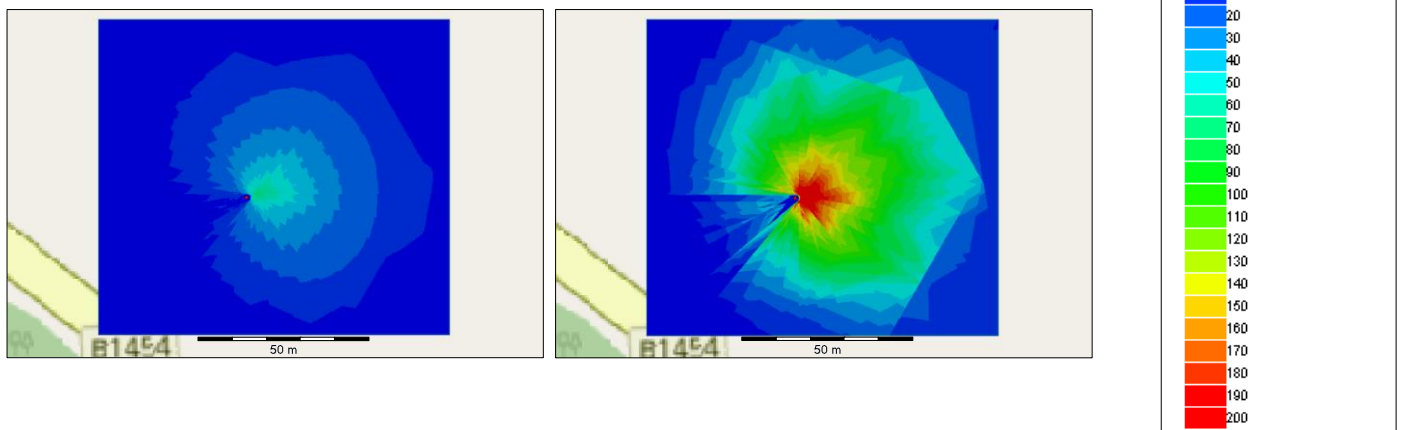
In this modelling, the percentile output from the model give the 36th highest concentration modelled at each output point and the exceedance output from the model provide the number of times a concentration exceeds 50 µg/m³ at each output point. The benefit of using the percentile option over the exceedances option is that concentrations are output, regardless if the output point exceeds the air quality objective or not (CERC, 2016). Hence, only the

percentile option was considered in this study. Waste fractions of PM_{2.5} were not present in the studied area using MLA particles size distribution analysis and therefore their UK limit were not considered for comparison in this study. The calculated ground-level long-term average airborne concentration for each source of activity taking into account the three different scenarios of wind speed for both emission rate values (min/max) are illustrated in Figure 50 versus their percentiles result of PM₁₀. The scale of maps used below is 1:1230 and are pointed to north direction.

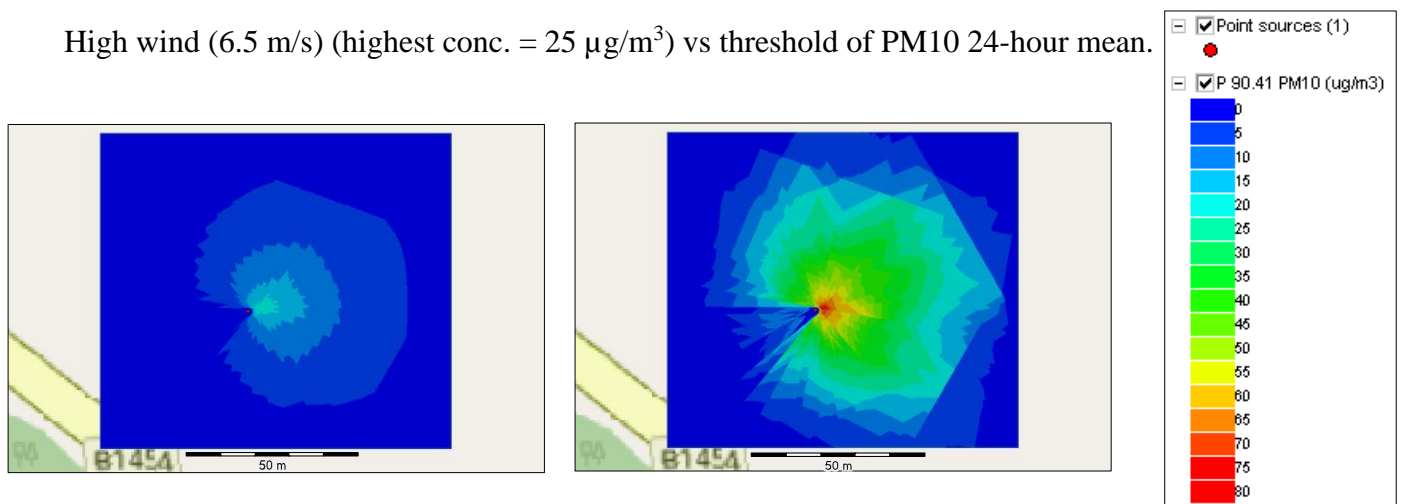
Line source of transport road is not considered in the ADMS models since boundaries have been drawn (grid extent) and set around the site.

Cover removal loading max. emission rates

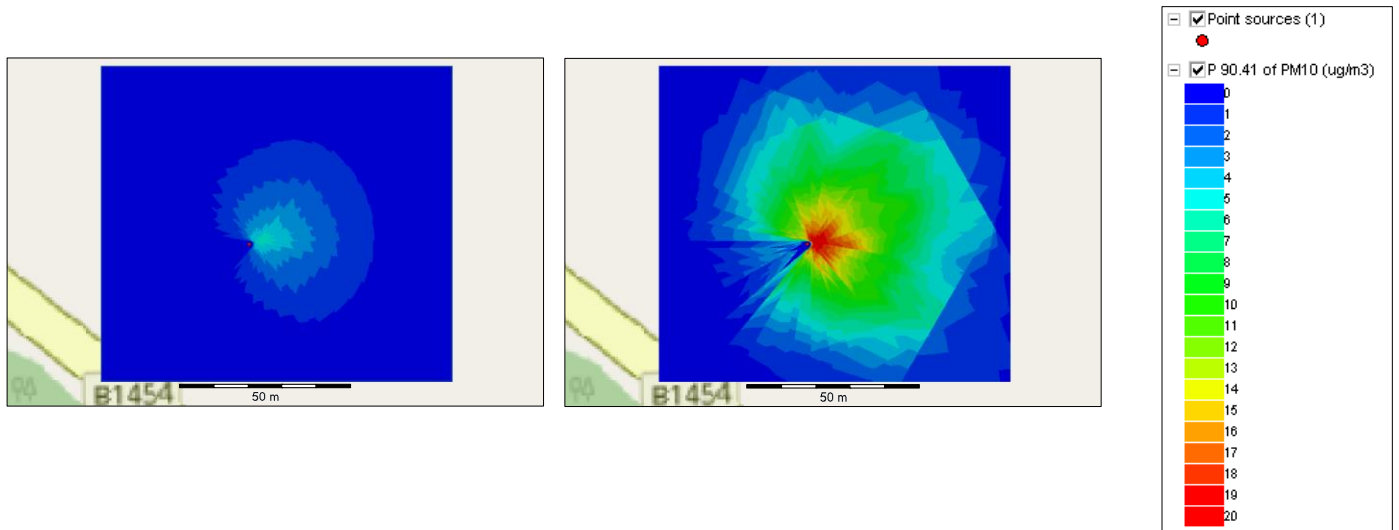
Low wind (2.5 m/s) (highest conc. = 70 µg/m³) vs threshold of PM₁₀ 24-hour mean.



High wind (6.5 m/s) (highest conc. = 25 µg/m³) vs threshold of PM₁₀ 24-hour mean.

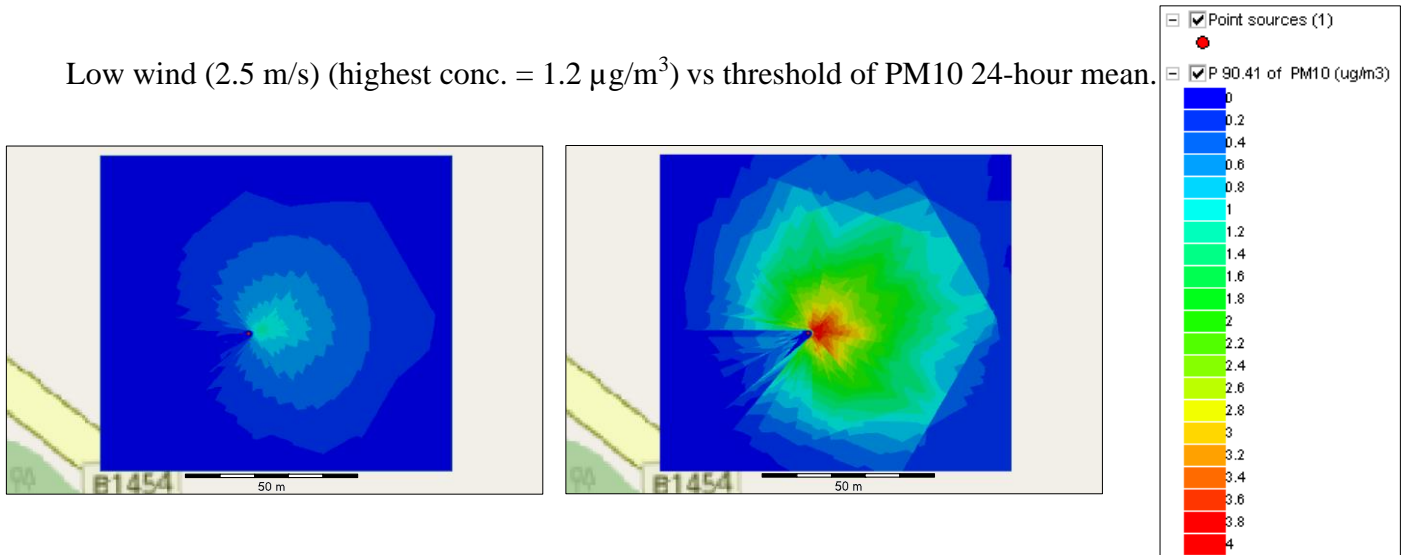


Extreme wind (21 m/s) (highest conc. = $7 \mu\text{g}/\text{m}^3$) vs threshold of PM10 24-hour mean.

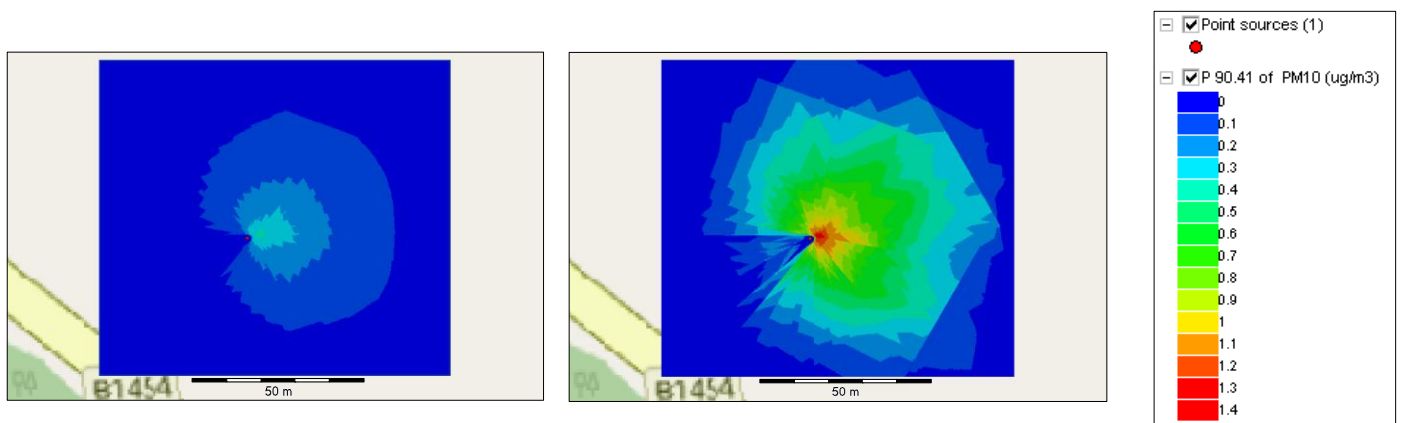


Cover removal loading min. emission rates

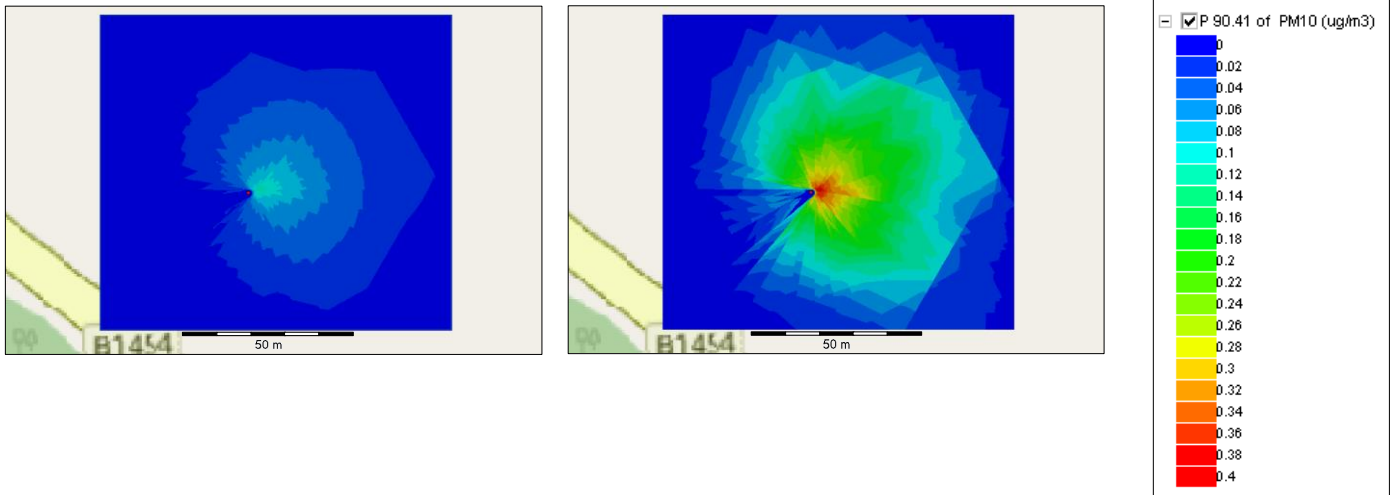
Low wind (2.5 m/s) (highest conc. = $1.2 \mu\text{g}/\text{m}^3$) vs threshold of PM10 24-hour mean.



High wind (6.5 m/s) (highest conc. = $0.4 \mu\text{g}/\text{m}^3$) vs threshold of PM10 24-hour mean.

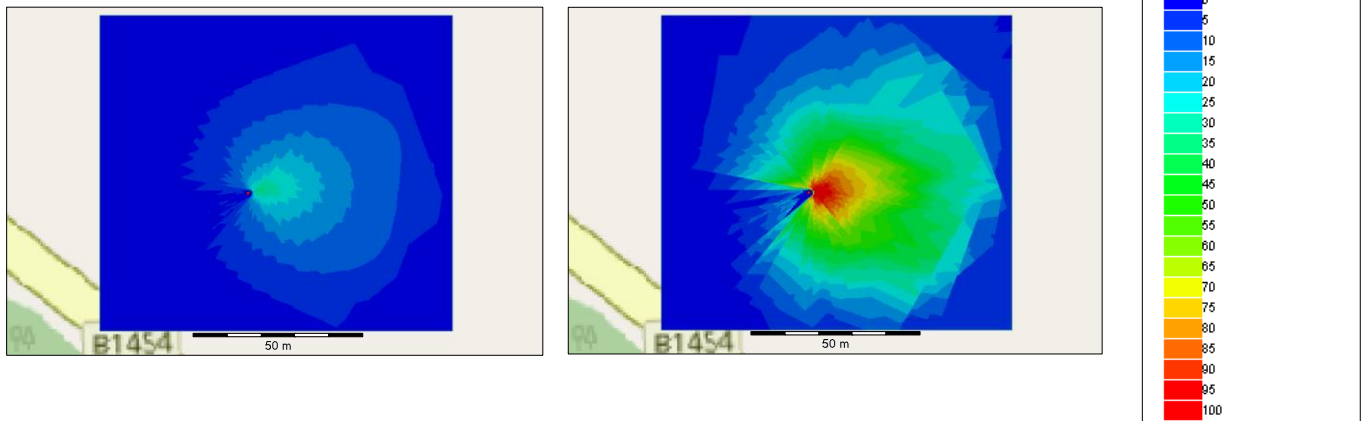


Extreme wind (21 m/s) (highest conc. = $0.12 \mu\text{g}/\text{m}^3$) vs threshold of PM10 24-hour mean.

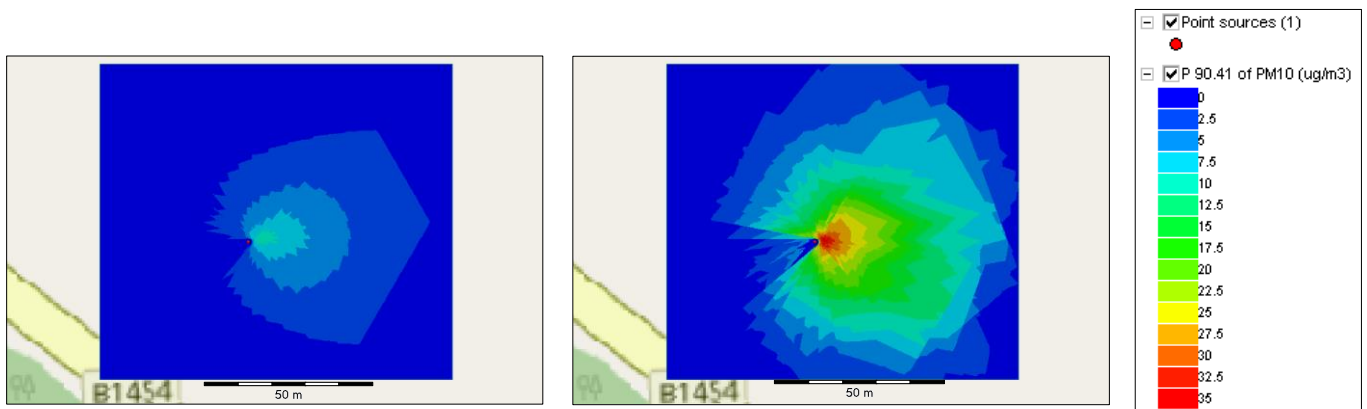


Cover removal unloading max. emission rates

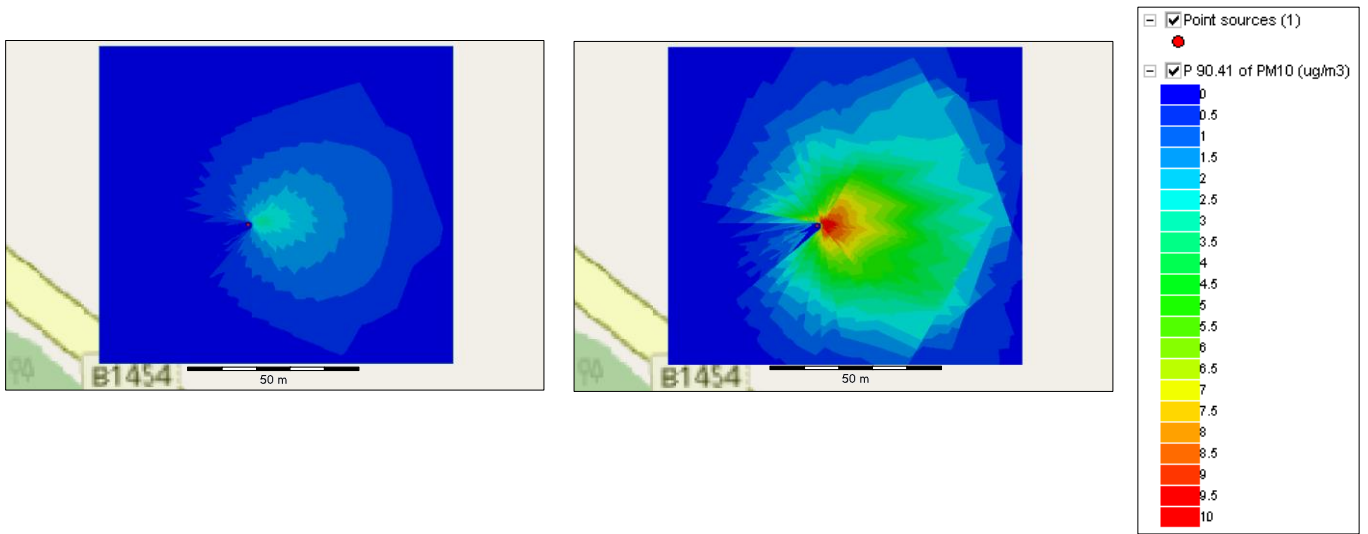
Low wind (2.5 m/s) (highest conc. = $35 \mu\text{g}/\text{m}^3$) vs threshold of PM10 24-hour mean.



High wind (6.5 m/s) (highest conc. = $12 \mu\text{g}/\text{m}^3$) vs threshold of PM10 24-hour mean.

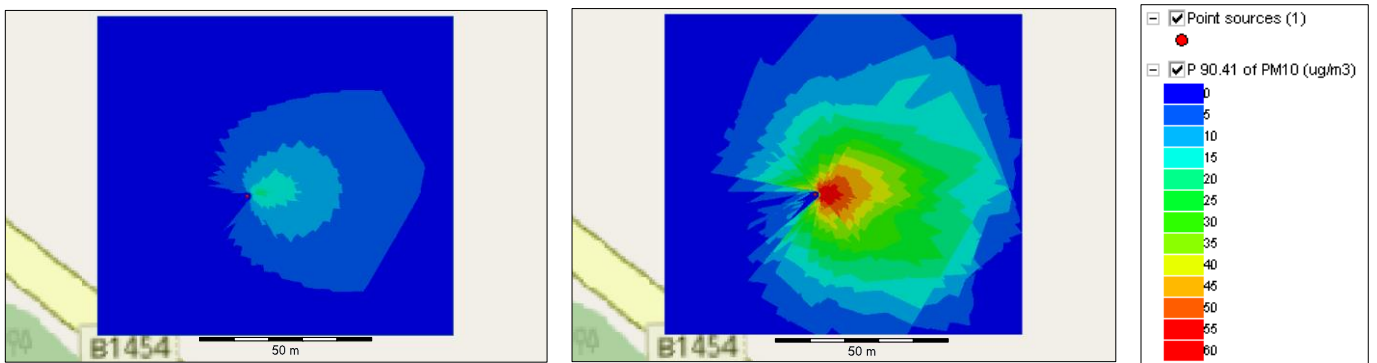


Extreme wind (21 m/s) (highest conc. = $3.5 \mu\text{g}/\text{m}^3$) vs threshold of PM10 24-hour mean.

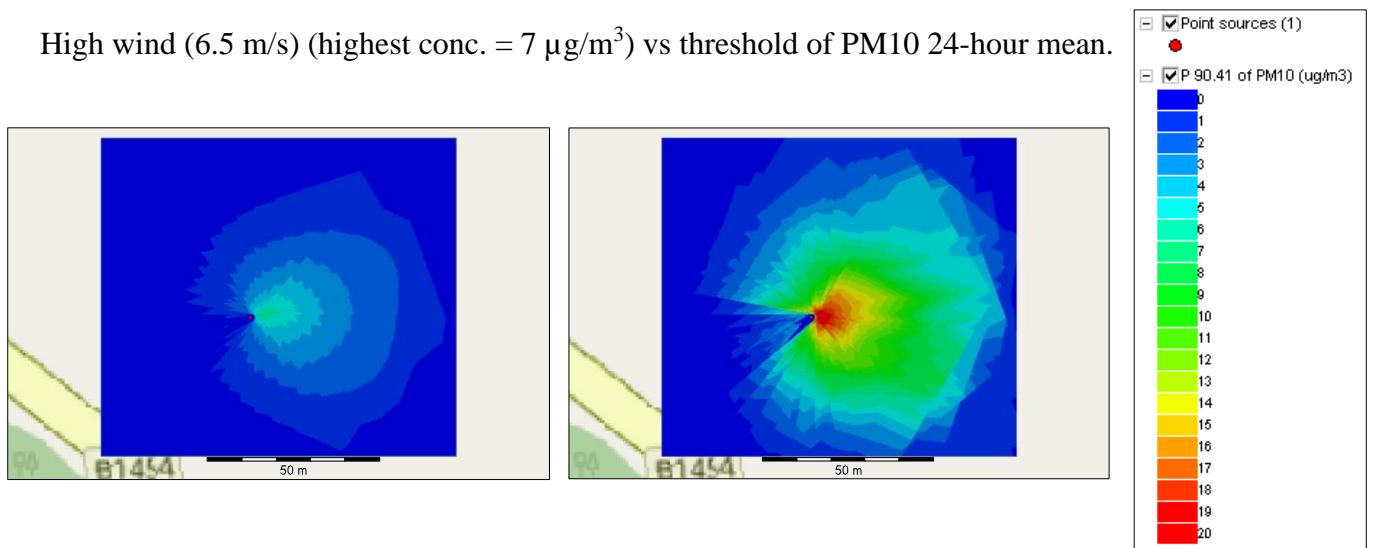


Cover removal unloading min. emission rates

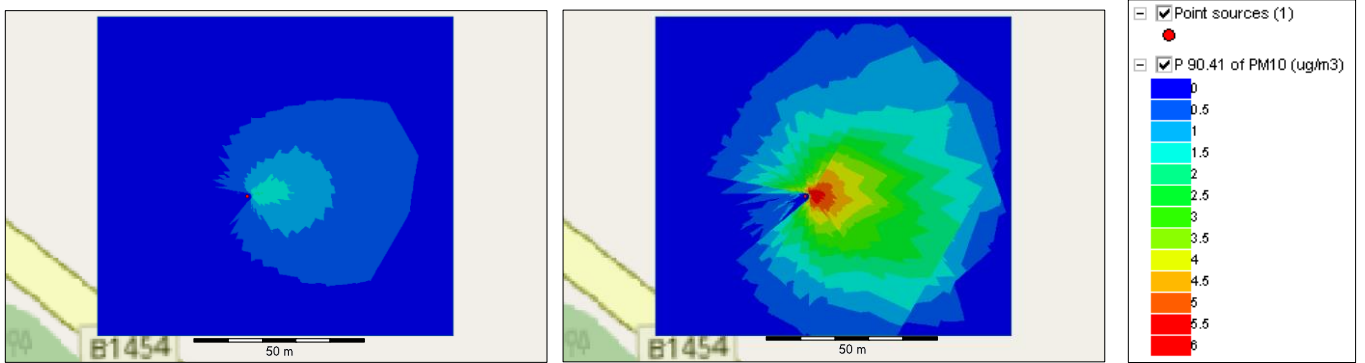
Low wind (2.5 m/s) (highest conc. = $20 \mu\text{g}/\text{m}^3$) vs threshold of PM10 24-hour mean.



High wind (6.5 m/s) (highest conc. = $7 \mu\text{g}/\text{m}^3$) vs threshold of PM10 24-hour mean.

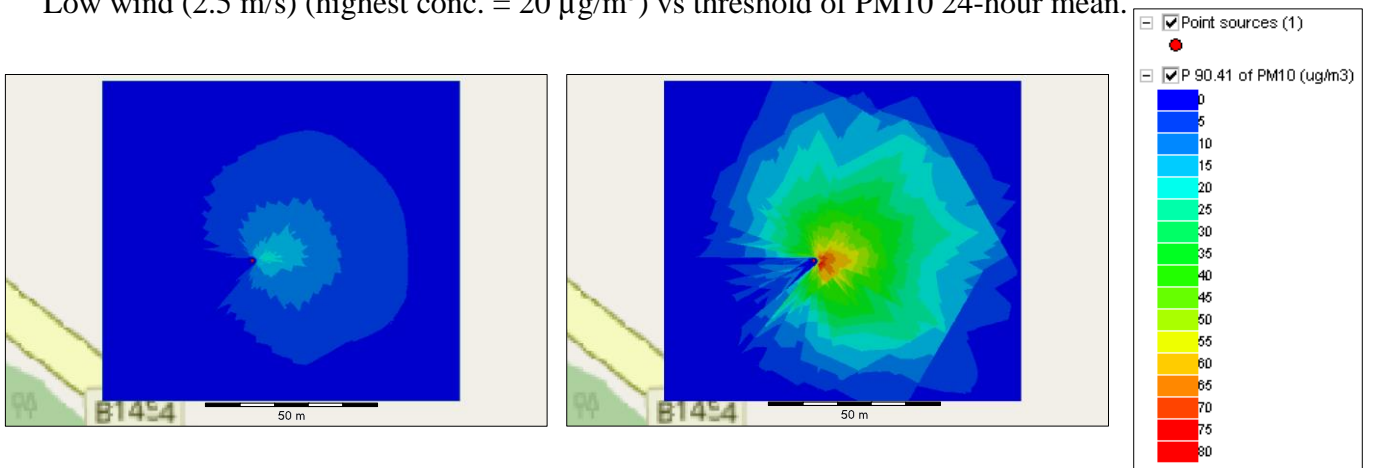


Extreme wind (21 m/s) (highest conc. = $2 \mu\text{g}/\text{m}^3$) vs threshold of PM10 24-hour mean.

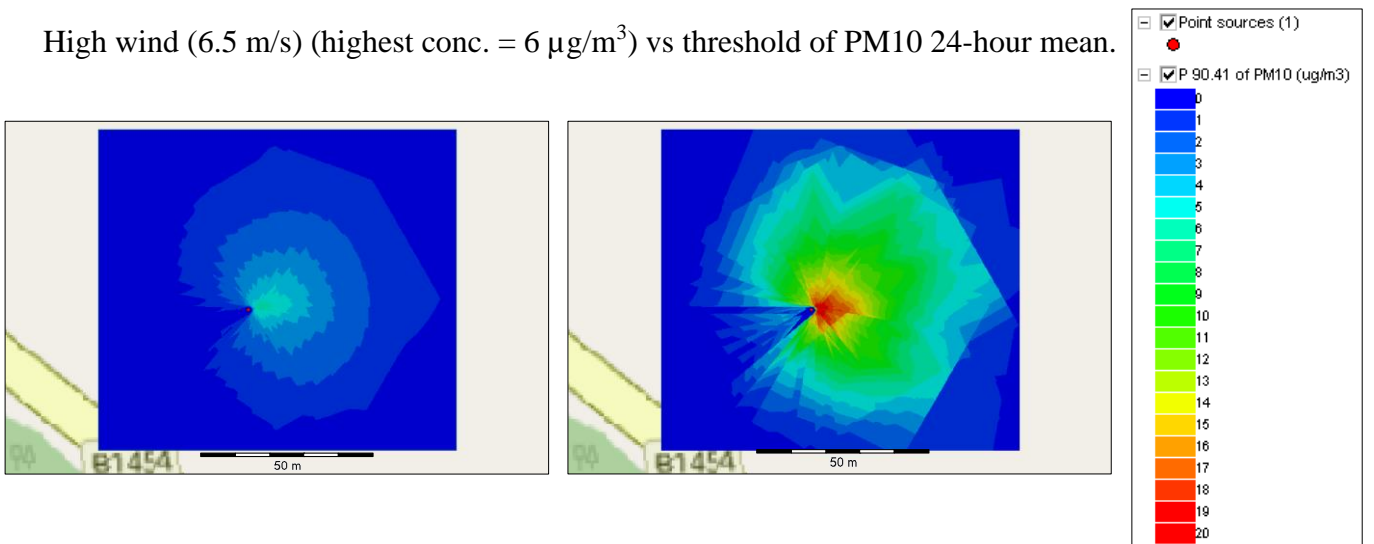


Recovered waste loading max. emission rates

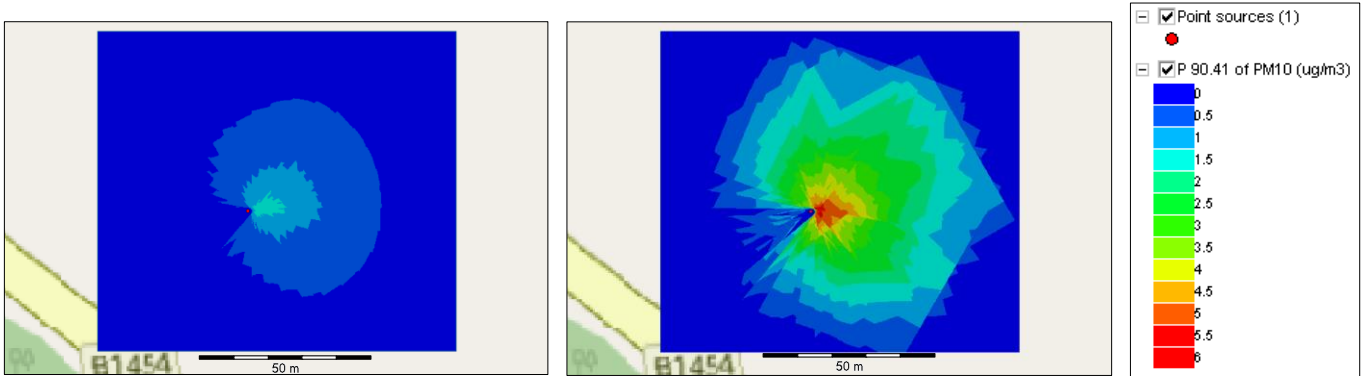
Low wind (2.5 m/s) (highest conc. = $20 \mu\text{g}/\text{m}^3$) vs threshold of PM10 24-hour mean.



High wind (6.5 m/s) (highest conc. = $6 \mu\text{g}/\text{m}^3$) vs threshold of PM10 24-hour mean.

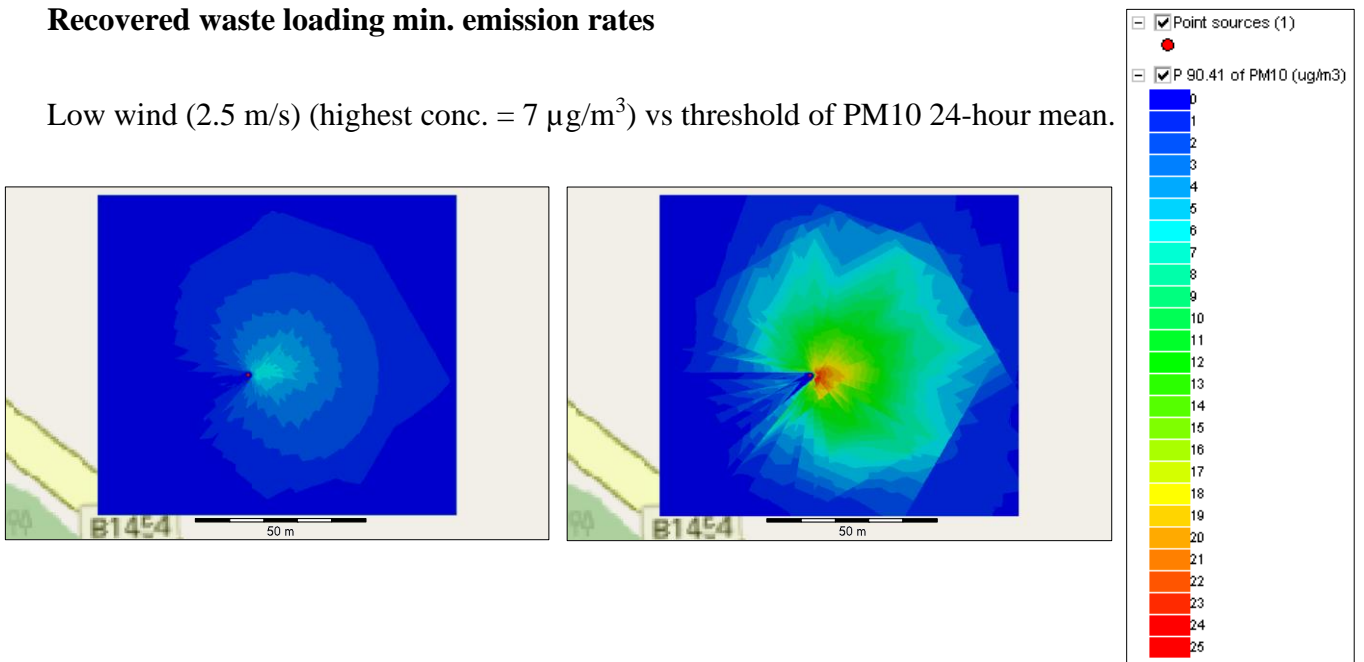


Extreme wind (21 m/s) (highest conc. = $1.8 \mu\text{g}/\text{m}^3$) vs threshold of PM10 24-hour mean.

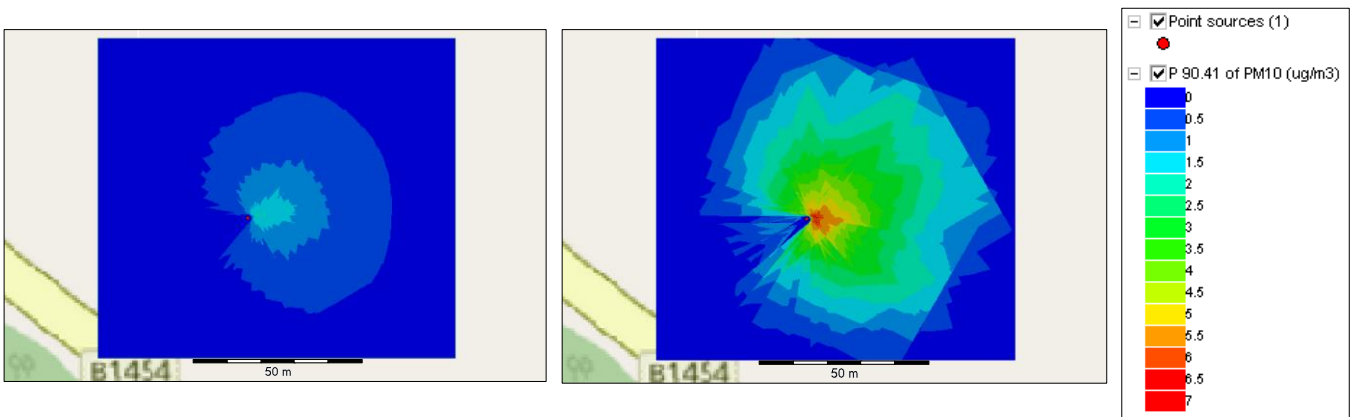


Recovered waste loading min. emission rates

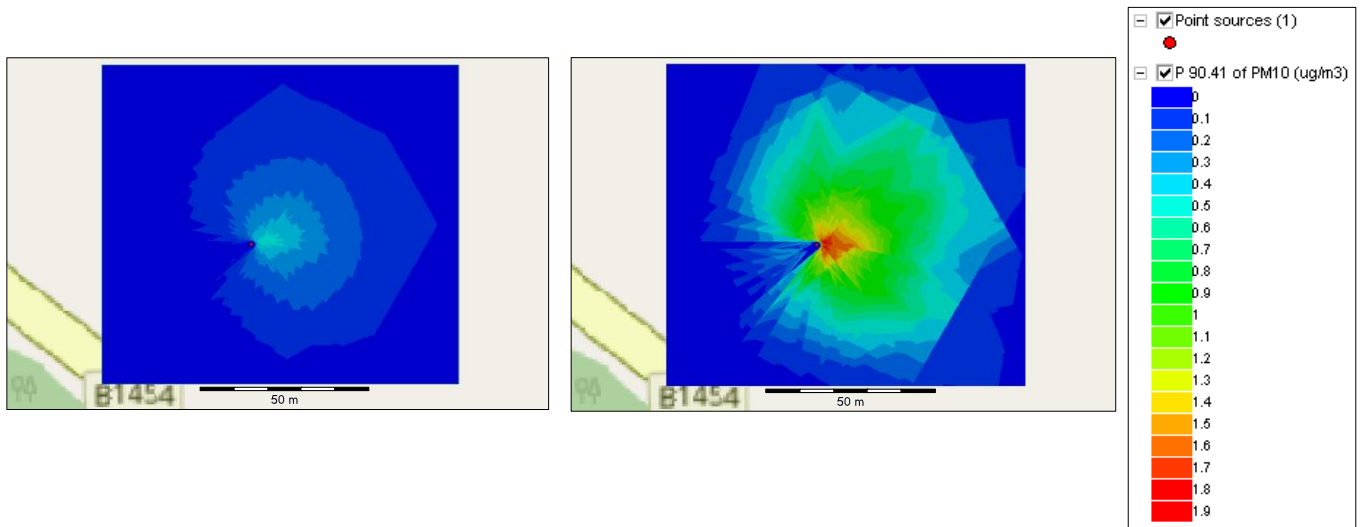
Low wind (2.5 m/s) (highest conc. = $7 \mu\text{g}/\text{m}^3$) vs threshold of PM10 24-hour mean.



High wind (6.5 m/s) (highest conc. = $2 \mu\text{g}/\text{m}^3$) vs threshold of PM10 24-hour mean.

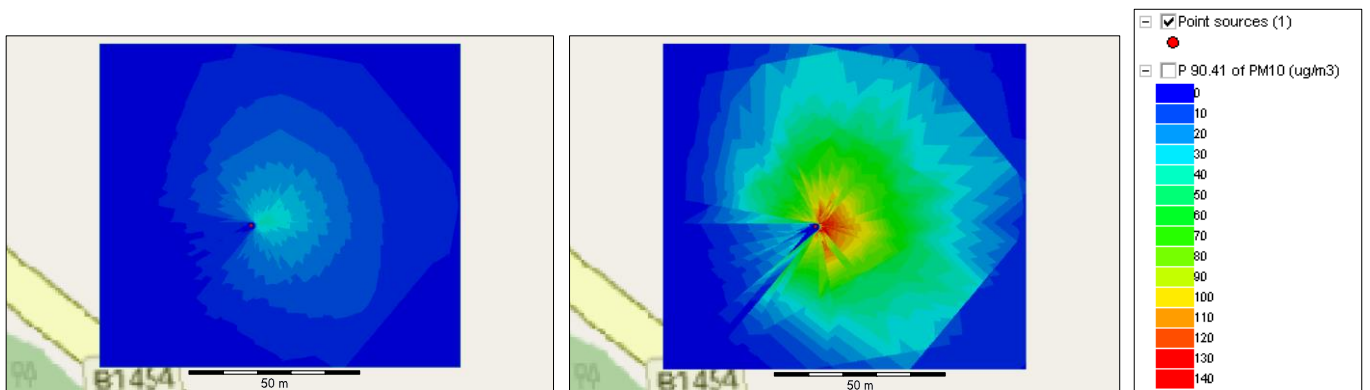


Extreme wind (21 m/s) (highest conc. = 0.5 $\mu\text{g}/\text{m}^3$) vs threshold of PM10 24-hour mean.

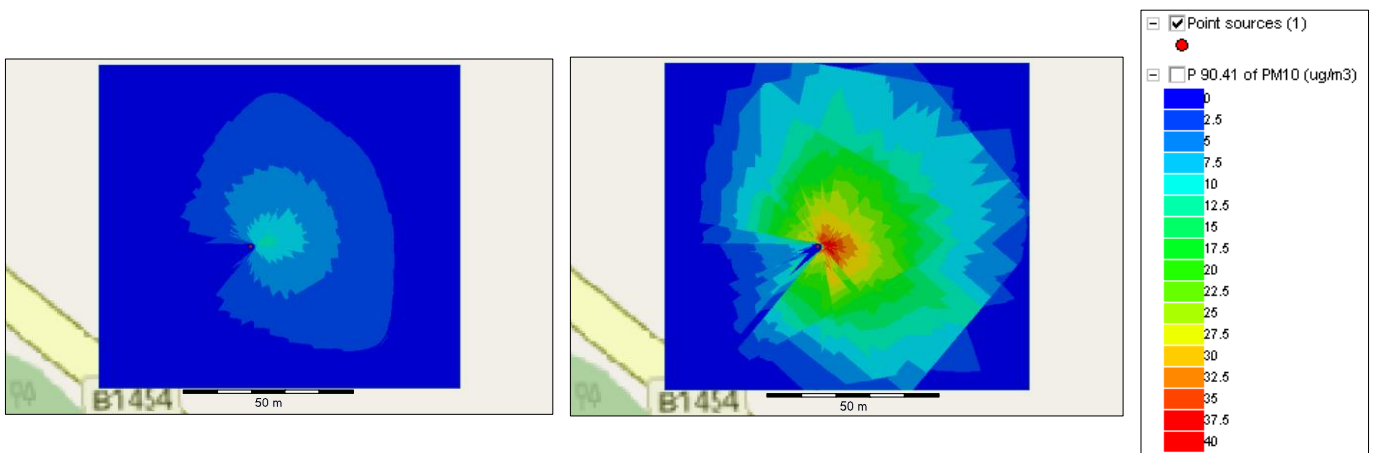


Recovered waste unloading max. emission rates

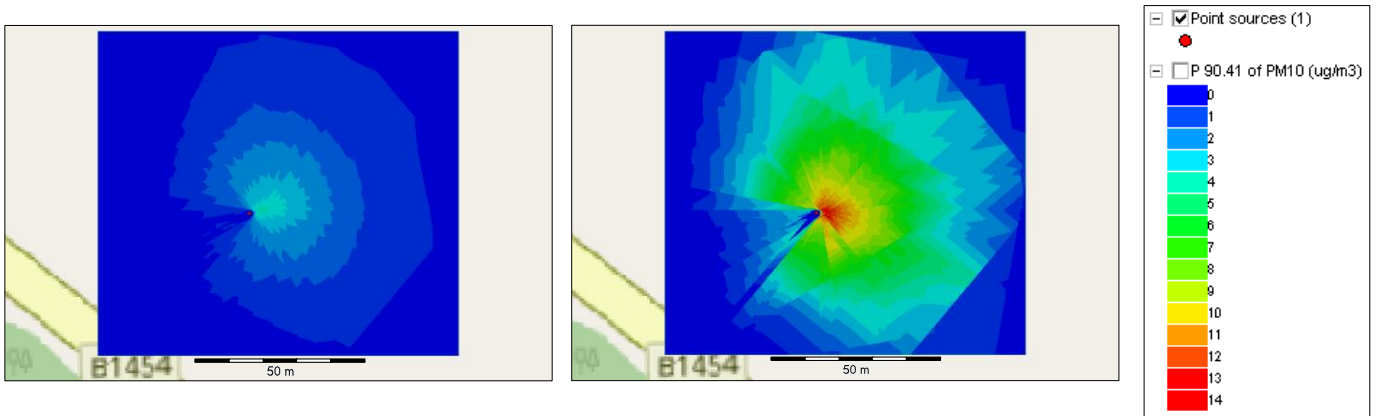
Low wind (2.5 m/s) (highest conc. = 40 $\mu\text{g}/\text{m}^3$) vs threshold of PM10 24-hour mean.



High wind (6.5 m/s) (highest conc. = 14 $\mu\text{g}/\text{m}^3$) vs threshold of PM10 24-hour mean.

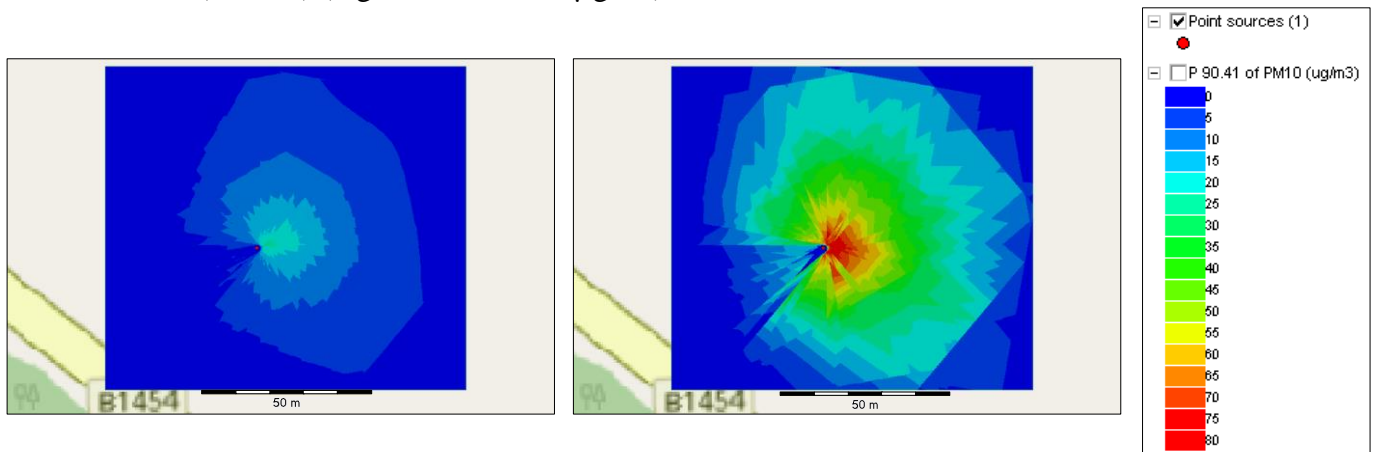


Extreme wind (21 m/s) (highest conc. = 4 $\mu\text{g}/\text{m}^3$) vs threshold of PM10 24-hour mean.

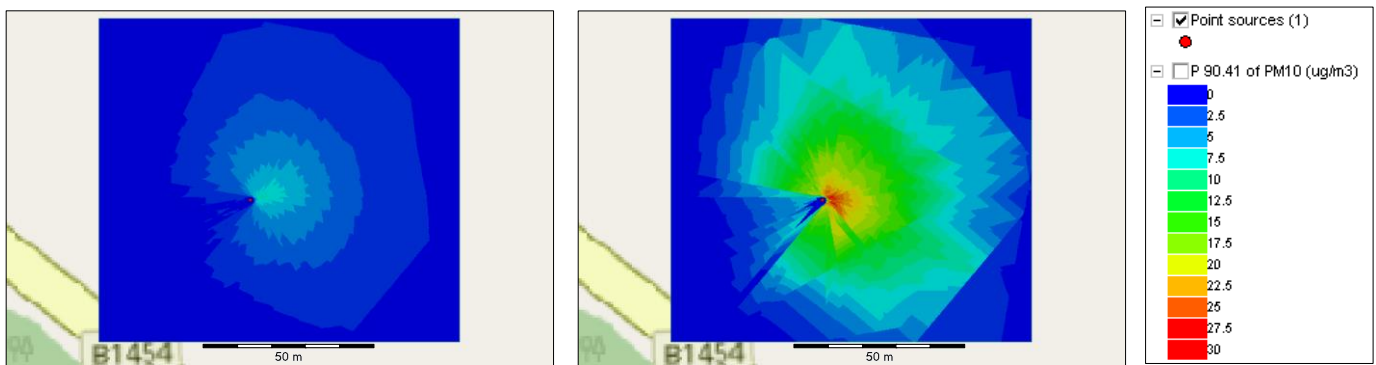


Recovered waste unloading min. emission rates

Low wind (2.5 m/s) (highest conc. = 30 $\mu\text{g}/\text{m}^3$) vs threshold of PM10 24-hour mean.



High wind (6.5 m/s) (highest conc. = 10 $\mu\text{g}/\text{m}^3$) vs threshold of PM10 24-hour mean.



Extreme wind (21 m/s) (highest conc. = 2.5 $\mu\text{g}/\text{m}^3$) vs threshold of PM10 24-hour mean.

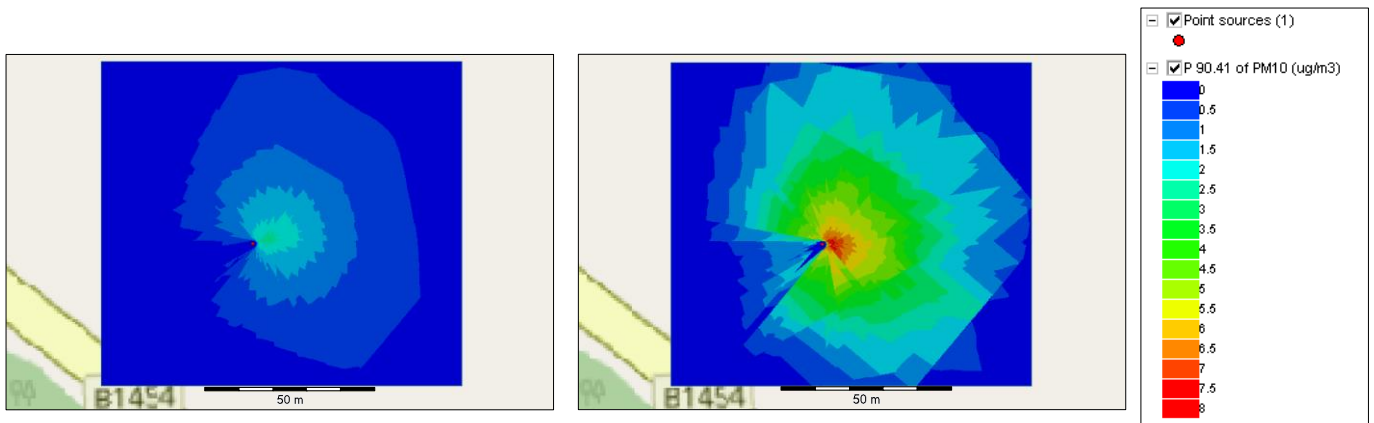
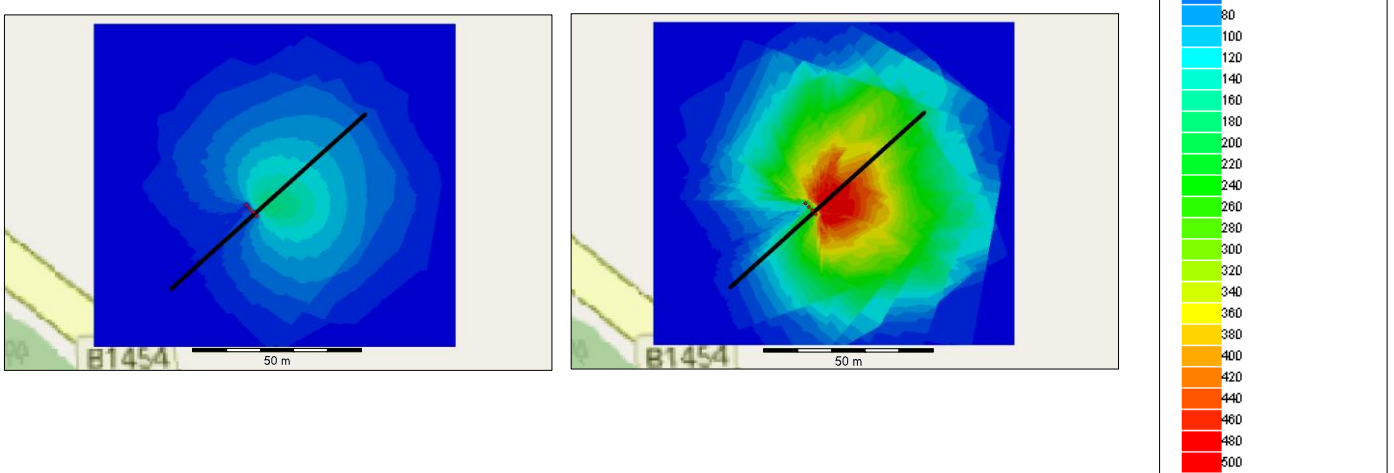


Figure 50. Contour plots of each individual activity source of the 3 wind speed scenarios considering maximum and minimum emissions rate against the UK regulatory standard for PM10 24-hour mean stated in terms of percentile.

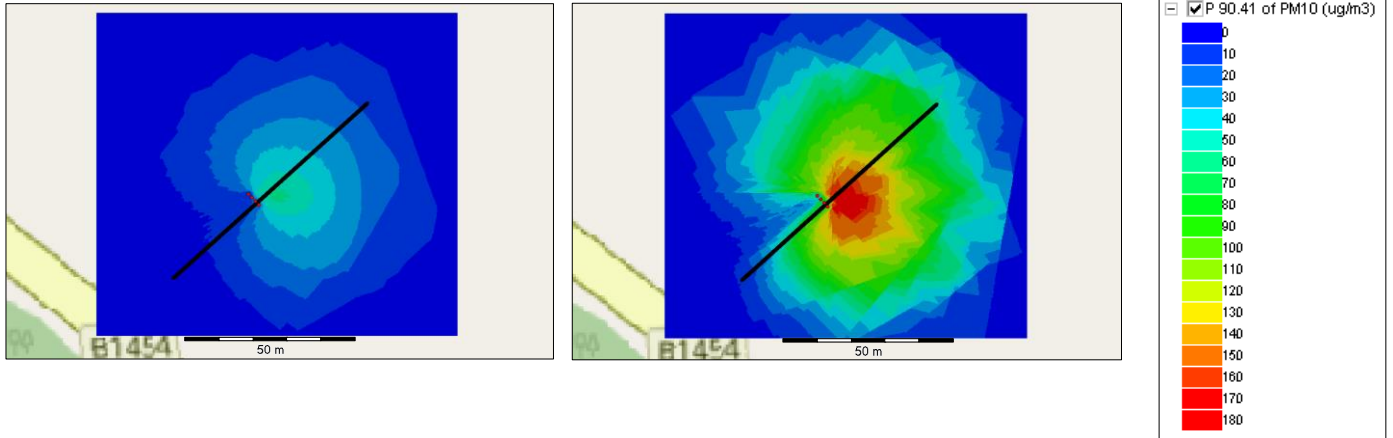
Haul road line and area sources were not displayed in the above figure since their emission rate values were very low in comparison with the activities of point sources, and thereby their air dispersion modelled concentrations will be within the UK regulatory standards. Figures 51 demonstrates the calculated ground-level long-term average airborne concentration with their percentiles for all 5 activity sources (in combination), taking into account the three different scenarios of winds and considering both maximum and minimum emission rate values.

All 5 sources (in combination) max. emission rates

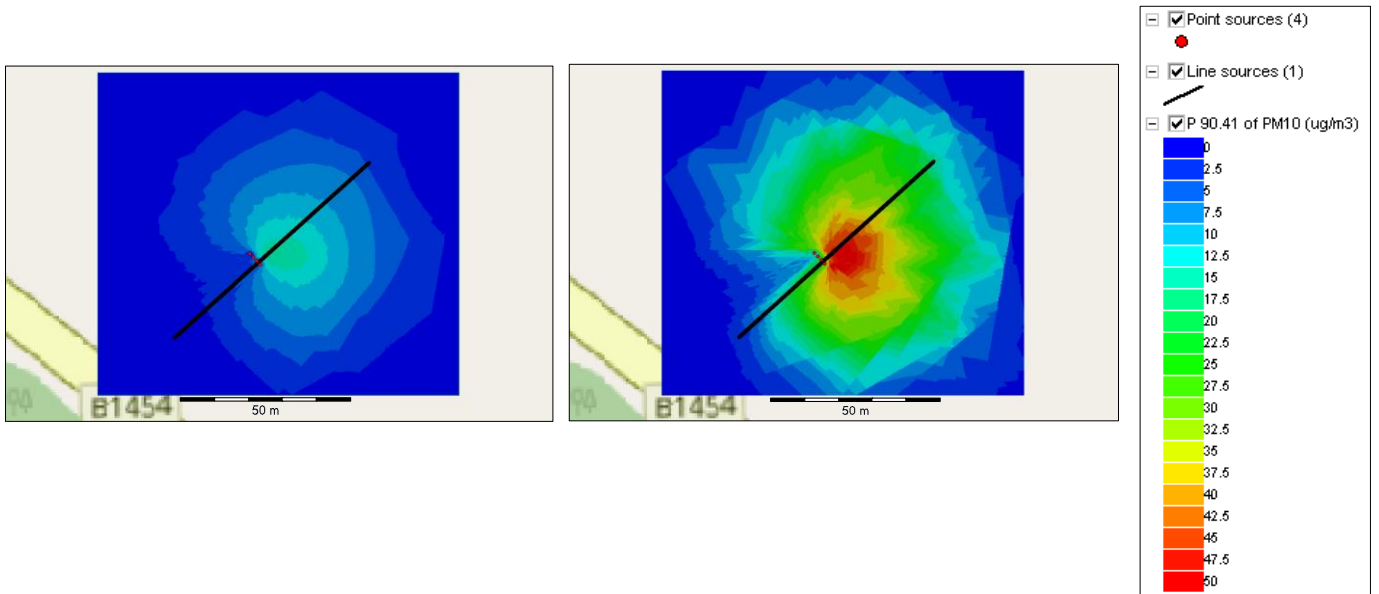
Low wind (2.5 m/s) (highest conc. = 180 $\mu\text{g}/\text{m}^3$) vs threshold of PM10 24-hour mean.



High wind (6.5 m/s) (highest conc. = 60 $\mu\text{g}/\text{m}^3$) vs threshold of PM10 24-hour mean.

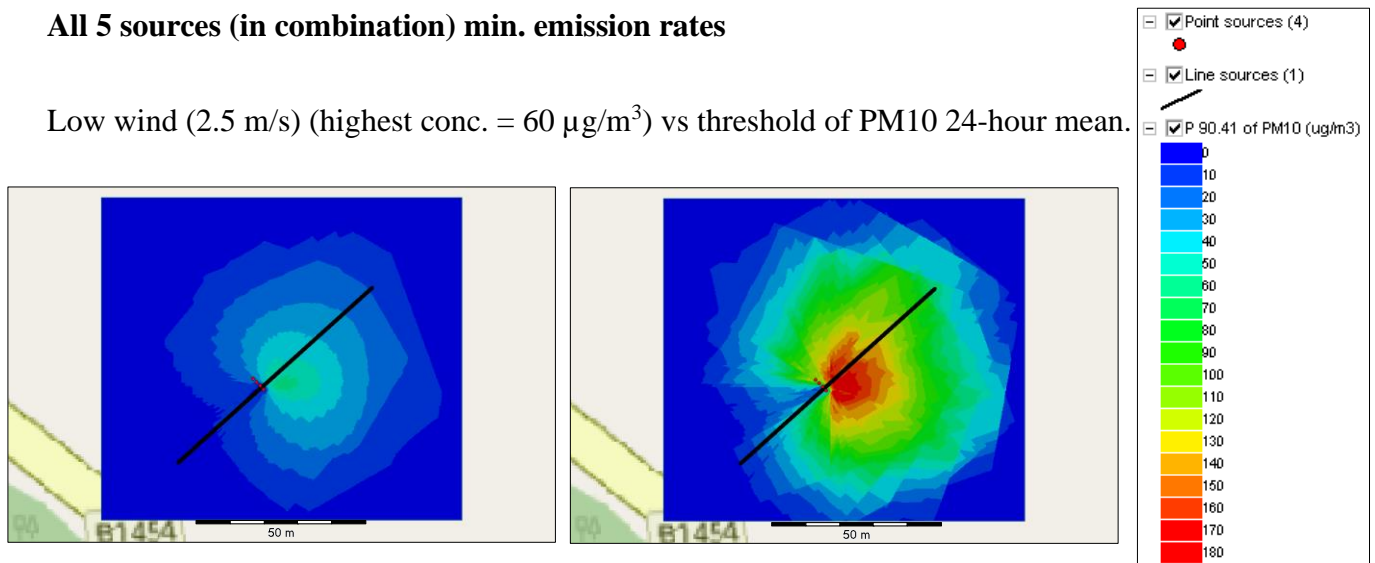


Extreme wind (21 m/s) (highest conc. = 16 $\mu\text{g}/\text{m}^3$) vs threshold of PM10 24-hour mean.

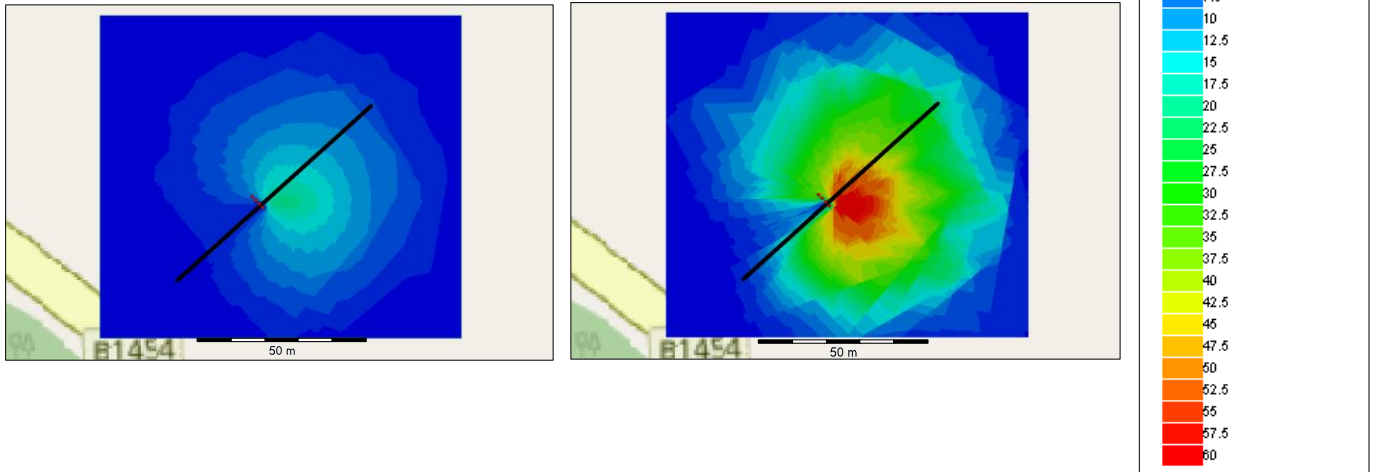


All 5 sources (in combination) min. emission rates

Low wind (2.5 m/s) (highest conc. = 60 $\mu\text{g}/\text{m}^3$) vs threshold of PM10 24-hour mean.



High wind (6.5 m/s) (highest conc. = 20 $\mu\text{g}/\text{m}^3$) vs threshold of PM10 24-hour mean.



Extreme wind (21 m/s) (highest conc. = 6 $\mu\text{g}/\text{m}^3$) vs threshold of PM10 24-hour mean.

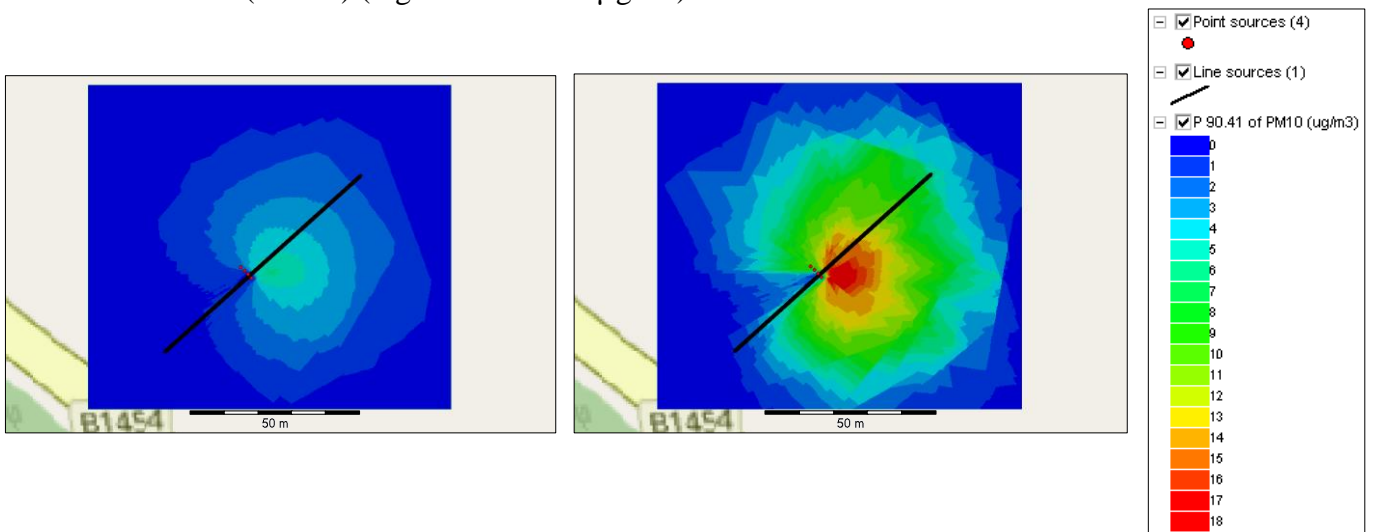


Figure 51. Contour plots of all five sources of activities of the 3 wind speed scenarios considering maximum and minimum emissions rate against the UK regulatory standards for PM10 24-hour mean stated in terms of percentile.

Area sources were not applied with the combination of all sources due to some file restrictions for the area sources. Thus, they were not included in the modelled air concentrations. However, their contributions to the total air dispersion modelling concentrations will be insignificant.

For every modelled scenario (side-by-side contour plots) in the figures above, one colour map scale is used for both concentrations (original concentrations versus percentile concentrations) to enable the ease of comparison between them.

Wind speed is a key factor in determining the modelled concentrations (Amoatey et al., 2018; Wang et al., 2022a). In most instances, concentrations usually decrease with increasing wind speed, as there is more turbulence and hence more dilution (CERC, 2016). This was clearly seen in the modelled concentrations of the three different wind speed scenarios. The predicted ground-level long-term average airborne concentrations of cover removal loading max. emission rate as an individual activity demonstrated the highest airborne concentrations following by recovered waste unloading max. emission rates, cover removal unloading max. emission rates, and recovered waste loading max. emission rates. These predicted concentrations are compatible with the calculated emission rates of each individual activity. The modelled all sources (in combination) max. emission rate revealed the greatest ground-level long-term average airborne concentrations at low wind scenario.

According to (Defra, 2007), if the percentile results of PM10 24-hour mean exceed the limit concentration of 50 ug/m^3 taking into accounts the allowed exceedances, risk is potential. On the other hand, if the percentile results are below the limit concentration, then there is no risk considered. This means if the percentile contour plots concentrations shown in the right side of the figures above exceed 50 ug/m^3 , risk is potential, which give the 36th highest concentration modelled at each output point. The limit of PM10 has been specified for the protection of human health and came into force from 01/01/2005 (Brookes et al., 2020). From the above results of the existing scenario, cover removal loading max. emission rate of low and high wind scenarios have exceeded the limit concentration of 50 ug/m^3 . In regard to cover removal unloading activity, max. and min. emission rate of low wind were the only scenario exceeded the limit. In addition, recovered waste loading max. emission rate of low wind was higher than the limit. Recovered waste unloading max. emission rate of low wind scenario has exceeded the limit concentration of 50 ug/m^3 . The minimum emission rate of recovered waste unloading at low wind scenario was also above the UK limit of PM10 24-hour mean. Regarding all 5

sources (in combination) modelled concentrations, max. emission rates of low and high wind scenarios have exceeded the limit, while the extreme wind scenario was at the limit. In contrast, all 5 sources min. emission rates of low and high wind scenarios were also above the limit.

The predicted 24-h ground-level long-term average airborne concentrations of air dispersion were carried out without the addition of background concentrations. According to (Defra, 2019) background mapping data for local authorities (North Norfolk District Council), the annual average of PM10 is 15 ug/m³. This means that some modelled activities classified to meet the UK regulatory standards could have exceeded the limit with the addition of background concentrations. Table 35 summarises the concentrations results of all modelled scenarios with their percentiles.

Normally, in order to compare the modelled concentration results against regulatory standards of PM10 24-hour average, it requires a long-term average concentration calculation to be carried out with a single year of hourly sequential meteorological data of a site (CERC, 2016). However, only 3 months of meteorological data was used for the studied site modelling analysis to be consistent with the calculated assumption of LFM timeframe of one phase. According to (CERC, 2016), it is possible to compare the data to the percentile of 24-hour averages for PM10 using only 3 months of met data, but it is not valid to officially compare the results against the PM10 24-hour mean standard (as this is defined in terms of a year). Hence, If the assumption made that one whole year of met. data was used in the meteorological data file, the predicted 24-h ground-level long-term average airborne concentrations would be less than the used 3 months meteorological data, and thereby the percentiles results will be also less as the percentiles are simply statistics relating directly to the modelled concentrations (Brookes et al., 2020). This inference was made by testing multiple modelling runs of different met. data periods of the same emission rates and source inputs in the ADMS, which is expected since emissions rates were applied for the first 3 months only. Nonetheless, if the assumption made

that one-year period of meteorological data is used in the analysis, the difference in concentration results is half of the 3 months period met. data and thereby percentiles result are also less. Table 35 also shows the predicted annual ground-level long-term average airborne concentrations results using 12 months period of meteorological data file with their percentiles. As percentiles result relationship were not simply clear as the predicted 24-h ground-level long-term average airborne concentrations relationship between the 3 months and one year period, an equation has been established by using regression line statistics to identify the percentile results concentration of the one-year period (instead of repeating all the analysis with one year met data with long run-times). The equation used was confirmed after ADMS modelling of only 6 analysed values using one year met. data and therefore, a strong positive relationship was identified ($P < 0.001$) ($R^2 = 0.997$) between the two different percentiles (Figure 52). The equation is shown in the centre of the regression line chart. The remaining percentile results of the 12 months period computed using the equation are shown in Table 35.

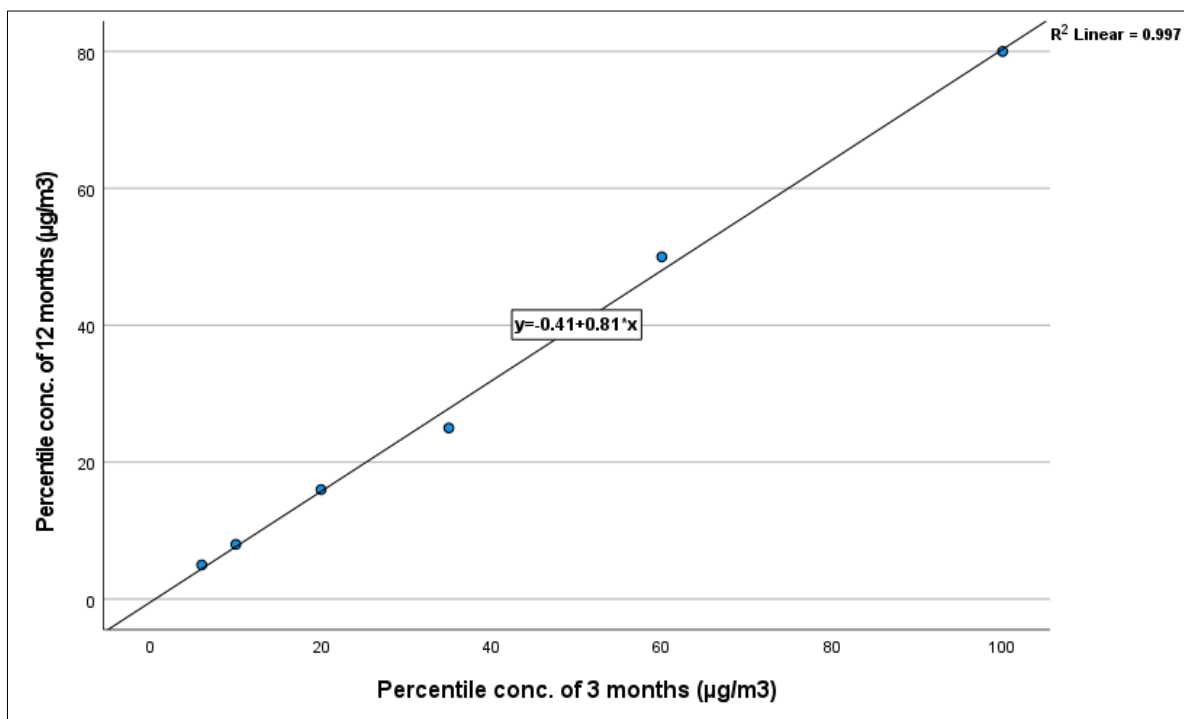


Figure 52. Correlation between the modelled percentiles concentration of three- and twelve-months meteorological data.

Having considered percentile concentrations of 12-months real-recorded meteorological data in comparison with the UK limits of PM10 24-hour average, the majority of results were classified the same as the percentile concentrations of 3-months excluding 3 values. Two of these values have fallen below the limit, whereas one value became at the limit. If the addition of background concentrations is considered using the 12-months real-recorded meteorological data of the same scenarios, then some modelled activities classified to meet the UK regulatory standards could have exceeded the limit with the addition of background concentrations.

Modelled air dispersed concentrations using one-year meteorological data have to be also compared against regulatory standards considering both UK air quality limits of PM10 (24-hour mean and annual mean) (CERC, 2016). If the concentrations results using 12 months met. data is compared against the UK limits of PM10 annual mean of (40 ug/m^3), It is noticed that only the all-sources max. emission rate event of low wind will exceed the limit. If the addition of background concentrations is considered using the 12-months real-recorded meteorological data of the same scenarios, then three values (that were below the limit) could have exceeded the limit. These values are cover removal loading max. emission rates of low wind scenario, all sources max. emission rates of high wind scenario, and all sources min. emission rates of low wind scenario. Considering the annual mean limit value relevance, the modelled concentrations values are directly compared to it as opposed to the 24-hour average conc., which is relevant to the percentile concentrations of allowed exceedances.

Table 35: Results of the modelled 24-h/annual ground-level long-term average airborne highest concentrations in (ug/m^3) and their respective percentiles of 24-hour average using 3- and 12-months meteorological data.

Activity	Concentrations of 3 months in (ug/m³)	Percentile conc. of 3 months in (ug/m³)	Concentrations of 12 months in (ug/m³)	Percentile conc. of 12 months in (ug/m³)
Cover removal loading Max. emission rates				
Low wind	70	200	35	161
High wind	25	80	12.5	64
Extreme wind	7	20	3.5	16
Cover removal loading Min. emission rates				
Low wind	1.2	4	0.6	3
High wind	0.4	1.4	0.2	.7
Extreme wind	0.12	0.4	0.06	0.3
Cover removal unloading Max. emission rates				
Low wind	35	100	17.5	80
High wind	12	35	6	25
Extreme wind	3.5	10	1.75	8
Cover removal unloading Min. emission rates				
Low wind	20	60	10	50
High wind	7	20	3.5	16
Extreme wind	2	6	1	5
Recovered waste loading Max. emission rates				
Low wind	20	80	10	64
High wind	6	20	3	16
Extreme wind	1.8	6	0.9	5
Recovered waste loading Min. emission rates				

Activity	Concentrations of 3 months in (ug/m³)	Percentile conc. of 3 months in (ug/m³)	Concentrations of 12 months in (ug/m³)	Percentile conc. of 12 months in (ug/m³)
Low wind	7	25	3.5	20
High wind	2	7	1	4
Extreme wind	0.5	1.9	0.25	1
Recovered waste unloading Max. emission rates				
Low wind	40	140	20	113
High wind	14	40	7	32
Extreme wind	4	14	2	11
Recovered waste unloading Min. emission rates				
Low wind	30	80	15	64
High wind	10	30	5	24
Extreme wind	2.5	8	1.25	6
All 5 sources Max. emission rates				
Low wind	180	500	90	403
High wind	60	180	30	145
Extreme wind	16	50	8	40
All 5 sources Min. emission rates				
Low wind	60	180	30	145
High wind	20	60	10	48
Extreme wind	6	18	3	14

Numbers displayed in red indicate potential risks (percentile concentrations >50 ug/m³).

It can be noted from the findings above that irrespective of the UK limit strategy of PM10 followed/ real-recorded meteorological data period considered, risk to the human health and the environment is potential, especially with the addition of background concentrations. This is clearly seen since some modelled values in $\mu\text{g}/\text{m}^3$ (whether percentile conc. of 3 or 12 months) have already exceeded the limit when considering only 3 months (one phase) of source of emissions in ADMS. Emission rates of around 12 months is used if all assumed 5 phases of LFM is considered and this will result in greatly increased airborne concentrations. It can be also inferred that the result of dust concentrations from cover removal loading as an individual activity possessed the greatest potential health hazards to exposed individuals nearby at low wind scenario followed by other unloading activities. This refers to the higher emission rate produced by the cover removal loading activity max. emission rate event. In terms of weather conditions, dispersion can pose the highest potential risk for the environment and human health under low wind speed meteorological condition events. This finding is congruent with the studies carried out by (Appleton et al., 2006; Pandey et al., 2014).

As discussed earlier, ADMS does not use the Pasquill-Gifford stability classes A to G. Instead, the stability is categorised using the parameter H/L_{MO} , where L_{MO} is the Monin-Obukhov length and H is the boundary layer height. Values of H and $1/L_{MO}$ of the analysed period of the real-recorded 3 months met. data were extracted from the ADMS mop output file in Excel as a comma-separated file. Calculation of the results showed that the real-recorded meteorological input dataset of the studied site is categorised under neutral stability conditions ($-0.3 \leq h/L_{MO} \leq 1$). According to (CERC, 2016), an inversion is present in the ADMS analysis when conditions are neutral or convective. This was validated by looking at the DELTATHETA data in the .mop file (this is column AU when viewed the file in Excel). If DELTATHETA is greater than 0, this means that ADMS has predicted an inversion (CERC, 2016). The calculated boundary layer height average by ADMS for the real-recorded meteorological data (3 months)

was approximately 429 m. However, in the weather conditions analysed of low wind scenario, the calculated boundary layer height average was found to be around 168 m. The lower boundary layer height promotes the accumulation of air pollutants in the atmosphere, leading to air quality deterioration (Cao et al., 2020; Fan et al., 2019; Ni et al., 2018; Pandey et al., 2014; Wang et al., 2016; Wang et al., 2022a; Zhao et al., 2018). In contrast, in the weather conditions analysed of extreme wind scenario, the calculated boundary layer height average was around 2587 m, indicating more turbulence of pollutants/dusts concentration. This finding was in agreement with the study by (Appleton et al., 2006; Du et al., 2022; Luo et al., 2021; Pandey et al., 2014; Wang et al., 2016). However, according to (CERC, 2016), low wind speeds do not always give rise to low boundary heights as it mainly depends on the stability. In stable and neutral conditions, a lower wind speed reduces the vertical mixing and hence reduces the height of the boundary layer. However, in convective conditions, there is vertical mixing driven by heating, in addition to the mechanical mixing due to the wind, so the boundary layer height can be large even if the wind speed is low (CERC, 2016). The boundary layer height average of the analysed high wind scenario (429 m) is most comparable to the Norfolk natural weather conditions, which equals to 553 m.

Some key points can be noted, resulting from the performed simulations:

- All receptors around a site can be potentially affected since wind direction is a variant factor through the year. This was in agreement with study by (Piras et al., 2014; Tian et al., 2014; Wang et al., 2014).
- The entered particle diameter and density values in the ADMS setup interface (palette) are used to calculate the particles deposition velocity and gravitational settling velocity to simulate the dispersion of a particulate plume (CERC, 2016).

- For more accurate comparison with regulatory standards of PM₁₀, only percentage of PM₁₀ should be used in the emission rate calculation and in the ADMS pollutant deposition parameters. The silt content of particles diameter around 50 microns was considered in the emission rate calculation in this study (known as total suspended particulate (TSP) matter) to take into account the dispersion of fine particles that could have potential environmental implications (e.g., travelling distance of particles in the plume), which is believed to settle very close to the point of emission (Luo et al., 2021).
- The results of the ground-level long-term average airborne concentrations analysed using the dry deposition model revealed that the level of precision is greater for the studied site during the analysed period since there was no rain recorded and modelling of the deposition takes into account the dilution effect with time (travel time from the source) for particles deposition (CERC, 2016). As the plume moves downwind, its strength decreases due to depletion at the surface from deposition (CERC, 2016). Thus, in terms of health and environmental impact, the results of the ground-level long-term average airborne concentrations analysed in this study using the dry deposition model are closer to the reality as opposed to other model options in ADMS.
- Mass fraction of the particle's diameters entered in the ADMS interface to calculate the deposition velocity were represented of the entire waste fractions of the studied landfill.
- The calculated mean dry deposition velocity of the analysed PM by the model is 6.9 cm/sec of all sources for the first 24 hours of meteorology, extracted from the output of .dep file.
- Although the height of the source entered is at ground level (0 m) in the ADMS interface, the plume from the source may still rise from the ground, due to momentum, buoyancy or mechanical mixing (CERC, 2016). The plume will then be subject to deposition in the same manner as a plume from an elevated source.

- The ADMS analysis carried out in this study predicted the worst-case possible scenarios of one LFM phase on a local level in terms of weather conditions. But regarding the percentage of size particles (silt content) considered in the emission inventory, it is not considered the worst because it was only accounted for the range of the analysed particles in this study

Among all modelled scenarios, extreme wind scenario of min. emission rate appeared to be the most preferred option in terms of the low concentrations of dust. This is in agreement with the study by (Appleton et al., 2006) who found that *"Higher wind speeds cause an elongation of the particulate plume and a reduction in the airborne concentration and deposition flux gradients observed near-source"* using ADMS model.

From health and environmental perspective, the best time of the year to carry out LFM in the studied area is when higher wind speed is dominated to allow for more dilution of dust, while at the same time ensuring airborne PM content is at a minimum within a landfill site especially fractions \leq PM₁₀ in diameter since higher wind speed generate higher emission rates (Richardson et al., 2019). If fine fractions are very large within a site, control measures should be in place, such as using surface watering control methods (Chang, 2004; Chaulya et al., 2019; Huertas et al., 2012a; Mishra et al., 2016). According to (Lilic et al., 2018; Richardson et al., 2019), the application of surface watering demonstrated an overall average control efficiency of 25% and 50%, respectively from the total emission rates within a mining region. The risk identified from the predicted analysis of one phase was restricted within the boundary of the landfill site as shown in the contour plots figures above. Therefore, strict measures should be in place if LFM occurs to ensure the safety of people working at the site from exposure as well as people living in proximity with the landfill site, especially in calm weather conditions. According to (Defra, 2016), if predicted environmental concentrations were above the limit, further actions should be taken. Performing a cost-benefit study of alternate waste recovery and

disposal options, or constructing new equipment, such as an abatement plant, are examples of further actions possibilities to reduce the impact on the environment (Defra, 2016).

Predicting particulate matter pollution prior to the initiation of any LFM project is now possible with the adoption of surface mining activities using equations to calculate the suspended emission rate for each individual LFM related activity. As a result, efficient mitigation measures may be designed at the planning stage. These findings can be used to visualize future environmental scenarios and improve decision-making to a wide range of LFM projects regarding license permission. The findings may also help to create safer workplaces and healthier environments around landfill mines.

Chapter 7: Conclusions and Further Work

7.1 Introduction

The research's conclusion is presented in this chapter along with an overview of key findings. The overall summary of how each objective was covered in the thesis is also restated and highlighted. The novelty of this research and the contributions to new knowledge with regard to health and environmental impact assessment of LFM activities are also discussed. Before proposing recommendations for future research, the chapter also takes into account the limitations of this research

7.2 Review of the Thesis Objectives

Each of the objective outlined in the thesis is reviewed and discussed in this part.

Objective 1: To identify the landfill pollutant linkages based on site specific conditions.

A comprehensive review of desk-based research of the site under the study in Chapter 3 revealed that the site can cause potential health and environmental risks to the surrounding medium, particularly due to the legacy waste deposited prior to Landfill and Waste Directives. A Conceptual Site Model of the study area was established to identify potential contaminants linkage. The Conceptual site model represented the area of concern, contaminant sources, the environmental media that can be affected, and the processes that control the transport of contaminants to potential receptors. Atmospheric transport showed that it is likely to be the most significant among all the major transport pathways in terms of potential risk to human health and the environment as potential contaminants are directly exposed to the air during LFM activities and can travel a considerable distance from the source of emission. Therefore, it was the pathway considered in this research scope.

Objective 2: To characterize the landfill waste to determine the state of degradation and its relevant impact for determining the suitability for landfill mining.

A number of parameters were identified (physical, chemical, and biological) in Chapter 4 to help in assessing the degradation state of the landfill site studied for determining the suitability for LFM. These parameters are MC, leaching test, pH, COD, and TOC. leaching test was performed in order to enable the analysis of pH and COD. MC and pH were analysed in this research to understand their roles in the biodegradation of waste materials and predict the waste degradation stage as well as its behaviour in the surroundings, respectively. COD was analysed to identify the landfill waste stage and its potential impact that could have on the oxygen levels of receiving waters through LFM activities. TOC was determined in order to identify the airborne methane during LFM activities and its potential impact on human health. From the data obtained, the waste degradation stage was concluded to be in an advanced state of degradation, which is regarded suitable for LFM activities from this perspective. MC was also investigated in Chapter 5 and 6 to meet objective number 4 which is discussed later.

Objective 3: To identify the components within the waste known for their established health impact based on chemical analysis.

Chapter 4 analysed and critically discussed a vast range of metals and minerals found within the waste components known for their established health impact with particular focus on fine fractions as it poses the highest risk to the human health. The instrumentation utilised for the analysis are ICP-OES and SEM-MLA techniques. The following metals were analysed: Pb, Cd, Zn, Cu, Cr, Co, As, Ni, Ba, and Mn, which were selected as being of greatest concern in European and American communities. Some minerals that can be potentially harmful to the human health were detected in the site under the study. Additionally, waste size fractions ≤ 10 and >3 microns were also found in the studied site.

Objective 4: To estimate the dust that can be airborne during landfill mining activities.

A method for computing the amount of dust, coupled with adoption of surface mining activities equations was proposed for each individual LFM activity and discussed in details in Chapter 5 and 6. These activities are cover removal loading, recovered waste loading, cover removal unloading, recovered waste unloading, haul road, transport road, exposed cover removal waste, exposed pit surface, and screening plant. A LFM assumed process plan was produced to divide the study area into several phases according to its unit area and select one phase out of five divided phases in the calculation of emission rate as generally LFM projects are implemented at different stages. A range of each formula component was given for modelling emission rate variability to predict maximum and minimum emission values. Parameters identified in the equations were adjusted to LFM applications and for local weather conditions. Some parameters analysed in Chapter 4 (MC and PSD) were used in the calculation of the emission rate to allow behaviour prediction of fine fractions in different mechanical processing activities and obtain represented values of the study area. Moreover, an assumed waste volume range according to 1 phase was computed for the studied landfill site to generate an assumed processes plan flowsheet illustrating the LFM processes and define volumetric throughput ranges for each unit operation. Furthermore, an equation has been established to enable estimation of the cumulative emissions over the lifetime of the LFM operation.

Objective 5: To model dust emissions impact of landfill mining activities on air quality.

In Chapter 5 and 6, extensive work has been undertaken to enable the modelling analysis of dust dispersion impact stemming from LFM activities with the addition to the work carried out to meet objective 4. Factors affecting the dispersion of pollutants/dust in the atmosphere were highlighted to comprehend their main roles in dust dispersion at first. Then, a review of air dispersion models was carried out to select the preferred model and software for dust emissions

impact assessment of LFM activities. After that, an ADMS model option was selected for the modelling analysis based on the research aim. Meanwhile, the equation established to enable the estimation of the cumulative emissions over the lifetime of the LFM operation was also used for the determination of time period of meteorological data applied in the ADMS modelling. Following this, a great deal of statistical analysis of the study site's real-recorded meteorological data for the years from 2016 to 2019 was conducted to form a specific number of scenarios for weather conditions. These number of scenarios were established and applied for the maximum and minimum emission values in the ADMS analysis to find out under what scenario is dispersion an environmental/health risk and under what meteorological conditions is dispersion worst/best for each individual LFM activity and all sources of activities (in combination).

Objective 6: To quantify the risk compared to appropriate standards and legislation.

All the results were related to appropriate standards and legislation. The results of the COD test showed that some values exceeded the standard limit for effluent discharge regulations, but they are within the standard limit when considering the average value. The COD results indicated that there are still some non-degraded residuals found within the studied wells. In terms of the pH results, they were within the current waste acceptance criteria (thresholds) for non-hazardous landfills. Regarding the TOC results, the waste acceptance criterion (threshold) of TOC is 5% for non-hazardous landfills in the UK. This categorised the Norfolk landfill with an average TOC of 1.5%, indicating that it is in an advanced methanogenic state. However, the TOC results were not within the recommended safe methane concentration for workers during an 8-hour period and thus, methane needs to be routinely monitored at the working face of a LFM site due to its potential risk for ignition.

Heavy metals concentrations were compared against the generic assessment criteria of the UK SGVs based on the corresponding land use. The concentrations of As, Cd, Cr, Pb, Cu, and Zn were above permissible limits set for soil in the UK with different land uses. Results of heavy metals were also assessed against maximum allowable limit of heavy metal concentrations in soil for different countries and significant accumulation of some metals were found to be above the limits including As, Pb, Cu, Zn, Cd, Cr, and Cu in some countries. Additionally, heavy metals results were used to derive pollution and health impact indices for pollution and health assessment. Regarding the I_{geo} and CF values, the concentrations of heavy metals were in the following order: Cu>Pb>Cd>As>Ni. The pollution load index was >1, indicating that unacceptable pollution could arise. The study predicts that the landfill could pose a significant risk to human health due to LFM, with potential non-carcinogenic risks of Zn and Pb being higher than the levels set by the USEPA. Carcinogenic assessment suggests that Cr was the most prominent metal followed by As, which could cause human health impacts.

Dust modelled concentrations by ADMS were related to the AQS limit of PM₁₀ (24-hour mean and annual mean) for England. The analysis of air dispersion modelling showed that some dust concentrations values were beyond the limit, and thereby with potential risk to the human health and the environment, especially with the addition of background concentrations.

Besides, discussion of the results and critical analysis were provided throughout the thesis to highlight the significance of the findings/methods/chosen-parameters and broaden understanding by means of interpretations with others' similar work, respectively. This involves comparison of the research findings with literature available work of similar data and appropriate statistical analysis to draw meaningful interpretation, identify patterns and trends of parameters, and support the research findings.

7.3 Contribution to Knowledge

The following are the contribution to new knowledge that this study provides:

1. Identification of the knowledge gap in literature regarding LFM activities.
2. The methods/parameters used for determining the waste state of degradation and mineral composition/abundance and their potential related risks were addressed and applied for the first time in relation to LFM activities.
3. This research is the first to determine the concentration and extent of heavy metal pollution and the associated health and environmental risks in the view of LFM.
4. This research presents a novel approach for calculating and assessing the potential risks of potentially toxic elements to human health in the application of LFM activities.
5. A method for calculating the amount of dust emissions was proposed for each individual LFM activity for the first time.
6. A method for modelling dust air concentrations of LFM activities based on an advanced Gaussian model was introduced and applied for the first time.
7. ADMS model can be used as predictive tool in the estimation of dust/heavy metals concentrations and their plume in the air when their emission inventory is known.
8. The potential impacts of LFM activities on human health and the environment have become evident which may allow fuller implementation of LFM activities.
9. The assessment of health and environmental impact correlated with LFM activities is significant to the waste management industry since this assessment will enable sustainable reuse of waste from LFM, strategies development for preventing and controlling dust as the significant emission, and safe working practice assurance.
10. This research findings will also enable selection of suitable remediation strategies and suppression measures to avoid future costs, which is of value at the site-specific LFM feasibility stage.

11. These insights have allowed for a critical assessment of the research methodology, which has highlighted the limitation of the research and suggested areas for additional work.

7.4 Limitations of the Research

Although the intended achievement of this research towards the aim and objectives was attained, the research has some limitations that should be readily acknowledged. These include:

- Using borehole logs instead of rotary drilling rig during excavation would allow for classification of each individual sample depth in terms of parameters quantification and their relationship to depth, and thereby further critical analysis.
- Additional extensive systematic sampling regimes covering the complete landfill area of the site might confirm presence of undetected materials, certain waste size fraction, and more elevated potentially toxic elements within the landfill site.
- Only one sample was available for MLA particle size distribution.
- More classification analysis using MLA can enable or help in establishing a methodology for health risk assessment using SEM-MLA in the application of LFM activities. Due to closure of Nanoscale and Microscale Research Centre at the University of Nottingham caused by Covid-19 pandemic, continuation of work on the SEM-MLA analysis could not be completed, which was planned to investigate mineral locking percentage of different mineral phases and elemental distribution that can identify in which minerals/phases certain elements (heavy metals) occur and in which proportions from health risk assessment perspective. Therefore, these data will lead to investigation of heavy metals emission rate estimation since PM emission rate is already known.

- All PM emission factor equations require input parameters such as moisture, wind speed, silt content, area, and drop height etc. These formulae are empirical in nature and were developed to estimate the emission factor from mine operations under specific mine geometry and meteorological conditions. Therefore, these relationships may not hold true in general.
- Note that by default, ADMS 5 does not model calm conditions. Any lines of meteorological data for which the wind speed at 10 m is calm (less than 0.75 m/s) were skipped by the model, and output was given as -999 for that line of meteorological data.
- Dry density of the studied size particles was not measured and therefore were estimated. However, multiple ADMS runs were made with different density values of each particle diameter, and the difference in the results of the ground-level long-term average airborne concentrations were found to be negligible.

7.5 Future Work and Recommendations

- Obtaining samples representative of the whole landfill site was not possible and further work is required to consider the statistically valid number of samples required.
- For a better understanding of mobility/bioavailability and environmental fate of heavy metals in the fine fraction of studied landfill waste, sequential extraction method is suggested for further work.
- Experimentally based derivation of robust emissions factors relevant to activities of a LFM site is necessary to minimise over- or under-estimation of emissions. This could be further validated by the monitoring of actual emissions during LFM activities.
- The present study was conducted at one proposed LFM site. Therefore, similar studies should be conducted for different sites to compare the emission rates and modelled concentrations of dust which will provide an improved understanding for the range of emissions, whilst being necessarily site-specific.

- Future research can be carried out to identify heavy metals emission concentrations in the air using ADMS model once their emission inventory is known, and thereby they can be related to the Ambient Air Directive Limit/Target Values and UK Air Quality Strategy Objectives.
- Given that some predicted and modelled LFM impacts may be deemed unacceptable, the practicalities associated with devising a cover to enclose operational LFM activities to restrict emissions dispersion, whilst ensuring safety for occupational health, should be scoped.
- Extending dust modelling work is suggested taking into consideration the total deposition (including wet deposition/humidity) of similar meteorological conditions, considering different time periods to compare with the current results in terms of removal efficiency of PM concentrations as observed in the study by (Mishra et al., 2016; Pandey et al., 2014; Wu et al., 2018). According to (Luo et al., 2021), relative humidity can play an important role in dust concentrations/dispersion as humidity levels greater than 70% maintain safe air quality conditions in the area (Huertas et al., 2014).
- Future research may focus on the uncertainty estimates of air quality risk analysis in decision-making using Monte Carlo simulation since it is considered to be the ideal method for assessing uncertainty of pollutants concentrations in the atmosphere (Holnicki and Nahorski, 2015).

7.6 Conclusion

This research is novel in being the first to determine the concentration and extent of heavy metal pollution and potential associated health and environmental risks from LFM, a previously neglected area in the published literature. The characterisation of MSW samples analysed here provides an indication of the components within the waste from a landfill site that are typical

of those in the UK and that could be considered suitable for LFM. MSW samples were recovered from four different wells of an aged landfill in the UK. The samples were analysed for physical, chemical, and biological properties for the purpose of identifying the extent of potential pollution and emissions during LFM activities. Well-established statistical methods and environmental and health risk indices were used in the assessment. A one-way analysis of variance followed by least significant difference *post hoc* analysis was used to estimate statistically significant differences among the four wells and to compare the heavy metal contents of the MSW samples. Pearson's correlation analysis using a 2-tailed test was used to identify correlations between various variables in the MSW samples. Box and whisker plots were produced to display the range of environmentally available heavy metal concentrations in the four different wells.

Waste fractions of different sizes demonstrated similar behaviours in the four different wells; approximately 56% of the excavated waste materials were ≤ 2.3 mm in size, whereas fine particles approximately ≤ 1.5 mm accounted for more than 50% of the total mass of excavated waste and contained predominantly soil-like materials. The results of the TOC and pH analysis were within the waste acceptance criteria thresholds set for UK landfills.

The concentrations of As, Cd, Cr, Pb, Cu, and Zn in the present study were above the permissible limits set for soil in the UK. The Zn and Pb concentrations were found to be the highest in wells 1901 and 1904, respectively, compared to the UK SGVs. The concentrations also varied significantly among the four wells and decreased in the following order: Zn>Mn>Pb>Cu>Ba>Cr>Ni>As>Co>Cd. Regarding the I_{geo} and CF values, the concentrations of heavy metals were in the following order: Cu>Pb>Cd>As>Ni. The PLI was >1, indicating pollution. The study found that the landfill posed a major risk to human health when LFM occurred, with the non-carcinogenic risks of Zn and Pb being higher than the levels set by the USEPA. The carcinogenic effect revealed that Cr was the most prominent metal, followed by

As, which could impact human health. To this end, a method for computing the amount of dust, coupled with adoption of surface mining activities equations was proposed for each individual LFM activity. The results of the calculated emission rates (dust) revealed that point source activities were the major sources of estimated emissions. The calculated emissions were then used for the air quality analysis using an advanced atmospheric dispersion modelling system (ADMS). Analysis of the ADMS air dispersing modelling results suggest that dust concentrations are most intense in low wind and maximum emission rate scenarios. The analysis also showed that some dust concentrations values were beyond the AQS limit of PM10 for England and thereby, with potential risk to human health and the environment, especially with the addition of background concentrations.

This research highlights the novelty of the approach used to calculate and assess potential risks to human health in the application of LFM activities and reveals useful information that needs to be considered in policy development for environmentally sustainable reuse of waste from LFM and when designing feasibility studies. This approach can be used beyond the UK, while ensuring that the use of SGVs is representative of all exposure routes of specific land uses in the considered country to allow for variation in numerical values, definition, and inference methods of SGVs.

This research puts a spotlight on potential risks that LFM can cause to the human health and the environment that could enable a wider implementation of LFM activities. This study provides a basis for more detailed studies on the environmental and health risk management of LFM. From an international scientific viewpoint, the findings of this research and the role of LFM in the transport of environmental contaminants might become highly significant in the coming decades owing to climate change and the increasing pressure on land use and redevelopment, which can substantially increase the potential for dust emissions and transport.

This research provides qualitative and quantitative evidence demonstrating the need for LFM regulations in order to protect residents from potential emissions into the environment. Implementation of LFM processes must be given adequate attention to allow safe practices from an occupational health perspective (protection of site workers), human health off-site, and the surrounding environment. From a policy point of view, understanding and managing the risk to make them acceptable is a significant step forward.

References

- Abba SI, Elkiran G. Effluent prediction of chemical oxygen demand from the astewater treatment plant using artificial neural network application. *Procedia computer science* 2017; 120: 156-163.
- Abril GA, Diez SC, Pignata ML, Britch J. Particulate matter concentrations originating from industrial and urban sources: validation of atmospheric dispersion modeling results. *Atmospheric Pollution Research* 2016; 7: 180-189.
- Abu-Daabes M, Qdais HA, Alsyouri H. Assessment of heavy metals and organics in municipal solid waste leachates from landfills with different ages in Jordan. *Journal of Environmental Protection* 2013; 4: 344.
- Adelopo A, Haris PI, Alo B, Huddersman K, Jenkins R. Multivariate analysis of the effects of age, particle size and landfill depth on heavy metals pollution content of closed and active landfill precursors. *Waste Management* 2018; 78: 227-237.
- Adelopo AO, Alo B, Haris PI, Huddersman K, Jenkins RO. Seasonal variations in moisture content and the distribution of total organic carbon in landfill composites: case of active and closed landfills in Lagos, Nigeria. 2017.
- Adhikari B, Dahal K, Khanal SN. A review of factors affecting the composition of municipal solid waste landfill leachate. *International Journal of Engineering Science and Innovative Technology (IJESIT)* 2014; 3: 273-281.
- Adimalla N, Wang H. Distribution, contamination, and health risk assessment of heavy metals in surface soils from northern Telangana, India. *Arabian Journal of Geosciences* 2018; 11: 684.
- Afzali A, Rashid M, Afzali M, Younesi V. Prediction of air pollutants concentrations from multiple sources using AERMOD coupled with WRF prognostic model. *Journal of Cleaner Production* 2017; 166: 1216-1225.

- Agency E. Waste Sampling and Testing for Disposal to Landfill. 2013.
- Aihong M, Qinghai L, Jinyan J, ZHANG Y. Effect of moisture on partitioning of heavy metals in incineration of municipal solid waste. *Chinese Journal of Chemical Engineering* 2012; 20: 1008-1015.
- Aiman U, Mahmood A, Waheed S, Malik RN. Enrichment, geo-accumulation and risk surveillance of toxic metals for different environmental compartments from Mehmood Booti dumping site, Lahore city, Pakistan. *Chemosphere* 2016; 144: 2229-2237.
- Aksoyoglu S, Prévôt AS. Modelling nitrogen deposition: dry deposition velocities on various land-use types in Switzerland. *International Journal of Environment and Pollution* 2018; 64: 230-245.
- Al-Ani T, Sarapää O. Clay and clay mineralogy. Physical-chemical properties and industrial uses 2008.
- Al-Hemoud A, Al-Sudairawi M, Al-Rashidi M, Behbehani W, Al-Khayat A. Temperature inversion and mixing height: critical indicators for air pollution in hot arid climate. *Natural Hazards* 2019; 97: 139-155.
- Albright WH, Benson CH, Gee GW, Abichou T, Tyler SW, Rock SA. Field performance of three compacted clay landfill covers. *Vadose Zone Journal* 2006; 5: 1157-1171.
- Allen A. Containment landfills: the myth of sustainability. *Engineering geology* 2001; 60: 3-19.
- Allen B. UK landfill sites could each contain £90m of valuable metals. *edie news*. edie UK, 2015.
- ALS E. Waste acceptance criteria: thresholds, UK, 2017.

- Amin M, Prajati G, Humairoh GP, Putri RM, Phairuang W, Hata M, et al. Characterization of size-fractionated carbonaceous particles in the small to nano-size range in Batam city, Indonesia. *Heliyon* 2023.
- Amoatey P, Omidvarborna H, Baawain M. The modeling and health risk assessment of PM_{2.5} from Tema Oil Refinery. *Human and Ecological Risk Assessment: An International Journal* 2018; 24: 1181-1196.
- Appleton T, Kingman S, Lowndes I, Silvester S. The development of a modelling strategy for the simulation of fugitive dust emissions from in-pit quarrying activities: a UK case study. *International journal of surface mining, reclamation and environment* 2006; 20: 57-82.
- Araújo IP, Costa DB, De Moraes RJ. Identification and characterization of particulate matter concentrations at construction jobsites. *Sustainability* 2014; 6: 7666-7688.
- Asif Z, Chen Z, Han Y. Air quality modeling for effective environmental management in the mining region. *Journal of the Air & Waste Management Association* 2018; 68: 1001-1014.
- Athanassiadou M, Baker J, Carruthers D, Collins W, Girnary S, Hassell D, et al. An assessment of the impact of climate change on air quality at two UK sites. *Atmospheric Environment* 2010; 44: 1877-1886.
- Atia A. Methane (CH₄) Safety, Alberta, 2004.
- Atkinson J. Landfill mining regulation: how do we start? In: McCaffrey R, editor. *Global Landfill Mining Conference and Exhibition*, 2010.
- Barry D, Gregory B, Harries C. Minimizing methane emissions from MSW landfill. *Atkins Environment*, UK 2004.
- Bastian K, Alexander M, Daniel H, Robert R. Landfill mining of a mixed municipal solid waste and commercial waste landfill: application of existing processing technology –

- opportunities and limitations In: Jones PT, Machiels L, editors. 4th International Symposium On Enhanced Landfill Mining, Mechelen, Belgium, 2018.
- Bäumler R, Kögel-Knabner I. Spectroscopic and wet chemical characterization of solid waste organic matter of different age in landfill sites, Southern Germany. *Journal of environmental quality* 2008; 37: 146-153.
- Bhalla B, Saini M, Jha M. Effect of age and seasonal variations on leachate characteristics of municipal solid waste landfill. *International Journal of Research in Engineering and Technology* 2013; 2: 223-232.
- Bhatti SS, Kumar V, Kumar A, Kirby JK, Gouzos J, Correll R, et al. Potential carcinogenic and non-carcinogenic health hazards of metal (loid) s in food grains. *Environmental Science and Pollution Research* 2020: 1-11.
- Bisutti I, Hilke I, Raessler M. Determination of total organic carbon—an overview of current methods. *TrAC Trends in Analytical Chemistry* 2004; 23: 716-726.
- Bour O, Berger S, Couturier C, Riquier L. Determination of guidance values for closed landfill gas emissions. 10. *International waste management and landfill Symposium (Sardinia), 2005, pp. NC.*
- Bourgkard E, Wild P, Courcot B, Diss M, Ettliger J, Goutet P, et al. Lung cancer mortality and iron oxide exposure in a French steel-producing factory. *Occupational and environmental medicine* 2009; 66: 175-181.
- Bozkurt S, Moreno L, Neretnieks I. Long-term fate of organics in waste deposits and its effect on metal release. *Science of the Total Environment* 1999; 228: 135-152.
- Bozkurt S, Moreno L, Neretnieks I. Long-term processes in waste deposits. *Science of the total environment* 2000; 250: 101-121.

- Brand E, de Nijs TC, Dijkstra JJ, Comans RN. A novel approach in calculating site-specific aftercare completion criteria for landfills in The Netherlands: policy developments. *Waste Management* 2016; 56: 255-261.
- Brand JH. Assessing the risk of pollution from historic coastal landfills. PhD. Queen Mary University of London, 2017.
- Brand JH, Spencer KL, O'shea FT, Lindsay JE. Potential pollution risks of historic landfills on low-lying coasts and estuaries. *Wiley Interdisciplinary Reviews: Water* 2018; 5: e1264.
- Briki M, Zhu Y, Gao Y, Shao M, Ding H, Ji H. Distribution and health risk assessment to heavy metals near smelting and mining areas of Hezhang, China. *Environmental Monitoring and Assessment* 2017; 189: 458.
- Brookes DM, Stedman JR, Kent AJ, Whiting SL, Rose RA, Williams CJ, et al. Technical report on UK supplementary assessment under the Air Quality Directive (2008/50/EC), The Air Quality Framework Directive (96/62/EC) and Fourth Daughter Directive (2004/107/EC) for 2018, UK, 2020.
- Brown D, Shaw S, Gergory R, Robinson H, Robinson T. Landfill aftercare scoping study, UK, 2018.
- Brown T. Silica exposure, smoking, silicosis and lung cancer—complex interactions. *Occupational medicine* 2009; 59: 89-95.
- Brusca S, Famoso F, Lanzafame R, Mauro S, Garrano AMC, Monforte P. Theoretical and experimental study of Gaussian Plume model in small scale system. *Energy Procedia* 2016; 101: 58-65.
- Bučinskas A, Kriipsalu M, Denafas G. Proposal for feasibility assessment model for landfill mining and its implementation for energy generation scenarios. *Sustainability* 2018; 10: 2882.

- Burlakovs J, Jani Y, Kriipsalu M, Vincevica-Gaile Z, Kaczala F, Celma G, et al. On the way to 'zero waste' management: recovery potential of elements, including rare earth elements, from fine fraction of waste. *Journal of Cleaner Production* 2018; 186: 81-90.
- Burlakovs J, Kaczala F, Vincevica-Gaile Z, Rudovica V, Orupold K, Stapkevica M, et al. Mobility of metals and valorization of sorted fine fraction of waste after landfill excavation. *Waste and Biomass Valorization* 2016; 7: 593-602.
- Burlakovs J, Kriipsalu M, Arina D, Kaczala F, Shmarin S, Denafas G, et al. Former dump sites and the landfill mining perspectives in Baltic countries and Sweden: the status. *Proceedings of the 13th SGEM GeoConference on Science and Technologies in Geology, Exploration and Mining* 2013; 1: 485-492.
- Burlakovs J, Kriipsalu M, Klavins M, Bhatnagar A, Vincevica-Gaile Z, Stenis J, et al. Paradigms on landfill mining: from dump site scavenging to ecosystem services revitalization. *Resources, Conservation and Recycling* 2017; 123: 73-84.
- Burnett RT, Pope III CA, Ezzati M, Olives C, Lim SS, Mehta S, et al. An integrated risk function for estimating the global burden of disease attributable to ambient fine particulate matter exposure. *Environmental health perspectives* 2014; 122: 397-403.
- Camacho I, Rajabi-Estarabadi A, Eber AE, Griggs JW, Margaret SI, Nouri K, et al. Fiberglass dermatitis: clinical presentations, prevention, and treatment—a review of literatures. *International journal of dermatology* 2019; 58: 1107-1111.
- Canopoli L, Coulon F, Wagland ST. Degradation of excavated polyethylene and polypropylene waste from landfill. *Science of the Total Environment* 2020; 698: 134125.

- Cao B, Wang X, Ning G, Yuan L, Jiang M, Zhang X, et al. Factors influencing the boundary layer height and their relationship with air quality in the Sichuan Basin, China. *Science of the Total Environment* 2020; 727: 138584.
- Capella S, Bellis D, Fioretti E, Marinelli R, Belluso E. Respirable inorganic fibers dispersed in air and settled in human lung samples: Assessment of their nature, source, and concentration in a NW Italy large city. *Environmental Pollution* 2020; 263: 114384.
- Carruthers D, Holroyd R, Hunt J, Weng W, Robins A, Apsley D, et al. UK-ADMS: a new approach to modelling dispersion in the earth's atmospheric boundary layer. *Journal of wind engineering and industrial aerodynamics* 1994; 52: 139-153.
- Castrillón L, Fernández-Nava Y, Ulmanu M, Anger I, Marañón E. Physico-chemical and biological treatment of MSW landfill leachate. *Waste Management* 2010; 30: 228-235.
- CAT. Caterpillar equipment selection and application guide for waste landfills, 2008.
- CERC. Atmospheric dispersion modelling system (ADMS 5) user guide version 5.2, 2016.
- Chakraborty M, Ahmad M, Singh R, Pal D, Bandopadhyay C, Chaulya S. Determination of the emission rate from various opencast mining operations. *Environmental Modelling & Software* 2002; 17: 467-480.
- Chandana N, Goli VSNS, Mohammad A, Singh DN. Characterization and utilization of landfill-mined-soil-like-fractions (LFMSF) for sustainable development: a critical appraisal. *Waste and Biomass Valorization* 2020: 1-22.
- Chandana N, Goli VSNS, Mohammad A, Singh DN. Characterization and utilization of landfill-mined-soil-like-fractions (LFMSF) for sustainable development: a critical appraisal. *Waste and Biomass Valorization* 2021; 12: 641-662.

- Chang C-T. Assessment of influential range and characteristics of fugitive dust in limestone extraction processes. *Journal of the Air & Waste Management Association* 2004; 54: 141-148.
- Chaulya S. Emission rate formulae for surface iron ore mining activities. *Environmental Modeling & Assessment* 2006; 11: 361-370.
- Chaulya S, Ahmad M, Singh R, Bandopadhyay LK, Bondyopadhyay C, Mondal G. Validation of two air quality models for Indian mining conditions. *Environmental Monitoring and Assessment* 2003; 82: 23-43.
- Chaulya S, Chakraborty M, Ahmad M, Singh R, Bondyopadhyay C, Mondal G, et al. Development of empirical formulae to determine emission rate from various opencast coal mining operations. *Water, Air, and Soil Pollution* 2002; 140: 21-55.
- Chaulya S, Tiwary R, Mondal S, Mondal G, Singh T, Singh S, et al. Air quality impact assessment and management of mining activities around an international heritage site in India. *Mining, Metallurgy & Exploration* 2022; 39: 573-590.
- Chaulya S, Trivedi R, Kumar A, Tiwary R, Singh R, Pandey P, et al. Air quality modelling for prediction of dust concentrations in iron ore mines of Saranda region, Jharkhand, India. *Atmospheric pollution research* 2019; 10: 675-688.
- Chen H, Teng Y, Lu S, Wang Y, Wang J. Contamination features and health risk of soil heavy metals in China. *Science of the Total Environment* 2015; 512: 143-153.
- Cheriyar R, Chandrakaran S. Suitability of iron oxide-rich industrial waste material in clay soil as a landfill liner. *Problematic Soils and Geoenvironmental Concerns*. Springer, 2021, pp. 215-228.
- Chu C-C, Fang G-C, Chen J-C, Lin I-C. Ambient air dry deposition and ionic species analysis by using various deposition collectors in Shalu, central Taiwan. *Atmospheric Research* 2008; 88: 212-223.

- Chuan M, Shu G, Liu J. Solubility of heavy metals in a contaminated soil: effects of redox potential and pH. *Water, Air, and Soil Pollution* 1996; 90: 543-556.
- Commission E. Circular economy—implementation of the circular economy action plan. 2018.
- Cortés S, Zúñiga-Venegas L, Pancetti F, Covarrubias A, Ramírez-Santana M, Adaros H, et al. A positive relationship between exposure to heavy metals and development of chronic diseases: a case study from Chile. *International Journal of Environmental Research and Public Health* 2021; 18: 1419.
- Cossu R, Hogland W, Salerni E. Landfill mining in Europe and USA. *ISWA Yearbook* 1996: 107-114.
- Cossu R, Lai T, Sandon A. Standardization of BOD5/COD ratio as a biological stability index for MSW. *Waste management* 2012; 32: 1503-1508.
- Costa A, Macedonio G, Folch A. A three-dimensional Eulerian model for transport and deposition of volcanic ashes. *Earth and Planetary Science Letters* 2006; 241: 634-647.
- Costa R, Orriols R. Man-made mineral fibers and the respiratory tract. *Archivos de Bronconeumología (English Edition)* 2012; 48: 460-468.
- Council E. Council Directive 1999/31/EC of 26 April 1999 on the landfill of waste. *Official Journal of the European Communities* 1999; 16: 1999.
- Council E. Council Decision 2003/33/EC of 19 December 2002 establishing criteria and procedures for the acceptance of waste at landfills pursuant to Article 16 of and Annex II to Directive 1999/31/EC. *Official Journal of the European Communities* 2003; 16: L11.
- Csavina J, Field J, Félix O, Corral-Avitia AY, Sáez AE, Betterton EA. Effect of wind speed and relative humidity on atmospheric dust concentrations in semi-arid climates. *Science of the Total Environment* 2014; 487: 82-90.

- Csavina J, Field J, Taylor MP, Gao S, Landázuri A, Betterton EA, et al. A review on the importance of metals and metalloids in atmospheric dust and aerosol from mining operations. *Science of the Total Environment* 2012; 433: 58-73.
- Cuculeanu V, Lupu A, Grigoras G, Popescu I, Toma A. Dispersion model for low wind and atmospheric calm part i: description. *Romanian Reports in Physics* 2019; 71: 712.
- Damigos D, Menegaki M, Kaliampakos D. Monetizing the social benefits of landfill mining: evidence from a contingent valuation survey in a rural area in Greece. *Waste Management* 2016; 51: 119-129.
- Danthurebandara M. Environmental and economic performance of enhanced landfill mining. KU Leuven, 2015.
- Danthurebandara M, Van Passel S, Vanderreydt I, Van Acker K. Environmental and economic performance of plasma gasification in enhanced landfill mining. *Waste Management* 2015; 45: 458-467.
- Datta M, Somani M, Ramana G, Sreekrishnan T. Feasibility of re-using soil-like material obtained from mining of old MSW dumps as an earth-fill and as compost. *Process Safety and Environmental Protection* 2020.
- Davidson CI, Phalen RF, Solomon PA. Airborne particulate matter and human health: a review. *Aerosol Science and Technology* 2005; 39: 737-749.
- Davies BM. Validation of ADMS for dispersion in convective conditions. *Air Pollution Modeling and Its Application XI*. Springer, 1996, pp. 683-685.
- Defra. The air quality strategy for England, Scotland, Wales and Northern Ireland (Volume 1), 2007.
- Defra. Environmental protection act 1990: part 2A. Contaminated land statutory guidance. Department of Environment, Food and Rural Affairs London, 2012.
- Defra. Background mapping data for local authorities 15 April 2022, UK, 2019.

- Defra, Agency E. Model procedures for the management of land contamination. Contaminated Land Report 11, Bristol: Environment Agency, 2009.
- Defra Ea. Air emissions risk assessment for your environmental permit, 2016.
- Dhar A. Landfill mining - a comprehensive literature review, 2015.
- Dickinson W. Landfill mining comes of age. *Solid Waste Technologies* 1995; 9: 42–47.
- Dijkstra J, Van Zomeren A, Comans R, Brand E, Claessens J. Calculating site-specific emission criteria for sustainable landfills: the Dutch approach. *Proceedings Sardinia 2013, Fourteenth International Waste Management and Landfill Symposium, Cagliari, Italy; 30 September–4 October 2013. CISA Publisher Italy, 2013.*
- Dino GA, Mehta N, Rossetti P, Ajmone-Marsan F, De Luca DA. Sustainable approach towards extractive waste management: two case studies from Italy. *Resources Policy* 2018; 59: 33-43.
- Directive E. Directive 2008/98/EC of the European Parliament and of the Council of 19 November 2008 on waste and repealing certain Directives. *Official Journal of the European Union L* 2008; 312.
- Doležalová Weissmannová H, Mihočová S, Chovanec P, Pavlovský J. Potential ecological risk and human health risk assessment of heavy metal pollution in industrial affected soils by coal mining and metallurgy in Ostrava, Czech Republic. *International Journal of Environmental Research and Public Health* 2019; 16: 4495.
- Douglas P, Hayes ET, Williams W, Tyrrel SF, Kinnersley R, Walsh K, et al. Use of dispersion modelling for environmental impact assessment of biological air pollution from composting: progress, problems and prospects. *Waste management* 2017; 70: 22-29.
- Douglas P, Tyrrel S, Kinnersley RP, Whelan M, Longhurst PJ, Walsh K, et al. Sensitivity of predicted bioaerosol exposure from open windrow composting facilities to ADMS

- dispersion model parameters. *Journal of environmental management* 2016; 184: 448-455.
- DP T, TR D. Assessment and modelling of dust concentration in an opencast coal mine in India. 2015.
- Du C, Wang J, Wang Y. Study on environmental pollution caused by dumping operation in open pit mine under different factors. *Journal of Wind Engineering and Industrial Aerodynamics* 2022; 226: 105044.
- Dubey B, Pal AK, Singh G. Trace metal composition of airborne particulate matter in the coal mining and non-mining areas of Dhanbad Region, Jharkhand, India. *Atmospheric Pollution Research* 2012; 3: 238-246.
- Edina. Geology. <https://digimap.edina.ac.uk/geology> (accessed 18 October 2019), 2019.
- Edina. Environment. <https://digimap.edina.ac.uk/environment> (accessed 14 March 2021), 2022a.
- Edina. Historic. <https://digimap.edina.ac.uk/historic> (accessed 9 October 2020), 2022b.
- Ehrig H, Krümpelbeck I. The emission behaviour of old landfills in the aftercare phase. *Proceedings Sardinia, 2001*, pp. 313-323.
- EI-Harbawi M, Rashid ZA. Air pollution modelling, simulation and computational methods: a review. *Proceedings International Conference on Environmental Research and Technology. Universiti Sains Malaysia, 2008*.
- Einhäupl P, Krook J, Svensson N, Van Acker K, Van Passel S. Enhanced landfill mining at the Remo Site: Assessing stakeholders' perspectives for implementation. *Proceedings of the 4th International Symposium on Enhanced Landfill Mining, 2018*, pp. 367-377.
- Einhäupl P, Van Acker K, Peremans H, Van Passel S. The conceptualization of societal impacts of landfill mining—A system dynamics approach. *Journal of Cleaner Production* 2021; 296: 126351.

- El-Fadel M, Abi-Esber L. Simulating industrial emissions using atmospheric dispersion modeling system: model performance and source emission factors. *Journal of the Air & Waste Management Association* 2012; 62: 336-349.
- Elmes M, Gasparon M. Sampling and single particle analysis for the chemical characterisation of fine atmospheric particulates: a review. *Journal of Environmental management* 2017; 202: 137-150.
- Emerson EW, Hodshire AL, DeBolt HM, Bilsback KR, Pierce JR, McMeeking GR, et al. Revisiting particle dry deposition and its role in radiative effect estimates. *Proceedings of the National Academy of Sciences* 2020; 117: 26076-26082.
- EN B. Characterisation of waste-leaching-compliance test for leaching of granular waste materials and sludges: part 2. One stage batch test at a liquid to solid ratio of 10 l/kg for materials with particle size below 4 mm (without or with size reduction). European Committee for Standardization Brussels, 2002.
- Environment Agency. Model procedures for the management of land contamination. Environment Agency Bristol, 2004.
- Environment Agency. Updated technical background to the CLEA model. ScienceReport: SC050021/SR33, UK, 2009a.
- Environment Agency. Using science to create a better place. Updated technical background to the CLEA model. Science Report SC050021/SR3. Environment Agency Bristol, 2009b.
- Environment Agency b. The surrender of permits for the permanent deposit of waste. In: Environment Agency B, UK, Version 1: p. 24., editor, 2010.
- EPA NSW. Approved methods for the modelling and assessment of air pollutants in New South Wales. Department of Environment and Conservation, Sydney 2005.

- Esakku S, Kurian J, Nagendran R. Methodological constraints and challenges in sampling and characterization for dumpsite rehabilitation. Proceeding Sardinia. Citeseer, 2005.
- Esakku S, Palanivelu K, Joseph K. Assessment of heavy metals in a municipal solid waste dumpsite. Workshop on sustainable landfill management. 35. Citeseer, 2003, pp. 139-145.
- Fan W, Qin K, Xu J, Yuan L, Li D, Jin Z, et al. Aerosol vertical distribution and sources estimation at a site of the Yangtze River Delta region of China. Atmospheric research 2019; 217: 128-136.
- Fatta D, Papadopoulos A, Loizidou M. A study on the landfill leachate and its impact on the groundwater quality of the greater area. Environmental Geochemistry and Health 1999; 21: 175-190.
- Femi BB. Municipal solid waste: pre-treatment options and benefits on landfill emissions. World Academy of Science, Engineering and Technology, International Journal of Chemical, Molecular, Nuclear, Materials and Metallurgical Engineering 2011; 5: 1007-1011.
- Feng X, Wang S, Guo J. Temperature inversions in the lower troposphere over the Sichuan Basin, China: Seasonal feature and relation with regional atmospheric circulations. Atmospheric Research 2022; 271: 106097.
- Ferreira-Baptista L, De Miguel E. Geochemistry and risk assessment of street dust in Luanda, Angola: A tropical urban environment. Atmospheric Environment 2005; 39: 4501-4512.
- Filgueiras A, Lavilla I, Bendicho C. Chemical sequential extraction for metal partitioning in environmental solid samples. Journal of Environmental Monitoring 2002; 4: 823-857.
- Fisher C, Maurice C, Lagerkvist A. Gas emission from landfills—an overview of issues and research needs. Swedish Environmental Protection Agency, Stockholm 1999.

- Ford S, Warren K, Lorton C, Smithers R, Read A, Hudgins M. Feasibility and viability of landfill mining and reclamation in Scotland. Scoping Study. Final Report.. Zero Waste Scotland 2013.
- Francois V, Feuillade G, Skhiri N, Lagier T, Matejka G. Indicating the parameters of the state of degradation of municipal solid waste. *Journal of hazardous materials* 2006; 137: 1008-1015.
- Frändegård P, Krook J, Svensson N, Eklund M. Resource and climate implications of landfill mining: a case study of Sweden. *Journal of Industrial Ecology* 2013; 17: 742-755.
- Frank R, Cipullo S, Garcia J, Davies S, Wagland ST, Villa R, et al. Compositional and physicochemical changes in waste materials and biogas production across 7 landfill sites in UK. *Waste Management* 2017; 63: 11-17.
- Fryer M, Collins CD, Ferrier H, Colvile RN, Nieuwenhuijsen MJ. Human exposure modelling for chemical risk assessment: a review of current approaches and research and policy implications. *Environmental Science & Policy* 2006; 9: 261-274.
- Fubini B, Arean CO. Chemical aspects of the toxicity of inhaled mineral dusts. *Chemical Society Reviews* 1999; 28: 373-381.
- García J, Davies S, Villa R, Gomes D, Coulon F, Wagland ST. Compositional analysis of excavated landfill samples and the determination of residual biogas potential of the organic fraction. *Waste Management* 2016; 55: 336-344.
- Gautam S, Patra AK, Sahu SP, Hitch M. Particulate matter pollution in opencast coal mining areas: a threat to human health and environment. *International Journal of Mining, Reclamation and Environment* 2018; 32: 75-92.
- Gautam S, Prasad N, Patra AK, Prusty BK, Singh P, Pipal AS, et al. Characterization of PM_{2.5} generated from opencast coal mining operations: a case study of Sonepur Bazari Opencast Project of India. *Environmental technology & innovation* 2016; 6: 1-10.

- Gerlach RW, Dobb DE, Raab GA, Nocerino JM. Gy sampling theory in environmental studies. 1. Assessing soil splitting protocols. *Journal of Chemometrics: A Journal of the Chemometrics Society* 2002; 16: 321-328.
- Ghorbel M, Munoz M, Solmon F. Health hazard prospecting by modeling wind transfer of metal-bearing dust from mining waste dumps: application to Jebel Ressay Pb–Zn–Cd abandoned mining site (Tunisia). *Environmental Geochemistry and Health* 2014; 36: 935-951.
- Ghose M, Majee S. Assessment of the impact on the air environment due to opencast coal mining—an Indian case study. *Atmospheric Environment* 2000; 34: 2791-2796.
- Giardina M, Buffa P. A new approach for modeling dry deposition velocity of particles. *Atmospheric Environment* 2018; 180: 11-22.
- Gregory B. Landfill aftercare scoping study. *Landfill Aftercare Decision Support System (LANDSS) Forum Meeting, Birmingham, 2018.*
- Grimmer A. Contaminated land inspection report (potential landfill, Docking Common (Docking No1), Fakenham Road, Docking, Norfolk, 2018.
- Gu Y. Automated scanning electron microscope based mineral liberation analysis an introduction to JKMRC/FEI mineral liberation analyser. *J. Miner. Mater. Charact. Eng* 2003; 2: 33-41.
- Gujre N, Rangan L, Mitra S. Occurrence, geochemical fraction, ecological and health risk assessment of cadmium, copper and nickel in soils contaminated with municipal solid wastes. *Chemosphere* 2021; 271: 129573.
- Gutiérrez-Gutiérrez SC, Coulon F, Jiang Y, Wagland S. Rare earth elements and critical metal content of extracted landfilled material and potential recovery opportunities. *Waste Management* 2015; 42: 128-136.

- Gworek B, Dmuchowski W, Koda E, Marecka M, Baczevska AH, Brągoszewska P, et al. Impact of the municipal solid waste Łubna landfill on environmental pollution by heavy metals. *Water* 2016; 8: 470.
- Hakanson L. An ecological risk index for aquatic pollution control. A sedimentological approach. *Water Research* 1980; 14: 975-1001.
- Hanna SR, Egan BA, Purdum J, Wagler J. Evaluation of the ADMS, AERMOD, and ISC3 dispersion models with the OPTTEX, Duke Forest, Kincaid, Indianapolis and Lovett field datasets. *International Journal of Environment and Pollution* 2001; 16: 301-314.
- Hassaan MA, El Nemr A, Madkour FF. Environmental assessment of heavy metal pollution and human health risk. *American Journal of Water Science and Engineering* 2016; 2: 14-19.
- Health UDo, Services H. Agency for toxic substances and disease registry-ATSDR. 1999.
- Heyer K-U, Hupe K, Ritzkowski M, Stegmann R. Pollutant release and pollutant reduction—impact of the aeration of landfills. *Waste Management* 2005; 25: 353-359.
- Hogland M, Hogland W, Jani Y, Kaczala F, de Sá Salomão AL, Kriipsalu M, et al. Experiences of three landfill mining projects in the baltic sea area: with focus on machinery for material recovery. *Linnaeus Eco-Tech* 2014.
- Hogland W. Remediation of an old landsfill site. *Environmental Science and Pollution Research* 2002; 9: 49-54.
- Hogland W, Marques M, Nimmermark S. Landfill mining and waste characterization: a strategy for remediation of contaminated areas. *Journal of Material Cycles and Waste Management* 2004; 6: 119-124.
- Holm O, Hansen E, Lassen C, Stuer-Lauridsen F, Jesper K. Heavy metals in waste—final report. European Commission DG ENV. E3, Project ENV. E. 2002.

- Holmes N, Morawska L. A review of dispersion modelling and its application to the dispersion of particles: an overview of different dispersion models available. *Atmospheric Environment* 2006; 40: 5902-5928.
- Holnicki P, Nahorski Z. Emission data uncertainty in urban air quality modeling—case study. *Environmental Modeling & Assessment* 2015; 20: 583-597.
- Holtslag A, Van Ulden A. A simple scheme for daytime estimates of the surface fluxes from routine weather data. *Journal of Applied Meteorology and Climatology* 1983; 22: 517-529.
- Hölzle I. Contaminants in landfill soils—Reliability of prefeasibility studies. *Waste Management* 2017; 63: 337-344.
- Hölzle I. Dry screening—assessing the effectiveness of contaminant reduction in recovered landfill soils. *Journal of Cleaner Production* 2018; 172: 1998-2008.
- Hölzle I. Contaminant patterns in soils from landfill mining. *Waste Management* 2019; 83: 151-160.
- Hölzle I, Somani M, Ramana G, Datta M. Heavy metals in soil-like material from landfills—Resource or contaminants? *Journal of Cleaner Production* 2022; 369: 133136.
- Hosford M. Human health toxicological assessment of contaminants in soil: Environment Agency, 2009.
- Hu X, Zhang Y, Ding Z, Wang T, Lian H, Sun Y, et al. Bioaccessibility and health risk of arsenic and heavy metals (Cd, Co, Cr, Cu, Ni, Pb, Zn and Mn) in TSP and PM_{2.5} in Nanjing, China. *Atmospheric Environment* 2012; 57: 146-152.
- Huang SX, Jaurand M-C, Kamp DW, Whysner J, Hei TK. Role of mutagenicity in asbestos fiber-induced carcinogenicity and other diseases. *Journal of Toxicology and Environmental Health, Part B* 2011; 14: 179-245.

- Huertas J, Huertas M, Cervantes G, Díaz J. Assessment of the natural sources of particulate matter on the opencast mines air quality. *Science of the Total Environment* 2014; 493: 1047-1055.
- Huertas JI, Camacho DA, Huertas ME. Standardized emissions inventory methodology for open-pit mining areas. *Environmental Science and Pollution Research* 2012a; 19: 2784-2794.
- Huertas JI, Huertas ME, Izquierdo S, González ED. Air quality impact assessment of multiple open pit coal mines in northern Colombia. *Journal of environmental management* 2012b; 93: 121-129.
- Hull RM, Krogmann U, Strom PF. Composition and characteristics of excavated materials from a New Jersey landfill. *Journal of Environmental Engineering* 2005; 131: 478-490.
- Hupe K, Heyer K, Stegmann R. Water infiltration for enhanced in situ stabilization. *Proceedings Sardinia, 2003*, pp. 6-10.10.
- Hussein M, Yoneda K, Mohd-Zaki Z, Amir A, Othman N. Heavy metals in leachate, impacted soils and natural soils of different landfills in Malaysia: An alarming threat. *Chemosphere* 2021; 267: 128874.
- Hussein M, Yoneda K, Zaki ZM, Amir A. Leachate characterizations and pollution indices of active and closed unlined landfills in Malaysia. *Environmental Nanotechnology, Monitoring & Management* 2019; 12: 100232.
- Ilse B, Patrick B, Jan P, Yves T. Development of an early warning system for the closing the circle project at the remo landfill site. *4th International Symposium On Enhanced Landfill Mining, Mechelen, Belgium, 2018*.
- ISWA. *Landfill operational guidelines 3rd edition*. International Solid Waste Association, 2019.

- Jacobs J. Accelerated methane production prior to mining. Global Landfill Mining Conference, Royal School of Arts, London, 9 October 2008, 2008.
- Jain P, Kim H, Townsend TG. Heavy metal content in soil reclaimed from a municipal solid waste landfill. *Waste Management* 2005; 25: 25-35.
- Jain P, Townsend TG, Johnson P. Case study of landfill reclamation at a Florida landfill site. *Waste Management* 2013; 33: 109-116.
- Jani Y, Kaczala F, Marchand C, Hogland M, Kriipsalu M, Hogland W, et al. Characterisation of excavated fine fraction and waste composition from a Swedish landfill. *Waste Management & Research* 2016; 34: 1292-1299.
- Jia Q, Huang Y, Al-Ansari N, Knutsson S. Dust emissions from landfill deposition: a case study in Malmberget mine, Sweden. *Journal of Earth Sciences and Geotechnical Engineering* 2013; 3: 25-34.
- Johansson N. Why don't we mine the landfills? Linköping University Electronic Press, 2013.
- Johnson C, Ander E, Cave M, Palumbo-Roe B. Normal background concentrations (NBCs) of contaminants in English soils: final project report. 2012.
- Jones PT, Geysen D, Tielemans Y, Van Passel S, Pontikes Y, Blanpain B, et al. Enhanced Landfill Mining in view of multiple resource recovery: a critical review. *Journal of Cleaner Production* 2013; 55: 45-55.
- Joseph G, Lowndes I, Hargreaves D. A computational study of particulate emissions from Old Moor Quarry, UK. *Journal of Wind Engineering and Industrial Aerodynamics* 2018; 172: 68-84.
- Kaartinen T, Sormunen K, Rintala J. Case study on sampling, processing and characterization of landfilled municipal solid waste in the view of landfill mining. *Journal of Cleaner Production* 2013; 55: 56-66.

- Kaczala F, Mehdinejad MH, Lääne A, Orupold K, Bhatnagar A, Kriipsalu M, et al. Leaching characteristics of the fine fraction from an excavated landfill: physico-chemical characterization. *Journal of Material Cycles and Waste Management* 2017; 19: 294-304.
- Kakosimos KE, Assael MJ, Lioumbas JS, Spiridis AS. Atmospheric dispersion modelling of the fugitive particulate matter from overburden dumps with numerical and integral models. *Atmospheric Pollution Research* 2011; 2: 24-33.
- Kampa M, Castanas E. Human health effects of air pollution. *Environmental pollution* 2008; 151: 362-367.
- Kamunda C, Mathuthu M, Madhuku M. Health risk assessment of heavy metals in soils from Witwatersrand gold mining basin, South Africa. *International Journal of Environmental Research and Public Health* 2016; 13: 663.
- Kappos AD, Bruckmann P, Eikmann T, Englert N, Heinrich U, Höpfe P, et al. Health effects of particles in ambient air. *International journal of hygiene and environmental health* 2004; 207: 399-407.
- Kartal S, Özer U. Determination and parameterization of some air pollutants as a function of meteorological parameters in Kayseri, Turkey. *Journal of the Air & Waste Management Association* 1998; 48: 853-859.
- Kasemodel M, Sakamoto I, Varesche M, Rodrigues V. Potentially toxic metal contamination and microbial community analysis in an abandoned Pb and Zn mining waste deposit. *Science of the Total Environment* 2019; 675: 367-379.
- Kiepper B. Understanding laboratory wastewater tests: I. Organics (BOD, COD, TOC, O&G). *The University of Georgia College of Agricultural and Environmental Sciences ...*, 2010.

- Kilburn KH, Powers D, Warshaw RH. Pulmonary effects of exposure to fine fibreglass: irregular opacities and small airways obstruction. *Occupational and Environmental Medicine* 1992; 49: 714-720.
- Kim H, Tae S, Yang J. Calculation methods of emission factors and emissions of fugitive particulate matter in south Korean construction sites. *Sustainability* 2020; 12: 9802.
- Kim K-H, Kabir E, Jahan SA. Airborne bioaerosols and their impact on human health. *Journal of Environmental sciences* 2018; 67: 23-35.
- Kim K-H, Kabir E, Kabir S. A review on the human health impact of airborne particulate matter. *Environment international* 2015; 74: 136-143.
- Kim S-y, Kim C, Lee KJ, Chang SH, Elmasri H, Beeley PA. Development of an environmental radiation analysis research capability in the UAE. *Applied Radiation and Isotopes* 2013; 81: 190-195.
- Kirpichtchikova TA, Manceau A, Spadini L, Panfili F, Marcus MA, Jacquet T. Speciation and solubility of heavy metals in contaminated soil using X-ray microfluorescence, EXAFS spectroscopy, chemical extraction, and thermodynamic modeling. *Geochimica et Cosmochimica Acta* 2006; 70: 2163-2190.
- Kjeldsen P, Barlaz MA, Rooker AP, Baun A, Ledin A, Christensen TH. Present and long-term composition of MSW landfill leachate: a review. *Critical reviews in environmental science and technology* 2002; 32: 297-336.
- Kloog I, Ridgway B, Koutrakis P, Coull BA, Schwartz JD. Long-and short-term exposure to PM_{2.5} and mortality: using novel exposure models. *Epidemiology (Cambridge, Mass.)* 2013; 24: 555.
- Kolawole TO, Olatunji AS, Jimoh MT, Fajemila OT. Heavy metal contamination and ecological risk assessment in soils and sediments of an industrial area in Southwestern Nigeria. *Journal of Health and Pollution* 2018; 8: 180906.

- Kowalska JB, Mazurek R, Gąsiorek M, Zaleski T. Pollution indices as useful tools for the comprehensive evaluation of the degree of soil contamination—a review. *Environmental Geochemistry and Health* 2018; 40: 2395-2420.
- Krogmann U, Qu M. Landfill mining in the United States. *Proceedings Sardinia '97. Sixth International Landfill Symposium, Cagliari, 1997*, pp. 543–552.
- Król A, Mizerna K, Bożym M. An assessment of pH-dependent release and mobility of heavy metals from metallurgical slag. *Journal of hazardous materials* 2019: 121502.
- Krook J, Svensson N, Eklund M. Landfill mining: a critical review of two decades of research. *Waste Management* 2012; 32: 513-520.
- Krook J, Svensson N, Van Passel S, Van Acker K. What do recent assessments tell us about the potential and challenges of landfill mining? *Sustainable Resource Recovery and Zero Waste Approaches*. Elsevier, 2019, pp. 267-281.
- Kumar A, Patil RS, Dikshit AK, Islam S, Kumar R. Evaluation of control strategies for industrial air pollution sources using American Meteorological Society/Environmental Protection Agency Regulatory Model with simulated meteorology by Weather Research and Forecasting Model. *Journal of Cleaner Production* 2016; 116: 110-117.
- Kurian J, Esakku S, Palanivelu K, Selvam A. Studies on landfill mining at solid waste dumpsites in India. *Proceedings Sardinia. 3. Citeseer, 2003*, pp. 248-255.
- Kylefors K, Ecke H, Lagerkvist A. Accuracy of COD test for landfill leachates. *Water, Air, and Soil Pollution* 2003; 146: 153-169.
- Lal B, Tripathy SS. Prediction of dust concentration in open cast coal mine using artificial neural network. *Atmospheric Pollution Research* 2012; 3: 211-218.
- Laner D. *Understanding and evaluating long-term environmental risks from landfills: na*, 2011.

- Laner D, Cencic O, Svensson N, Krook J. Quantitative analysis of critical factors for the climate impact of landfill mining. *Environmental science & technology* 2016; 50: 6882-6891.
- Laner D, Crest M, Scharff H, Morris JW, Barlaz AM. A review of approaches for the long-term management of municipal solid waste landfills. *Waste management* 2012a; 32: 498-512.
- Laner D, Fellner J, Brunner PH. Site-specific criteria for the completion of landfill aftercare. *Waste Management & Research* 2012b; 30: 88-99.
- Lang J, Cheng S, Li J, Chen D, Zhou Y, Wei X, et al. A monitoring and modeling study to investigate regional transport and characteristics of PM_{2.5} pollution. *Aerosol and Air Quality Research* 2013; 13: 943-956.
- Lee A, Nikraz H, Hung Y. Characterization of acetogenic and methanogenic leachates generated from a sanitary landfill site. *Proceedings of the International Conference on Environmental Engineering and Technology*. World Academy of Science, Engineering and Technology, 2010, pp. 24-29.
- Lee H, Coulon F, Beriro D, Wagland S. Recovering metal (loids) and rare earth elements from closed landfill sites without excavation: Leachate recirculation opportunities and challenges. *Chemosphere* 2022a; 292: 133418.
- Lee H, Coulon F, Beriro D, Wagland S. Increasing recovery opportunities of metal (loid) s from municipal solid waste via landfill leachate recirculation. *Waste Management* 2023; 158: 116-124.
- Lee H, Coulon F, Wagland S. Influence of pH, depth and humic acid on metal and metalloids recovery from municipal solid waste landfills. *Science of The Total Environment* 2022b; 806: 150332.

- Leelőssy Á, Molnár F, Izsák F, Havasi Á, Lagzi I, Mészáros R. Dispersion modeling of air pollutants in the atmosphere: a review. *Open Geosciences* 2014; 6: 257-278.
- Legislation E. The Urban waste water treatment (England and Wales) regulations. <https://www.legislation.gov.uk/ukxi/1994/2841/schedule/3/paragraph/5/made?view=plain> (accessed 22 October 2020) 1994.
- Leroy C, Maro D, Hébert D, Solier L, Rozet M, Le Cavelier S, et al. A study of the atmospheric dispersion of a high release of krypton-85 above a complex coastal terrain, comparison with the predictions of Gaussian models (Briggs, Doury, ADMS4). *Journal of environmental radioactivity* 2010; 101: 937-944.
- Lesovik V, Zagorodnyuk L, Ryzhikh V, Lesovik R, Fediuk R, Vatin N, et al. Granular aggregates based on finely dispersed substandard raw materials. *Crystals* 2021; 11: 369.
- Lewinski N, Graczyk H, Riediker M. Human inhalation exposure to iron oxide particles. *BioNanoMaterials* 2013; 14: 5-23.
- Li G, Liang L, Yang J, Zeng L, Xie Z, Zhong Y, et al. Pulmonary hypofunction due to calcium carbonate nanomaterial exposure in occupational workers: a cross-sectional study. *Nanotoxicology* 2018; 12: 571-585.
- Li Z, Ma Z, van der Kuijp TJ, Yuan Z, Huang L. A review of soil heavy metal pollution from mines in China: pollution and health risk assessment. *Science of the Total Environment* 2014; 468: 843-853.
- Lilic N, Cvjetic A, Knezevic D, Milisavljevic V, Pantelic U. Dust and noise environmental impact assessment and control in Serbian mining practice. *Minerals* 2018; 8: 34.
- Lippmann M. Toxicological and epidemiological studies on effects of airborne fibers: coherence and public health implications. *Critical reviews in toxicology* 2014; 44: 643-695.

- Liu P, Wu Q, Hu W, Tian K, Huang B, Zhao Y. Effects of atmospheric deposition on heavy metals accumulation in agricultural soils: Evidence from field monitoring and Pb isotope analysis. *Environmental Pollution* 2023; 121740.
- LLC. Landfill reclamation demonstration project. Innovative Waste Consulting Services, Florida, 2009.
- López CG, Küppers B, Clausen A, Pretz T. Landfill mining: a case study regarding sampling, processing and characterization of excavated waste from an Austrian landfill. *Detritus* 2018; 2: 29-45.
- Lopez CG, Ni A, Parrodi JH, Küppers B, Raulf K, Pretz T. Characterization of landfill mining material after ballistic separation to evaluate material and energy recovery potential. *Detritus* 2019; 8: 5-23.
- Losacco C, Perillo A. Particulate matter air pollution and respiratory impact on humans and animals. *Environmental Science and Pollution Research* 2018; 25: 33901-33910.
- Lucas HI, García López C, Hernández Parrodi J, Vollprecht D, Raulf K, Pomberger R, et al. Quality assessment of nonferrous metals recovered by means of landfill mining: A case study in Belgium. *Detritus* 2019a; 8: 79-90.
- Lucas MSH, Li MSC, López MSCG, Hernández MSJC, Gürsel D, Pretz IT, et al. Primary evaluation of the use and refining of Al scrap recovered from a landfill in Belgium. EMC, Dusseldorf, Germany 2019b: 51-61.
- Luo H, Zhou W, Jiskani IM, Wang Z. Analyzing characteristics of particulate matter pollution in open-pit coal mines: Implications for Green Mining. *Energies* 2021; 14: 2680.
- Machiels L, Arnout L, Yan P, Jones PT, Blanpain B, Pontikes Y. Transforming enhanced landfill mining derived gasification/vitrification glass into low-carbon inorganic

- polymer binders and building products. *Journal of Sustainable Metallurgy* 2017; 3: 405-415.
- MacKinnon M. The measurement of the volatile organic fraction of the TOC in seawater. *Marine Chemistry* 1979; 8: 143-162.
- Macklin Y, Kibble A, Pollitt F. Impact on health from emissions from landfill sites: Advice from the health protection agency. Centre for radiation. Health Protection Agency UK, 2011.
- Maheshi D. Environmental and economic assessment of 'open waste dump' mining in Sri Lanka. *Resources, Conservation and Recycling* 2015; 102: 67-79.
- Manisalidis I, Stavropoulou E, Stavropoulos A, Bezirtzoglou E. Environmental and health impacts of air pollution: a review. *Frontiers in public health* 2020; 8: 14.
- Mariraj Mohan S. An overview of particulate dry deposition: measuring methods, deposition velocity and controlling factors. *International journal of environmental science and technology* 2016; 13: 387-402.
- Márquez AJC, Cassettari Filho PC, Rutkowski EW, de Lima Isaac R. Landfill mining as a strategic tool towards global sustainable development. *Journal of Cleaner Production* 2019; 226: 1102-1115.
- Masi S, Caniani D, Grieco E, Lioi D, Mancini I. Assessment of the possible reuse of MSW coming from landfill mining of old open dumpsites. *Waste Management* 2014; 34: 702-710.
- Mathew RA. Analysis of ground water quality over Chennai and consequent requirement of sanitary landfill. *International Journal of Earth And Atmospheric Science* 2017.
- Mathlener R, Heimovaara T, Oonk H, Luning L, van der Sloot H, van Zomeren A. Opening the black box: process based design criteria to eliminate aftercare of landfills, Dutch

sustainable landfill foundation, s'-Hertogenbosch, The Netherlands, ISBN-10: 90-73573-30-0, 2006.

- Meegoda JN, Li B, Patel K, Wang LB. A review of the processes, parameters, and optimization of anaerobic digestion. *International journal of environmental research and public health* 2018; 15: 2224.
- Mehta N, Cocerva T, Cipullo S, Padoan E, Dino GA, Ajmone-Marsan F, et al. Linking oral bioaccessibility and solid phase distribution of potentially toxic elements in extractive waste and soil from an abandoned mine site: case study in Campello Monti, NW Italy. *Science of the Total Environment* 2019; 651: 2799-2810.
- Mehta N, Dino GA, Passarella I, Ajmone-Marsan F, Rossetti P, De Luca DA. Assessment of the possible reuse of extractive waste coming from abandoned mine sites: case study in Gorno, Italy. *Sustainability* 2020; 12: 2471.
- Meng C, Cheng T, Gu X, Shi S, Wang W, Wu Y, et al. Contribution of meteorological factors to particulate pollution during winters in Beijing. *Science of The Total Environment* 2019a; 656: 977-985.
- Meng X, Wu Y, Pan Z, Wang H, Yin G, Zhao H. Seasonal characteristics and particle-size distributions of particulate air pollutants in Urumqi. *International journal of environmental research and public health* 2019b; 16: 396.
- Met-Office. UK actual and anomaly maps (Maps of climate variables for previous months, seasons and years). <https://www.metoffice.gov.uk/research/climate/maps-and-data/uk-actual-and-anomaly-maps> (accessed 22 July 2020). Met Office, 2020.
- Mishra SR, Pradhan RP, Prusty B, Sahu SK. Meteorology drives ambient air quality in a valley: a case of Sukinda chromite mine, one among the ten most polluted areas in the world. *Environmental Monitoring and Assessment* 2016; 188: 1-17.
- Mohajan H. Acid rain is a local environment pollution but global concern. 2018.

- Mönkäre TJ, Palmroth MR, Rintala JA. Characterization of fine fraction mined from two Finnish landfills. *Waste Management* 2016; 47: 34-39.
- Moreira D, Vilhena M, Tirabassi T, Buske D, Cotta R. Near-source atmospheric pollutant dispersion using the new GILTT method. *Atmospheric Environment* 2005; 39: 6289-6294.
- Morris JW, Barlaz MA. A performance-based system for the long-term management of municipal waste landfills. *Waste Management* 2011; 31: 649-662.
- Morris JW, Crest M, Barlaz MA, Spokas KA, Åkerman A, Yuan L. Improved methodology to assess modification and completion of landfill gas management in the aftercare period. *Waste management* 2012; 32: 2364-2373.
- Muller G. Index of geoaccumulation in sediments of the Rhine River. *Geojournal* 1969; 2: 108-118.
- Nathanail P, McCaffrey C, Gillett A, Ogden R, Nathanail J. *The LQM/CIEH S4ULs for human health risk assessment*: Land Quality Press, 2015.
- Neghab M, Abedini R, Soltanzadeh A, Kashkooli AI, Ghayoomi S. Respiratory disorders associated with heavy inhalation exposure to dolomite dust. *Iranian Red Crescent Medical Journal* 2012; 14: 549.
- Neshuku MN. Comparison of the performance of two atmospheric dispersion models (AERMOD and ADMS) for open pit mining sources of air pollution. University of Pretoria, 2012.
- Nguyen F, Ghose R, Isunza Manrique I, Robert T, Dumont G. Managing past landfills for future site development: a review of the contribution of geophysical methods. *Proceedings of the 4th International Symposium on Enhanced Landfill Mining*, 2018, pp. 27-36.

- Ni Z-z, Luo K, Zhang J-x, Feng R, Zheng H-x, Zhu H-r, et al. Assessment of winter air pollution episodes using long-range transport modeling in Hangzhou, China, during World Internet Conference, 2015. *Environmental pollution* 2018; 236: 550-561.
- Oben M, Boum AN, Besack F. Influence of the composition of the municipal solid waste (MSW) on the physicochemical parameters of leachate at the municipal solid waste landfill in Nkolfoulou–Yaounde. *Current Journal of Applied Science and Technology* 2019: 1-8.
- Oettle NK, Matasovic N, Kavazanjian E, Rad N, Conkle C. Characterization and placement of municipal solid waste as engineered fill. *Global Waste Management Symposium, San Antonio, Texas, 2010.*
- Ogundiran M, Osibanjo O. Mobility and speciation of heavy metals in soils impacted by hazardous waste. *Chemical Speciation & Bioavailability* 2009; 21: 59-69.
- Oguntoke O, Ojelede ME, Annegarn HJ. Frequency of mine dust episodes and the influence of meteorological parameters on the Witwatersrand area, South Africa. *International Journal of Atmospheric Sciences* 2013; 2013.
- Omar H, Rohani S. Treatment of landfill waste, leachate and landfill gas: a review. *Frontiers of Chemical Science and Engineering* 2015; 9: 15-32.
- Omrani M, Ruban V, Ruban G, Lamprea K. Assessment of atmospheric trace metal deposition in urban environments using direct and indirect measurement methodology and contributions from wet and dry depositions. *Atmospheric Environment* 2017; 168: 101-111.
- Onder M, Yigit E. Assessment of respirable dust exposures in an opencast coal mine. *Environmental monitoring and assessment* 2009; 152: 393-401.

- Ortner ME, Knapp J, Bockreis A. Landfill mining: objectives and assessment challenges. Proceedings of the Institution of Civil Engineers-Waste and Resource Management. 167. Thomas Telford Ltd, 2014, pp. 51-61.
- Osinubi O, Gochfeld M, Kipen HM. Health effects of asbestos and nonasbestos fibers. Environmental health perspectives 2000; 108: 665-674.
- Oury TD, Sporn TA, Roggli VL. Pathology of asbestos-associated diseases: Springer, 2014.
- Øygaard JK, Måge A, Gjengedal E. Estimation of the mass-balance of selected metals in four sanitary landfills in Western Norway, with emphasis on the heavy metal content of the deposited waste and the leachate. Water research 2004; 38: 2851-2858.
- Padoan E, Romè C, Mehta N, Dino G, De Luca D, Ajmone-Marsan F. Bioaccessibility of metals in soils surrounding two dismissed mining sites in Northern Italy. International Journal of Environmental Science and Technology 2020: 1-12.
- Pandey B, Agrawal M, Singh S. Assessment of air pollution around coal mining area: emphasizing on spatial distributions, seasonal variations and heavy metals, using cluster and principal component analysis. Atmospheric pollution research 2014; 5: 79-86.
- Pandey B, Agrawal M, Singh S. Ecological risk assessment of soil contamination by trace elements around coal mining area. Journal of Soils and Sediments 2016; 16: 159-168.
- Park S-H. Types and health hazards of fibrous materials used as asbestos substitutes. Safety and health at work 2018; 9: 360-364.
- Parker T, Dottridge J, Kelly S. Investigation of the composition and emissions of trace components in landfill gas. Environment Agency, R&D Technical Report P1-438/TR, Bristol 2002.

- Parodi A, Feuillade-Cathalifaud G, Pallier V, Mansour A. Optimization of municipal solid waste leaching test procedure: assessment of the part of hydrosoluble organic compounds. *Journal of hazardous materials* 2011; 186: 991-998.
- Parrodi JC, Lucas H, Gigantino M, Sauve G, Esguerra JL, Einhäupl P, et al. Integration of resource recovery into current waste management through (enhanced) landfill mining. *Detritus* 2019a; 8: 141-156.
- Parrodi JCH, Höllen D, Pomberger R. Characterization of fine fractions from landfill mining: a review of previous investigations. *Composites* 2018a; 6: 4.0.
- Parrodi JCH, Höllen D, Pomberger R. Potential and main technological challenges for material and energy recovery from fine fractions of landfill mining: a critical review. *Detritus* 2018b; 3: 19-29.
- Parrodi JCH, López CG, Küppers B, Raulf K, Vollprecht D, Pretz T, et al. Case study on enhanced landfill mining at Mont-Saint-Guibert landfill in Belgium: Characterization and potential of fine fractions. *Detritus* 2019b; 8: 47-61.
- Parrodi JCH, Raulf K, Vollprecht D, Pretz T, Pomberger R. Case study on enhanced landfill mining at Mont-Saint-Guibert landfill in Belgium: Mechanical processing of fine fractions for material and energy recovery. *Detritus* 2019c; 8: 62-78.
- Parrodi JCH, Vollprecht D, Pomberger R. Case study on enhanced landfill mining at Mont-Saint-Guibert landfill in Belgium: physico-chemical characterization and valorization potential of combustibles and inert fractions recovered from fine fractions. *Detritus* 2020; 10: 44-61.
- Parsa VA, Salehi E, Yavari AR, van Bodegom PM. Analyzing temporal changes in urban forest structure and the effect on air quality improvement. *Sustainable Cities and Society* 2019; 48: 101548.

- Pastre G, Griffiths Z, Val J, Tasiu AM, Camacho-Dominguez EV, Wagland S, et al. A decision support tool for enhanced landfill mining. *Detritus* 2018; 1: 91-101.
- Patra AK, Gautam S, Kumar P. Emissions and human health impact of particulate matter from surface mining operation—a review. *Environmental Technology & Innovation* 2016; 5: 233-249.
- Pecorini I, Iannelli R. Characterization of excavated waste of different ages in view of multiple resource recovery in landfill mining. *Sustainability* 2020; 12: 1780.
- Pelletier J. Sensitivity of playa windblown-dust emissions to climatic and anthropogenic change. *Journal of Arid Environments* 2006; 66: 62-75.
- Peña-Castro M, Montero-Acosta M, Saba M. A critical review of asbestos concentrations in water and air, according to exposure sources. *Heliyon* 2023.
- Pérez IA, García M, Sánchez M, Pardo N, Fernández-Duque B. Key points in air pollution meteorology. *International Journal of Environmental Research and Public Health* 2020; 17: 8349.
- Pimolthai P, Wagner J-F. Soil mechanical properties of MBT waste from Luxembourg, Germany and Thailand. *Songklanakarin J Sci Technol* 2014; 36: 701-709.
- Piras L, Dentoni V, Massacci G, Lowndes IS. Dust dispersion from haul roads in complex terrain: the case of a mineral reclamation site located in Sardinia (Italy). *International Journal of Mining, Reclamation and Environment* 2014; 28: 323-341.
- Prechthai T, Padmasri M, Visvanathan C. Quality assessment of mined MSW from an open dumpsite for recycling potential. *Resources, Conservation and Recycling* 2008; 53: 70-78.
- Qi G, Yue D, Liu J, Li R, Shi X, He L, et al. Impact assessment of intermediate soil cover on landfill stabilization by characterizing landfilled municipal solid waste. *Journal of environmental management* 2013; 128: 259-265.

- Quaghebeur M, Laenen B, Geysen D, Nielsen P, Pontikes Y, Van Gerven T, et al. Characterization of landfilled materials: screening of the enhanced landfill mining potential. *Journal of Cleaner Production* 2013; 55: 72-83.
- Raga R, Cossu R. Landfill in-situ aeration process and technology. *Linnaeus Eco-Tech* 2010: 43-50.
- Rahman SH, Khanam D, Adyel TM, Islam MS, Ahsan MA, Akbor MA. Assessment of heavy metal contamination of agricultural soil around Dhaka Export Processing Zone (DEPZ), Bangladesh: implication of seasonal variation and indices. *Applied Sciences* 2012; 2: 584-601.
- Reed W, Control CfD. Significant dust dispersion models for mining operations. Vol 9478: Createspace Independent Pub, 2005.
- Reed W, Westman E, Haycocks C. The introduction of a dynamic component to the ISC 3 model in predicting dust emissions from surface mining operations. *APCOM 2002: 30th International Symposium on the Application of Computers and Operations Research in the Mineral Industry*, 2002, pp. 659-667.
- Reinhart DR, McCreanor PT, Townsend T. The bioreactor landfill: its status and future. *Waste Management & Research* 2002; 20: 172-186.
- Reyes A, Cuevas J, Fuentes B, Fernández E, Arce W, Guerrero M, et al. Distribution of potentially toxic elements in soils surrounding abandoned mining waste located in Taltal, Northern Chile. *Journal of Geochemical Exploration* 2021; 220: 106653.
- Riber C, Fredriksen GS, Christensen TH. Heavy metal content of combustible municipal solid waste in Denmark. *Waste management & research* 2005; 23: 126-132.
- Richardson C, Rutherford S, Agranovski I. Particulate emission rates for open surfaces in Australian open cut black coal mines. *Journal of environmental management* 2019; 232: 537-544.

- Riddle A, Carruthers D, Sharpe A, McHugh C, Stocker J. Comparisons between FLUENT and ADMS for atmospheric dispersion modelling. *Atmospheric environment* 2004; 38: 1029-1038.
- Roberts N. Should the UK start digging up its landfill sites? *Materials Recycling World.*, UK, 2013.
- Rodríguez J, Castrillon L, Maranon E, Sastre H, Fernandez E. Removal of non-biodegradable organic matter from landfill leachates by adsorption. *Water Research* 2004; 38: 3297-3303.
- Rodríguez MG, Rivera BH, Heredia MR, Heredia BR, Segovia RG. A study of dust airborne particles collected by vehicular traffic from the atmosphere of southern megalopolis Mexico City. *Environmental Systems Research* 2019; 8: 1-17.
- Rodríguez N, Machiels L, Jones PT, Binnemans K. Towards near-zero-waste recycling of mine tailings and metallurgical process residues through a novel solvometallurgical process based on deep eutectic solvents. *Proceedings of the 4th International Symposium on Enhanced Landfill Mining (ELFM IV)*, Mechelen (Belgium), 5-6 February 2018. Eds PT Jones and L. Machiels, 2018, pp. 95-100.
- Rong L, Zhang C, Jin D, Dai Z. Assessment of the potential utilization of municipal solid waste from a closed irregular landfill. *Journal of Cleaner Production* 2017; 142: 413-419.
- Ronowijoyo TA, Budiharjo MA, Sumiyati S. Analysis of ambient air quality conditions of tsp parameters and its source in Temon district. *E3S Web of Conferences*. 202. EDP Sciences, 2020, pp. 02009.
- Sahu SP, Patra AK, Kolluru SSR. Spatial and temporal variation of respirable particles around a surface coal mine in India. *Atmospheric Pollution Research* 2018; 9: 662-679.

- Sairanen M, Pursio S. Near field modelling of dust emissions caused by drilling and crushing. *SN Applied Sciences* 2020; 2: 1-15.
- Sánchez-Ccoyllo O, de Fatima Andrade M. The influence of meteorological conditions on the behavior of pollutants concentrations in São Paulo, Brazil. *Environmental Pollution* 2002; 116: 257-263.
- Sauve G, Van Acker K. To mine or not to mine: a review of the effects of waste composition, time and long-term impacts of landfills in the decision making for ELM. *Proceedings of the 4th International Symposium on Enhanced Landfill Mining*, 2018, pp. 379-388.
- Savage GM, Golueke CG, von Stein E, L. "Landfill mining: past and present". *Biocycle* 1993; 34: 58.
- Schirmer W, Jucá J, Schuler A, Holanda S, Jesus L. Methane production in anaerobic digestion of organic waste from Recife (Brazil) landfill: evaluation in refuse of different ages. *Brazilian Journal of Chemical Engineering* 2014; 31: 373-384.
- Scott DI, Longman M, Wilson S. Reclaiming historic landfill sites for residential development: a UK case study. *Journal of Environmental Engineering and Science* 2019; 15: 71-79.
- Seaman NL. Meteorological modeling for air-quality assessments. *Atmospheric environment* 2000; 34: 2231-2259.
- Sharifi Z, Hossaini SM, Renella G. Risk assessment for sediment and stream water polluted by heavy metals released by a municipal solid waste composting plant. *Journal of Geochemical Exploration* 2016; 169: 202-210.
- Singh A, Chandel MK. Effect of ageing on waste characteristics excavated from an Indian dumpsite and its potential valorisation. *Process Safety and Environmental Protection* 2020; 134: 24-35.

Singh A, Chandel MK. Mobility and environmental fate of heavy metals in fine fraction of dumped legacy waste: Implications on reclamation and ecological risk. *Journal of Environmental Management* 2022; 304: 114206.

Smart-Ground. Report on the environmental issues, 2017.

Smart-Ground. Enhanced landfill mining toolkit for municipal solid waste streams, Europ, 2018.

Somani M, Datta M, Ramana G, Sreekrishnan T. Investigations on fine fraction of aged municipal solid waste recovered through landfill mining: case study of three dumpsites from India. *Waste Management & Research* 2018; 36: 744-755.

Somani M, Datta M, Ramana G, Sreekrishnan T. Leachate characteristics of aged soil-like material from MSW dumps: sustainability of landfill mining. *Journal of Hazardous, Toxic, and Radioactive Waste* 2019; 23: 04019014.

Somani M, Datta M, Ramana G, Sreekrishnan TR. Contaminants in soil-like material recovered by landfill mining from five old dumps in India. *Process Safety and Environmental Protection* 2020; 137: 82-92.

Song Y-S, Yun J-M, Hong W-P, Kim T-H. Investigation of solid waste soil as road construction material. *Environmental Geology* 2003; 44: 203-209.

Sormunen K, Ettala M, Rintala J. Detailed internal characterisation of two Finnish landfills by waste sampling. *Waste Management* 2008; 28: 151-163.

Sripaiboonkij P, Sripaiboonkij N, Phanprasit W, Jaakkola MS. Respiratory and skin health among glass microfiber production workers: a cross-sectional study. *Environmental health* 2009; 8: 1-10.

Srivastava A, Kumar A, Elumalai SP. Evaluating dispersion modeling of inhalable particulates (pm 10) emissions in complex terrain of coal mines. *Environmental Modeling & Assessment* 2021; 26: 385-403.

- Staley BF, Francis L, Barlaz MA. Effect of spatial differences in microbial activity, pH, and substrate levels on methanogenesis initiation in refuse. *Appl. Environ. Microbiol.* 2011; 77: 2381-2391.
- Standard D. Water analysis: guidelines for the determination of total organic carbon (TOC) and dissolved organic carbon (DOC). DS/EN 1997; 1484: 1997.
- Stegmann R, Heyer K, Hupe K, Ritzkowski M. Discussion of criteria for the completion of landfill aftercare. *Proceedings Sardinia*. 3, 2003, pp. 6-10.
- Stewart AG. Mining is bad for health: a voyage of discovery. *Environmental Geochemistry and Health* 2019: 1-13.
- Sun Y, Wang J, Guo G, Li H, Jones K. A comprehensive comparison and analysis of soil screening values derived and used in China and the UK. *Environmental Pollution* 2020; 256: 113404.
- Tang W-W, Zeng G-M, Gong J-L, Liang J, Xu P, Zhang C, et al. Impact of humic/fulvic acid on the removal of heavy metals from aqueous solutions using nanomaterials: a review. *Science of the Total Environment* 2014; 468: 1014-1027.
- Tang Z, Zhang L, Huang Q, Yang Y, Nie Z, Cheng J, et al. Contamination and risk of heavy metals in soils and sediments from a typical plastic waste recycling area in North China. *Ecotoxicology and Environmental Safety* 2015; 122: 343-351.
- Tartakovsky D, Broday DM, Stern E. Evaluation of AERMOD and CALPUFF for predicting ambient concentrations of total suspended particulate matter (TSP) emissions from a quarry in complex terrain. *Environmental Pollution* 2013; 179: 138-145.
- Tartakovsky D, Stern E, Broday DM. Dispersion of TSP and PM₁₀ emissions from quarries in complex terrain. *Science of the Total Environment* 2016; 542: 946-954.

- Tenebe IT, Emenike CP, Chukwuka CD. Prevalence of heavy metals and computation of its associated risk in surface water consumed in Ado-Odo Ota, South-West Nigeria. *Human and Ecological Risk Assessment: An International Journal* 2018.
- Thermo Fisher Scientific. Comparison of ICP-OES and ICP-MS for trace element analysis. <https://www.thermofisher.com/sa/en/home/industrial/environmental/environmental-learning-center/contaminant-analysis-information/metal-analysis/comparison-icp-oes-icp-ms-trace-element-analysis.html> (accessed 2 February 2021), 2015.
- Thomas RG. An air quality baseline assessment for the Vaal airshed in South Africa. University of Pretoria, 2009.
- Tian G, Qiao Z, Xu X. Characteristics of particulate matter (PM₁₀) and its relationship with meteorological factors during 2001–2012 in Beijing. *Environmental pollution* 2014; 192: 266-274.
- Timur H, Öztürk I. Anaerobic sequencing batch reactor treatment of landfill leachate. *Water Research* 1999; 33: 3225-3230.
- Tomlinson D, Wilson J, Harris C, Jeffrey D. Problems in the assessment of heavy-metal levels in estuaries and the formation of a pollution index. *Helgoländer Meeresuntersuchungen* 1980; 33: 566-575.
- Toyokuni S. Mechanisms of asbestos-induced carcinogenesis. *Nagoya J Med Sci* 2009; 71: 1-10.
- Triantafyllou A. PM₁₀ pollution episodes as a function of synoptic climatology in a mountainous industrial area. *Environmental Pollution* 2001; 112: 491-500.
- Triantafyllou A, Kapageridis I, Gkaras S, Pavloudakis F. Development of emission factor equations for surface mining activities: the case of the stacker. *Materials Proceedings* 2021; 5: 15.

- Triantafyllou A, Kassomenos P. Aspects of atmospheric flow and dispersion of air pollutants in a mountainous basin. *Science of the total environment* 2002; 297: 85-103.
- Trinh TT, Trinh TT, Le TT, Tu BM. Temperature inversion and air pollution relationship, and its effects on human health in Hanoi City, Vietnam. *Environmental geochemistry and health* 2019; 41: 929-937.
- Tsiouri V, Kakosimos KE, Kumar P. Concentrations, sources and exposure risks associated with particulate matter in the Middle East Area—a review. *Air Quality, Atmosphere & Health* 2015; 8: 67-80.
- Turner DB. *Workbook of atmospheric dispersion estimates: an introduction to dispersion modeling*: CRC press, 2020.
- USEPA. *Compilation of air pollutant emission factors, AP-42*. Office Of Air Quality Standards, Emission Inventory Branch, US Environmental ..., 1995.
- USEPA. *Supplemental guidance for developing soil screening levels for superfund sites, peer review draft*. Washington, DC: US Environmental Protection Agency Office of Solid Waste and Emergency Response, OSWER 9355 9355, 2002, pp. 4-24.
- Utell MJ, Maxim LD. Refractory ceramic fibers: fiber characteristics, potential health effects and clinical observations. *Toxicology and applied pharmacology* 2018; 361: 113-117.
- van der Sloot HA, van Zomeren A. Characterisation leaching tests and associated geochemical speciation modelling to assess long term release behaviour from extractive wastes. *Mine Water and the Environment* 2012; 31: 92-103.
- Van der Zee D, Achterkamp M, De Visser B. Assessing the market opportunities of landfill mining. *Waste management* 2004; 24: 795-804.
- Van Passel S, Dubois M, Eyckmans J, De Gheldere S, Ang F, Jones PT, et al. The economics of enhanced landfill mining: private and societal performance drivers. *Journal of cleaner production* 2013; 55: 92-102.

- Vardoulakis S, Valiantis M, Milner J, ApSimon H. Operational air pollution modelling in the UK—Street canyon applications and challenges. *Atmospheric Environment* 2007; 41: 4622-4637.
- Vergara SE, Tchobanoglous G. Municipal solid waste and the environment: a global perspective. *Annual Review of Environment and Resources* 2012; 37: 277-309.
- Vollprecht D, Parrodi JCH, Lucas HI, Pomberger R. Case study on enhanced landfill mining at Mont-Saint-Guibert landfill in Belgium: Mechanical processing, physico-chemical and mineralogical characterization of fine fractions < 4.5 mm. *Detritus* 2020; 10: 26-43.
- Wagland ST, Coulon F, Canopoli L. Developing the case for enhanced landfill mining in the UK. 2019.
- Wagner TP, Raymond T. Landfill mining: case study of a successful metals recovery project. *Waste Management* 2015; 45: 448-457.
- Wang L, Liang T, Zhang Q, Li K. Rare earth element components in atmospheric particulates in the Bayan Obo mine region. *Environmental Research* 2014; 131: 64-70.
- Wang X, Dan Z, Cui X, Zhang R, Zhou S, Wenga T, et al. Contamination, ecological and health risks of trace elements in soil of landfill and geothermal sites in Tibet. *Science of the Total Environment* 2020; 715: 136639.
- Wang X, Wang K, Su L. Contribution of atmospheric diffusion conditions to the recent improvement in air quality in China. *Scientific reports* 2016; 6: 1-11.
- Wang Y-n, Xu R, Kai Y, Wang H, Sun Y, Zhan M, et al. Evaluating the physicochemical properties of refuse with a short-term landfill age and odorous pollutants emission during landfill mining: a case study. *Waste Management* 2021a; 121: 77-86.
- Wang Z-M, Zhou W, Jiskani IM, Ding X-H, Liu Z-C, Qiao Y-Z, et al. Dust reduction method based on water infusion blasting in open-pit mines: a step toward green mining.

- Energy Sources, Part A: Recovery, Utilization, and Environmental Effects 2021b: 1-15.
- Wang Z, Zhou W, Jiskani IM, Ding X, Luo H. Dust pollution in cold region Surface Mines and its prevention and control. *Environmental Pollution* 2022a; 292: 118293.
- Wang Z, Zhou W, Jiskani IM, Luo H, Ao Z, Mvula EM. Annual dust pollution characteristics and its prevention and control for environmental protection in surface mines. *Science of The Total Environment* 2022b; 825: 153949.
- Warren K, Read A. Landfill mining: goldmine or minefield.
http://www.ismenvis.nic.in/Database/Landfill_Mining-Goldmine_or_Minefield_5478.aspx (accessed 11 October 2018), 2014.
- Wei M, Chen J, Sun Z, Lv C, Cai W. Distribution of heavy metals in different size fractions of agricultural soils closer to mining area and its relationship to TOC and Eh. *Proceedings of the World Congress on New Technologies, Barcelona, Spain, 2015*, pp. 200-206.
- Weiner ER. *Applications of environmental aquatic chemistry: a practical guide*: CRC press, 2012.
- Weng Y-C, Fujiwara T, Houg HJ, Sun C-H, Li W-Y, Kuo Y-W. Management of landfill reclamation with regard to biodiversity preservation, global warming mitigation and landfill mining: Experiences from the Asia–Pacific region. *Journal of Cleaner Production* 2015; 104: 364-373.
- Weng Y-C, Furuichi T, Ishii K. Proposal of an integrated evaluation approach on final disposal sites with regard to future reclamation—a case study of Moereruma Park, Sapporo city. *J Jpn Soc Civ Eng Ser G* 2013; 69: 313-320.
- Westwood D. *The determination of chemical oxygen demand in waters and effluents*. Environment Agency, National Laboratory Service, UK 2007.

- Wijaya I, Soedjono E. Physicochemical characteristic of municipal wastewater in tropical area: case study of Surabaya City, Indonesia. IOP Conference Series: Earth and Environmental Science. 135. IOP Publishing, 2018, pp. 012018.
- Wolfsberger T, Aldrian A, Sarc R, Hermann R, Höllen D, Budischowsky A, et al. Landfill mining: resource potential of Austrian landfills—evaluation and quality assessment of recovered municipal solid waste by chemical analyses. Waste Management & Research 2015; 33: 962-974.
- Wreford K, Atwater J, Lavkulich L. The effects of moisture inputs on landfill gas production and composition and leachate characteristics at the Vancouver Landfill Site at Burns Bog. Waste management & research 2000; 18: 386-392.
- WSDH. Fiberglass.
<https://www.doh.wa.gov/communityandenvironment/airquality/indoorair/fiberglass>
(accessed 8 November 2021). Washington State Department of Health.
- Wu Y, Liu J, Zhai J, Cong L, Wang Y, Ma W, et al. Comparison of dry and wet deposition of particulate matter in near-surface waters during summer. PloS one 2018; 13: e0199241.
- Wuana RA, Okieimen FE. Heavy metals in contaminated soils: a review of sources, chemistry, risks and best available strategies for remediation. International Scholarly Research Notices 2011; 2011.
- Xiaoli C, Shimaoka T, Xianyan C, Qiang G, Youcai Z. Characteristics and mobility of heavy metals in an MSW landfill: Implications in risk assessment and reclamation. Journal of hazardous materials 2007; 144: 485-491.
- Xu A, Chang H, Zhao Y, Tan H, Wang Y, Zhang Y, et al. Dispersion simulation of odorous compounds from waste collection vehicles: Mobile point source simulation with ModOdor. Science of the Total Environment 2020; 711: 135109.

- Yang K, Yoo K-C, Jung J. Quantitative analysis of asbestos-containing materials using various test methods. *Minerals* 2020; 10: 568.
- Yao Q, Wang X, Jian H, Chen H, Yu Z. Characterization of the particle size fraction associated with heavy metals in suspended sediments of the Yellow River. *International Journal of Environmental Research and Public Health* 2015; 12: 6725-6744.
- Yilmaz T, Aygün A, Berktaş A, Nas B. Removal of COD and colour from young municipal landfill leachate by Fenton process. *Environmental technology* 2010; 31: 1635-1640.
- Zhang X-l, Kou J, Sun C-b, Zhang R-y, Su M, Li S-f. Mineralogical characterization of copper sulfide tailings using automated mineral liberation analysis: a case study of the Chambishi Copper Mine tailings. *International Journal of Minerals, Metallurgy and Materials* 2021; 28: 944-955.
- Zhang X, Chen W, Ma C, Zhan S. Modeling particulate matter emissions during mineral loading process under weak wind simulation. *Science of the total environment* 2013; 449: 168-173.
- Zhao B, Sha H, Li J, Cao S, Wang G, Yang Y. Static magnetic field enhanced methane production via stimulating the growth and composition of microbial community. *Journal of Cleaner Production* 2020; 271: 122664.
- Zhao S, Yu Y, Yin D, Qin D, He J, Dong L. Spatial patterns and temporal variations of six criteria air pollutants during 2015 to 2017 in the city clusters of Sichuan Basin, China. *Science of the total environment* 2018; 624: 540-557.
- Zhao Y, Song L, Huang R, Song L, Li X. Recycling of aged refuse from a closed landfill. *Waste Management & Research* 2007; 25: 130-138.
- Zhou C, Gong Z, Hu J, Cao A, Liang H. A cost-benefit analysis of landfill mining and material recycling in China. *Waste Management* 2015; 35: 191-198.

- Zilenina V, Ulanova O, Begunova L. Problem of landfilling environments pollution by heavy metals. IOP Conference Series: Earth and Environmental Science. 87. IOP Publishing, 2017, pp. 042028.
- Ziyang L, Bin D, Xiaoli C, Yu S, Youcai Z, Nanwen Z. Characterization of refuse landfill leachates of three different stages in landfill stabilization process. Journal of Environmental Sciences 2009; 21: 1309-1314.
- Ziyang L, Luochun W, Nanwen Z, Youcai Z. Martial recycling from renewable landfill and associated risks: a review. Chemosphere 2015; 131: 91-103.
- Zomeren Av, Hjelmar O, van der Sloot H, Hyks J, Saveyn H, Eder P, et al. Study on methodological aspects regarding limit values for pollutants in aggregates in the context of the possible development of end-of-waste criteria under the EU Waste Framework Directive. ECN, 2014.
- Zornberg JG, Jernigan BL, Sanglerat TR, Cooley BH. Retention of free liquids in landfills undergoing vertical expansion. Journal of Geotechnical and Geoenvironmental Engineering 1999; 125: 583-594.
- Zou B, Zhan FB, Wilson JG, Zeng Y. Performance of AERMOD at different time scales. Simulation Modelling Practice and Theory 2010; 18: 612-623.

Appendices

Appendix 1. Mean values of (COD, pH, and MC) in different wells

		Descriptives							
		N	Mean	Std. Deviation	Std. Error	95% Confidence Interval for Mean		Minimum	Maximum
						Lower Bound	Upper Bound		
COD mg/L	1901.00	15	141.4000	10.97920	2.83482	135.3199	147.4801	119.00	150.00
	1904.00	15	84.2467	15.28009	3.94530	75.7848	92.7085	60.40	116.00
	1906.00	15	94.6467	21.31612	5.50380	82.8422	106.4511	62.00	134.00
	1907.00	15	118.2800	22.30600	5.75938	105.9274	130.6326	89.90	150.00
	Total	60	109.6433	28.39729	3.66607	102.3075	116.9791	60.40	150.00
pH	1901.00	15	7.3220	.07655	.01977	7.2796	7.3644	7.20	7.45
	1904.00	15	7.6113	.17780	.04591	7.5129	7.7098	7.22	7.85
	1906.00	15	7.4553	.09884	.02552	7.4006	7.5101	7.33	7.66
	1907.00	15	7.5267	.14936	.03857	7.4440	7.6094	7.23	7.80
	Total	60	7.4788	.16716	.02158	7.4357	7.5220	7.20	7.85
MC %	1901.00	15	25.8689	2.87314	.74184	24.2779	27.4600	21.46	32.20
	1904.00	15	22.9941	3.08734	.79715	21.2844	24.7038	17.45	28.28
	1906.00	15	23.0597	2.97328	.76770	21.4131	24.7062	19.26	31.72
	1907.00	15	22.8037	1.54257	.39829	21.9494	23.6579	20.33	26.14
	Total	60	23.6816	2.91783	.37669	22.9278	24.4354	17.45	32.20

Appendix 2. One-Way ANOVA test of (COD, pH, and MC) for all wells

		ANOVA				
		Sum of Squares	df	Mean Square	F	Sig.
COD mg/L	Between Groups	29294.529	3	9764.843	29.909	.000
	Within Groups	18283.419	56	326.490		
	Total	47577.947	59			
pH	Between Groups	.675	3	.225	12.938	.000
	Within Groups	.974	56	.017		
	Total	1.649	59			
MC %	Between Groups	96.221	3	32.074	4.423	.007
	Within Groups	406.091	56	7.252		
	Total	502.311	59			

Appendix 3. Multiple comparisons analysis between (COD, pH, and MC) of the four wells

Multiple Comparisons							
LSD							
Dependent Variable	(I) Well no.	(J) Well no.	Mean Difference (I-J)	Std. Error	Sig.	95% Confidence Interval	
						Lower Bound	Upper Bound
COD mg/L	1901.00	1904.00	57.15333*	6.59787	.000	43.9362	70.3705
		1906.00	46.75333*	6.59787	.000	33.5362	59.9705
		1907.00	23.12000*	6.59787	.001	9.9029	36.3371
	1904.00	1901.00	-57.15333*	6.59787	.000	-70.3705	-43.9362
		1906.00	-10.40000	6.59787	.121	-23.6171	2.8171
		1907.00	-34.03333*	6.59787	.000	-47.2505	-20.8162
	1906.00	1901.00	-46.75333*	6.59787	.000	-59.9705	-33.5362
		1904.00	10.40000	6.59787	.121	-2.8171	23.6171
		1907.00	-23.63333*	6.59787	.001	-36.8505	-10.4162
	1907.00	1901.00	-23.12000*	6.59787	.001	-36.3371	-9.9029
		1904.00	34.03333*	6.59787	.000	20.8162	47.2505
		1906.00	23.63333*	6.59787	.001	10.4162	36.8505
pH	1901.00	1904.00	-.28933*	.04815	.000	-.3858	-.1929
		1906.00	-.13333*	.04815	.008	-.2298	-.0369
		1907.00	-.20467*	.04815	.000	-.3011	-.1082
	1904.00	1901.00	.28933*	.04815	.000	.1929	.3858
		1906.00	.15600*	.04815	.002	.0595	.2525
		1907.00	.08467	.04815	.084	-.0118	.1811
	1906.00	1901.00	.13333*	.04815	.008	.0369	.2298
		1904.00	-.15600*	.04815	.002	-.2525	-.0595
		1907.00	-.07133	.04815	.144	-.1678	.0251
	1907.00	1901.00	.20467*	.04815	.000	.1082	.3011
		1904.00	-.08467	.04815	.084	-.1811	.0118
		1906.00	.07133	.04815	.144	-.0251	.1678
MC %	1901.00	1904.00	2.87487*	.98330	.005	.9051	4.8447
		1906.00	2.80928*	.98330	.006	.8395	4.7791
		1907.00	3.06527*	.98330	.003	1.0955	5.0351
	1904.00	1901.00	-2.87487*	.98330	.005	-4.8447	-.9051
		1906.00	-.06559	.98330	.947	-2.0354	1.9042
		1907.00	.19040	.98330	.847	-1.7794	2.1602
	1906.00	1901.00	-2.80928*	.98330	.006	-4.7791	-.8395
		1904.00	.06559	.98330	.947	-1.9042	2.0354
		1907.00	.25599	.98330	.796	-1.7138	2.2258
	1907.00	1901.00	-3.06527*	.98330	.003	-5.0351	-1.0955
		1904.00	-.19040	.98330	.847	-2.1602	1.7794
		1906.00	-.25599	.98330	.796	-2.2258	1.7138

*. The mean difference is significant at the 0.05 level.

Appendix 4. Correlation analysis between variables of (COD, pH, and MC) for all wells using Pearson's correlation (2-tailed) analysis

		Correlations		
		COD mg/L	pH	MC %
COD mg/L	Pearson Correlation	1	-.513**	.263*
	Sig. (2-tailed)		.000	.042
	N	60	60	60
pH	Pearson Correlation	-.513**	1	-.114
	Sig. (2-tailed)	.000		.386
	N	60	60	60
MC %	Pearson Correlation	.263*	-.114	1
	Sig. (2-tailed)	.042	.386	
	N	60	60	60

** . Correlation is significant at the 0.01 level (2-tailed).
 * . Correlation is significant at the 0.05 level (2-tailed).

Appendix 5. Multiple linear regression analysis between COD and (MC and pH) for all wells

Model	Variables Entered	Variables Removed	Method
1	MC % , pH ^b	.	Enter

a. Dependent Variable: COD mg/L
 b. All requested variables entered.

Model	R	R Square	Adjusted R Square	Std. Error of the Estimate
1	.553 ^a	.306	.281	24.07466

a. Predictors: (Constant), MC % , pH

Model		Sum of Squares	df	Mean Square	F	Sig.
1	Regression	14541.354	2	7270.677	12.545	.000 ^b
	Residual	33036.594	57	579.589		
	Total	47577.947	59			

a. Dependent Variable: COD mg/L
 b. Predictors: (Constant), MC % , pH

Appendix 6. Correlation analysis between variables of the studied site (COD, MC, and pH) and the 7 previous landfill sites in the UK using Pearson's correlation (2-tailed) analysis

		Correlations			
		COD mg/L	pH	MC %	Landfill age
COD mg/L	Pearson Correlation	1	-.478	.170	-.738 [*]
	Sig. (2-tailed)		.231	.687	.037
	N	8	8	8	8
pH	Pearson Correlation	-.478	1	-.470	.310
	Sig. (2-tailed)	.231		.240	.454
	N	8	8	8	8
MC %	Pearson Correlation	.170	-.470	1	-.054
	Sig. (2-tailed)	.687	.240		.899
	N	8	8	8	8
Landfill age	Pearson Correlation	-.738 [*]	.310	-.054	1
	Sig. (2-tailed)	.037	.454	.899	
	N	8	8	8	8

*. Correlation is significant at the 0.05 level (2-tailed).

Appendix 7. Descriptive statistics of heavy metals within the different wells

		Descriptives							
		N	Mean	Std. Deviation	Std. Error	95% Confidence Interval for Mean		Minimum	Maximum
						Lower Bound	Upper Bound		
As	1901.00	5	24.4839	8.15977	3.64916	14.3522	34.6156	17.49	37.08
	1904.00	5	27.7156	9.76064	4.36509	15.5961	39.8350	16.57	42.70
	1906.00	5	36.3447	15.37871	6.87757	17.2495	55.4399	21.82	60.39
	1907.00	5	40.2800	14.55131	6.50754	22.2122	58.3478	25.91	62.58
	Total	20	32.2060	13.08064	2.92492	26.0841	38.3280	16.57	62.58
Pb	1901.00	5	187.6486	57.47944	25.70559	116.2784	259.0187	146.40	285.12
	1904.00	5	985.7612	284.85630	127.39161	632.0654	1339.4570	623.29	1356.16
	1906.00	5	195.5766	67.12045	30.01718	112.2355	278.9176	140.27	304.21
	1907.00	5	204.1422	69.78803	31.21015	117.4889	290.7955	129.19	311.79
	Total	20	393.2822	378.09635	84.54491	216.3276	570.2367	129.19	1356.16
Zn	1901.00	5	1814.1432	356.98772	159.64976	1370.8844	2257.4020	1298.07	2205.56
	1904.00	5	505.3972	163.90183	73.29913	301.8862	708.9082	315.57	746.75
	1906.00	5	443.7638	189.64639	84.81245	208.2868	679.2409	231.94	688.95
	1907.00	5	560.0290	191.02725	85.42998	322.8373	797.2206	357.95	850.35
	Total	20	830.8333	623.52432	139.42428	539.0150	1122.6517	231.94	2205.56
Mn	1901.00	5	1621.5210	334.17913	149.44945	1206.5828	2036.4592	1162.10	2039.16
	1904.00	5	499.7738	173.41252	77.55243	284.4538	715.0939	318.31	766.20
	1906.00	5	619.3617	247.08391	110.49928	312.5665	926.1569	339.00	930.83
	1907.00	5	547.9399	147.13545	65.80097	365.2472	730.6327	388.67	755.29
	Total	20	822.1491	522.84448	116.91158	577.4504	1066.8479	318.31	2039.16
Cd	1901.00	5	1.3498	.41859	.18720	.8300	1.8695	1.02	2.05
	1904.00	5	1.2189	.80535	.36017	.2189	2.2189	.59	2.55
	1906.00	5	1.7168	.61574	.27537	.9522	2.4813	.94	2.64
	1907.00	5	.3721	.48163	.21539	-.2260	.9701	.09	1.23
	Total	20	1.1644	.74660	.16695	.8150	1.5138	.09	2.64
Ba	1901.00	5	172.6271	62.17079	27.80362	95.4319	249.8224	122.70	273.92
	1904.00	5	147.5127	60.23468	26.93777	72.7215	222.3039	94.28	245.89
	1906.00	5	220.9992	87.54616	39.15183	112.2963	329.7021	136.15	358.36
	1907.00	5	343.5505	149.98633	67.07592	157.3179	529.7831	201.34	579.96
	Total	20	221.1724	117.96715	26.37826	165.9621	276.3827	94.28	579.96
Ni	1901.00	5	31.9031	12.24070	5.47421	16.7043	47.1019	21.57	51.68
	1904.00	5	32.2289	13.37064	5.97953	15.6271	48.8308	19.36	53.69
	1906.00	5	42.3132	17.75854	7.94186	20.2631	64.3633	25.48	69.97
	1907.00	5	49.8591	19.96834	8.93011	25.0652	74.6531	29.88	79.80
	Total	20	39.0761	16.69585	3.73331	31.2622	46.8900	19.36	79.80
Cr	1901.00	5	109.8506	41.49720	18.55811	58.3250	161.3762	70.17	172.75
	1904.00	5	95.1470	35.55273	15.89966	51.0025	139.2916	58.34	148.48
	1906.00	5	82.0604	25.43428	11.37456	50.4796	113.6412	54.37	118.38
	1907.00	5	69.7496	26.29035	11.75740	37.1058	102.3934	40.44	107.77
	Total	20	89.2019	33.83547	7.56584	73.3664	105.0374	40.44	172.75
Co	1901.00	5	10.8264	3.59702	1.60864	6.3602	15.2927	7.63	16.46
	1904.00	5	11.4146	3.97251	1.77656	6.4821	16.3471	7.21	17.48
	1906.00	5	14.0411	5.36995	2.40152	7.3734	20.7088	8.48	22.18
	1907.00	5	15.2932	5.57868	2.49486	8.3664	22.2201	9.43	23.52
	Total	20	12.8938	4.71497	1.05430	10.6872	15.1005	7.21	23.52
Cu	1901.00	5	215.8985	170.01551	76.03325	4.7964	427.0007	104.05	514.12
	1904.00	5	237.4202	182.02544	81.40425	11.4057	463.4346	49.18	532.52
	1906.00	5	239.5895	261.05054	116.74535	-84.5475	563.7266	72.04	695.74
	1907.00	5	257.2063	297.89471	133.22257	-112.6788	627.0915	60.06	775.82
	Total	20	237.5286	215.21169	48.12280	136.8065	338.2508	49.18	775.82

Appendix 8. One-Way ANOVA test of heavy metals for all wells

ANOVA						
		Sum of Squares	df	Mean Square	F	Sig.
As	Between Groups	810.570	3	270.190	1.771	.193
	Within Groups	2440.389	16	152.524		
	Total	3250.959	19			
Pb	Between Groups	2340890.117	3	780296.706	33.267	.000
	Within Groups	375290.073	16	23455.630		
	Total	2716180.190	19			
Zn	Between Groups	6479824.225	3	2159941.408	38.101	.000
	Within Groups	907044.840	16	56690.302		
	Total	7386869.065	19			
Mn	Between Groups	4296173.128	3	1432057.709	25.522	.000
	Within Groups	897787.572	16	56111.723		
	Total	5193960.700	19			
Cd	Between Groups	4.851	3	1.617	4.508	.018
	Within Groups	5.740	16	.359		
	Total	10.591	19			
Ba	Between Groups	113794.117	3	37931.372	4.030	.026
	Within Groups	150614.607	16	9413.413		
	Total	264408.724	19			
Ni	Between Groups	1125.441	3	375.147	1.439	.268
	Within Groups	4170.835	16	260.677		
	Total	5296.277	19			
Cr	Between Groups	4455.539	3	1485.180	1.374	.287
	Within Groups	17296.399	16	1081.025		
	Total	21751.938	19			
Co	Between Groups	67.677	3	22.559	1.018	.411
	Within Groups	354.710	16	22.169		
	Total	422.387	19			
Cu	Between Groups	4296.666	3	1432.222	.026	.994
	Within Groups	875708.709	16	54731.794		
	Total	880005.375	19			

Appendix 9. Multiple comparisons analysis between heavy metal values of the four wells

Multiple Comparisons										
LSD										
Dependent Variable	(i) Well	(j) Well	Mean Difference (i-j)	Std. Error	Sig.	95% Confidence Interval				
						Lower Bound	Upper Bound			
As	1901.00	1904.00	-3.23188	7.81087	.685	-19.7900	13.3266			
		1906.00	-11.86084	7.81087	.148	-28.4192	4.6975			
	1907.00	1904.00	-15.75814	7.81087	.000	-32.3544	-7.6252			
		1906.00	3.23188	7.81087	.685	-13.3266	19.7900			
	1904.00	1901.00	-8.62916	7.81087	.286	-25.1675	7.9292			
		1907.00	-12.56446	7.81087	.127	-29.1228	-3.9939			
	1906.00	1901.00	11.86084	7.81087	.148	-4.6975	28.4192			
		1904.00	8.62916	7.81087	.286	-7.9292	25.1675			
	1907.00	1901.00	-3.93529	7.81087	.621	-20.4936	12.6230			
		1904.00	15.75814	7.81087	.000	-7.622	32.3544			
	Pb	1901.00	1904.00	-790.11267	96.86202	.000	-1002.4509	-582.7743		
			1906.00	-7.92797	96.86202	.936	-213.2663	197.4103		
		1907.00	1904.00	-16.49382	96.86202	.867	-221.9319	188.8447		
			1906.00	798.11267	96.86202	.000	592.7743	1003.4509		
		1904.00	1901.00	790.18466	96.86202	.000	584.8463	995.5230		
			1907.00	791.81901	96.86202	.000	576.2807	986.9573		
1906.00		1901.00	7.92797	96.86202	.936	-197.4103	213.2663			
		1904.00	-790.18466	96.86202	.000	-995.5230	-584.8463			
1907.00		1901.00	-8.56565	96.86202	.931	-213.9040	196.7727			
		1904.00	16.49382	96.86202	.867	-188.8447	221.8319			
Zn		1901.00	1904.00	-781.61901	96.86202	.000	-986.9573	-576.2807		
			1906.00	8.56565	96.86202	.931	-196.7727	213.9040		
		1904.00	1901.00	1308.74606	150.58593	.000	889.5182	1627.9740		
			1906.00	1370.37940	150.58593	.000	1051.1515	1689.6073		
		1906.00	1901.00	1254.11426	150.58593	.000	834.8864	1573.3422		
			1904.00	-1308.74606	150.58593	.000	-1627.9740	-989.5182		
	1907.00	1901.00	61.83334	150.58593	.688	-257.5946	380.8612			
		1904.00	-54.83180	150.58593	.722	-373.8597	264.5961			
	1904.00	1901.00	-1370.37940	150.58593	.000	-1689.6073	-1051.1515			
		1906.00	-61.83334	150.58593	.688	-380.8612	257.5946			
	1906.00	1901.00	-116.26514	150.58593	.451	-435.4930	202.9628			
		1904.00	1254.11426	150.58593	.000	-1573.3422	-934.8864			
	Mn	1901.00	1904.00	54.83180	150.58593	.722	-264.5961	373.8597		
			1906.00	116.26514	150.58593	.451	-202.9628	435.4930		
		1904.00	1901.00	1121.74715	149.81552	.000	804.1524	1439.3419		
			1906.00	1002.15937	149.81552	.000	684.5646	1319.7540		
1906.00		1901.00	1073.58104	149.81552	.000	755.9863	1391.1757			
		1904.00	-1121.74715	149.81552	.000	-1439.3419	-804.1524			
1907.00		1901.00	-119.56782	149.81552	.436	-437.1625	198.0269			
		1904.00	-48.16611	149.81552	.752	-365.7608	269.4286			
1904.00		1901.00	-1002.15937	149.81552	.000	-1319.7540	-684.5646			
		1906.00	119.56782	149.81552	.436	-198.0269	437.1625			
1906.00		1901.00	71.42171	149.81552	.640	-246.1730	389.0164			
		1904.00	-1073.58104	149.81552	.000	-1391.1757	-755.9863			
1907.00		1901.00	48.16611	149.81552	.752	-269.4286	365.7608			
		1904.00	-71.42171	149.81552	.640	-389.0164	246.1730			
Cd		1901.00	1904.00	13981	37880	.734	-6721	9339		
			1906.00	-36700	37880	.347	-11700	4360		
	1904.00	1901.00	97727	37880	.020	1747	17807			
		1906.00	-49791	37880	.734	-9339	6721			
	1906.00	1901.00	84681	37880	.040	4838	16488			
		1904.00	36700	37880	.347	-4360	11700			
	1907.00	1901.00	49791	37880	.207	-3051	13009			
		1904.00	1.34472	37880	.003	5417	2.1477			
	Ba	1901.00	1904.00	-77727	37880	.020	-1.7807	-1.747		
			1906.00	-84681	37880	.040	-1.6498	-1.0438		
		1904.00	1901.00	-1.34472	37880	.003	-2.1477	-5.417		
			1906.00	25.11442	61.36257	.688	-104.9684	55.1973		
		1906.00	1901.00	-48.37209	61.36257	.442	-178.4549	81.7108		
			1904.00	-170.82337	61.36257	.013	-301.0062	-40.8405		
		1904.00	1901.00	-25.11442	61.36257	.688	-155.1073	104.9684		
			1906.00	-73.48850	61.36257	.249	-203.5693	56.5863		
1906.00		1901.00	-196.03779	61.36257	.006	-326.1206	-65.9550			
		1904.00	48.37209	61.36257	.442	-81.7108	178.4549			
1907.00		1901.00	73.48850	61.36257	.249	-56.5863	203.5693			
		1904.00	-122.55129	61.36257	.063	-252.6341	7.5316			
Ni		1901.00	1904.00	170.92337	61.36257	.013	40.8405	301.0062		
			1906.00	196.03779	61.36257	.006	65.9550	326.1206		
		1904.00	1901.00	122.55129	61.36257	.063	-7.5316	252.6341		
			1906.00	-32586	10.21131	.975	-21.9729	21.3212		
	1906.00	1901.00	-18.41011	10.21131	.323	-32.6571	11.2369			
		1904.00	-17.95805	10.21131	.398	-39.6031	3.6810			
	1904.00	1901.00	32586	10.21131	.975	-21.3212	21.9729			
		1906.00	-10.08426	10.21131	.338	-31.7313	11.5628			
	1906.00	1901.00	-17.63019	10.21131	.104	-39.2772	4.0168			
		1904.00	10.41011	10.21131	.323	-11.2369	32.0571			
	1907.00	1901.00	10.08426	10.21131	.338	-11.5628	31.7313			
		1904.00	-7.54593	10.21131	.471	-29.1929	14.1011			
	Cr	1901.00	1904.00	17.89805	10.21131	.098	-3.8916	39.6031		
			1906.00	17.63019	10.21131	.104	-4.0168	39.2772		
		1904.00	1901.00	7.54593	10.21131	.471	-14.1011	29.1929		
			1906.00	14.70380	20.79447	.490	-29.3787	58.7859		
1906.00		1901.00	27.79822	20.79447	.200	-16.2921	71.8725			
		1904.00	40.10104	20.79447	.072	-3.9813	84.1833			
1904.00		1901.00	-14.70380	20.79447	.490	-58.7859	29.3787			
		1906.00	13.08862	20.79447	.538	-30.9957	57.1689			
1906.00		1901.00	25.39744	20.79447	.240	-18.6849	69.4797			
		1904.00	-27.79822	20.79447	.200	-71.8725	16.2921			
Co		1901.00	1904.00	-13.08862	20.79447	.538	-57.1689	30.9957		
			1906.00	-25.39744	20.79447	.240	-69.4797	18.6849		
		1904.00	1901.00	13.08862	20.79447	.538	-30.9957	57.1689		
			1906.00	12.31082	20.79447	.562	-31.7715	56.3931		
		1906.00	1901.00	-40.10104	20.79447	.072	-84.1833	3.9813		
			1904.00	-25.39744	20.79447	.240	-69.4797	18.6849		
	1907.00	1901.00	-12.31082	20.79447	.562	-56.3931	31.7715			
		1904.00	-58816	2.97789	.846	-6.9010	5.7247			
	1906.00	1901.00	-3.21483	2.97789	.296	-8.9274	3.0882			
		1904.00	-4.48679	2.97789	.153	-10.7756	1.8480			
	1904.00	1901.00	58816	2.97789	.846	-5.7247	6.9010			
		1906.00	-2.82847	2.97789	.391	-8.9393	3.0883			
	1907.00	1901.00	-3.87882	2.97789	.211	-10.1914	2.4342			
		1904.00	3.21483	2.97789	.296	-3.0882	9.5274			
	1906.00	1901.00	2.62847	2.97789	.391	-3.6863	8.9393			
		1904.00	-1.25210	2.97789	.680	-7.5650	5.0607			
Cu	1901.00	1904.00	4.48679	2.97789	.153	-1.8480	10.7796			
		1906.00	3.87882	2.97789	.211	-2.4342	10.1914			
	1904.00	1901.00	1.25210	2.97789	.680	-5.0607	7.5650			
		1906.00	-21.52163	147.96188	.886	-335.1868	292.1435			
	1906.00	1901.00	-22.69102	147.96188	.875	-337.3562	289.9741			
		1904.00	-41.30782	147.96188	.784	-354.9730	272.3574			
	1904.00	1901.00	21.52163	147.96188	.886	-292.1435	335.1868			
		1906.00	-2.16939	147.96188	.988	-315.8346	311.4958			
	1906.00	1901.00	-19.78619	147.96188	.895	-333.4514	293.8790			
		1904.00	23.69102	147.96188	.875	-289.9741	337.3562			
	1907.00	1901.00	21.6939	147.96188	.888	-311.4958	315.8346			
		1904.00	-17.61880	147.96188	.907	-331.2628	286.0484			
	1907.00	1901.00	41.30782	147.96188	.784	-272.3574	354.9730			
		1904.00	19.78619	147.96188	.895	-293.8790	333.4514			
	1906.00	1901.00	17.61880	147						

Appendix 10. Correlation analysis between various heavy metals using Pearson's correlation (2-tailed) analysis

		Correlations									
		As	Pb	Zn	Mn	Cd	Ba	Ni	Cr	Co	Cu
As	Pearson Correlation	1	.040	-.068	.008	.199	.917**	.988**	.466*	.987**	.846**
	Sig. (2-tailed)		.869	.775	.975	.401	.000	.000	.038	.000	.000
	N	20	20	20	20	20	20	20	20	20	20
Pb	Pearson Correlation	.040	1	-.220	-.255	.031	-.166	.010	.348	.074	.231
	Sig. (2-tailed)	.869		.351	.279	.896	.484	.966	.133	.757	.328
	N	20	20	20	20	20	20	20	20	20	20
Zn	Pearson Correlation	-.068	-.220	1	.986**	.217	.006	.036	.620**	.039	.210
	Sig. (2-tailed)	.775	.351		.000	.357	.981	.881	.004	.871	.375
	N	20	20	20	20	20	20	20	20	20	20
Mn	Pearson Correlation	.008	-.255	.986**	1	.316	.037	.103	.668**	.113	.261
	Sig. (2-tailed)	.975	.279	.000		.175	.878	.666	.001	.634	.266
	N	20	20	20	20	20	20	20	20	20	20
Cd	Pearson Correlation	.199	.031	.217	.316	1	.002	.196	.465*	.244	.390
	Sig. (2-tailed)	.401	.896	.357	.175		.993	.407	.039	.299	.089
	N	20	20	20	20	20	20	20	20	20	20
Ba	Pearson Correlation	.917**	-.166	.006	.037	.002	1	.942**	.316	.903**	.743**
	Sig. (2-tailed)	.000	.484	.981	.878	.993		.000	.175	.000	.000
	N	20	20	20	20	20	20	20	20	20	20
Ni	Pearson Correlation	.988**	.010	.036	.103	.196	.942**	1	.529*	.993**	.862**
	Sig. (2-tailed)	.000	.966	.881	.666	.407	.000		.017	.000	.000
	N	20	20	20	20	20	20	20	20	20	20
Cr	Pearson Correlation	.466*	.348	.620**	.668**	.465*	.316	.529*	1	.579**	.705**
	Sig. (2-tailed)	.038	.133	.004	.001	.039	.175	.017		.008	.001
	N	20	20	20	20	20	20	20	20	20	20
Co	Pearson Correlation	.987**	.074	.039	.113	.244	.903**	.993**	.579**	1	.872**
	Sig. (2-tailed)	.000	.757	.871	.634	.299	.000	.000	.008		.000
	N	20	20	20	20	20	20	20	20	20	20
Cu	Pearson Correlation	.846**	.231	.210	.261	.390	.743**	.862**	.705**	.872**	1
	Sig. (2-tailed)	.000	.328	.375	.266	.089	.000	.000	.001	.000	
	N	20	20	20	20	20	20	20	20	20	20

** . Correlation is significant at the 0.01 level (2-tailed).
* . Correlation is significant at the 0.05 level (2-tailed).

Appendix 11. Correlation analysis between TOC and heavy metals using Pearson's correlation (2-tailed) analysis

		Correlations between TOC and various heavy metals of the same size fractions										
		TOC	Cr	Ba	Ni	Co	As	Cu	Mn	Zn	Cd	Pb
TOC	Pearson Correlation	1	.978	.970	.919	.896	.838	.833	.660	.621	.162	.004
	Sig. (2-tailed)		.000	.000	.000	.000	.002	.003	.038	.055	.655	.991
	N	10	10	10	10	10	10	10	10	10	10	10

Appendix 12. Descriptive statistics of minerals within the four different wells

		Descriptives							
		N	Mean	Std. Deviation	Std. Error	95% Confidence Interval for Mean		Minimum	Maximum
						Lower Bound	Upper Bound		
Quartz	1901.00	2	41.3400	1.76777	1.25000	35.4572	57.2228	40.09	42.59
	1904.00	2	39.4950	.64347	.46500	33.7137	45.2763	39.04	39.95
	1906.00	2	38.1450	.38062	.25500	34.9049	41.3951	37.89	38.40
	1907.00	2	34.5200	.21213	.15000	32.6141	36.4259	34.37	34.67
	Total	8	38.3750	2.76801	.97864	36.0609	40.6891	34.37	42.59
Stilpnomelane	1901.00	2	2.2700	.39598	.28000	-1.2877	5.8277	1.99	2.55
	1904.00	2	2.4750	.28991	.20500	-1.298	5.0798	2.27	2.68
	1906.00	2	3.3550	.31820	.22500	.4961	6.2139	3.13	3.58
	1907.00	2	3.4850	.20506	.14500	1.6426	5.3274	3.34	3.63
	Total	8	2.8963	.61384	.21702	2.3831	3.4094	1.99	3.63
Hematite	1901.00	2	2.2600	.12728	.09000	1.1164	3.4036	2.17	2.35
	1904.00	2	2.8650	.14849	.10500	1.5308	4.1992	2.76	2.97
	1906.00	2	3.2650	.10607	.07500	2.3120	4.2180	3.19	3.34
	1907.00	2	3.8200	.16971	.12000	2.2953	5.3447	3.70	3.94
	Total	8	3.0525	.61796	.21848	2.5359	3.5691	2.17	3.94
Calcite	1901.00	2	1.8800	.16971	.12000	3.3553	3.4047	1.76	2.00
	1904.00	2	1.0400	.07071	.05000	.4047	1.6753	.99	1.09
	1906.00	2	1.2700	.07071	.05000	.6347	1.9053	1.22	1.32
	1907.00	2	2.7450	.09192	.06500	1.9191	3.5709	2.68	2.81
	Total	8	1.7338	.70993	.25100	1.1402	2.3273	.99	2.81
Orthoclase	1901.00	2	5.5100	.33941	.24000	2.4605	8.5595	5.27	5.75
	1904.00	2	5.4400	.25456	.18000	3.1529	7.7271	5.26	5.62
	1906.00	2	5.1000	.15556	.11000	3.7023	6.4977	4.99	5.21
	1907.00	2	4.8000	.15556	.11000	3.4023	6.1977	4.69	4.91
	Total	8	5.2125	.35346	.12497	4.9170	5.5080	4.69	5.75
Muscovite	1901.00	2	1.7750	.07778	.05500	1.0762	2.4738	1.72	1.83
	1904.00	2	1.4250	.03536	.02500	1.1073	1.7427	1.40	1.45
	1906.00	2	2.9950	.04950	.03500	2.5503	3.4397	2.96	3.03
	1907.00	2	3.7450	.09192	.06500	2.9191	4.5709	3.68	3.81
	Total	8	2.4950	.99778	.35277	1.6508	3.3192	1.40	3.81
Chamosite	1901.00	2	4.450	.23335	.16500	-1.6515	2.5415	.28	.61
	1904.00	2	6.550	.36062	.25500	-2.5851	3.8951	.40	.91
	1906.00	2	4.950	.28991	.20500	-2.1098	3.0998	.29	.70
	1907.00	2	3.650	.14849	.10500	-5.962	1.6992	.26	.47
	Total	8	4.900	.23312	.08242	.2951	6.849	.26	.91
Old battery ZnMn	1901.00	2	4.100	.01414	.01000	.2829	5.371	.40	.42
	1904.00	2	0.500	.00000	.00000	.0500	0.500	.05	.05
	1906.00	2	0.850	.00707	.00500	.0215	1.485	.08	.09
	1907.00	2	0.250	.00707	.00500	-.0385	0.885	.02	.03
	Total	8	1.425	.16680	.05997	.0031	2.819	.02	.42
Ferroan Clay	1901.00	2	25.8200	1.40007	.99000	13.2409	38.3991	24.83	26.81
	1904.00	2	31.8750	.99702	.70500	22.9171	40.8329	31.17	32.58
	1906.00	2	30.5500	.29698	.21000	27.8817	33.2183	30.34	30.76
	1907.00	2	26.9350	.19092	.13500	25.2197	28.6503	26.90	27.07
	Total	8	28.7950	2.74726	.97130	28.4992	31.9918	24.83	32.58
Zircon	1901.00	2	1.150	.00707	.00500	.0515	1.795	.11	.12
	1904.00	2	2.400	.01414	.01000	.1129	3.671	.23	.25
	1906.00	2	2.100	.00000	.00000	.2100	2.100	.21	.21
	1907.00	2	1.450	.00707	.00500	.0815	2.085	.14	.15
	Total	8	1.775	.05365	.01897	.1326	2.224	.11	.25
Epidote	1901.00	2	7.2150	.79903	.56500	0.960	14.3940	6.65	7.78
	1904.00	2	3.3700	.26870	.19000	.9558	5.7842	3.18	3.56
	1906.00	2	4.9250	.36062	.25500	1.6849	8.1651	4.67	5.18
	1907.00	2	8.0250	.26163	.18500	5.6744	10.3756	7.84	8.21
	Total	8	5.8838	2.00356	.70837	4.2087	7.5588	3.18	8.21
Sodic glass	1901.00	2	3.2100	.28284	.20000	.6688	5.7512	3.01	3.41
	1904.00	2	3.3850	.68589	.48500	-2.7775	9.5475	2.90	3.87
	1906.00	2	2.7050	.57278	.40500	-2.4410	7.8510	2.30	3.11
	1907.00	2	2.6200	.52326	.37000	-2.0913	7.3213	2.25	2.99
	Total	8	2.9800	.53407	.18992	2.5335	3.4285	2.25	3.87
Albite	1901.00	2	5.0200	.04243	.03000	4.6298	5.4012	4.99	5.05
	1904.00	2	5.4750	.02121	.01500	5.2844	5.6656	5.46	5.49
	1906.00	2	4.5800	.02828	.02000	4.3259	4.8341	4.56	4.60
	1907.00	2	4.3950	.02121	.01500	4.2044	4.5856	4.38	4.41
	Total	8	4.8675	.44721	.15811	4.4936	5.2414	4.38	5.49
Dolomite	1901.00	2	2.2550	.02121	.01500	.0644	4.456	.24	.27
	1904.00	2	0.950	.00707	.00500	.0315	1.585	.09	.10
	1906.00	2	0.950	.00707	.00500	.0315	1.585	.09	.10
	1907.00	2	1.100	.00000	.00000	1.000	1.000	.10	.10
	Total	8	1.362	.07386	.02611	.0745	1.980	.09	.27
Bixbyite	1901.00	2	2.000	.01414	.01000	.0729	3.271	.19	.21
	1904.00	2	0.300	.00000	.00000	.0300	0.300	.03	.03
	1906.00	2	0.200	.00000	.00000	.0200	0.200	.02	.02
	1907.00	2	0.000	.00000	.00000	.0000	0.000	.00	.00
	Total	8	0.625	.08592	.03034	-.0092	1.342	.00	.21
Lead or Galena	1901.00	2	0.850	.07778	.05500	-.6138	7.638	.03	.14
	1904.00	2	3.250	.04950	.03500	-1.197	7.697	.29	.36
	1906.00	2	2.450	.23335	.16500	-1.8515	2.3415	.08	.41
	1907.00	2	5.000	.42426	.30000	-3.3119	4.3119	.20	.80
	Total	8	2.888	.24544	.08678	.0836	4.939	.03	.80
Ankerite	1901.00	2	9.250	.00707	.00500	8.615	9.885	.92	.93
	1904.00	2	6.350	.00707	.00500	5.715	6.985	.63	.64
	1906.00	2	8.550	.00707	.00500	7.915	9.185	.85	.86
	1907.00	2	1.1850	.02121	.01500	.9944	1.3756	1.17	1.20
	Total	8	9.000	.21003	.07426	.7244	1.0756	.63	1.20
Fe TiCr oxide	1901.00	2	0.600	.00000	.00000	.0600	0.600	.06	.06
	1904.00	2	0.700	.00000	.00000	.0700	0.700	.07	.07
	1906.00	2	0.850	.00707	.00500	.0915	1.285	.06	.07
	1907.00	2	0.850	.00707	.00500	.0215	1.485	.08	.09
	Total	8	0.700	.01069	.00378	.0611	0.799	.06	.09
Glass fibres	1901.00	2	5.850	.00707	.00500	5.215	6.485	.58	.59
	1904.00	2	2.100	.00000	.00000	.2100	2.100	.21	.21
	1906.00	2	2.500	.01414	.01000	1.229	3.771	.24	.26
	1907.00	2	1.5300	.07071	.05000	.8947	2.1653	1.48	1.58
	Total	8	6.438	.56938	.20131	1.677	1.1198	.21	1.58
Rutile	1901.00	2	2.500	.01414	.01000	1.229	3.771	.24	.26
	1904.00	2	3.300	.04243	.03000	-.0512	7.112	.30	.36
	1906.00	2	3.050	.03536	.02500	-.0127	6.227	.28	.33
	1907.00	2	2.750	.02121	.01500	.0844	4.656	.26	.29
	Total	8	2.900	.03964	.01402	.2569	3.231	.24	.36
Hornblende	1901.00	2	3.350	.00707	.00500	2.715	3.985	.33	.34
	1904.00	2	2.200	.01414	.01000	.0929	3.471	.21	.23
	1906.00	2	3.100	.01414	.01000	1.929	4.371	.30	.32
	1907.00	2	3.100	.01414	.01000	1.929	4.371	.30	.32
	Total	8	2.938	.04779	.01890	.2538	3.337	.21	.34
Cu oxide	1901.00	2	0.300	.04243	.03000	-.3512	4.112	.00	.06
	1904.00	2	2.850	.17678	.12500	-1.3033	1.8733	.16	.41
	1906.00	2	1.900	.16971	.12000	-1.3347	1.7147	.07	.31
	1907.00	2	3.950	.07778	.05500	-.3038	1.0938	.34	.45
	Total	8	2.250	.17378	.06144	.0797	.3703	.00	.45

Appendix 13. One-Way ANOVA test of minerals for all wells

		ANOVA				
		Sum of Squares	df	Mean Square	F	Sig.
Quartz	Between Groups	49.919	3	16.640	17.921	.009
	Within Groups	3.714	4	.929		
	Total	53.633	7			
Stilpnomelane	Between Groups	2.253	3	.751	7.821	.038
	Within Groups	.384	4	.096		
	Total	2.638	7			
Hematite	Between Groups	2.595	3	.865	44.186	.002
	Within Groups	.078	4	.020		
	Total	2.673	7			
Calcite	Between Groups	3.481	3	1.160	98.222	<.001
	Within Groups	.047	4	.012		
	Total	3.528	7			
orthoclase	Between Groups	.646	3	.215	3.772	.116
	Within Groups	.228	4	.057		
	Total	.875	7			
Muscovite	Between Groups	6.951	3	2.317	509.216	<.001
	Within Groups	.018	4	.005		
	Total	6.969	7			
Chamosite	Between Groups	.090	3	.030	.412	.754
	Within Groups	.291	4	.073		
	Total	.380	7			
Old battery ZnMn	Between Groups	.194	3	.065	864.222	<.001
	Within Groups	.000	4	.000		
	Total	.195	7			
Ferroan Clay	Between Groups	49.753	3	16.584	21.546	.006
	Within Groups	3.079	4	.770		
	Total	52.832	7			
Zircon	Between Groups	.020	3	.007	88.222	<.001
	Within Groups	.000	4	.000		
	Total	.020	7			
Epidote	Between Groups	27.191	3	9.064	39.877	.002
	Within Groups	.909	4	.227		
	Total	28.100	7			
Sodic glass	Between Groups	.844	3	.281	.977	.487
	Within Groups	1.152	4	.288		
	Total	1.997	7			
Albite	Between Groups	1.396	3	.465	531.981	<.001
	Within Groups	.003	4	.001		
	Total	1.400	7			
Dolomite	Between Groups	.038	3	.013	91.242	<.001
	Within Groups	.001	4	.000		
	Total	.038	7			
Bixbyte	Between Groups	.051	3	.017	342.333	<.001
	Within Groups	.000	4	.000		
	Total	.052	7			
Lead or Galena	Between Groups	.179	3	.060	.981	.486
	Within Groups	.243	4	.061		
	Total	.422	7			
Ankerite	Between Groups	.308	3	.103	684.889	<.001
	Within Groups	.001	4	.000		
	Total	.309	7			
Fe TiCr oxide	Between Groups	.001	3	.000	9.333	.028
	Within Groups	.000	4	.000		
	Total	.001	7			
Glass fibres	Between Groups	2.264	3	.755	575.019	<.001
	Within Groups	.005	4	.001		
	Total	2.269	7			
Rutile	Between Groups	.007	3	.002	2.631	.187
	Within Groups	.004	4	.001		
	Total	.011	7			
Hornblende	Between Groups	.015	3	.005	31.462	.003
	Within Groups	.001	4	.000		
	Total	.016	7			
Cu oxide	Between Groups	.144	3	.048	2.818	.171
	Within Groups	.068	4	.017		
	Total	.211	7			